1996

Electrokinetically induced movement of organic coal tar constituents in clay soils

Gary P. Newhart
Lehigh University

Newhart, Gary P.

Electrokinetically Induced Movement of Organic Coal Tar Constituents in Clay Soils

January 12, 1997

ELECTROKINETICALLY INDUCED MOVEMENT OF ORGANIC COAL TAR CONSTITUENTS IN CLAY SOILS

By

Gary P. Newhart

A Thesis

Presented to the Graduate and Research Committee,

of Lehigh University

in Candidacy for the Degree of

Master of Science

in

Civil and Environmental Engineering

Lehigh University

December 1996

This Thesis is accepted and approved in partial fulfillment of the requirements for the Master of Science.

Dr. Sibel Pamukcu

Professor of Civil Engineering

Thesis Advisor

Dr. Le-Wu Lu

Chairman Civil and Environmental Engineering

Acknowledgments

I would like to express my sincere appreciation to my research advisor, Dr. Sibel Pamukcu, for her support throughout this work. I am also extremely appreciative of the late Dr. Irwin J. Kugelman, former chairman of the Civil Engineering Department, and Dr. Paul B. Myers of the Earth and Environmental Studies Department for their interest in, and encouragement of graduate research in Environmental and Geotechnical Engineering at Lehigh University. Additionally, I'd like to thank Dr. Kenneth Whittle of Electro-Petroleum, Inc., Wayne PA., Dr. Eric Lindgren of Sandia National Laboratories, Albuquerque, NM., and Alan Brown, Superfund Removal Branch, Hazardous Waste Division, United States Environmental Protection Agency, Region III, Philadelphia, PA., for their time and helpful guidance.

This research was funded by Illinois Power and Light Utility Company of Champaign Urbana, Illinois as administered by the Electric Power Research Institute (EPRI) through the Energy Research Center, Lehigh University, Bethlehem, Pennsylvania, and in part by the Office of Technology Development, Office of Environmental Restoration and Waste Management, United States Department of Energy, managed by Argonne National Laboratory, Chicago, Illinois.

TABLE OF CONTENTS

ABSTRACT

Organic chemical contamination of the soil and ground water presents a threat to the Ecosystem as a whole, and a potential health threat to the inhabitants of affected communities. Previous waste disposal techniques practiced at industrial and non-industrial sites over many years as well as uncontrolled chemical releases have contributed to the deterioration of our soil, surface and ground water supplies. Due to a heightened awareness, an effort has been undertaken by the scientific community to address chemical contaminants, their fate and transport in the environment, and remedial techniques capable of safely removing those contaminants from our water and soil. Present remedial techniques need to be improved in concert with the development of new, more efficient treatment processes. Present remedial techniques for soil treatment include removal and containment in a landfill, soil washing, soil vitrification, and aerobic and anaerobic Bioremediation (U.S. EPA 1985). Surface and ground water treatment processes include air striping, ion exchange resins, carbon adsorption, ultra violet (UV) destruction, and ozonation. Recently, electrokinetics has been demonstrated to be a promising tool in the arsenal of remedial tools used to remove inorganic contaminants from both saturated and unsaturated soils. The electrokinetic process is also being studied as a possible tool to decontaminate soils affected by organic contaminants.

Electrokinetics is the application of an electric field between two electrodes, causing the migration of chemical species which lie in the path of the electrodes. Electrokinetic remediation of soils is a technique employing three fundamental physical factors: **Electromigration**, **Electrophoresis**, and **Electroosmosis**. Electromigration and Electrophoresis involve the movement of ionic and charged species and particles toward oppositely charged electrodes. Electroosmosis is the induced flow of water toward an electrode, most often from the anode to the cathode. These processes are presented in Figure 1. These phenomena transport contaminants through the soil matrix to the respective electrodes for further treatment or removal. The direction and relative movement of the target compounds are determined by a number of factors which include the type and concentration of the contaminant, soil type (chemical makeup and physical matrix structure), interfacial chemistry of the soil water system, and the conductivity of the soil pore water system.

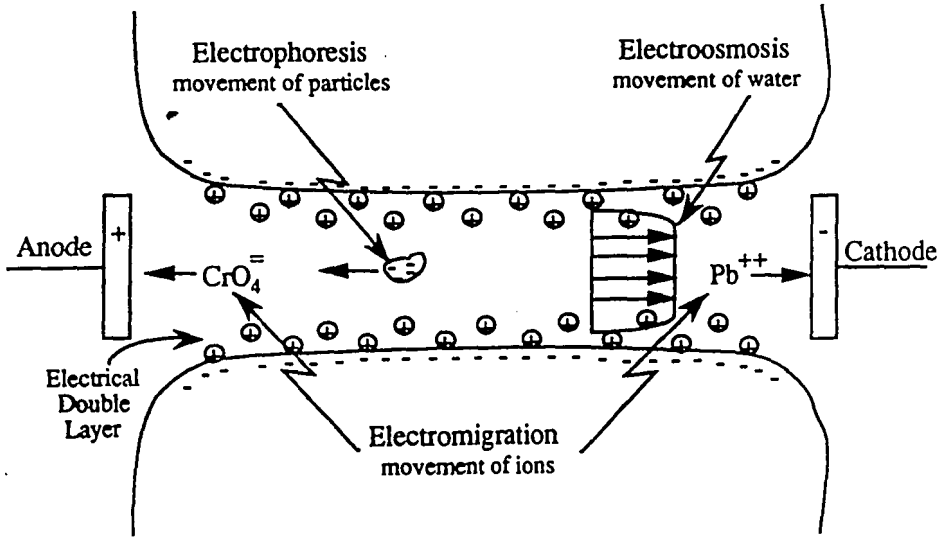

Figure 1 : Electrokinetic Migration

The study presented here was undertaken to determine, at the laboratory bench scale, the feasibility of using the electrokinetic remediation process to remove coal tar constituents, specifically Polycyclic Aromatic Hydrocarbons (PAHs), from clay soils. The laboratory analyses measured the movement of coal tar as source material, and the movement of it's lighter molecular weight constituents. The soil which was examined and tested was retrieved from a former manufactured gas plant (MGP) site, located in Champaign Urbana, Illinois. The samples were treated electrokinetically using (1) simulated site ground water containing concentrations of inorganic compounds typical of site ground water conditions[1], (2) ground water and an anionic surface active agent [surfactant (sodium dodecyl sulfate)], and (3) ground water with the surfactant and a co-surfactant (butanol).

The bench scale studies indicated that the removal of the lighter fraction ionic and water soluble PAH compounds occurs readily, due to electroosmotic flow. An increase in the mobility of the water insoluble, no net charge organic coal tar constituent compounds was achieved to a limited degree by the addition of the anionic surfactant to the ground water system. Movement of the insoluble organic compounds was not enhanced further by the combination of the particular surfactant and the co-surfactant in this work. It appears that the cosurfactant disrupted the micellar envelope, causing a scattering of the organic compounds toward the anode by electromigration, and toward the cathode with electroosmotic flow. The soils which were treated without the addition of the surfactant/co-surfactant, showed increased removal of the contaminants with increased pore water flow through the sample. The treated samples exhibited an accumulation or stacking of the

contaminants at the cathode end of the soil. Stacking also occurred at the anode end of the soil sample, hypothesized to be due to the electrolytic separation of the various size and mass organic compounds. The greatest removal of the PAHs treated with the addition of the anionic surfactant occurred when the surfactant was injected into the cathode chamber of the test apparatus. The anionic surfactant-enveloped PAH compounds electromigrated to the anode end of the soil sample.

The results of the laboratory investigations presented in this work demonstrate that the electrokinetic enhancement of organic chemical transport through soils is a promising remedial process which, with continued research, would be developed into an effective in-situ treatment tool to remove organic contaminants (e.g. PAHs) from soils. The further development of the electrokinetic process to effectively remove PAH contaminants from the soil should include, but not be limited to: 1) a detailed evaluation of the vertical and horizontal contaminant distribution through the soil matrix, 2) a more complete understanding of the specific soil - contaminant interaction, and 3) an in-depth understanding of the transient physical and electrochemical processes which occur at the soil/fluid interface, causing the movement of the organic species through the soil matrix. The interim transient processes should also be studied, including the physical and chemical interactions between the soil and the contaminant; the effect of the pore fluid chemistry on the removal of the contaminant from the soil matrix; and the distribution and speciation of the contaminants throughout the soil matrix.

The laboratory results have demonstrated that the movement of organic species through the soil matrix is primarily dependent on the organic species being removed from, and it's chemical and physical interactions with, the matrix, rather than the soil matrix itself. Chemical enhancements such as pH control, complexing or solubilizing compounds, and physical enhancements may be necessary to effectively mobilize and remove the targeted organic species from the soils. Chemical enhancement occurs when the contaminant's chemistry is altered by oxidation and reduction (redox) reactions due to the soil and competing chemical species, chemical and biological weathering of the contaminants, and the adsorption capacity of the soil matrix (Dragun 1988). Physical parameters such as the soil matrix's water content, bulk density or porosity, hydraulic conductivity, clay content, surface area, and total organic carbon (TOC) content significantly influence the movement of the contaminant through the soil matrix (McBride 1994).

CHAPTER 1

INTRODUCTION

1.1 Introduction

In the United States, coal gasification for energy consumption was common during the late 1800s and early to mid 1900s, peaking in the 1930s and declining into the 1950s. In the process of coal gasification, volatile gasses were released from the solid coal and used directly as an energy source in industrial and commercial boilers, as well as municipal power generation units. The residual by-product compounds, known as coal tars, were disposed of by selling the tars to other industries for use in the manufacture of "tar" related products. If the by-products were not marketable, the residues were stored at the industrial site or power plants or, as often occurred, were land filled at their generation site. Today, due to the pervasiveness of the contamination, coal tar contamination has become an environmental clean-up challenge (Pamukcu 1994).

The United States Environmental Protection Agency (U.S.EPA) has estimated that approximately 1,500 former manufactured gas plants (MGP) facility sites exist within the borders of the United States. Wastes associated with the gasification processes have contaminated these sites, leaving behind residual polycyclic aromatic hydrocarbons (PAH), light aromatic hydrocarbons and an array of inorganic contaminants. Complex environmental

processes govern the release, transport and exposure of theses MGP contaminants. Utilities face the daunting task of investigating and cleaning up these MGP sites (U.S. EPA 1995).

This study evaluated the feasibility of applying an emerging technology variably known as electrokinetics, electrokinetic remediation, electro-reclamation, electrokinetic soil processing, and electrokinetic decontamination electrochemical treatment (Probstein 1990), to remediate soil contaminated by coal tar constituents.

The technique of electrokinetics is becoming a noted technology in the cadre of soil remediation techniques for the clean-up of inorganic soil contaminants, and a tool which is potentially capable of addressing organic soil and ground water contamination. **Electrokinetics** refers to the movement of water, ionic and non-ionic species relative to each other as a response to an applied direct current electric field. The process is an in-situ or ex-situ technique, capable of mobilizing and transporting ionic and non ionic compounds to an electrode for collection and removal from the target area. This is achieved by applying a direct current (DC) voltage at an electrode (anode), which is capable of flowing through a media (soil), to a companion electrode (cathode). The charged or ionized compounds are transported to it's oppositely charged, companion electrode, while the water soluble compounds are swept along as the water in the cell is transported to the cathode.

Electrokinetics, as applied to the remediation of soils contaminated with organic contaminants involves three processes: **Electroosmosis**, **Electromigration**, and **Electrophoresis**. Electroosmosis produces the rapid flow of fluid (vadose zone, saturated zone), and is considered to be the dominant process in low permeability soils. Electromigration refers to the migration of ionic and polar species which are present in the matrices pore water. Electrophoresis is the process of mobilization and migration of charged colloids, with respect to an electric potential gradient. In soils which are more permeable than clays, such as sands, electrophoresis may play a significant role in transport. In soils with low permeabilities, such as clays, electrophoresis is not a major transport mechanism due to size exclusion of the colloids by the soil matrix.

Electromigration is the action which causes the dissociation of the water molecule into hydrogen (H^+)and hydroxyl (OH^-) ions. This is the driving force in a soil-water system, responsible for the directional sweeping of the pore fluid and the chemical species contained within the fluid, charged or otherwise. The reaction of H_2O dissociating to H^+ and OH^- is the cause for the migration of an acid front (H^+), which is generated at the anode by the oxidation of water to $H^+(aq) + O_2(g)$, toward the cathode. Conversely, the reaction which occurs at the cathode is the cause of the migration of a basic front toward the anode as water is reduced to $H_2(g) + OH^-$. Though logic initially suggests that the two fronts would buffer each other, there are two factors which cause the acid front to dominate in an unchecked system. First, hydrogen ions electromigrate more quickly through a soil water matrix than the hydroxide ion. Secondly, the enhancement created by the electroosmotic motion sweeping the pore fluid

from the anode to the cathode, carries the hydrogen ion toward the cathode (Wittle et al. 1993).

1.2 Objectives of the Study

The objective of this research was to determine the feasibility of transporting organic coal tar constituents through clay soils. Specifically, the target contaminants are PAH compounds which are constituents of coal tar, commonly associated with contaminants found at MGP facility sites. Soil samples contaminated by coal tar constituents collected from a MGP facility were treated electrokinetically. Movement of the target organic PAH compounds were monitored for their mobility through the soil matrix, as a current was applied to the soil system.

1.3 Scope of the Study

The investigation of the coal tar contaminated soil samples was conducted from May 1992 through May 1993. Soil samples (predominantly illite clay) were collected in Shelby tube samplers during a field investigation in December, 1991, at a former MGP facility, located in Champaign-Urbana, Illinois. Existing electrokinetic apparatus (Lehigh University's Geotechnical Laboratories, Bethlehem, Pennsylvania) was modified to perform the tests on the coal tar contaminated clays. The electrokinetic evaluations were performed in the Geotechnical Laboratories at Lehigh University. Additional electrokinetic soil

decontamination studies were performed at the Sandia National Laboratories in Albuquerque, New Mexico (Summer 1993).

Decontamination experiments were performed to test the removal of target PAHs from artificially contaminated soil samples and from soil samples collected from the subsurface at the MGP site. Experimentation times ranged from 24 hours for the artificially contaminated soils, to up to eight weeks for the surfactant enhanced electrokinetic experiments. The physical phenomenon associated with electrokinetics were evaluated in this research with respect to their role in organic compound transport. Also the effects of adding a surfactant alone, and a surfactant with a co-surfactant to the contaminated clays was evaluated with respect to the electrokinetic processes.

CHAPTER 2

BACKGROUND

2.1 Development of Environmental Remediation Techniques for Organic Compounds in the Subsurface and Ground Water

The impact of surface water, soil and ground water contamination on environmental resources is becoming an increasingly difficult problem to manage. The increasing costs of litigation and the technical complexity of contaminant removal at hazardous waste sites is driving remediation costs skyward (Shineldecker 1992). A need for technically sound water and soil remedial options, which can be performed relatively safely (without additional environmental damage), economically, and in a timely fashion, is tantamount to the further development of remedial treatment options (Probstein 1991; Grube, et al. 1992; U.S. EPA 1988).

Physical and chemical soil and ground water remedial treatment methods depend both on the contaminant and the soil and ground water matrix (Sawyer et al. 1978). The adsorption capacity of the soil for the contaminant depends largely on the contaminant's solubility, the octanol-water partition coefficient (K_{ow}), and the chemical structure of the contaminant Krauskopf, et al. 1979; Knox, et al. 1993). Additionally, the contaminant may undergo volatilization, biological degradation, hydrolysis, oxidation and reduction, and dehalogenation. The higher the K_{ow}, the more likely the contaminant will adsorb to soils. The chemical

structure and net electric charge determines the contaminant's polarity and physical size, thus defining whether or not the species is able to bind to the soil matrix. These factors ultimately influence the contaminant's pathway of movement through the soil to the aquifer. Once the contaminant has reached the aquifer, the same physical and chemical parameters affect the species movement in the aquifer in addition to the aquifer's chemical and physical parameters (Lyman, et al. 1990).

Pure compound recovery is only possible when the contaminant is not entirely soluble in the aqueous phase, or the concentration of the contaminant exceeds the aqueous saturation point causing phase separate hydrocarbon (PSH) accumulation. If the organic compound is in solution, then the technique of pure compound recovery will not be a viable remedial technology. If the compound is not soluble in water, then the relative position of the compound will depend on it's density relative to the water. Compounds whose specific gravity are greater than 1.0 (assuming water is the benchmark at 1.0) will sink through the aquifer; this group of compounds is commonly referred to as dense non-aqueous phase liquids (DNAPLs). Compounds whose specific gravity are less than 1.0 will float on top of the water table's surface; this group of compounds is commonly referred to as light non-aqueous phase liquids (LNAPLs) (Domenico, et al. 1990; Noonan, et al. 1990).

When volatile organic compounds (VOCs) are dissolved into the aqueous phase, aeration of the contaminated water is a method commonly used to remove those organic compounds. This technique relies on exposing the affected water to a contaminant free air supply. As the

air and water mix, the volatile compounds are stripped out of the aqueous phase, into the vapor phase, and scrubbed from the water. Common aeration technologies include slat tray aeration, diffused air aeration, spray aeration, cascade aeration, packed column aeration, and rotary stripper aeration. The key variables influencing the removal of VOCs from the aqueous phase are the Henry's Law constant and the overall mass transfer coefficient.

Some of the currently employed treatment and remediation technologies for soil impacted by organic contaminants are summarized below (Pignatello, et al. 1996; U.S. EPA 1985):

1. The use of granular activated carbon (GAC) adsorption is a well established treatment technology to remove organic compounds from the aqueous phase. Adsorption is the process in which liquid or gas molecules are attracted and held to the surface of a solid phase media. Physical adsorption refers to the attraction caused by the surface tension of a solid that causes organic compounds to be held to the surface of a solid phase media. Chemical adsorption refers to actual chemical bonding to a solid media's surface. Adsorption of organic compounds to GAC is of the physical nature. The advantages of this treatment technique is that carbon adsorption is very well suited to remove variable (low to high) dissolved phase concentrations of organic compounds from contaminated ground water.

2. Chemical oxidation of organic compounds found in ground water has been an effective treatment technology for hundreds of years. Oxidation involves the exchange of electrons between chemical species and subsequently effects a change in the oxidation number of the organic compound involved. Oxidation-reduction processes are referred to as redox reactions; one species gains electrons (reduced - valence state is reduced) while the concomitant species loses electrons (oxidized - valence state is increased). Oxygen (O_2), chlorine (Cl^-), ozone (O_3), and hydrogen peroxide (H_2O_2) are chemical oxidants commonly used to remove organic compounds from ground water.

3. Thermal oxidation, commonly referred to as incineration, is a treatment technique used to address both soil and ground water organic compound contamination. Incineration raises the temperature of the contaminant and the contaminated media (water or soil) in the presence of oxygen, to oxidize the organic contaminant to carbon dioxide (CO_2), water (H_2O), and ash.

4. Emerging treatment schemes such as solidification/vitrification, Bioremediation, dechlorination, soil washing, vapor extraction, thermal desorption, chemical treatments, and electrokinetic techniques all show promise in this expanding field of contaminant treatment. There does not appear to be one technology which is a preeminent technology in subsurface remediation. The individual technologies have limitations due to the soil matrix [fine grained versus coarse grained; ion exchange

capacity; total organic content (TOC); biological oxygen demand (BOD), etc.] and the hydraulic conductivity of the soil (degree of isotropy and homogeneity; permeabilities of layers and hydraulic accessibility).

2.2 The Coal Tar Environmental Problem

During the 1800s and into the early 1900s, coal was chemically altered for the production of gas for residential, commercial and industrial applications. The facilities producing the gas were known as Manufactured Gas Plants (MGP). Today many of these sites are the source of severe subsurface organic and inorganic chemical contamination. Wastes such as tars, ash and spent oxides were often left at the generation sites in lagoons, ponds, pits and lined and unlined vaults. Coal tars are a large portion of the hydrocarbon contamination found at these sites. It has been reported that more than 11 billion gallons of coal tar was produced in the United States during the late 1800s through the mid 1900s. Based on records accounting for the gas and the residual coal tar products, several billion gallons of coal tar material from the MGP facilities is missing (Pamukcu 1994).

Coal tars are a composite of many organic an inorganic compounds. Coal consists largely of the elements carbon, hydrogen and oxygen with small amounts of sulfur and other inorganic impurities. For purposes of energy analysis as a fuel, the contents of coal are given in terms of fixed carbon, volatile compounds and water. Coals are ranked by fuel ratio, which is the ratio of fixed carbon to volatile matter. Volatile compounds burn in the form of a gas and

produce a long smokey flame, whereas fixed carbon produces a short, hot, relatively smokeless flame. The lower ranking coals have a lower heating value than harder coals. Volatile compounds provide the gas for combustion in the lower ranking, softer coals.

Coal tars are composed mainly of PAHs, VOCs, phenolic compounds, and various inorganic compounds such as ammonia containing compounds, lead and cyanide. PAHs are the most dominant constituents of coal tars. Research in Environmental Toxicology has identified many of these compounds, which have been found in the soil and ground water near the former storage and disposal areas, as sources of human and environmental health risks.

PAH compounds are made up of successive aromatic ringed compounds. Generally, an increase in the number of aromatic rings in a chemical structure, and a corresponding increase in the compound's molecular weight will decrease the aqueous solubility of that compound. A decrease in the water solubility corresponds to an increase in the compound's octanol-water partition coefficient (K_{ow}). K_{ow} values for PAH compounds range from 2,500 for *naphthalene* to 6,300,000 for *benzo[ghi]perylene*. These values indicate that even the most water soluble PAH compound, *naphthalene*, would not be readily transported in the dissolved phase. Because of this physical characteristic (high K_{ow}), PAH compounds in ground water tend to partition and bind onto sediments, colloids and soil surfaces, rather than remain in the aqueous state. Significant volatilization of PAH compounds is unlikely to occur at ambient ground water and soil temperatures. PAHs are not easily bio-degraded and generally exhibit long food chain cycle lives.

The chemical composition of the residual coal tars is dependent on the composition of the parent coal, the type of process in which the coal gas was synthesized, and the gasification processing temperatures and operating parameters. Typical low molecular weight PAH compounds are: *Acenaphthene, Acenaphthylene, Anthracene, Fluorene, Naphthalene,* and *Phenanthrene.* Typical high molecular weight PAH compounds are: *Ben(a)pyrene, Benzo(b)fluoranthene, Benzo(k)fluoranthene, Benzo(g,h,i)perylene, Benzo(a)pyrene, Benzo(e)pyrene, Chrysene, Dibenz(a,h)anthracene,* and *Pyrene.* Another common constituent group of coal tars are the light aromatic compounds, such as *Benzene, Toluene* and *Xylene.* Generally, these chemicals are very water soluble and more mobile, and volatile. Inorganic constituents in coal tars range from trace amounts of metals, to cyanide and lead compounds. Coal tar contamination often exists in one, or a combination with one or more, of the following four fractions; 1) a solid or semi-solid fraction; 2) a lighter than water fraction (LNAPL); 3) a denser than water fraction (DNAPL); and, 4) a water soluble fraction (Jackman, et al. 1991; Pamukcu 1994; Sabatini, et al. 1991).

2.2.1 Applications for Soil and Ground Water Remediation

The electrokinetic technology is emerging as a viable alternative soil remediation technique. The technology has performed well on the bench and pilot scale, in removing inorganic and organic compounds from fine grained materials including sludge, fly ash, mine tailings, soil, and ground water Aiken, et al.1985; Alshawabkeh 1996; Shapiro, et al 1989; Shapiro 1990; Yin, et al. 1995).

2.3 The History and Development of Electrokinetics

The electrokinetic phenomenon was recognized in 1808 by Reuss, and expanded on by Helmholtz in 1879, by Pellat in 1904 and by Smoluchowski in 1921. The theory of electrokinetics was presented as the Helmholtz-Smoluchowski theory, which correlates electroosmotic velocity of a fluid with a defined viscosity and dielectric constant, through a surface charged medium with a determined zeta potential, under an electric gradient. Speigler contributed to the understanding of electrokinetics by evaluating the interactions of the mobile components of soil, water and ions, with each other and the frictional (shear) forces along the pore walls of the matrix. He theorized that the true electroosmotic flow was expressed as the difference between the measured water transport and the ion hydration in moles per Faraday.

2.3.1 Theoretical Development

Electrokinetics is a technique which involves the desorption of the contaminant (inorganic or organic) from a soil matrix, the transport of the contaminant through the matrix and the subsequent concentration of the contaminant in an area accessible for further treatment. The discovery of the electrokinetic phenomena is credited to Reuss during the early 1800s. He reported that when two reservoirs filled with water were bridged with a wet clay, and a direct electrical current (DC) was applied across the cell, water moved from the anode to the cathode, clouding the water in the anode chamber. The cloudiness was due to OH^- anions migrating toward the anode, reacting with available cations to form hydroxides (most of

which are white and relatively insoluble in water) and precipitate in the anode reservoir. Helmholtz developed an equation to describe electroosmotic velocities, which was modified by Schmoluchowski to apply to electrophoretic velocities, referred to as the Helmholtz-Smoluchowski equation.

Napier discriminated between the electrolytic process used for electrolysis and the electroosmotic process related to water movement through the soil matrix. Wiedemann demonstrated that the volume of fluid electrically transported through porous media was directly proportional to the applied current. He also reasoned that the weight of fluid to current ratio was inversely proportional to the to the electrical conductivity of the fluid medium. Further, Wiedemann reported that the manomeric pressure (gas pressure) was proportional to the current density, the thickness of the wall and the specific resistance of the fluid, and is inversely proportional to the cross sectional area of a cell. Quicke proposed that the reverse phenomenon of electroosmosis would give rise to the electric potential across the cell. He also reported that for a given electrical gradient across a cell, the increase in elevation of the manomeric fluid at the cathode was in fact proportional to the square of the radius of the cell's internal capillaries.

More recently, investigators such as Acar, Lingren, Pamukcu, Probstein, Shapiro, Wittle, and others have applied the electrokinetic processes to transport and ultimately remove inorganic and limited organic compounds from fine grained soils.

2.3.2 Applications in Civil Engineering

Investigators of the electrokinetic technique point to possible engineering applications the process (Cabera-Guzman, et al. 1990; Casagrande 1953):

- Soil Stability During Excavations
- Stabilization of Foundation Soils
- De-watering Dredged material
- De-watering Mill Tailings
- Damp Proofing Foundations
- Decreasing Pile Penetration Resistance
- Increasing Petroleum Production Rates
- Corrosion Control of Concrete Bridges
- Soil and Ground Water Treatment
- Chemical Grout Injections
- Filtration of Materials
- Removing Salts from Soils
- Mining Metals from the Ocean Floors
- Ground Water and Soil Barriers
- Consolidation Tests
- Measuring Pore Water Pressure
- Movement of Nutrients and Microorganisms to Specific Sites in the Subsurface

2.4 The Electrokinetic Process

The application of a DC Voltage in a wetted, porous medium leads to three transport phenomenon: (1) **Electrolytic migration**, (2) **Electrophoresis**, and (3) **Electroosmosis**. Ionic species will migrate through the soil water system toward an oppositely charged electrode by the electromigration process (Kuo, et al. 1996; Lingren, et al. 1991). The electrophoretic process is similar to electromigration in that particles or colloids migrate under the applied current toward the oppositely charged electrode. Electroosmosis is the bulk flow of pore water from one electrode toward the other. This phenomenon is the result of

a stationary soil phase having an electrical double layer of ions migrating toward the oppositely charged electrode thereby physically flushing the pore fluid through the soil matrix. This causes a dragging effect within the soil matrix, further enhancing species removal from the soil (Adamson, 1990).

The combination of these electrochemical phenomenon leads to the removal of ionic, charged and uncharged species from the contaminated soil-water system. The direction and migration rate of the "contaminant" species is determined by the magnitude and polarity of the charge on the species, the concentration of the species in the pore water and the concentration of the contaminant which is sorbed to the soil, the voltage gradient applied across the soil-water system, the electroosmotic flow velocity, and the pH gradient across the soil-water system. The electrokinetic process has been successfully applied in the laboratory for ionic species and compounds with a net charge. This research was intended to test the electrokinetic phenomenon on organic compounds with no net charge.

2.5 Fundamental Concepts

Electrokinetics as it applies to the remediation of hazardous waste sites, is a potentially powerful in-situ tool to efficiently move contaminants through soils and ground water (Banarjee, et al. 1988; Casagrande 1939; Kahn 1989; Pamukcu 1991).

2.5.1 The Electrokinetic Double Layer

The Electrokinetic double layer is a physical characteristic of the porous medium (soil) used in this research. The double layer is the region near the surface of a pore wall where the pore fluid possesses a charge equal to but opposite in sign of that charge which is inherent to the surface of the porous media.

To understand electrokinetic movement, one needs to understand the concept of the Electric Double Layer as the theory relates to the charged surface of soil, in this case clay. Clay consists of a group of minerals known as clay minerals. They are all essentially hydrous aluminum silicates. In some, magnesium (Mg) or iron (Fe) substitute in part for aluminum (Al). Alkalies or alkane earths may be present as essential constituents (Hurlbut, et al. 1977). If we hold to the tenant that a clay surface carries a negative charge, positively charged ions, or cations, are attracted to the surface of the particle. Helmholtz and Shapiro suggested that counter-ions are attracted from the surrounding pore water solution to the particle surface to maintain electro-neutrality, that is counter the existing charges without additional free charges. Helmholtz's theory included the assumption that this formed a monolayer on the surface of the particle. Guoy-Chapman modified this assumption to include in the model, Brownian motion of ions, which would result in a distribution of ions in a random cloud around the particle's surface, rather than the monolayer assumption. This layer of distributed ions is what is commonly referred to as the electric double layer (Figure 2). Stern (1924) presented a theory which includes a monolayer acting as the counter ions to the particle's

charged surface (the Stern layer) surrounded by a cloud of ions in a diffused double layer (Guoy Chapman layer). It is assumed that the diffuse double layer provides the ions for electroosmotic flow through the soil system (Thompson 1992).

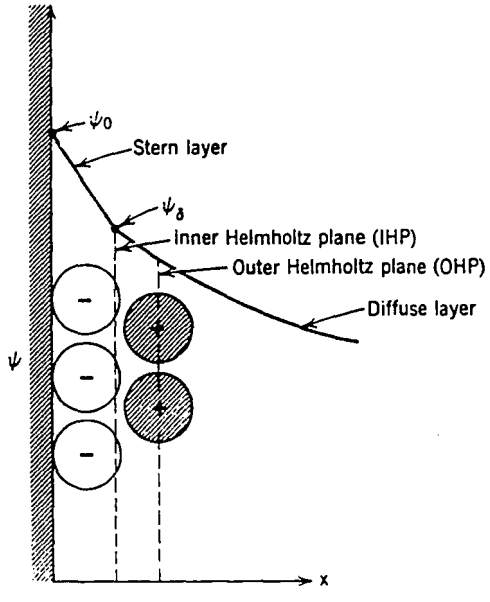

Figure 2: Stern Double Layer

The applied electric field causes a force to be exerted on the fluid in the double layer, causing movement parallel to the direction of the electric field's stream lines. This movement of fluid causes a viscous gradient to be developed within the cell, which is responsible for the movement or dragging of fluids and compounds not directly entrained within the primary fluid.

2.5.2 Electroosmosis

Electroosmosis is the movement of water from one electrode to another electrode, as the result of an applied electric field gradient (Fleureau, et al. 1988). As previously described, clay particles carry a negative charge, which attracts cations from the pore fluid, creating the electric double layer. When an electrical field is applied to the system, the cations in the diffuse double layer are attracted to the cathode, whereas the anions are attracted to the anode. The clay particles, being negatively charged are also attracted to the anode. Because the clay particles are immobile, the ions in the double layer are able to migrate. Therefore the cations are mobilized toward the cathode, dragging the fluid in the pores toward the cathode. Anions are mobilized toward the anode, also carrying pore fluid. But the cations (specifically H^+ ions) appear to migrate more quickly than the anions (specifically OH^-) migrate, therefore creating an overall electroosmotic movement from the anode to the cathode. It is postulated that the movement of ions is not a free stream of ions, but rather the exchanging of an ion with a similar ion on the down gradient side of the flow. Additionally, H^+ is a strong cation exchanger, and therefore will tend to replace the cations in the diffuse double layer and on the surface of the soil particles, further enhancing movement in the pore fluid.

In the dissociation of water, $H_2O = H^+ + OH^-$, the hydrogen ion's migration velocity is greater than the hydroxide ion. Though the reasons for this greater velocity are numerous, the cause may be dominated by the size of the molecule and the ease in which the H^+ ion spring boards itself to the next bonding site, pushing the formerly occupied H^+ ion to the next

down gradient binding site. The OH^- ion is larger and does not have the ability to displace and push molecules as efficiently as the H^+ ion, therefore causing the movement of the liquid phase toward the cathode. The ion migration causes an electron gradient to be developed within the immediate vicinity of the ion movement, causing the dragging of the pore fluid. This is "electroosmotic flow". If the double layer was reversed with respect to charge, (the surface of the stationary media held a net positive charge) and the double layer had a net negative charge, the electroosmotic flow would be toward the anode.

2.5.3 Electrophoresis

Electrophoresis is the migration of charged colloids or particles toward the oppositely charged electrode, as result of the application of an electric gradient (Fleureau, et al. 1988).

2.5.4 Electrolysis and Electromigration

Electrolysis is the oxidation and reduction of water (H_20), as a result of an applied external current, into $O_2(g)$, $H^+(aq)$, $H_2(g)$, and $OH^-(aq)$, respectively. As previously described, it is assumed that this is the predominant force causing the movement of contaminants within the soil-water system. The chemical reactions involved in electrolysis are:

$$2H_2O - 4e^- = O_2 + 4H^+ \text{ (oxidation at the Anode)}$$

$$4H_20 + 4e^- = H_2 + 4OH^- \text{ (reduction at the Cathode)}$$

At the anode, H^+ is evolved, causing the acidification of the pore fluid in the immediate vicinity of the anode, and the propagation of an acidic front toward the cathode. At the cathode, OH^- is liberated, causing the development of an alkaline front in the immediate vicinity of the cathode, and the propagation of alkaline front toward the anode.

Electromigration is defined as the ion migration in response to an applied electric field. The ions which contribute to electromigration are present in the diffuse double layer as counter-ions and co-ions, and as free-ions in the pore fluid. The soil medium will act as a conductor for the movement of the ions toward their oppositely charged electrodes. The flow is based on the concentration of the ions present and the characteristics of the soil matrix. The electrical gradient generated across the soil matrix depends on the conductivity of that matrix and the concentration of ions within the pore fluid and the double layer. As the conductivity increases, electroosmotic flow decreases as a result of the decrease in the electrical potential gradient. Because of this, the increase in the concentration of ions in the pore fluid will cause a decrease in electroosmotic flow.

Due to the electrolysis of the water, the electrolyte concentration within the pore water will increase resulting in an increase in conductivity in the immediate vicinity of the anode region. As the H^+ ion front propagates toward the cathode, causing saturation of the pore voids with ions which causes the formation of the electron rich double layer, the conductivity in the cathode region and the propagated front increases by an order of magnitude higher than the H^+ front alone. The fact that the H^+ ions bind preferentially to the clay soil matrix causes the

increase in conductivity. As the H^+ front approaches the advancing OH front, water molecules are formed, causing a decrease in the bulk ion concentration in the pore fluid and the double layer in the vicinity of the cathode. A direct consequence of this phenomenon is the decrease in electroosmotic flow in the vicinity of the anode and a subsequent increase in the osmotic flow in the cathode region. Another consequence is the increase in electrical gradients leading to an increase in the electrical potential difference across the electrodes (Adamson 1990; Pamukcu 1994).

2.5.5 Diffusion

It should also be noted that diffusion plays a role in the movement of these organic compounds in the soil-water matrix (Brusseau 1992; Rao 1990). Diffusion will occur as a result of an initial concentration gradient, and then as a result of the contaminant concentration gradient, as the contaminant's leading edge moves toward the respective electrode. As the leading edge advances due to the electroosmotic flow, the trailing edge will, due to diffusion, move in the opposite direction. As that edge's concentration drops lower than before, the conductivity decreases which effectively causes an increase in osmotic flow in that micro-region. This increases the flow toward the advancing front; as the concentration in the trailing edge increases, the osmotic flow drops off, diffusion away from the bulk flow occurs, and the process repeats itself.

2.6 Contaminant Transport

Solutes move with soil water, and within the soil water in response to contaminant concentration gradients. In addition to water movement, contaminants (solutes) interact with the soil matrix in a continuous dynamic of interrelated physical and chemical processes. These interactions involve variables such as acidity, temperature, oxidation-reduction potential (ORP), composition and concentration of the soil solution. Rao (1990) described the difference between sorption related non-equilibrium and transport related non-equilibrium. Sorption related non-equilibrium includes Vacarri's (1988) kinetic and mass transfer models into one group. Transport related non-equilibria is stated as being more appropriate for non-heterogeneous systems (field conditions). In this case, the rate of mass sorbed and desorbed from a fixed media (soil matrix) is limited to diffusion, a relatively slow process compared to the convective transport occurring at and through the macro pores. Brusseau (1992) stated that the transport related non-equilibrium is relatively unimportant in homogeneous laboratory type systems. Retarded intra-particle and/or intra-organic matter diffusion is more likely to occur and be the driving force behind contaminant non-equilibrium in such systems. Ahlert's (1989) work supports this hypothesis. In considering solute movement, three mechanisms are commonly discussed; convective transport, diffusion of solutes, and hydrodynamic dispersion (Butcher, et al. 1989; Freeze and Cherry 1979; Rieger 1987; Wilkowe 1992).

The mass flow or convective transport of soil water can be described as Darcian flow, where the convective flux of solutes J_c is proportional to their concentration c, as defined in the following equation (Equation 1):

$$J_c = qc = -c(KdH/dx)$$

where $q = -K\, dh/dx$ is Darcy's law which mathematically describes ground water flow, q is the volume of liquid flowing through a unit area, perpendicular to the direction of flow per unit time, and c is the mass of solute per unit volume of solution; J_c is defined in terms of mass of solute passing through a unit cross-sectional area of a soil matrix per unit time (Hillel, 1980).

To estimate the travel distance of solute per unit time, the average apparent velocity v of the flowing solution is defined by the following equation (Equation 2):

$$v = q/\Theta$$

where Θ is the volumetric wetness, and v is given as the straight line length of path traversed within the matrix per unit time. Realizing that the term v does not take into account anisotropic conditions or at the least tortuosity, v as defined is an approximation. Therefore the following equation (Equation 3) is given:

$$J_c = v\Theta c$$

To develop an equation for the average distance L_t of convective transport per unit time t, the following equations lead to the desired convective transport equation (Equation 4):

$$t_r = L/v$$

where t_r is the average residence time within a layer of soil of thickness L. If the flow is not dependent on forces other than gravity, for purposes of this development one can assume that the movement of liquid is dependent on the hydraulic conductivity K of the matrix which is in turn dependent on the wetness Θ of the matrix.

Therefore, the following equation is presented (Equation 5):

$$q = K(\Theta)$$

and manipulating $v = q/\Theta$ with $t_r = L/v$, the following equation develops (Equation 6):

$$t_r = L\Theta/K(\Theta)$$

Equation 7 for average convective distance follows:

$$L_t = tK(\Theta)/\Theta$$

Diffusion processes occur within the gas and liquid phases due to Brownian motion and random collisions and deflections of the molecules within the fluid. The result is the tendency to equilibrate the distribution of diffusible components in any multi-component system (Freeze and Cherry, 1979; Hillel, 1980).

If solutes in a multi-component fluid begin in disequilibrium, the components will tend to diffuse from a higher concentration to a lower concentration to achieve phase equilibrium. Because of this, diffusion is very important for solutes in the liquid phase diffusing into the solid phase.

Beginning with solutes which are not in equilibrium with a solution, concentration gradients will exist with the solute tending to diffuse from areas of higher concentration to the lower concentration solution.

For an uncontaminated volume of water, the rate of diffusion into the bulk water, J_d can be related by Fick's Law to the concentration c as (Equation 8):

$$J_d = -D_o \, dc/dx$$

where D_o is the diffusion coefficient for the solute diffusing in bulk water, and dc/dx is the concentration gradient.

In general, the diffusion of a solute into the liquid phase of a saturated soil is less than the diffusion of the solute into bulk water. This is because the maximum liquid phase content in a soil matrix is equal to the porosity of the soil. The soil's pore passages are tortuous, so the path length of diffusion is greater than a bulk water's physically unrestricted length. In an unsaturated soil, the soil wetness is decreased and the path length increases.

Considering only the water volume Θ and the tortuosity ζ of the soil matrix, the diffusion coefficient in soil D_s could be defined by the following equation (Equation 9):

$$D_s = D_o \Theta \zeta$$

Tortuosity, ζ, is defined as the ratio of the straight line length of a soil sample to the average circuitous path length through the soil's voids which molecules and ions travel. Generally, tortuosity decreases with decreasing water volume (Θ). Based on this relationship, the diffusion coefficient in soil, D_s, multiplied by the fractional water volume, Θ, is equal to the solute's diffusion coefficient in bulk water, D_o. This is expressed in Equation 10:

$$D_o = D_s(\Theta)$$

Based on this mathematical reasoning, the rate of liquid phase diffusion in an unsaturated soil may be written as Equation 11:

$$J_d = -D_s(\Theta)dc/dx$$

It should be noted that over time (travel distance), the concentration of solute available to diffuse into a liquid or onto a solid phase decreases, based on the corresponding decrease in available solute concentration. This is written as Fick's second law (Equation 12):

$$\partial c/\partial t = D_s \partial^2 c/\partial x^2$$

Describing the diffusion of solutes in the soil water is complicated by factors not described in the previously described equations. The soil matrix varies in space and in time. Solutes interact with and may modify the soil's physical and chemical properties. This may modify the pore structure and vary the tortuosity of the path way. Different contaminants in the solute phase may interact with each other, and with those in the adsorbed phase. The convective flow of the solution and the solute may affect the diffusion process by changing the distribution of solutes and by inducing hydrodynamic dispersion.

Hydrodynamic dispersion is the motion of a heterogeneous fluid in a porous body, in which the initially heterogeneous solution mixes and eventually reaches equilibrium between the different portions of the flowing solutions. Some portions of a flowing solution move more

quickly than other portions which cause an incoming solution to mix with or disperse within an antecedent solution. The degree of mixing depends on such parameters as average flow velocity, pore-size distribution, degree of saturation, and concentration gradients. When convective velocity is great enough, the effect of hydrodynamic dispersion can greatly exceed that of molecular diffusion, and the latter can be neglected in the analysis of solute movement. Conversely, when a soil fluid is at rest, hydrodynamic dispersion is not a component of mixing and contaminant transport (Hillel, 1980).

Empirically, hydrodynamic dispersion depends directly on the average flow velocity. Thee dispersion coefficient is mathematically defined in Equation 13:

$$D_h = av$$

where D_h is a dispersion coefficient, v is the average velocity, and a is an empirically derived parameter.

The diffusion and dispersion terms are often added to describe a diffusion-dispersion coefficient, D_{sh}. The diffusion-dispersion coefficient is a function of the water volume Θ and the average velocity v (Equation 14):

$$D_{sh}(\Theta,v) = D_s(\Theta) + D_h(v)$$

The three mechanisms convection, diffusion, and hydrodynamic dispersion can be combined to define a total solute flux term.

The total solute flux equation can be further simplified by combining the diffusion and hydrodynamic dispersion terms as (Equation 15):

$$J_t = v\Theta c - D_{sh}(\Theta,v)dc/dx$$

where J_t is the total mass of solute transported across a unit cross-sectional area of soil per unit time (D_{sh} is the diffusion-dispersion coefficient, v is the average pore-water velocity, Θ is the volumetric wetness, c is the solute concentration, and dc/dx is the solute gradient). The preceding total solute flux equation is limited to steady state processes.

A transient-state process where fluxes and concentrations vary in time and space is defined in Equation 16 as:

$$\partial(c\Theta)/\partial t = -\partial J/\partial x$$

2.7 Contaminant Transport by Electrokinetics

Organic contaminant transport processes in soils under electric fields is accomplished by diffusion, electroosmosis, electromigration, and electrophoresis. Many factors determine the relative contribution of the aforementioned processes to movement of contaminant species. Those factors include the soil matrix's mineralogy, permeant fluid chemical composition and degree of conductivity, introduced chemical species in the pore fluid, and the geotechnical parameters of the soil matrix (permeability, ion exchange potential, available pore size, tortuosity). The transport mechanisms are countered by sorption processes in the soil, precipitation and dissolution, and other aqueous phase reactions in the pore water. The technique has been successfully demonstrated to transport the organic species phenol, acetic acid, hexachlorobutadiene, and hexachlorobenzene in both enhanced and unenhanced bench-scale experiments (Shapiro et al. 1989; Acar et al. 1992; Acar et al. 1993; Shapiro and Probstein 1993; Whittle and Pamukcu 1993).

In the case of the unenhanced transport of the PAHs through a clay matrix, electroosmosis appears to be the major transport mechanism, with electromigration being the minor contributing mechanism (Acar et al. 1989; Pamukcu 1993). Electrophoresis, which is the transport of charged particles due to an electric field, becomes significant in electrokinetics when surfactants are introduced. The relative contribution of electroosmosis is often maximized when the matrix is a low activity clay having a high moisture content.

Changes in the soil electrochemistry in the test cell will result in vary chemical reactions, including the solubilization and subsequent precipitation of salts and minerals. Chemical species transport in the pore water fluid is influenced by the dissolution of minerals and the formation of new precipitates (Hamed et al. 1991).

The advancement of the acid front (from anode to cathode) is expected to cause the solution of most of the encountered precipitates through the soil test cell. The base front generated at the cathode will cause the precipitation of sodium and aluminum hydroxides commonly associated with clay soils.

2.8 Surfactant Enhanced Contaminant Transport

With respect to the removal of the target organic compounds from the test cell soils, the electrokinetic process relies primarily on electroosmosis, and to a lesser degree electromigration, to remove the organic contaminants. A surfactant (surface active agent) controls both surface charge and the hydrophobic-hydrophilic nature of a surface. When the surfactant sodium dodecyl sulfate is used in electrokinetic applications, the effect of inter-particle interactions and surface charge are of key interest Gabr, et al. 1995). The subsequent balance between the hydrophobic and hydrophilic nature of the surfactant represents the component necessary to enhance organic contaminant movement through the soil cell. In aqueous systems there exists two predominant mechanisms for surfactant adsorption: hydrophobic interaction and ionic interactions. On non-polar particle surfaces, adsorption

occurs by Van der Waals attraction of the non polar tails to the hydrophobic surface, forming a micelle. This causes the polar hydrophilic constituent to be oriented toward the aqueous phase. Hydrophilic surface adsorption occurs primarily by electrostatic interactions between the polar head group and the oppositely charged surface groups. Because of this, the surfactant molecule becomes oriented with the hydrophobic group toward the aqueous phase which causes the surface to become less wetted. Upon the saturation of the sites of the organic molecule, a micelle is formed. Micelle formation occurs above a critical concentration of surfactant monomers. This is referred to as the critical micelle concentration (CMC), which will vary for every surfactant/target organic system. A high CMC may cause precipitation of the surfactant, and will inhibit the effectiveness of the surfactant toward the removal of the target organic compounds. Also, surfactant selection for contaminant removal should consider the possibility that the surfactant will encapsulate organic compounds indigenous to the vadose zone. Multi-layer adsorption may occur at higher surfactant concentrations, akin to the electrical double layer previously discussed. The second multi-layer adsorbs through the Van der Waals forces based on the need for the hydrophobic tails of the micelle to be removed from the aqueous system. The encapsulated surface becomes the hydrophilic surface, with the polar group oriented toward the bulk phase, allowing removal from the system (Fountain, et al. 1992; Yoem, et al. 1995).

If the micelles are regarded as a separate phase, then adding excess solubilizate phase means that there are three phases present in the system. Although no gross phase separation can be observed in a surfactant enhanced system, techniques measuring light scattering in aqueous

systems suggest that the increase in light scattering is due to the formation of a colloidal phase. Explanations of this phenomenon indicate that in the region of the CMC aggregation, the long chain electrolytes begin to form charged units. The units are micelles. Micelles are often narrowly dispersed in size and often contain 50 to 100 monomer units. Micelles are charged if the monomer unit is an electrolyte, as is the case of sodium dodecyl sulfate. Since it is the long chain ion that aggregates while the opposite charged, the counterions, remain unaggregated. The presence of a large charge on the micelle is evident from their electrophoretic mobility. The net charge may be less than the degree of aggregation because, presumably, some of the counterions attach to the micelle, presumably as part of the Stern double layer (Adamson 1990).

The published work on the solubilization of relatively insoluble organic compounds is based on the phase separation model of the micelle. Solubilization has been treated as a partitioning of solubilizate molecules between a micellar phase and the intra-micellar bulk phase. The partition coefficient is usually defined as the ratio of the mole fraction of solubilizate in the micelles (molecules of solubilizate per micelle per total solubilizate plus surfactant molecules per micelle) to the concentration of solubilizate in the solution outside of the micelle. Presentations of the formation of micelles have previously been based on mass-action approaches (Moroi 1992). Solubilization has also been discussed with respect to the Gibbs phase rule (Adamson 1990).

The morphology of the micelle structure has been discussed and disputed by physical chemists; a clear picture of the shape of the colloid has not been definitively established. Hartley proposed a spherical shape while McBain has presented evidence that a lamellar form also exists. Nuclear Magnetic Resonance (NMR) studies indicate that a spherical lattice structure would allow the micelle to be encapsulated in a relatively fluid environment.

When a surfactant is added to the aqueous system, the extent that the organic will concentrate in the micelle is defined through the octanol-water partition coefficient (K_{ow}) of the target organic. The larger the K_{ow} of the organic contaminant, the greater the tendency of the organic compound to concentrate in the micellular envelope. In the saturated zone of the soil, the interface between the water and the organic contaminant-surfactant is characterized by the interfacial tension (IFT) which develops. The force which encapsulates the organic is dominated by capillarity (adhesive-cohesive force) which is proportional to the IFT at the water-organic interface. It has been postulated that in order to achieve optimal movement through the soil, the surfactant-organic micelle system needs to be compressed by the addition of a co-surfactant. The co-surfactant system used during this research was butanol. The co-surfactant compresses the micelle by binding the tails of the surfactant more tightly than allowed by surface charge interactions of a non co-surfactant system.

CHAPTER 3

MATERIALS AND METHODS

3.1 Sample Collection

The soil samples and coal tar colloidal suspension used for this research were collected from a former MGP facility, located in Champaign Urbana, Illinois during December of 1991. The sampling program was drafted to include areas of suspected heavy coal tar contamination and areas considered clean. These areas were identified in an Environmental Assessment report for the former MGP site in June, 1989, by John Mathes, Geotechnical Engineers of St. Louis, Missouri. During the initial (1989) field investigation, the geotechnical engineers and scientists evaluated the subsurface using field techniques common to environmental investigations. Ground water monitor wells were installed as soil cores were screened for relative levels of contamination. Screening was accomplished by visual inspection, an HNu photo ionization detector (PID), and by chemical laboratory evaluation of the soil samples. Upon completion of the monitor well installation, soil and ground water sampling and chemical evaluations, site maps presenting the suspected extent of the contamination, and characteristics of the contamination were prepared of the former MGP site. Based on the available information, a sampling grid was developed, and soil cores were retrieved via Shelby tubes for the electrokinetic experiments to evaluate the feasibility of applying this process to decontaminate the soil at the Champaign-Urbana site (Figure 3).

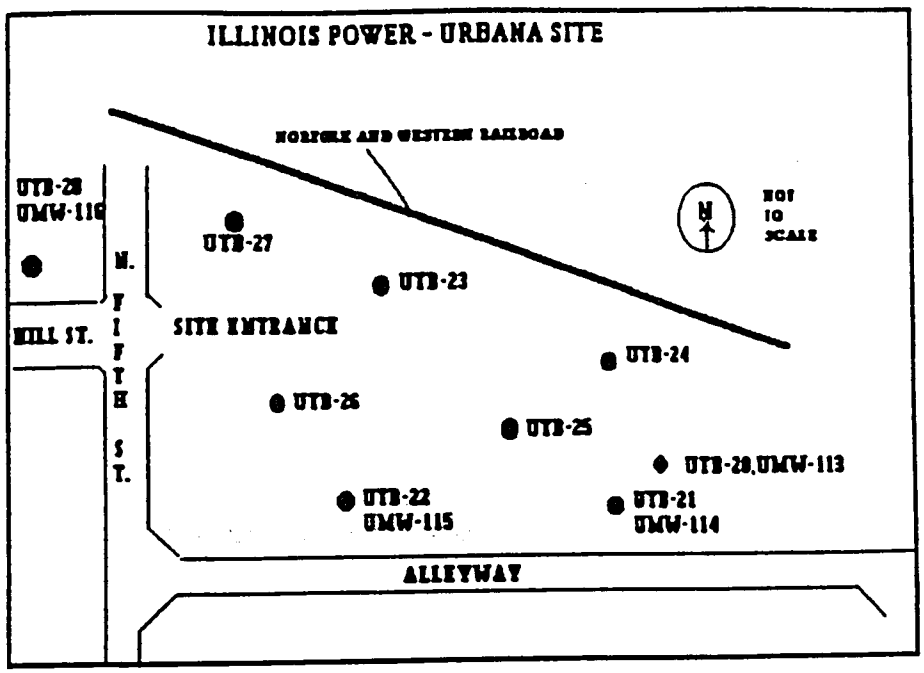

Figure 3: Sample Locations at the MGP Site

The soil core samples were retrieved in 7 centimeter (cm) inner diameter (ID), 76 cm long steel Shelby tubes. Soil cores were recovered at two foot intervals, at depth below ground surface (bgs) ranging from 8 to 10 feet bgs, 10 to 12 feet bgs, 18 to 20 feet bgs, and 20 to 22 feet bgs. The collected Shelby tubes were sealed with a paraffin wax on both ends, capped and taped to preserve the moisture content of the sample. The soil samples were shipped via overnight courier to Lehigh University and stored at 4 degrees centigrade (^{0}C) until the experiments began. To begin the experiments, the soil cores were removed from the chosen Shelby tube. To remove an undisturbed soil sample from the Shelby tube, two longitudinal cuts were made by a table saw fitted with a carborundum blade. Upon opening the Shelby tube, the soil core and steel tube were wrapped in aluminum foil, with the edges of the foil

taped to preserve the integrity of the sample until the electrokinetic testing process was initiated. The soil samples were stored after removal from the Shelby tubes and following the initiation of testing, at approximately 4 °C in one of Lehigh University's cold room refrigeration units.

3.2 Testing Program

The electrokinetic tests were performed in the Geotechnical Engineering Laboratory and in the Organic Chemistry Laboratories at Lehigh University. Physical parameters were evaluated in Lehigh's Department of Earth and Environmental Sciences Laboratories, and the Geotechnical Engineering Laboratory. The soil samples were stored and maintained at 4 °C in a walk in refrigeration unit located in Lehigh's Seeley G. Mudd Chemistry building. The electrokinetic testing apparatus was designed for and dedicated to this research. The initial chemical analyses were performed by Heritage Environmental Laboratories, Indianapolis, Indiana. As the research progressed, the chemical analyses were performed at Lehigh University's chemistry department gas chromatography facility. The initial research was carried out between 1992 and 1993.

3.2.1 Contaminants

Coal tar is a complex mixture of hydrocarbons. The constituents of coal tar and coal tar distillates are generally defined as coal, petroleum fuels, pitch, and solvents. The raw materials, intermediate products, final products, and waste products generated during the manufacture and use of manufactured gas are:

- Acetone
- Acridine
- Aniline
- Arsenic
- Creosote
- Cresol
- Lead
- Naphthalene
- Phenols
- PAHs
- Benzene
- Benzol
- Toluene
- Xylene
- Ethyl benzene

The target compounds analyzed for during this study were PAHs commonly associated with coal tar residuals. The specific PAH compounds analyzed for were *Naphthalene*, *Pyrene*, *Acenaphthene*, *Fluorene*, *Phenanthrene*, *Anthracene*, *Fluoranthene*, Benz(a)pyrene, *Benzo(a)anthracene*, *Benzo(b)fluoranthene*, *Benzo(g,h,i)perylene*, *Benzo(k)fluoranthene*, *Chrysene*, *Dibenzo(a,h)anthracene*, and *Indeno(1,2,3-c,d)pyrene* (Pamukcu 1994; Schwarzenbach, et al. 1993). The specific PAH compounds analyzed for are grouped into two categories; those which are deemed potentially carcinogenic and those which are not carcinogenic.

3.2.2 Testing Equipment

The electrokinetic testing equipment used for this study was designed based on previous working apparatus used in electrokinetic studies carried out at Lehigh University (Kahn, Pamukcu, et al. 1989). The testing apparatus consists of a two component system and an external power supply. The first component is the cell which houses the soil, the electrodes, porous frits to separate the soil from the electrode, anode and the cathode fluid reservoirs, and gas expulsion valves for the release and subsequent measurement of the gasses collected during the experimentation in the electrode chambers. The second component of the testing apparatus is a panel which holds two graduated burettes which feed the anode chamber of the cell system, and receive the effluent waters from the cathode chamber of the cell system. The cell and the panel were connected by chemical resistant Teflon™ tubing. The cell, manufactured by Ace Glass of Vineland, New Jersey, is constructed of Pyrex™ glass fitted with three sampling ports along the length of the tube. The reservoirs are connected to the feed burettes by chemical resistant Teflon adapters. Though Teflon is inert, it is porous and can harbor contaminants; this may have provided a sink for the contaminants during the testing procedure. The fluid reservoirs were also constructed of Pyrex, and fitted with an inlet and outlet port, a electrode connector port, and a gas expulsion port. The inlet and outlet ports were fitted with a glass and Teflon stopcock to allow flow control to the reservoirs when necessary. The expulsion port was initially fitted with a glass and Teflon stopcock to allow gas venting during the tests, but during the course of the research, stainless steel relief valves were used in lieu of the glass stopcock. The frits were a sintered glass frit

with a permeability of approximately 10^{-3} cm/sec. This is more permeable than the soil is considered to be (approximately 10^{-7} cm/sec), and therefore did not hinder the osmotic flows during this research. The electrodes used were constructed of carbon rods supplied by Carbone of America, Ultra Carbon Division, Bay City, Michigan. Stainless steel electrodes were tested during the course of the research, and were found to perform adequately. Due to the lower cost of the graphite electrodes, the graphite rods were chosen.

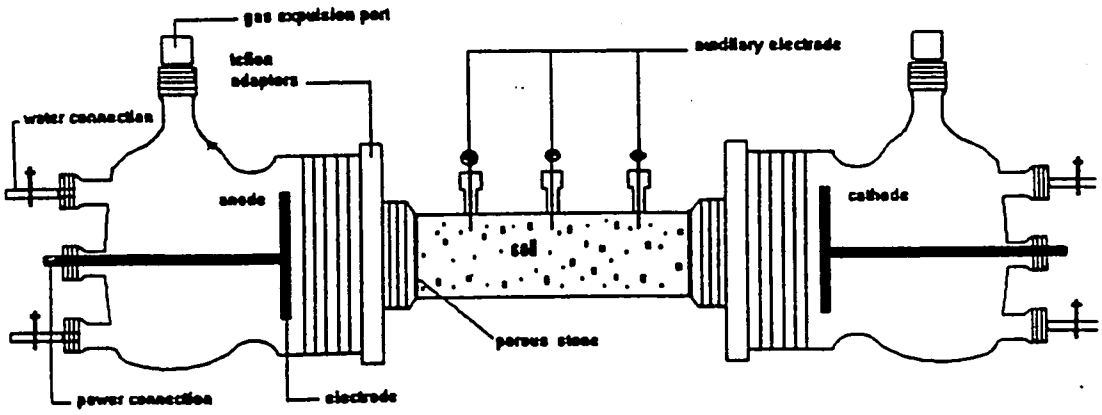

Figure 4: Electrokinetic Test Cell

3.2.3 Sample Preparation

Soil core samples were collected in Shelby tubes from the MGP facility, and held upright in a cooler at the site. Following the completion of the site sampling, the Shelby tubes were shipped by over night courier to the Fritz Engineering Laboratories at Lehigh University, where the samples were transferred to a refrigerated storage unit in the Mudd Chemistry building. The cold room maintained the soil samples at a constant temperature of 4°C. When the electrokinetic testing apparatus was being prepared, the selected Shelby tube was removed from the cold room, taken to the engineering machine shop, and opened. The tubes were opened by making two longitudinal cuts on opposite sides of the tube. Following opening of the tube, the sample was returned to the cold room for additional preparation. The soil sample was reviewed, and observations were noted. An approximate 12 cm section of visually homogeneous (soil type, color) soil was removed from the Shelby tube, trimmed, and pushed into the glass sample chamber. In an effort to maintain the soils' native, undisturbed status, handling and manipulation of the soil sample was minimized. Once the soil sample was inserted into the sample chamber, the sintered glass frits were placed in the recessed ends of the chamber. Following the frits, butadiene O-rings were placed on both ends of the Teflon coupler, and the coupler was attached to the sample chamber. The electrode chamber was fitted with the graphite electrode, which exited through the center of the end of the chamber, and sealed with a butadiene O-ring and a threaded Teflon fitting. The electrode chamber was attached to the soil sample chamber, and the four glass and Teflon stopcock valves were

installed on both ends of the electrode chambers. The three measuring ports on the dorsal side of the soil sample chamber were fitted with graphite sampling electrodes, and sealed with butadiene O-rings and threaded Teflon fittings (Figure 4). At this point in the sample apparatus preparation, the chamber was removed from the cold room to the testing laboratory to complete the sample testing set-up.

To complete the test cell set-up, the two electrode chambers of the electrokinetic cell were filled, by removing the chambers' valve, with the chosen permeant fluid, and sealed with the stopcock closed. The cell was then placed in a cradle to maintain the upright status of the cell and the electrical and fluid connections to the cell were completed. After the panel burettes were filled with the permeant fluid, the valves between the cell chamber and burette were opened, and the gas expulsion port on the chamber was bled to fully fill the chambers with the permeant fluid. Following this procedure, the burettes were filled to a starting volume, the volume was recorded, and the electrokinetic apparatus was ready for experimentation (Figure 5).

The permeant fluid used, unless otherwise noted, was a synthetic ground water solution based on United States Geological Survey (USGS) records (1989) of ground water from Jefferson County, Idaho, the constituents of which are given in Table 3-1.

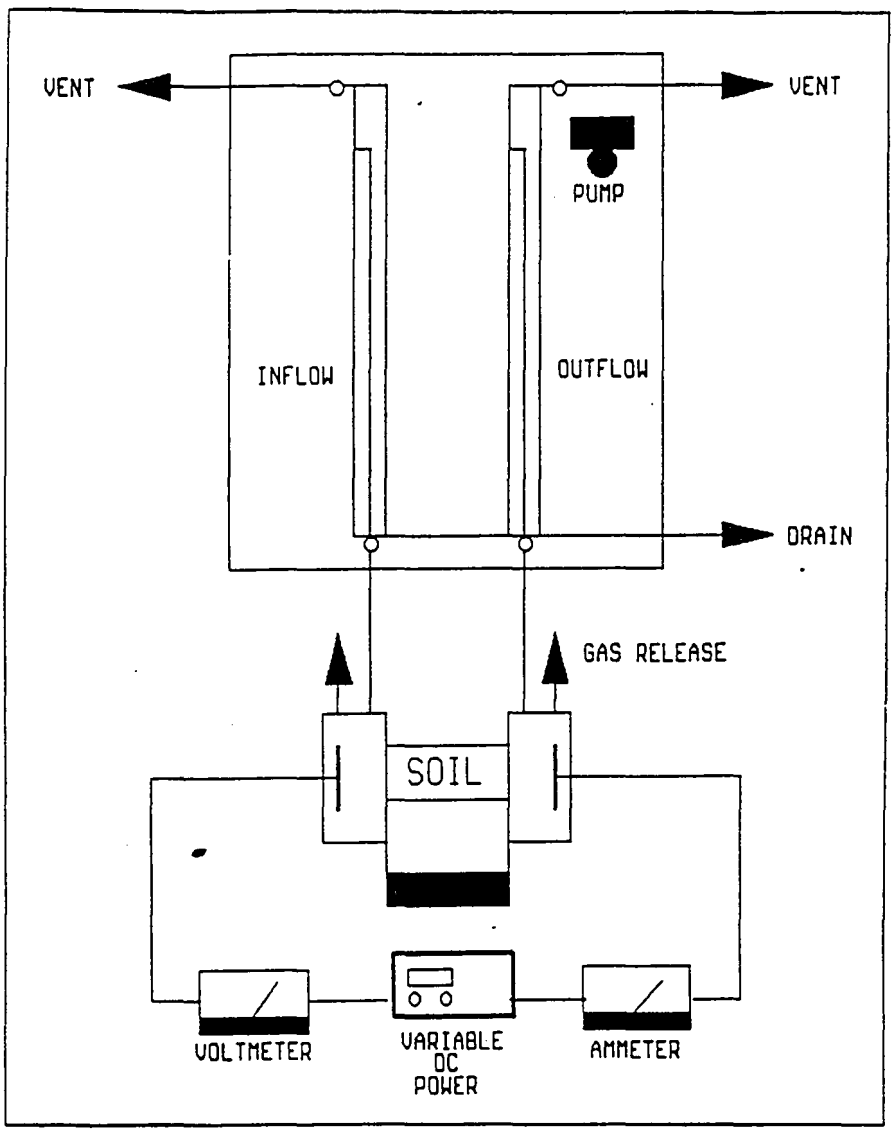

Figure 5: Schematic diagram of the Electrokinetic Test Apparatus

Table 3-1

Synthetic Ground Water Solution Constituents

Ground Water Constituent	Jefferson County, Idaho	Synthetic Ground Water
pH	7.69	7.90
Ca	46.75 mg/L	47.06 mg/L
Mg	13.9 mg/L	14.00 mg/L
Bicarbonate	212.5 mg/L	90.51 mg/L
Chloride	33.69 mg/L	83.43 mg/L
Sodium	31.88 mg/L	32.04 mg/L
Potassium	3.41 mg/L	3.51 mg/L
Sulfate	29.37 mg/L	55.34 mg/L
Fluoride	0.31 mg/L	--
Silica	28.75 mg/L	--Nitrogen, Nitrate 0.01 mg/L--
Nitrogen, NO_2 and NO_3	2.54 mg/L	--
Arsenic	1.87 ug/L	2.01 ug/L
Barium	55.38 ug/L	54.95 ug/L
Beryllium	0.5 ug/L	--
Cadmium	1.0 ug/L	0.98 ug/L
Strontium	173.75 ug/l	171.61 ug/L
Zinc	45 ug/L	173.66 ug/L

ug/L = micrograms per Liter

3.2.4 Testing Procedure

During the assemblage of the electrokinetic cell, the soil which was trimmed from the ends of the cell was collected and analyzed for geotechnical parameters. The parameters included: soil moisture content, mineral content, specific gravity, and particle size distribution.

Prior to the initiation of the electrokinetic testing, the trimmed soil samples were evaluated for the target PAH compound concentrations. These concentrations were recorded as the initial concentrations of each sample's PAH compounds.

The individual electrokinetic tests ranged from 2 to 4 weeks in duration. During the tests, fluid flow (volumetric decrease in the anode chamber burette; volumetric increase in the cathode chamber burette) measurements were recorded. The power source was maintained at a constant 30 Volts (V); the voltage drop across the cell and the current across the cell was recorded at regular intervals. The voltage through the soil cell was measured via the anode and cathode power connections; the voltage drop across the soil cell was measured via the dorsal mounted electrodes. Data was collected and recorded at the initiation of the experiment, and 15 minutes, 30 minutes, 60 minutes, and 120 minutes into the test. During the shorter experiments, data was further collected at intervals of 120 minutes and 180 minutes. During the longer experiments, data was collected, following the initial intervals then at 720 minute (12 hour) intervals. Permeation fluid generally moved from the anode burette, through the soil cell, and accumulated in the cathode burette. In addition to fluid movement, gas was generated at the anode and cathode, and was collected in their respective electrode chambers. The gas was expelled from the chambers, and the depleted burette was replenished of fluid, recording the volume of the added fluid. The fluid which was transported through the cell was collected for analysis; observations such as color, accumulation of precipitate, and the volume of the fluid was recorded.

Following the completion of the electrokinetic experiment, observations of the anode and cathode water were recorded (color, presence of sheen, odor). The pH of the anode and cathode waters were measured and recorded. The pH of the water was measured using a Beckman Digital pH meter, fitted with a standard probe. Samples of the anode and cathode fluids were collected and later analyzed for the targeted PAH compounds; the water samples were preserved by refrigeration at 4° C, and were analyzed within seven days of collection.

Observations of the soil were also collected and recorded. The soil was pressed out of the sample cell and cut into five sections. The pH of the soil sections were measured and recorded. The pH of the soil was measured using a Orion 91360 probe. The anode and cathode end, and the center soil samples were collected and refrigerated (unpreserved except for the lower temperatures), and analyzed for the targeted PAH compounds within seven days of sample collection.

3.2.5 Surfactant Addition

The use of a sodium dodecyl sulfate, an anionic surfactant, was investigated in this research. The surfactant was donated by the Union Carbide Chemicals and Plastics Company; there was no purity information supplied with the chemical, and it was used as it was received. The surfactant was added to the synthetic ground water solution to achieve a concentration of 1,000 milligrams per Liter (mg/L). This is above the critical micelle concentration (CMC) of approximately 500 mg/L. Two co-surfactants were tested during this work. Ethanol and

butanol were tested, separately, at a 20% volume of the co-surfactant to an 80% volume of the surfactant solution. Both the ethanol and butanol were supplied by The Fisher Scientific Company, and were 99.9% high performance liquid chromatography (HPLC) grade. This system was then added to the electrode chamber, and evaluated for PAH removal efficiency. The "system" used during the tests presented here were the surfactant sodium dodecyl sulfate (SDS) and the co-surfactant butanol. Based on the evaluation of the data presented in this thesis, the surfactant/synthetic ground water system was more effective in mobilizing the target PAH compounds than the ground water without surfactant. Also, the surfactant system alone was more effective in mobilizing the target organic compounds than the surfactant and co-surfactant ground water system.

3.3 Chemical Analyses

Soil and water samples collected prior to and following the electrokinetic testing were analyzed for target PAH compounds. Samples were analyzed at an independent laboratory (Heritage Laboratories, Inc.), and at Lehigh University Laboratories. The samples selected for chemical evaluation, qualitative level of contamination, pore volume flow (PVF), test duration, and general comments are outlined in Table 3-2.

3.3.1 Gas Chromatography

Gas Chromatography has developed into an extremely versatile instrument for selective and sensitive analysis of organic materials. This analytical technique has proven, since it's development in the early 1950s, to be successful for micrograms per Kilogram (ug/Kg) or microgram per Liter (ug/L) quantitative analysis of chemical compounds.

Gas Chromatography (GC) involves the vaporization of a liquid sample followed by the separation of the constituent gaseous components so those components can be qualitatively and quantitatively identified. The basic components of a GC are a source of carrier gas, a valving mechanism to control gas flow rate, an injection port for sample introduction, a chromatographic column, a heating and cooling mechanism to control the column's temperature, and a detector (Shiner, et al 1980).

The carrier gas source is an inert gas such as hydrogen, helium, or nitrogen which flows through the column at a constant flow rate. A sample of analyte in the liquid phase is

Table 3-2

Sample Identification and Observations

SAMPLE ID	CONTAMINATION	PORE VOLUME FLOW (PVF)	TEST DURATION (weeks)	COMMENTS
UTB-23-G1	Heavy	2.4	2	Oily Sheen in Cathode Water
UTB-23-G4	Heavy	5.8	3	Oily Sheen in Cathode Water; Tar residue in Cathode Frit
UTB-23-G5	Very Heavy	9.0	3	Control Specimen for UTB-23-S1.S2.S3
UTB-23-S1	Very Heavy	7.6	3	Surfactant used in Cathode Water
UTB-23-S2	Very Heavy	5.5	3	Surfactant and a co-surfactant in Cathode Water
UTB-23-S3	Very Heavy	8.0	3	Surfactant and a co-surfactant in Cathode Water
UTB-23-A2	Moderate	5.8	3	Surfactant injected into Cathode Water
UTB-23B-8/10	Light to Moderate	3.3	2	Oily Sheen in Cathode Water; High ionic content in Cathode Water; Constant Current Density
UTB-24T-10:12	Light to Moderate	4.3	2	Oily Sheen in Cathode Water; Constant Current Density

injected, via the injection port, and is flash vaporized. The analyte's constituents are converted into the gaseous state, entrained into the carrier gas (mobile phase) stream, and carried through the chromatographic column. The gaseous organic constituents travel through the column at differing rates, due to the compounds' affinity for the column (adsorption). Components of the sample are separated by their relative abilities to be adsorbed by the supported stationary phase. The presence of the individual components is detected (detector) and recorded when the components are swept to the end of the column by the carrier gas. Separation of the sample is a function of both the polarity and volatility of the samples' constituent components. Typical chromatographs from this study are found in Appendix A. The time which is required from injection to detection is referred to as the components retention time. The detector transmits a signal which is translated into a discernable electronic or physically measurable peak. The detector used in this study was a flame ionization detector (FID). The flame ionization detector measures sample content by burning the eluted sample in a hydrogen generated flame, and counting the ions which are produced.

In this study, an integrator collected the data and converted the resultant electronic counts into a measurable peak. The area under the peak is proportional to the concentration of the component in that sample. The detected compounds peak areas are compared to peak areas generated by known concentrations of known standard compounds. Qualitative and quantitative analysis is based on the comparisons of the library of known compounds and

concentrations with those peak signals of the unknown sample.

The analyses completed at the Lehigh University Laboratories were performed using a Hewlet Packard 5880A Series Gas Chromatograph, equipped with a 5880A series Gas Chromatograph (level four) terminal integrator. The column used during for the analyses was a 30 meters (m) long, 0.053 millimeters (mm) inner diameter (ID), 5 micrometer df column, Cross Bonded 100% Dimethyl Polysiloxane column [RTX-1, Restek, Inc., Bellefonte, Pennsylvania (Appendix A)].

3.3.2 Nuclear Magnetic Resonance

With respect to electrolyte solution investigations, Nuclear Magnetic Resonance (NMR) spectroscopy is a powerful analytical tool which can be used to investigate (1) the structure of organic molecules in solution, (2) the influence of a surface on the structure of solutions, (3) the dynamics of solutions, and (4) the permeability and pore geometry of porous media. During this investigation, NMR was used to confirm the movement of organic species through the soil matrix, by evaluating the spectra for the presence of aromatic (PAH) compounds.

Protons and electrons possess properties of spin. Both have two nuclear spin states, +1/2 and -1/2, which are degenerate or equal in energy. A proton has a spinning charge, with a magnetic moment coinciding with the axis of rotation. In the presence of an induced

magnetic field, the two nuclear spin states no longer have equal energy and are split. The state in which the nuclear magnetic moment is aligned with the magnetic field is a lower energy state than when the nuclear magnetic moment is opposing the magnetic field. The energy difference between the two states corresponds to the radio frequency region of the electromagnetic spectrum. A sample is placed in the presence of a magnetic field and causes spin splitting to occur. Based on Boltzman's distribution, 50% of the spins will be in a lower energy state and the remaining 50% of the spins will be in a the higher energy state. Upon application of a radio frequency (RF) signal, protons in the lower energy spin state gain sufficient energy to reach the higher energy spin state. As the excited protons return to their original spin state, the energy released during the relaxation is detected, and recorded (Silverstein, et al. 1981).

The NMR spectrometer used during this work used electromagnets which operated in a complementary manner; the source was maintained at a constant 60 megahertz (MHz) while the magnetic field strength was varied to allow the energy gap between the spin states to match that of the source.

Absorption of a specific frequency is governed by the characteristics of the sample. A plot of the frequencies of absorption peaks versus intensities is a NMR spectra. The difference in the absorption position of a particular proton to that of a reference proton [tetramethylsilane (TMS)] is referred to as the chemical shift. Different chemical environments for protons give rise to differing chemical shifts. Chemical shifts are typically

described by delta units as parts per million, or ppm.

What makes NMR spectroscopy an outstanding analytical tool for structure determination is that protons in different environments experience varying degrees of shielding, and have different chemical shifts. Shielding is defined by the organic compounds number of electrons which shield the bound proton from the induced magnetic field. Increased shielding requires a greater magnetic field to achieve resonance. Chemical shifts are the changes in the resonance position of a nucleus which is brought about by it's molecular environment. The nature of the bonding in the molecule affects the chemical shift.

During this work, NMR spectroscopy was used to analyze extracted soil samples to identify compound movement through the soil cell. Samples were collected prior to and following the application of the electrokinetic experiments.

CHAPTER 4

RESULTS

4.1 Introduction

The experiments performed to test and evaluate the theories presented herein were carried out from 1991 through 1993 at Lehigh University. The premise of the research was to evaluate the probability and subsequent efficacy to remove organic coal tar constituents from soil which was recovered from the Illinois Power - Champaign Urbana former MGP facility site. The primary soil matrix encountered in this study was clay, predominantly illite with kaolinite clays. Some medium to fine sands were also encountered in the collected soil samples [American Society for Testing Material (ASTM) guidelines]. The samples evaluated from the Illinois Power site (referred to as IP-Champaign Urbana) were collected in December 1991. The soil sampling locations were chosen by the consulting engineers for Illinois Power (John Mathes Consulting Geotechnical Engineers, Columbia, Missouri), Illinois Power Environmental Engineering personnel, and Dr. Sibel Pamukcu. Soil samples were collected at suspected or previously documented areas of significant coal tar contamination, of moderate contamination, and areas of the site which were deemed "clean". Additionally, coal tar emulsion was collected from an abandoned coal tar holding pit located on the IP-Champaign Urbana site. The experiments performed were modeled after the experimental techniques previously established at Lehigh University (Kahn, et al. 1989; Pamukcu 1991;

Pamukcu, et al. 1992; Pamukcu 1994).

4.2 General Discussions

The predominant mechanisms which mobilized the PAH compounds through the clay test chamber were electroosmosis and electrolytic migration. The target PAH compounds which were the least mobilized toward the cathode were the compounds with the greatest molecular weights. Separation occurred with the lowest molecular weight compounds apparently were mobilized toward the cathode, and the highest molecular weight compounds remaining at the cathode. PAH compounds with a mid range molecular weight were detected in the greatest concentration in the center of the test chamber. For example, the relatively low molecular weight *naphthalene* (MW = 128.2) was concentrated at the cathode section of the test cell while the highest molecular weight compound *dibenzo(ah)anthracene* (MW = 278.4) was concentrated in the anode portion of the test cell. A mid-range molecular weight PAH, *pyrene* (MW = 202), concentrated in the center of the test cell.

With the addition of the anionic surfactant to the cathode chamber, the major concentrations of the target PAH compounds were mobilized toward either the anode portion of the test cell or the cathode portion of the test cell, leaving the center of the chamber relatively target PAH compound free. The major concentration of the PAH compounds were mobilized toward the anode portion of the test cell.

The addition of the surfactant with the butanol cosurfactant into the cathode chamber caused the low molecular weight target PAH compounds to concentrate toward the cathode chamber. The higher molecular weight compounds tended to concentrate in the anode portion of the electrokinetic test cell. The mid range molecular weight compounds also tended to concentrate in the anode portion of the test cell. The surfactant with cosurfactant permeate did not remove the PAH compounds from the center portion of the test cell as the surfactant alone had.

4.3 Experimental Results

The soil core samples were retrieved from the MGP located in Champaign-Urbana, Illinois during December of 1991, in steel Shelby tubes. Following collection of the Shelby tubes, the ends of the tubes were sealed with a paraffin wax, supplied by Mathes Geotechnical Services, and shipped to Lehigh University's Geotechnical Laboratories. The contents of the Shelby tubes were analyzed in the Geosciences and Geotechnical Engineering Laboratories at Lehigh University.

The soil core from the bore hole labeled underground test boring - 23 (UTB-23) was found to be in primarily in the silt and clay size range, described as 70% to 90% passing through the #200 sieve. The mineralogy is dominated by illite clay, with quartz and some chlorite (Appendix B).

Clay minerals are phyllosilicates, which are silicates with continuous sheet structures like mica. The clays have a characteristic structure made up of alternating layers or sheets of two kinds. One sheet consists of the ions Al^{3+}, O^{2-}, and OH^-. The negative ions form an octahedra around the Al^{3+}, the relative numbers of O^{2-} and OH^- being adjusted to satisfy the valence of the entire structure; the O^{2-} and OH^- are shared between adjacent octahedra, so that the structure is continuous in two dimensions. The second kind of sheet is made up of Si^{4+}, O^{2-}, and OH^- ions. Each Si^{4+} is the center of a tetrahedron of oxygen ions. The tetrahedron all face the in same direction with the oxygens linked at their bases so as to forma hexagonal rings. This sheet is the tetrahedral sheet or the silica sheet of the clay structure.

Chemically, clay is best described as hydrous aluminum silicates. Many clays contain other metals in addition to aluminum, particularly magnesium and iron. Crude molecular formulas of the principal clays can be written as $H_4Al_2Si_2O_9$, which is Kaolinite, and $HAlSi_2O_6$, which is montmorillonite. One of the ions most firmly held by montmorillonite is potassium (K^+), which is a relatively large atom which fits well and is held strongly between the layers of the clay structure. Clays which are lacking a positive charge, due largely to substitution in the tetrahedral sheets hold the K^+ especially strongly, with the consequence that only part of it is replaceable by other ions. These clays, which are held together with successive K^+ ions are illite clays. Clays whose layers are held together by the attraction of K^+ for strong negative charges in the tetrahedron sheets. These three layered clays have a strong net negative charge, and can be pushed apart by adsorbed water (Krauskopf, 1979).

The soil core from bore hole UTB-24 was found to contain more granular material than UTB-23, with 10% to 20% passing through the #200 sieve. The mineralogy varies from that of UTB-23 in that there are more carbonate minerals in the 8 to 10 feet bgs section of the bore hole, and more quartz minerals in the 10 to 12 feet bgs section . The increased presence of quartz with increasing depth is supported by the decrease in clay and silt sized material with increasing depth.

Table 4-1

Soil Index Properties

Sample	Bulk Density (g/cm^3)	Average Bulk Density (g/cm^3)	Dry Density (g/cm^3)	Water Content + before EK Test (%) (1)	Water Content after EK Test (%)	Average Void Ratio (2)	Sat'd before EK Test (%)	Average Sat'd after EK Test (%) (3)
UTB-23-G1	1.83	–	1.42	28.5 *	30.1	0.77	92.5	99.9
UTB-23-G4	1.83	–	1.40	31.0 *	32.7	0.80	96.4	99.9
UTB-23-G5	1.70	–	1.39	22.0	29.3	0.84	67.8	87.2
UTB-23-S1	1.82	–	1.42	28.0	33.4	0.83	90.2	98.1
UTB-23-S2	1.67	–	1.26	32.4	43.1	1.07	80.8	98.2
UTB-23-S3	1.85	–	1.45	27.5 *	32.5	0.81	92.8	94.2
UTB-23-A2	1.79	1.12	1.26	41.7	35.5	1.00	99.9	92.9
UTB-24B-8/10	2.14	2.45	1.87	14.4	13.8	0.40	95.5	89.7
UTB-24T-10/12	2.09	2.27	1.83	14.4	14.2	0.44	88.2	82.5

- = Not evaluated

(1) = Water content by dry weight (Weight $_{(water)}$/Weight $_{(solids)}$

; (2) = Void Ratio = (Volume $_{(voids)}$/Volume $_{(solids)}$)

(3) = Based on average water content at the anode, center, and cathode locations

The average specific gravity of the UTB-23 soil sample was measured to be 2.54; the average specific gravity of the UTB-24 soil sample was measured to be 2.60. The measured index properties for the collected soil samples and the quantity of electrokinetically enhanced water flow through each test soil sample are provided in Table 4-1.

4.3.1 Electrical Potential Gradients and Flow

Throughout the tests, water flow was enhanced by electroosmosis, as evidenced by consistent water flow through the electrokinetic cells. Current efficiencies, defined as the quantity of water flow per unit of electrical charge [equal to the electricity transferred by a current of one ampere in one second (Coulomb)] generally remained constant through the cells. Following an initial spike of current flow through the cells, steady state flows were achieved.

4.3.2 pH Profiles

The pH distributions in the soil and the water chambers, following the electrokinetic tests exhibited a consistent pattern. Consistent soil pH gradients developed through the tests, and generally followed the pattern without deviance. The soil toward the anode section of the cell was generally in the pH range of 5 units, whereas the soil toward the cathode portion of the cell approached a pH of 10 units. The pH value trends in the aqueous chambers were consistent with the pH trends observed in the soil. The pH values in the anode chambers were consistently in the range of 2 to 3 units, whereas the pH in the cathode chamber ranged from

10 to 12 units.

4.3.3 Conductivity

The conductivity of the electrokinetic cell was measured in terms of a voltage drop, monitored between the anode and the cathode. The voltage drop and current were monitored between the ports located on the upper surface of the electrokinetic chamber (anode-P1, P1-P2, P2-P3, and P3-cathode). The voltage and measured current were used to compute the resistance in ohms, between the sections of the test soil. The figures found in Appendix C present the resistance developed in the test soils during the electrokinetic treatments.

The resistance was generally higher at the Anode to P1 interval, than in the other measured intervals. Both the anode to P1 and P3 to cathode intervals exhibited an initial "trough" of resistance, followed by a relaxation of the "trough" to a more constant value over a 24 to 48 hour test period. Overall, the resistance values within the test soil (P1-P2, P2-P3) fell into the 1 to 2 K-ohms range. An exception to this generalization was demonstrated by test soil UTB-23-A2, where the anode-P1 and P3-cathode interval resistances were effectively equal to or less than that within the soil chamber.

4.3.4 Energy Expenditure

During the electrokinetic tests, substantial pore volumes of water were moved through the soil chambers while generally constant current efficiencies were observed (Pamukcu 1994). The current variations and water flow through the test soil cells for samples UTB-23-8/10, UTB-24-8/10, and UTB-24-10/12 are presented in Appendix C. Water flow equilibrated in the majority of the soils during the experimental procedures. The center sections of sample UTB-23-8/10 did not achieve a steady state flow during the testing procedures. Non-steady state flow or unsaturated flow was exhibited in samples UTB-23-G4, G5, S1, S2, and S3. The total inflow and total outflow data are presented in Table 4-2 below.

During the electrokinetic tests, the current through the test cells was generally constant, baring the sample UTB-23-A2 (Pamukcu 1994). As shown in Appendix C, the current in sample UTB-23-A2 varied from approximately 11 mA to 2 mA. As presented in Table 4-1, the sample's soil index properties show that UTB-23-A2 had the greatest initial water content and a low dry bulk density. This suggests mineral dissolution which would provide a greater initial current; as the test proceeded, the concentration of ions decreased, the current decreased to a stable concentration. The average current density was calculated to be 0.34 mA/cm^2.

Table 4-2

Electrokinetic Flow Data for the Soil Samples

Sample ID	Volume of Inflow (cm^3)	Volume of Outflow (cm^3)	E-K Duration (hours)	Pore Volumes Flow (PVF)	Average Current (mA)	Average Current Density (mA/cm^2)
UTB-23-A1	170.4	153.0	512	4.6	2.85	0.3
UTB-23-G1	61.1	25.9	333	2.4	1.32	0.2
UTB-23-G4	149.2	36.2	559	5.8	2.72	0.5
UTB-23-G5	237.7	23.5	519	9.0	2.08	0.4
UTB-23-S1[1]	199.7	49.6	511	7.6	2.81	0.5
UTB-23-S2[2]	163.7	38.4	511	5.5	2.30	0.4
UTB-23-S3[3]	209.7	32.5	525	8.0	1.89	0.3
UTB-23-S4[4]	220.0	221.2	442	5.8	7.04	0.7
UTB-24T-8/10	95.9	81.6	333	4.5	2.69	0.3
UTB-24B-8/10	72.2	79.0	334	3.3	1.95	0.2
UTB-24T-10/12	99.5	87.9	352	4.3	3.05	0.3
UTB-24B-10/12	119.5	102.1	336	6.4	5.74	0.6

PVF = pore volume flow (Volume of Inflow)

Average current = Current averaged over the duration of Electrokinetic treatment

[1] = Anionic surfactant injected into the cathode chamber

[2] = Anionic surfactant and co-surfactant injected into the cathode chamber

[3] = Anionic surfactant and co-surfactant injected into the cathode chamber

[4] = Anionic surfactant injected into the anode chamber

The current efficiencies of the electrokinetic test cells, which is the unit of electric charge equal to the electricity transferred by a current of one ampere in one second (Coulomb), were calculated. Steady state current efficiencies indicate that the test samples reached equilibrium. A decrease in the current efficiency indicates that there has been an increase in the ionic strength of the pore water in the test sample, and that electromigration is strongly contributing to the electrokinetic flow through the sample. An increase in the current efficiency indicates the reverse, that the ionic strength in the pore water has decreased and the electrokinetic flow is dominated by electroosmosis.

Table 4-3

Electrokinetic Current Efficiency Data of the Field Soil Samples

Sample ID	Current Efficiency (M^{-1})	R^2	Geometric Average (M^{-1})	Arithmetic Average (M^{-1})
UTB-23-A1	74.7	0.98	139	154
UTB-23-G1	123.0	0.98	139	154
UTB-23-G4	92.7	0.99	139	154
UTB-23-G5	202.7	0.96	139	154
UTB-23-A5	44.6	0.98	44	44
UTB-23-S1	134.0	0.98	166	155
UTB-23-S2	122.7	0.97	166	155
UTB-23-S3	208.6	0.99	166	155
UTB-24T-8/10	149.2	0.99	111.5	114
UTB-24B-8/10	127.8	0.99	111.5	114
UTB-24T-10/12	106.0	0.99	111.5	114
UTB-24B-10/12	73.2	0.98	111.5	114

The average current efficiencies are presented above, in Table 4-3. The greatest current efficiency was demonstrated in the soil sample with the surfactant and co-surfactant introduced into the cathode chamber (UTB-23-S3). The lowest current efficiency was demonstrated in the soil sample with the ground water and surfactant enhancement introduced into the anode chamber (UTB-23-A2). The current efficiency values are presented as the pore volume fraction of inflow per moles of electrons transferred. The moles of electrons is the cumulative current multiplied by the elapsed time, divided by the Faraday constant [(*ampere x seconds*)/(*Coulomb/mole*).

The current efficiencies ranged from 166 Mole $^{-1}$ to 44 Mole $^{-1}$ for all of the specimens tested. There is not much difference between the UTB-23 samples that did not receive the surfactant enhancement, and the UTB-24 samples that also did not receive the surfactant enhancement. This figure shows that the data deviates from the straight line relationship. The flattening of the current efficiency curve may be due to the increase in ion (in pore water) concentration as a result of the solution of naturally occurring minerals (aluminum, calcium) bound to the clay mineral surface, or the mobilization of charged contaminant molecules. The increase in ion strength increases the participation of electromigration to the overall electrokinetic flow. The increase in the curve slope is due to the decrease of ions in the pore water. A decrease in ion concentration decreases the participation of electromigration to the electrokinetic flow. It appears that the current efficiency was related to the degree of PAH contamination. The greater the level of organic contamination, the higher the calculated current efficiency. Conversely, the lesser the organic contamination, the lower the calculated current efficiency.

4.3.5 Organic Compound Removal

As outlined in section 3.2.1, the target PAH contaminants which were tracked through the electrokinetic experiments ranged from two ringed compounds to six ringed compounds. The targeted compounds were: (1) *naphthalene*, (2) *acenaphthylene*, (3) *acenaphthene*, (4) *fluorene*, (5) *phenanthrene*, (6) *anthracene*, (7) *fluoranthene*, (8) *pyrene*, (9) *chrysene*, (10) *benz(a)anthracene*, (11) *benzo(b)fluoranthene*, (12) *benzo(k)fluoranthene*, (13) *benzo(a)pyrene*, (14) *dibenzo(a,h)anthracene*, (15) *benzo(g,h,i)perylene*, and (16) *indeno(1,2,3-c,d)pyrene*. Following the electrokinetic tests, the collected soil samples and collected anode and cathode water samples were analyzed and evaluated against the samples' starting chemical concentrations. The proceeding table (Table 4-4) presents the molecular weights and the maximum aqueous phase concentrations, at room temperature (25°C), of the target PAH compounds. The values were empirically derived from the partitioning of PAH compounds from coal tar samples.

The solubility and the maximum aqueous phase concentrations of the listed PAH compounds decreases with the increase of the compounds molecular weight. In addition to these findings, it has been demonstrated that the PAH compounds' solubility in water generally decreases as the compounds' physical structure (number of benzene rings) and molecular weight increases. The efficiency of the removal of the targeted PAHs ranged from a low of 4% removal to a high of 90% removal. *Naphthalene* (a two ring compound), the most soluble of the target compounds, was identified in the electrode chambers as the highest concentration PAH

compound.

Table 4-4

Molecular Weights and Maximum Aqueous Phase Concentrations

Compound	Molecular Weight	Maximum Aqueous Phase Concentration, (mg/L)
Naphthalene	128.2	14
Acenaphthylene	152.2	1.4
Acenaphthene	154.2	0.3
Fluorene	166.2	0.3
Phenanthrene	178.2	0.4
Anthracene	178.2	0.07
Fluoranthene	202.0	0.01
Pyrene	202.0	0.1
Chrysene	228.2	0.006
Benz(a)anthracene	228.2	0.0057
Benzo(a)pyrene	252.0	0.001

mg/L = milligrams per Liter

4.4 Gas Chromatography

The results of the analytical investigation using gas chromatography, can be found in Appendix D. Procedural blanks were analyzed periodically during the sample evaluations. Detectable levels of PAHs were not measured in any of the analyzed blanks. Perylene was used as an internal standard, and was monitored following every sample evaluation. The detection limits for the target PAH compounds varied from 1 ug/L to 10 ug/L (parts per billion). As a matter of course, the lower detection limits of the target compounds were set at 20 ug/L. At a minimum, a three point (a five point curve was often generated) standard

curve was generated prior to each daily run, to audit the gas chromatographs performance. The percent recovery of the individual target PAH compounds met at least 90% and not greater than 110% of that standard's published value to be considered within acceptable instrument operating parameters (Personal communication, Restek, Inc. 1992).

The results of the gas chromatography investigations are presented in Appendix E. The data has been graphed with normalized target PAH concentrations plotted against their relative location in the soil test cell (anode, center, and cathode).

4.5 Nuclear Magnetic Resonance Spectra

The results of the analytical investigation using Nuclear Magnetic Resonance spectral analysis, can be found in Appendix F. The spectral results qualitatively support the gas chromatography results. Tetramethylsilane (TMS) was used as a marker compound in the investigation. The TMS chemical shift is anchored at 0 parts per million (ppm), and is used throughout the evaluations as the reference peak. Deuterated chloroform was used as the solvent to prepare the soil samples for analysis. The sharp singlet which appears at 7.25 ppm is likely the protonated chloroform ($CHCL_3$) contaminant in the deuterated chloroform.

The original untreated soil sample shows evidence of the aromatic character of absorbed contaminants (PAHs) with broad bands ranging from the 7 to 8 ppm chemical shift peaks. The aromatic compounds are found in the anode, the center, and the cathode soil sections of

the sample. The spectra also identifies the presence of aliphatic hydrocarbons with peaks at 1 ppm, 1.25 ppm, and 1.5 ppm, which correspond to aliphatic $-CH_3$ and $-CH_2-$ structures.

In the UTB-23-8/10 sample, ground water alone was used as the pore fluid (permeate). Following the electrokinetic testing, the anode and the cathode water show no evidence of aromatic hydrogen bound carbon structures. The single sharp peak evidenced at 1.5 ppm corresponds to an unknown aliphatic structure. The anode, center and cathode sections of the test soil all show evidence of aromatic structures (the PAHs) by the broad band at the 7 ppm to 8 ppm chemical shift peaks.

Secondly, the UTB-23-8/10 B sample, which was treated with the anionic sodium dodecyl sulfate surfactant shows no evidence of PAHs or aliphatic structures in the anode water sample. The surfactant was introduced at the cathode water chamber of the test cell. The cathode water shows no evidence of aromatic structures. However, peaks at approximately 1.9 ppm and at approximately 2.25 ppm are detected, which indicates the presence of a long methylene chain containing hydrocarbon structure. The anode and center soil sections show evidence of PAHs whereas the cathode extracted soil shows no evidence of any PAHs. Also, there does not appear to be any surfactant (aliphatic structure) in the cathode soil sample.

Finally, the UTB-23-8/10 C sample was treated with a surfactant and cosurfactant; the surfactant/co-surfactant was also introduced into the cathode chamber of the test cell. The spectra shows no evidence of PAHs in the anode or cathode waters. The cathode water does

show significant evidence at approximately 1.25 ppm, 3.75 ppm, and at the 2.0 ppm shift of a long chain aliphatic-type hydrocarbon (ie, surfactant, long chain alcohol). The anode water show less evidence of containing aliphatic hydrocarbons. Both of the anode and the cathode soil samples both show significant evidence of PAHs, while very little evidence exists for the presence of PAHs in the center soil section.

CHAPTER 5

DISCUSSION OF RESULTS

5.1 Introduction

The electrokinetic phenomenon is the term associated with electrophoretic movement, electromigration, and electroosmosis. In this situation, with the target contaminants being essentially uncharged and non-ionic, the predominant force causing contaminant movement is the physical flushing action which accompanies electroosmotic flow. Though PAHs tend to be insoluble in water, some of the PAH compounds are slightly soluble. Thus the movement of water through the soil cell carries a dissolved portion of the contaminant. In this research, surfactant and surfactant/co-surfactant were added to the water to solubilize the PAH compounds. This treatment contributed to the movement of the otherwise insoluble compounds in the soil system. The addition of a surfactant to the purge waters allowed electromigration to occur. However, the predominant mobility of these contaminants is due to electroosmosis, and the associated dragging.

5.2 Parameters

Theoretically, in a homogeneous porous medium, nonreactive solutes in the aqueous phase will be carried in the direction of and at a rate equal to the velocity of the native pore water.

However, there is a diversion from the expected path of pore water flow due to hydrodynamic dispersion. The diversion occurs due to mechanical mixing as the solute/water phase moves through the soil matrix, and molecular diffusion of the solute in both saturated and unsaturated soil matrices and water in an unsaturated soil matrix due to kinetic energy.

The ultimate fate of the organic compounds evaluated in this research with respect to the subsurface environment, is dependent on the partitioning of those compounds between the solid phase (soil), the aqueous phase (ground water), and the vapor phase (dissolved and interstitial space of the vadose zone). The partitioning which occurs between the aqueous and gas phase is calculated from the aqueous solubility of a substance and the saturation vapor pressure of the compound. The partitioning between the solid and aqueous phases of PAH compounds may be estimated by applying two parameters: (1) the hydrophobicity via the octanol-water partition coefficient, and (2) the measurement of the solid phase hydrophobicity as defined by the weight fraction of organic carbon to non-organic carbon materials (Schwarzenbach, et al. 1993).

The octanol-water partition coefficient is used widely in the chemical literature to characterize the fugacity of the compound to move from it's so termed octanol-rich to water-rich phases. The octanol-water partition coefficient, K_{ow}, can be written as (Equation 17):

$$K_{ow} = \text{(Concentration in octanol phase)/(Concentration in aqueous phase)}$$

The value of K_{ow} is unitless. The parameter is measured with low solute concentrations, K_{ow} being a very weak function of solute concentration. Values of K_{ow} are commonly measured at 20 or 25 °C. Measured values for organic compounds range from 10^{-3} to 10^{7} (Lyman, Reehl, and Rosenblatt. 1990). In some cases, as in the instance of a plume of contaminant being formed, it is helpful to assume infinite dilution. At this point, the dominant factor in the determination of the K_{ow} is the activity coefficient of the individual compound in the water phase.

Additionally, the partitioning of the organic compound between the aqueous phase and the vapor phase can be understood by applying Henry's Law constants. The Henry's law constant K_H is simply the ratio of a compound's abundance in the gas phase to that in the aqueous phase, at equilibrium. K_H is defined as (Equation 18):

$$K_H = (P_i/C_w)\ (\text{atm L})\ (\text{mol}^{-1})$$

In the equation, P_i is the vapor phase partial pressure of the solute I, and C_w is the solute's molar concentration (Schwarzenbach, et. al. 1993). This relationship to the Henry's constant based on molar concentration, K_H, is (Equation 19):

$$K_H = (MW)(K_H)/10^6$$

where MW is the molecular weight of the solvent, in this instance ground water, and the units

being cubic meters per mole (m^3/mol).

Adsorption is another parameter to consider when determining the fate of the organic compounds in the subsurface environment. Within the vadose zone, organic compounds can partition by one of three mechanisms: (1) into the immobile solid matrix, (2) the mobile solid matrix, and (3) the mobile aqueous phase. In this research, the sorption onto colloidal particles and natural organic molecules was considered to be insignificant. Therefore, the adsorption of these organic compounds to the immobile soil matrix is considered to be predominant. Cations and other positively charged compounds can also be strongly sorbed to the negatively charged surface of these clayey soils. Ion exchange will cause desorption of these ionic species. The generation and propagation of an acid front through the soil will cause an exchange with free H^+ ions with the sorbed cations. It is theorized that this is a primary mechanism for the desorption of cations and positively charged species from the soil. The ion exchange mechanism is dependent on the surface charge characteristics of the soil, characteristics and the relative concentration of the species involved, and the availability of competing organic and carbonate species within the soil matrix (West, et al. 1995; Yin, et al. 1995).

The iso-electric point is defined as the pH at which the chemical (organic) compound has no net charge. At this point, the compound's zwitterion is at a maximum, and the two ions balance, causing electroneutrality and no further migration in the soil cell. During this research, banding of organic material was evident at specific points within the soil column

after extended treatment times. Whether these compounds were the organic compounds of interest or were ancillary organic compounds is not known; the rudimentary gas chromatographic analyses were unable to accurately identify the constituents of the bands. Regardless, the banding was probably caused by reaching the iso-electric point. If pH control was followed, ionized organic compound removal from the soil would be enhanced.

5.3 Experimental Results

The results of the electrokinetic tests performed during this work were quite interesting. In the unenhanced (ground water alone) soil test cells, the PAHs were mobilized toward the cathode, primarily by the electroosmotic mechanism. Stacking of the bulkier, higher molecular weight organic species occurs in the soil column as the contaminants move toward the cathode. The lighter species such as *naphthalene*, *fluorene*, and *acenaphthylene* electromigrated and were swept electroosmotically to toward the cathode. This has been shown in samples UTB-23-G1, UTB-23-G4, UTB-23-G5, UTB-23B-8/10, and UTB-24T-10/12). In the surfactant only-enhanced ground water permeate, the anionic surfactant sodium dodecyl sulfate was added at a concentration greater the necessary critical micellular concentration. This allowed the dynamic surfactant-ground water system to encapsulate much of the unbound PAH material. The PAH compounds generally electromigrated toward the anode. This was clearly demonstrated in the soil sample UTB-23-S1. In the surfactant with co-surfactant permeate water (SDS and Butanol), the results indicate that the PAHs were moved toward the anode and cathode, away from the center region of the test chamber.

This split movement was due to the co-surfactant expanding the micelle, and allowing some of the PAH material to be separated from the micelle encapsulated contaminants. Electroosmotic flow moved the "free" PAH material toward the cathode, where the micelle encapsulated material was electromigrated toward the anode. This was demonstrated in test samples UTB-23-S2 and UTB-23-S3. Movement toward the anode and cathode, out of the center region of the soil cell was very dramatic (Appendix F).

5.3.1 pH Profiles

The pH distribution in the test cell soils and in their electrode chambers are presented in the figures found in Appendix C. As expected from the dissociation of water, and the reduction/oxidation (redox) occurring at the electrodes due to electron transfer, the anode chamber fluid is acidic (pH ranging from 2 to 3) and the cathode chamber fluid is alkaline (pH ranging from 10 to 11).

In all of the test soil cells, a pH gradient developed from anode to cathode following an increasing trend (from a pH less than 7, to a pH greater than 7). The soil pH in the anode region of the soil cell did not drop to the low values in the anode chamber, but stabilized at approximately pH = 5. This is due to the buffering capacity of the soil, and the cell fluid movement away from the anode toward the cathode. This movement impedes electron transfer in the anode region. The soil pH in the cathode region did reach the higher values seen in the cathode chamber, ranging from pH 9 to pH 12. Researchers Lindgren, Probstein,

Acar, and Pamukcu have recognized the need for pH control to more effectively transport inorganic as well as organic constituents through soil matrices. In experiments conducted at the Sandia National Laboratories, Lindgren, Mattson, and Newhart demonstrated that pH control does in fact enhance transport of inorganic species through soil matrices. The buffering of the anode soils contributed to the PAH movement from the anode region to the cathode region. The addition of the surfactant caused an overall increase in the soil's pH. Since the CMC was exceeded, the binding sites on the soil were occupied by the excess surfactant, causing the soil to lose it's buffering capacity. Additionally, Grube (1992) stated that surfactant molecules could replace the available ions on the clay surface, thus causing an increased pore space and increased permeability because of a decreased hydraulic radius of the clay.

5.3.2 Conductivity

During the electrokinetic tests, the resistance was measured along the cell at the intervals: anode-P1, P1-P2, P2-P3, P3-cathode. A "peak" of resistance was observed at the anode-P1 and P3-cathode intervals; the anode-P1 peak being stronger (greater resistance). The initial peak at the anode-P1 interval is attributed to the initial conditions of the experiment. The porous frits used to separate the soil from the anode and cathode chambers is unsaturated and therefore is more resistant to electrical current flow. At the beginning of the electrokinetic test, dissociation of the permeant fluid has not occurred, and therefore the conductivity within the soil does not increase until the hydrogen ion (H^+) at the anode end, and the hydronium ion

(OH^-) begins to flow into the soil matrix, reducing the resistance (the reduction of the "peak" over time) within the soil. In soil cell UTB-23-A2, the anode-P1 and P3-cathode resistance was equal to or less than that of the soil matrix's resistance. This is attributed to the higher initial soil moisture content than other samples, and the greater initial concentration of ions in the soil water.

5.3.3 Energy Expenditure

Based on the observation that the majority of the PAH transport is due to electroosmotic flow, the dependence of contaminant movement to applied charge is minimal. Current flow is necessary to cause electroosmotic flow, but due to the nature of the PAH compounds, electromigration and electrophoresis are not the dominant force transporting the contaminants. In the case of the surfactant/water system, dependence on electromigration and electrophoresis is greater, but relatively insignificant. In soil test cells UTB-23-G4, UTB-23-S3, and UTB-24T-10/12, the resistance was greatest in the interval anode-P1, followed by the interval P3-cathode. The resistivity in the intervals P1-P2 and P2-P3 equilibrated following the 24 hour period, remaining constant throughout the period of electrokinetic testing. This data coupled with the chemical analyses indicate that electromigration and electrophoresis were minimal; electroosmosis was the predominant transporting force.

In soil test cells UTB-23-G5, UTB-23-S1, and UTB-23-A2, the resistance within the soil increased where PAH concentrations were decreased. In UTB-23-G5, the resistivity in the anode-P1 interval increased during the electrokinetic test; in UTB-23-S1, the resistivity in the P1-P2 interval increased during the test; in UTB-23-A2, the resistivity in the P1-P2 and P2-P3 intervals increased during the test following the introduction of the surfactant/water system. The increase in resistivity in the soil treated with the surfactant suggests that the surfactant exchanged with the available charged species sorbed to the surface of the soil matrix, mobilizing the charged species, leaving a no net charge void on the soil surface. This would localize the increase in resistivity. The chemical analyses of these soil intervals showed a decrease in the PAH concentration in these intervals. Furthermore, the chemical analyses of the UTB-23-G5 and UTB-23-S1 intervals with increased resistivity revealed overall PAH removal. This is attributed to the dissociation and subsequent ionization of the organic species, allowing electroosmosis to sweep the fragments, or daughter products through the soil matrix, and allowing limited electromigration. Dissociation would need to be to a level allowing the newly formed species to be small enough or, with the addition of a surfactant, "slippery" enough, to disallow size exclusion.

The increase in measured electrical resistivity suggests that one of the following: the removal or the neutralization of the charged surface species, the removal of or the electroneutrality of the charged species carried in the aqueous phase, or a decrease in the availability of the carrier which in these experiments is water. De-watering will also create a physical barrier to current flow, thus increasing resistivity through the matrix.

5.3.4 Efficiency of Organic Compound Removal

The target PAH contaminants which were tracked through the electrokinetic experiments ranged from two ringed compounds to six ringed compounds. The targeted compounds were: (1) *naphthalene*, (2) *acenaphthylene*, (3) *acenaphthene*, (4) *fluorene*, (5) *phenanthrene*, (6) *anthracene*, (7) *fluoranthene*, (8) *pyrene*, (9) *chrysene*, (10) *benz(a)anthracene*, (11) *benzo(b)fluoranthene*, (12) *benzo(k)fluoranthene*, (13) *benzo(a)pyrene*, (14) *dibenzo(a,h)anthracene*, (15) *benzo(g,h,i)perylene*, and (16) *indeno(1,2,3-c,d)pyrene*. The removal efficiency of the target organic compounds were assessed by comparing the soil's initial individual PAH concentrations (initial conditions were assumed to be a homogeneous PAH mixture across the tested soil sample), against the concentrations detected in the soils following the electrokinetic testing procedure. The three distinct intervals of the soil cell were evaluated, in the chemical evaluations, following the cessation of the tests. The anode interval, the center interval and the cathode interval. Also, the anode and cathode chamber fluid was periodically collected from the cathode chamber during the tests, and from the anode and cathode chambers following the electrokinetic testing. This was also analyzed for the target PAH compounds. Table 5-1 summarizes the results of the electrokinetic tests.

Table 5-1

Pre- and Post Electrokinetic Treatment Concentrations and Mass of PAHs Measured in the Soil

Sample ID	Initial +	Anode *	Center *	Cathode *	Initial Soil +	Final Soil +	Final Water +	Percent Removal
UTB-23-G1	2,851	580	1,605	2,811	307.6	176.4	0.005	43%
UTB-23-G4	3,037	2,243	3,038	3,093	327.7	314.5	0.02	4%
UTB-23-G5	4,584	676	643	3,749	461.5	117.4	0.07	75%
UTB-23-S1	4,584	755	492	2.8	483.2	47.9	6.5	90%
UTB-23-S2	4,548	598	2,771	1,472	450	215.2	57.2	52%
UTB-23-S3	5,980	2,393	1,735	847	631.4	179.2	ND	72%
UTB-23-A2	1,580	1,455	12.7	493	212.3	44.8	0.02	79%
UTB-24B-8/10	105.9	56.6	26.4	39.2	17.1	5.4	0.004	68%
UTB-24T-8/10	105.9	22.6	41.2	22.3	16.7	3.8	0.006	77%

* = Total PAH concentration in soil (mg/Kg)

+ = Total PAH calculated mass (mg)

ND = Not detected

The greatest concentration of PAH in the fluid collected from the cathode chamber was *naphthalene*. Due to the relative high solubility of *naphthalene* in aqueous systems, this was expected due to the predominance of the electroosmotic flow through the soil matrix. Presented in section 4.3.5 of this document, are the maximum aqueous phase concentration of the target PAH compounds. It has been shown that the solubility of a solute in water (X_w), is inversely proportional to K_{ow} (Lyman, et al. 1990).

The figures which pictorially describe the following test cell results are presented as bar graphs and line graphs. The first graph describes the initial PAH concentrations in the soil, followed by the resulting PAH concentrations in the anode, center, and cathode intervals. The second graph charts the individual PAH compound concentrations following the electrokinetic testing procedure, normalized to their initial concentration, as a concentration profile along the soil cell, from anode to cathode.

The figures in Appendix C present the distribution of the targeted PAH compounds in the soil test cells UTB-23-G1, UTB-23-G4, and UTB-23-G5, respectively. In the three test cells, in which the permeate fluid was synthetic ground water, overall the target PAH compounds were mobilized toward the cathode interval of the soil cell. Test cell UTB-23-G1 passed approximately 2.4 pore volumes (from the anode to the cathode) of permeate fluid during the test period. Test cell UTB-23-G4 passed approximately 5.8 pore volumes of permeate fluid during the test period, and test cell UTB-23-G5 passed approximately 9 pore volumes of permeate fluid during the test period.

In soil test sample UTB-23-G1, the concentration of the majority of the PAH compounds increased from the anode toward the cathode interval. This suggests that these compounds moved under the influence of the electrokinetic force. *Benz(k)fluoranthene* and *Dibenzo(a,h)anthracene* appear to have been mobilized preferentially toward the anode. *Fluoranthene* mobilized from the anode to the center and stacked in the center interval.

In soil test sample UTB-23-G4, the concentration of the majority of the PAH compounds again increased from the anode toward the cathode interval, though stacking in the center interval was the common occurrence. *Benzo(a)pyrene* appeared to be preferentially stacking at the center interval. Again, the *benz(k)fluoranthene* appeared to move preferentially toward the anode. *Naphthalene* moved away from the center of the soil sample, toward the cathode interval of the sample.

In soil test sample UTB-23-G5, PAH compounds were again mobilized from the anode to the cathode interval of the soil test cell. Approximately 9 pore volumes of permeate was moved through the cell during the test period. Interestingly, many of the target PAH compounds moved to toward the anode, more so than in the previous tests. The concentrations of *acenaphthene*, *fluorene*, *chrysene*, and *fluoranthene* were greater in the anode interval than the center interval, suggesting that: (1) movement from the anode interval was inhibited due to the soil's buffering capacity, (2) due to strong chemical adsorption occurring at the anode interval, these organic compounds were physically stabilized into the soil matrix, (3) the anode interval becomes more acidic, with a greater number of protons in the interval, electrostatically attracting the pi-electron rich organic compounds toward the anode, or (4) because the PAH compounds are electron rich, electromigration may influence the negatively charged portion of the compound, pulling the PAH compound toward the anode.

The figures in Appendix C present the distribution of the targeted PAH compounds in the soil test cells UTB-23-S1, UTB-23-S2, UTB-23-S3, and UTB-23-A2, respectively. In the test cell UTB-23-S1, the permeate fluid was surfactant and synthetic ground water, introduced into the test cell through the anode chamber. In test cell UTB-23-S2 and UTB-23-S3, the permeate was surfactant with a cosurfactant and synthetic ground water, introduced to the test cell through the anode chamber. In the test cell UTB-23-A2, the permeate fluid was surfactant and synthetic ground water, but introduced into the test cell through the cathode chamber. Test cell UTB-23-S1 passed approximately 6 pore volumes (from the anode to the cathode) of permeate fluid during the test period. Test cell UTB-23-S2 passed approximately 6 pore volumes of permeate fluid during the test period, test cell UTB-23-S3 passed approximately 6 pore volumes of permeate fluid during the test period, and test cell UTB-23-A2 passed approximately 6 pore volumes of permeate fluid during the test period.

5.4 Nuclear Magnetic Resonance Spectra

The NMR spectra generated during this research project support the observations and conclusions reached by evaluating the gas chromatography results. Qualitatively, the PAHs are present in the all of the sectioned soils when the ground water permeate alone is used in conjunction with the applied electric field. When a surfactant enhanced ground water permeate is introduced into the cathode chamber, the PAHs are (presumably) enveloped and move toward the anode chamber. When the surfactant with a co-surfactant is introduced into the cathode chamber, the PAHs move toward the anode region and the cathode region of the

test cell, with an elimination of the aromatic material from the enter portion of the test cell.

5.5 Stacking

Stacking is a capillary electrophoretic phenomena, where ions in a large injection plug are compressed into a narrow band. During the experimentation, the permeant (ground water) is injected at the anode end of the test cell. The electric field imposed over the soil cell is high due to the resistance of the injection solution. Using cations as an example to illustrate the stacking affect, electrophoretic mobility occurs in the direction of the negative electrode, the cathode. As the cations migrate from the injection zone, through the background electrolyte concentration in the soil cell, the cations become exposed to the lower electric field in the background electrolytic solution. This lower electric field causes the migrating cation velocity to decrease relative to the cations remaining in the injection zone. Those remaining cations continue to migrate a relatively high velocity. As a result, the ions compress or stack into a band at the front of the injection zone. Below is a visual example of the stacking phenomenon.

At the cathode, anions are migrating toward the anode. The movement is retarded due to the elctroosmotic flow from the anode to the cathode. The result is that the stacking occurs at the rear of the injection zone.

5.6 Isoelectric Focussing

The isoelectric point is the point where the pH of the environment causes ions to experience zero charge on the surface of the ion. The net adsorption of an acid or a base gives a surface charge on an ion, varying from the actual surface charge by some constant. This constant will vary with the pH at which the adsorption is measured. In cases where metals exist in the permeate or soil media, there can be complex pH effects if the inorganic compounds are hydrolyzable (Adamson 1990).

The banding effect which was observed in many of the soil samples following the electrokinetic testing may be due to in part to isoelectric focussing. Stacking which was previously discussed, may physically retard fluid movement through the soil matrix. This would disallow osmotic flow of uncharged species, and contribute to the broadening of the stacked bands, which has been observed.

CHAPTER 6

SUMMARY AND CONCLUSIONS

6.1 Summary

In summary, the electrokinetic movement of the target PAH compounds through the collected soil cores appeared to be driven by electrochemical reactions. The advancement of a band of organic material was visual evidence in the majority of the treated soil samples. The chemical analyses suggest that movement of the PAHs did occur within the soil matrix. It has been postulated that stacking and isoelectric focussing are the physical/chemical forces responsible for these observations.

The mass of the PAHs in the fluid samples collected from the anode and cathode chambers was lower than one would expect based on the soil's mass removal calculations. The low aqueous solubility of the targeted organic compounds inevitably contributed to the reduced removal via electroosmotic flow. Precipitate was often present in the electrode chambers, as well as the presence of a "oily" sheen. The precipitation was probably due to the formation of aluminum and calcium hydroxides, and in part due to degradation of the carbon electrodes. The sheen and the precipitation were not collected and analyzed for the target PAH compounds. In addition, the glass frits which held the soil in the test chambers were often stained with a dark material. An additional source of mass removal error may also lie in the

carbon electrodes themselves. Organic carbon adsorbs many organic compounds, and may have been a sink for the PAH compounds. It is very plausible to believe that these non-analyzed sources may contribute to the mass removal errors.

The greatest removal of PAHs was observed in sample UTB-23-S1. For this electrokinetic test, the anionic surfactant sodium dodecyl sulfate was incorporated into the cathode chamber fluid. Ignoring the surfactant enhanced data, the removal efficiency of PAH compounds is directly proportional to the volume of permeate fluid which flows through the test cell. There is an exception to this observation in the data from test sample UTB-23-G4. Though the data suggest that the PAH compounds are moving toward the cathode end of the test cell in sample UTB-23-G4, low removal is suggested. The low mass removal may be due to: (1) inhomogeneity of the initial soil core, (2) the banding of PAH compounds outside of the collected, and therefore non-analyzed soil sample, and (3) the movement of the PAH compounds through the soil cell into other sinks, such as the precipitate, the frit, and the carbon electrodes. The mass removal data for samples UTB-23-G1 and UTB-23-G5 suggest that PAH compounds are moved through the contaminated soil samples, predominantly by electroosmosis.

Table 6-1 presents the percent reduction data for the analyzed soil samples.

6.2 Conclusions

When technical feasibility of other remedial options prohibit their use at both organic compound and inorganic compound contaminated soil and ground water sites, electrokinetic remediation may be a viable alternative to treat the affected media. The technology has been successfully demonstrated on the bench and field scale to remediate soils contaminated by inorganic species. This work demonstrates that at the bench-scale, organic compound movement can be accomplished with this technique. Electrokinetic remedial techniques have taken significant forward strides through research and development at many laboratories through the world. With continued research into permeate enhancement techniques, pH control, surfactant/soil interface reactions, and methods to disallow precipitation and stacking in the soil matrix, electrokinetic movement of organic species will be a valuable remedial technology in the twenty first century.

TABLE 6-1

Average Percent Reduction of the PAH Compounds Concentration in Electrokinetically Treated Soil Samples

COMPOUND	UTB 23-G1	UTB 23-G4	UTB 23-G5	UTB 23-S1	UTB 23-S2	UTB 23-S3	UTB 23-A2	UTB 24B-8/10	UTB 24T-10/12	%[1]
Naphthalene	34	64	64	78	23	86	79	71	77	64
Pyrene	31	-	64	83	34	59	79	73	77	56
Acenapthylene	30	-	92	100	-	79	85	67	74	55
Acenapthene	3	-	57	95	55	85	55	74	66	54
Fluorene	33	-	74	86	42	79	82	68	71	60
Phenanthrene	27	-	71	100	77	83	77	67	66	65
Anthracene	79	-	100	100	35	92	75	66	73	69
Fluoranthene	83	-	58	78	25	75	77	62	-	51
Benz(a) pyrene	16	-	75	82	51	-	85	66	73	50
Benzo(a) anthracene	24	-	45	84	36	39	83	74	88	52
Benzo(b) fluoranthene	24	-	83	100	93	88	75	75	88	70
Benzo(g,h,i) perylene	17	8	BDL	BDL	BDL	92	78	74	79	58
Benzo(k) fluoranthene	-	-	82	92	68	100	26	77	88	59
Chrysene	20	-	34	57	-	91	85	29	87	45
Dibenzo(a,h) anthracene	73	-	BDL	BDL	BDL	91	97	64	88	69
Indeno (1,2,3-c,d) pyrene	17	-	79	100	100	93	78	65	86	69

TABLE 6-1

Average Percent Reduction of the PAH Compounds Concentration in Electrokinetically Treated Soil Samples

COMPOUND	UTB 23-G1	UTB 23-G4	UTB 23-G5	UTB 23-S1	UTB 23-S2	UTB 23-S3	UTB 23-A2	UTB 24B-8/10	UTB 24T-10/12	%[1]
Naphthalene	34	64	64	78	23	86	79	71	77	64
Pyrene	31	-	64	83	34	59	79	73	77	56
Acenapthylene	30	-	92	100	-	79	85	67	74	59
Acenapthene	3	-	57	95	55	85	55	74	66	54
Fluorene	33	-	74	86	42	79	82	68	71	60
Phenanthrene	27	-	71	100	77	83	77	67	66	63
Anthracene	79	-	100	100	35	92	75	66	73	69
Fluoranthene	83	-	58	78	25	75	77	62	-	51
Benz(a) pyrene	16	-	75	82	51	-	85	66	73	50
Benzo(a) anthracene	24	-	45	84	36	39	83	74	88	53
Benzo(b) fluoranthene	24	-	83	100	93	88	75	75	88	70
Benzo(g,h,i) perylene	17	8	BDL	BDL	BDL	92	78	74	79	58
Benzo(k) fluoranthene	-	-	82	92	68	100	26	77	88	59
Chrysene	20	-	34	57	-	91	85	29	87	45
Dibenzo(a,h) anthracene	73	-	BDL	BDL	BDL	91	97	64	88	69
Indeno (1,2,3-c,d) pyrene	17	-	79	100	100	93	78	65	86	69

[1] = Percent Reduction

- = Indicates no removal for which the average concentration is higher than the initial concentration of the compound

BDL = Below Detectable Limits

6.2.1 Recommendations for Further Studies

Recommendations for further study include:

- Evaluate to the soil following the electrokinetic testing in more depth by slicing and chemically evaluating more than three cross sections;
- Evaluate chemical treatments to solubilize precipitates within the soil column;
- Evaluate pH controls to enhance PAH movements through the soil column;
- Evaluate other surfactant / co-surfactant systems, with the goal of tightening the micelle rather than disrupt and expand the micellular envelope;
- Evaluate the geochemical reactions occurring between the organic compounds and the surface of the clay matrix.

REFERENCES

Abramson, H.A. (1934), "Electrokinetic Phenomena and Their Application to Biology and Medicine", *New York Chemical Catalogue Co, Inc.*

Acar, Y., Gale, R., Putnam, G., Hamed, J., and Wong, R. (1989), "Electrochemical Processing of Soils : Theory of pH Gradient Development by Diffusion, Migration and Linear Convection", *Journal of Electro Analytical Chemistry*, Louisiana State University.

Acar, Yalcin B., and Alshawabkeh, Akram N. (1996), "Electrokinetic Remediation I : Pilot-Scale Tests with Lead-Spiked Kaolinite", *Journal of Geotechnical Engineering*, pp. 173-185.

Adamson, Arthur W. (1990), "Physical Chemistry of Surfaces, Fifth Edition", Wiley Interscience, New York.

Ahlert, W.K. (1989), "An Examination of the Primary Adsorption and Secondary Uptake of Benzene and Toluene By Two Aquifer Solids." Ph.D. Dissertation, Graduate School of Rutgers University, New Brunswick, New Jersey.

Aiken, George R., Mcknight, Diane M., Wershaw, Robert L., and Maccarthy, Patrick. (1985), "Humic Substances in Soil, Sediment, and Water: Geochemistry, Isolation, and Characterization", Wiley Interscience, New York.

Alshawabkeh, Akram N., Acar, Yalcin B. (1996), "Electrokinetic Remediation. II : Theoretical Model", *Journal of Geotechnical Engineering*, pp. 186-196.

Banarjee, S., Horng, J., Ferguson, P., and Nelson, O. (1988), "Field-scale Feasibility Study of Electrokinetic Remediation". U.S. EPA Risk Reduction Engineering Laboratory, Office of Research and Development.

Brusseau, M.L. (!992), "Non-equilibrium Transport of Organic Chemicals: The Impact of Pore Water Velocity." *Journal of Contaminant Hydrology*, Vol.9, pp. 353-368.

Butcher, B., Davidoff, B., Amacher, M.C., Hinz, C., Iskandar, K., and Selim, H.M. (1989), "Correlation of Freundlich K_d and n Retention Parameters with Soils and Elements", *Soil Science*, Vol. 148, No. 5, pp. 370-379.

Cabrera-Guzman, D.C., Schwartzbaugh, J.T., and Weisman, A.W. (1990), "The Use of Electrokinetics for Hazardous Site Waste Remediation", *Journal of Air Waste Management Association, Vol. 40*, pp. 1670-1676.

Casagrande, L. (1939), "Electroosmosis in Soils", *Geotechnique*, London, Vol. 1, No. 3, p. 159.

Casagrande, L. (1953), "Electroosmotic Stabilization of Soils", *Journal of the Boston Society of Civil Engineers*, Vol. 39, pp. 51-83.

Domenico, Patrick A., and Schwartz, Franklin W. (1990), "Physical and Chemical Hydrogeology", John Wiley and Sons, New York.

Dorn, E. (1880), "Weid Ann"., Vol. 10, p. 46, cited in Abramson, (1981).

Dragun, J. (1988), "The Soil Chemistry of Hazardous Materials", The Hazardous Materials Control Research Institute, Silver Spring, Maryland.

Fleureau, J., and Dupeyrat, M. (1988), "Influence of an Electric Field on the Interfacial Parameters of a Water/Oil/Rock System : Application to Oil Enhanced Recovery", *Journal of Colloid and Interface Science*, Vol. 123, No. 1, pp. 249-258.

Freeze, R.A., and Cherry, J.A. (1979), "Groundwater", Prentice-Hall, Inc., Englewood Cliffs, NJ.

Fountain, John C., Starr, Robert C., Middleton, Thomas, Beikirch, Michael, Taylor, Craig, and Hodge, Dennis. (1996), "A Controlled Field Test of Surfactant-Enhanced Aquifer Remediation", *Groundwater*, Vol. 34, No. 5, pp. 910-916.

Gabr, M.A., Bowders, J.J., and Shoblom, K.J. (1995), "Flushing of Polyaromatic Hydrocarbons from Soil Using SDS Surfactant", GEOENVIRONMENT 2000; Characterization, Containment, Remediation, and Performance in Environmental Geotechnics." *American Society of Civil Engineers, Geotechnical Special Publication*, Vol. 2, No. 46, pp.1321-1334.

Grube, W.E. Jr.(1992), "Slurry Trench Cut-Off Walls for Environmental Pollution Control." *Slurry Walls: Design, Construction, and Quality Control*, ASTM STP 1129, Philadelphia, Pennsylvania, pp 69-77.

Hamed, J., Acar, Y. B., and Gale, R. J. (1991), *ASCE Journal of Geotechnical Engineering*. Vol 112 (2), p. 241.

Hillel, Daniel. (1980), " Fundamentals of Soil Physics." Academic Press, Inc., Orlando, Florida.

Hurlbut Jr., Cornelius S., and Klein, Cornelis. (1977), " Manual of Mineralogy - 19th Edition", John Wiley & Sons, New York.

Jackman, Alan P., Powell, Robert L. (1991), "Hazardous Waste Treatment Technologies", Noyes Publications, Park Ridge, New Jersey.

Kahn, L. I., Pamukcu, S., and Kugelman, I. (1989), "Electroosmosis in Fine-Grained Soil", *Proceeding of the 2nd International Symposium on Environmental Geochronology*, Vol. 1, Lehigh University.

Knox, Robert C., Sabatini, David A., and Canter, Larry W. (1993), "Subsurface Transport and Fate Processes", Lewis Publishers, Boca Raton, Florida.

Krauskopf, Konrad B. (1979), "Introduction to Geochemistry, Second Edition", McGraw-Hill Book Company, New York.

Kuo, Cheng-Chueh and Papadopoulos, Kyriakos D. (1996), "Electrokinetic Movement of Settled Spherical Particles in Fine Capillaries." *Environmental Science and Technology*, 30 (4), pp. 1176 - 1179.

Lingren, E. R., Mattson, E. D., and Kozak, M. W. (1991), "Electrokinetic Remediation of Unsaturated Soils", Extended Abstract, I&EC Special Symposium, ACS, Atlanta, GA, Sept. 21, 1992, pp. 539-541.

Lyman, Warren J., Reehl, William F., and Rosenblatt, David H. (1990), "Handbook of Chemical Property Estimation Methods - Environmental behavior of Organic Compounds", American Chemical Society, Washington, D.C.

McBride, Murray B. (1994), "Environmental Chemistry of Soils", Oxford University Press.

Moroi, Yoshikiyo, Micelles. (1992), "Theoretical and Applied Aspects", Plenum Press, New York.

Noonan, David C. and Curtis, James T. (1990), "Groundwater Remediation and Petroleum, A Guide for Underground Storage Tanks", Lewis Publishers, Inc., Chelsea, Michigan.

Nyer, Evan K. (1992), "Groundwater Treatment Technology, Second Edition." Van Nostrand Reinhold, New York.

Pamukcu, Sibel. (1991), "Final Report : Electrokinetic Removal of Heavy Metals from a Former Substation Site of PSE&G".

Pamukcu, S. (1994), "Electrokinetic Removal of Coal Tar Constituents From Contaminated Soils : EPRI TR-103320s, Electric Power Research Institute", Lehigh University, Bethlehem, PA.

Pamucku, S., and Wittle, J.K. (1992), *Environmental Progress*, Vol 11(3), p. 241.

Pamukcu, Sibel, and Wittle, J. Kenneth. (1992), "Electrokinetics for Removal of Low-Level Radioactivity from Soil", Fourteenth Annual U.S. Department of Energy Low-Level Radioactive Waste Management Conference : Conference Proceedings", Phoenix, Arizona.

Pignatello, Joseph J., and Xing, Baoshan. (1996), "Mechanisms of Slow Sorption of Organic Chemicals to Natural Particles", Environmental Science and Technology, Vol. 30, No. 1, pp. 1-11.

Probstein, Ronald F., and Shapiro, Andrew P. (1990), "Electroosmotic Decontamination of Hazardous Waste Sites" Chemical Processing, pp. 35-40.

Rao, P.S.C. (1990), " Sorption of Organic Contaminants." *Water Science and Technology*, Vol.22, No.6, pp 1-6.

Restek Corp., personal Communication. (1993), "Analysis of Gasoline Range Organics in Soil and Water", The Restek Advantage, Restek Corporation, Bellefonte, Pa.

Restek Corp., personal Communication. (1993), "Analysis of Diesel Range Organics in Soil and Water", The Restek Advantage, Restek Corporation, Bellefonte, Pa.

Rieger, Philip H. (1987), "Electrochemistry", Prentice-Hall, Inc. Englewood Cliffs, NJ.

Sabatini, David A., and Knox, Robert C. (1991), "Transport and Remediation of Subsurface Contaminants : Colloidal, Interfacial, and Surfactant Phenomena", ACS Symposium Series 491.

Sawyer, Clair N., and McCarty, Perry L. (1978), "Chemistry for Environmental Engineering, Third Edition", McGraw-Hill Series in Water Resources and Environmental Engineering, McGraw-Hill Publishing Company, New York.

Schwarzenbach, Rene P., Gschwend, Philip M., and Imboden, Dieter M. (1993), "Environmental Organic Chemistry", John Wiley and sons, New York.

Shapiro, Andrew P. (1990), "Electroosmotic Purging of Contaminants From Saturated Soils", Doctor of Philosophy Dissertation, Massachusetts Institute of Technology, Cambridge, MA.

Shapiro, A. P., Renauld, P., and Probstein, R. F. (1989), *PhysicoChem. Hydrodyn.* Vol. 11, p. 785.

Shineldecker, Chris L. (1992), "Handbook of Environmental Contaminants, A Guide for Site Assessment", Lewis Publishers, Inc, Chelsea, Michigan.

Shriner, Ralph L., Fuson, Reynold C., Curtin, David Y. and Morrill, Terence C. (1980), "The Systematic Identification of Organic Compounds: A Laboratory Manual, Sixth Edition", John Wiley and Sons, New York.

Silverstein, Robert M., Bassler, G. Clayton, and Morrill, Terence C. (1981), "Spectrometric Identification of Organic Compounds : Fourth Edition", John Wiley and Sons, New York.

Thompson, Ronald G. (1992), "Practical Zeta Potential Determination Using Electrophoretic Light Scattering", *American Laboratory*, pp. 48-53.

U.S. EPA Handbook, Remedial Action at Waste Disposal Sites (Revised). (1985), Office of Emergency and Remedial Response, Washington DC 20460 and Office of Research and Development Hazardous Waste Engineering Research Laboratory, Cincinnati, OH 45268. EPA/625/6-85/006.

U.S. EPA. (1988), "Guidance on Remedial Actions for Contaminated Ground Water at Superfund Sites", Office of Emergency and Remedial Response, U.S. Environmental Protection Agency, Washington, DC. EPA/540/G-88/003, OSWER Directive 9283.1-2.

U.S. EPA. (1995) "Soil Transport and Fate Data Base : Chemical Characteristics."

Vacarri, D.A. (1988), "Modeling Hysteretic Adsorption/Desorption", Presented at the International Conference on Phsio-Chemical and Biological Detoxification of Hazardous Wastes, Atlantic City, New Jersey.

West, L. Jared, and Stewart, Douglas I. (1995), " Effect of Zeta Potential on Soil Electrokinetics", GEOENVIRONMENT 2000; Characterization, Containment, Remediation, and Performance in Environmental Geotechnics, American Society of Civil Engineers, Geotechnical Special Publication, Vol. 2, No. 46, pp.1535-1549.

Wilkowe, Amy. (1992), "A Modified Finite-Difference Model of Electrokinetic Transport in Porous Media", Master of Science Thesis, Lehigh University, Bethlehem, PA.

Wittle, J. K., and Pamukcu, S. (1993), "Electrokinetic Treatment of Contaminated Soils, Sludges and Lagoons; Final Report to Argonne National Laboratory; Electro-Petroleum: Wayne, Pa. Contract No. 02112406.

Yin, J., Finno, R. J., and Feldkamp, J. R. (1995), " Electro-Osmotic Mobility Measurement for Kaolinite Clay", GEOENVIRONMENT 2000; Characterization, Containment, Remediation, and Performance in Environmental Geotechnics. American Society of Civil Engineers, Geotechnical Special Publication, Vol. 2, No. 46, pp.1550-1563.

Yoem, Ick Tae, Ghosh, Mriganka M., Cox, Chris D., and Robinson, Kevin G. (1995), "Micellar Solubilization of Polynuclear aromatic Hydrocarbons In Coal Tar-Contaminated Soils", *Environmental Science and Technology*, Vol. 29, No. 12, pp. 3015-3021.

APPENDIX A

SAMPLE GAS CHROMATOGRAPHY PLOTS

Certificate of Analysis

Restek Corporation certifies that this material meets or exceeds QA/QC criteria established by the U.S. EPA for commercially purchased analytical standards. The exact composition of this mixture as determined by gravimetric techniques is listed on the opposite side of this certificate.

A complete data package for this mixture is available and includes: melting point (solids) or refractive index (liquids), GC/FID and GC/MS confirmation on all neat chemicals used. Also included is final product testing with statistical evaluation of the data to confirm the concentration of each analyte.

SV Calibration Mix #5
Catalog #31011
Lot #A001492

30m, 0.32mm ID, 1.0µm Rtx-5 (cat.#10254) · Hydrogen carrier @ 40cm/sec
Oven temp: 30°C (hold 4 min.) to 275°C @ 8°C/min (hold 33 min.) · Inj. 300°C; Det. 300°C, FID

Restek Corporation · 110 Benner Circle · Bellefonte, PA 16823-8812
Phone: 814-353-1300 FAX: 814-353-1309

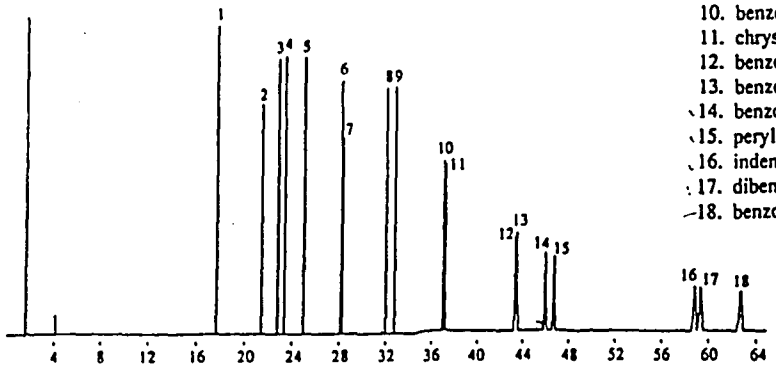

Component	Concentration
1. napthalene	2000µg/ml
2. 2-chloronaphthalene	Int. Std.
3. acenaphthylene	2000
4. acenaphthene	2000
5. fluorene	2000
6. phenanthrene	2000
7. anthracene	2000
8. fluoranthene	2000
9. pyrene	2000
10. benzo(a)anthracene	2000
11. chrysene	2000
12. benzo(b)fluoranthene	2000
13. benzo(k)fluoranthene	2000
14. benzo(a)pyrene	2000
15. perylene	Int. Std.
16. indeno(1,2,3-cd)pyrene	2000
17. dibenzo(a,h)anthracene	2000
18. benzo(g,h,i)perylene	2000

```
DATE (MO, DAY, YR)=? 01, 27, 93
TIME (24 HR CLOCK: HHMM)=? 1404

THRESHOLD 0

VALVE 5 ON

OVEN TEMP INITIAL VALUE 220

OVEN TEMP INITIAL TIME 3

OVEN TEMP PRGM RATE 8

OVEN TEMP LIMIT 305

OVEN TEMP FINAL VALUE 300

OVEN TEMP FINAL TIME 55

INJ 1 TEMP 220

DET 1 TEMP 300

OVEN TEMP EQUIB TIME 1

ATTN 2^5

CHART SPEED .1

LIST

OVEN TEMP=178°C  SETPT=220°C  LIMIT=305°C
   EQUIB TIME = 1.00 MIN

OVEN TEMP PROFILE:     (ANNOTATION OFF)
   INITIAL VALUE = 220°C
   INITIAL TIME = 3.00 MIN
   LEVEL 1
      PRGM RATE = 8.00°C/MIN
      FINAL VALUE = 300°C
      FINAL TIME = 55.00 MIN
   POST VALUE = ???
   POST TIME = ???

DET 1 TEMP=116°C  SETPT=300°C  LIMIT=405°C
DET 2 TEMP=0°C  SETPT=50°C(OFF)  LIMIT=405°C
INJ 1 TEMP=97°C  SETPT=220°C  LIMIT=405°C
INJ 2 TEMP=0°C  SETPT=50°C(OFF)  LIMIT=405°C
AUX 1 TEMP=0°C  SETPT=50°C(OFF)  LIMIT=405°C
AUX 2 TEMP=0°C  SETPT=50°C(OFF)  LIMIT=405°C

DEVICE 2: GC TERMINAL 1
   SIGNAL = B
   PLOT = ???
   CHART SPEED = 0.10 CM/MIN
```

```
   ATTN = 2↑5
   %OFFSET = 10
   ZERO = 0.00

DETECTOR B: FLAME IONIZATION
   CALIBRATION:  H=0  L1=0  L2=0

VALVES:
   VALVE  1 = OFF
   VALVE  2 = OFF
   VALVE  3 = OFF
   VALVE  4 = OFF
   VALVE  5 = ON
   VALVE  6 = OFF
   VALVE  7 = OFF
   VALVE  8 = OFF
   VALVE  9 = OFF
   VALVE 10 = OFF
   VALVE 11 = OFF
   VALVE 12 = OFF

THRESHOLD = 0
PEAK WIDTH = 0.04

AVAILABLE MEMORY (BYTES): 25280

PAGE
```

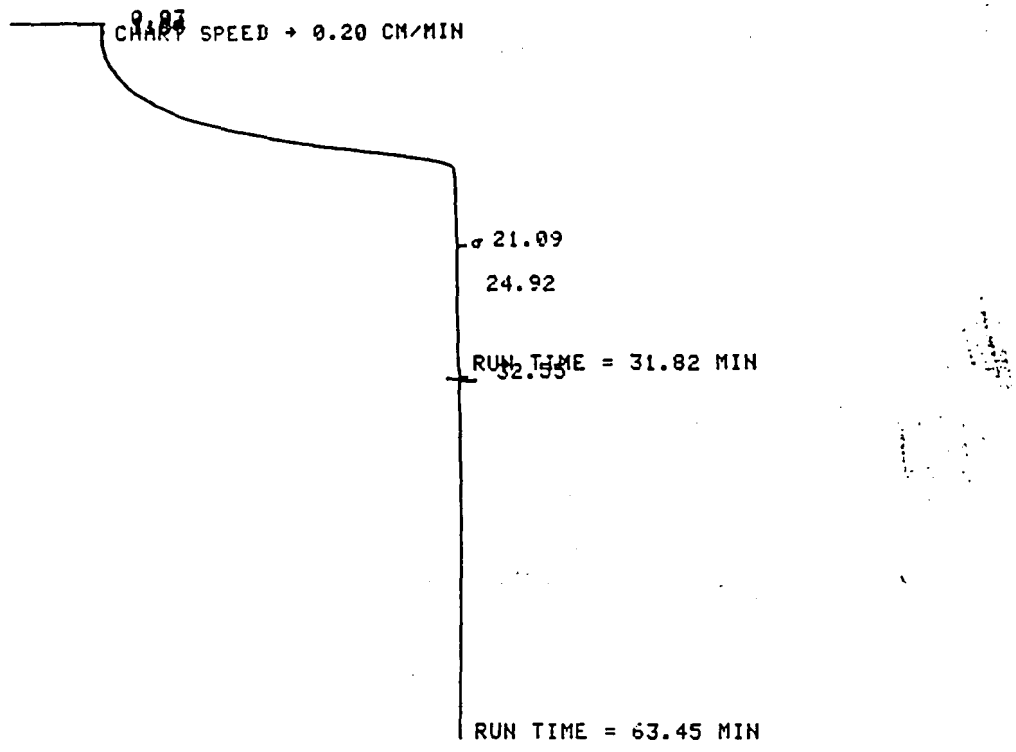

[hp] 5880A MANUAL INJECTION @ 14:36 JAN 27, 1993
AREA %

RT	AREA	TYPE	AREA %
1.54	0.47	BB	3.231
1.80	0.21	BB	1.472
21.09	11.85	BP	81.943
24.92	0.22	BB	1.522
32.55	1.71	BB	11.832

TOTAL AREA = 14.46
MULTIPLIER = 1

RESTEK PAH std 1.0 µL

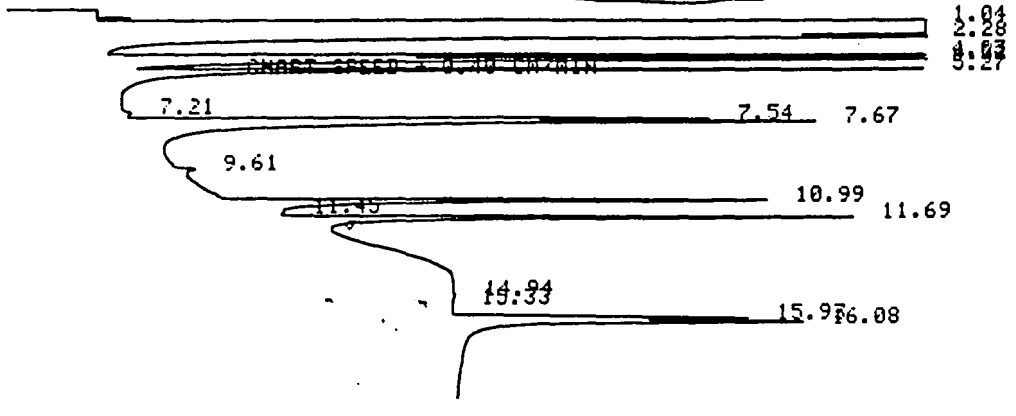

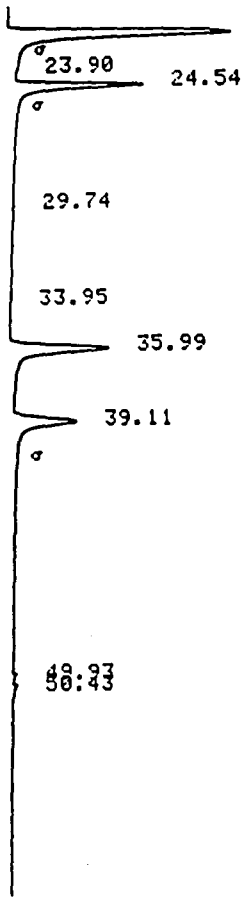

[hp] 5880A MANUAL INJECTION @ 15:42 JAN 27, 1993
AREA %

RT	AREA	TYPE	AREA %
1.04	1338140.00	BV	95.852
2.28	16118.40	VB	1.155
4.03	5394.33	BV	0.386
4.32	9442.33	VV	0.676
5.27	5660.08	VB	0.405
7.21	20.28	BB	0.001
7.54	1884.17	BV	0.135
7.67	4703.20	VB	0.337
9.61	57.44	BB	0.004
10.99	2002.70	BV	0.143
11.45	38.45	VV	0.003
11.69	2820.40	VV	0.202
14.94	8.92	BB	0.001
15.33	0.16	BB	0.000
15.93	1144.04	BV	0.082
16.08	2153.62	VB	0.154
22.32	2830.24	BV	0.203
23.90	0.07	BB	0.000
24.54	1207.97	BV	0.087
29.74	0.05	BB	0.000
33.95	0.90	BB	0.000

39.11	1062.17	BV	0.076
49.93	20.75	BV	0.001
50.43	21.87	VB	0.002

TOTAL AREA = 1396050.00
MULTIPLIER = 1

1.0 ml UTB 21-8110-B Octane cut

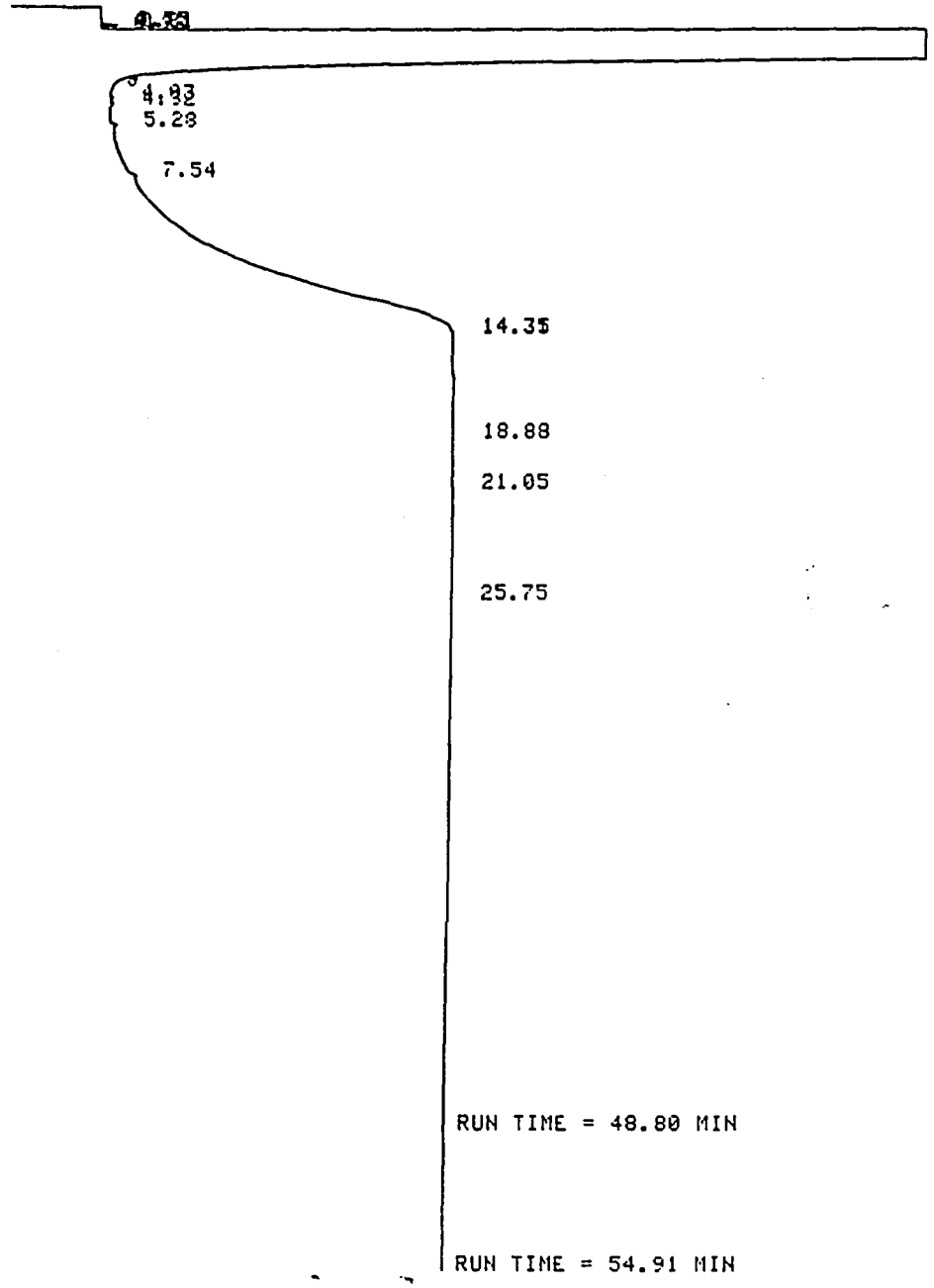

[hp] 5880A MANUAL INJECTION @ 16:45 JAN 27, 1993
AREA %

PT	AREA	TYPE	AREA %

0.75	1.24	BV	0.000
0.81	2.23	PB	0.000
0.92	0.26	BB	0.000
1.01	2497360.00	PV	99.998
4.03	13.99	BB	0.001
4.32	15.36	PB	0.001
5.28	13.08	BB	0.001
14.31	0.66	BV	0.000
14.35	0.24	VB	0.000
18.38	0.06	BB	0.000
21.05	0.03	BB	0.000
25.75	0.17	BB	0.000

TOTAL AREA = 2497400.00
MULTIPLIER = 1

1.0 µL UTB-21 - 8/10 - B CATHODE CUT.

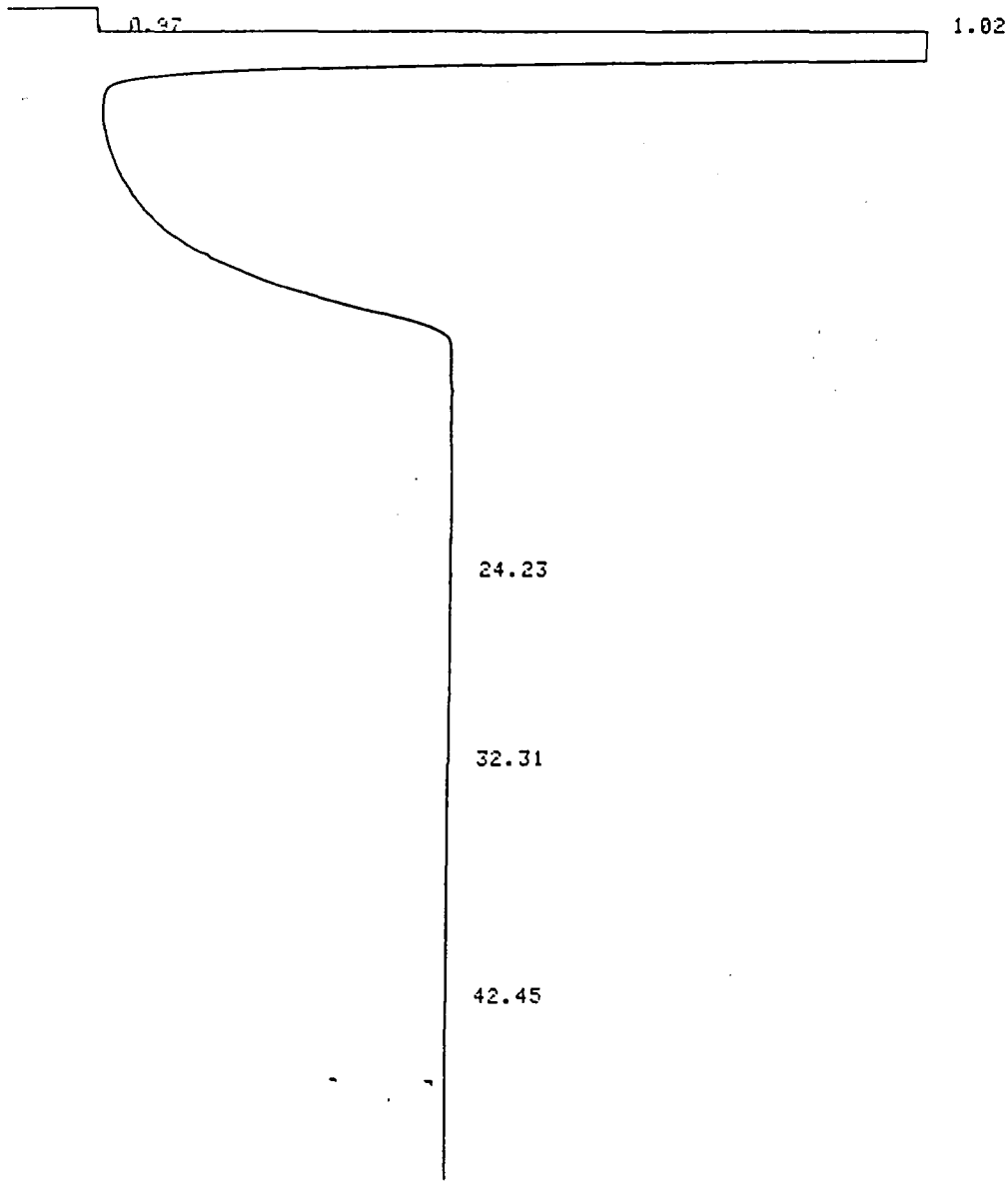

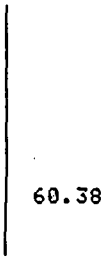

[hp] 5880A MANUAL INJECTION @ 17:42 JAN 27, 1993
AREA %

RT	AREA	TYPE	AREA %
1.02	2364220.00	BB	100.000
24.23	0.09	BB	0.000
32.31	0.09	BB	0.000
42.45	0.06	BB	0.000
60.38	0.07	BB	0.000

TOTAL AREA = 2364220.00
MULTIPLIER = 1

OVEN TEMP INITIAL VALUE 40

PAGE

```
 15.27          0.19   BB      3.242
 17.36          0.13   BB      2.288
 20.43          5.28   BB     89.912
 26.32          0.14   BP      2.384

TOTAL AREA = 5.87
MULTIPLIER = 1

OVEN TEMP LIMIT 300

OVEN TEMP FINAL VALUE 275

OVEN TEMP PRGM RATE 8

OVEN TEMP FINAL VALUE 275

OVEN TEMP FINAL TIME 35

OVEN TEMP INITIAL VALUE 40

OVEN TEMP INITIAL TIME 4

OVEN TEMP INITIAL TIME 5

LIST

OVEN TEMP=40°C  SETPT=40°C  LIMIT=300°C
   EQUIB TIME = 1.00 MIN

OVEN TEMP PROFILE:     (ANNOTATION OFF)
   INITIAL VALUE = 40°C
   INITIAL TIME = 5.00 MIN
   LEVEL 1
      PRGM RATE = 8.00°C/MIN
      FINAL VALUE = 275°C
      FINAL TIME = 35.00 MIN
   POST VALUE = ???
   POST TIME = ???

DET 1 TEMP=220°C  SETPT=220°C  LIMIT=405°C
DET 2 TEMP=0°C  SETPT=50°C(OFF)  LIMIT=405°C
INJ 1 TEMP=150°C  SETPT=150°C  LIMIT=405°C
INJ 2 TEMP=0°C  SETPT=50°C(OFF)  LIMIT=405°C
AUX 1 TEMP=0°C  SETPT=50°C(OFF)  LIMIT=405°C
AUX 2 TEMP=0°C  SETPT=50°C(OFF)  LIMIT=405°C

DEVICE 2: GC TERMINAL 1
   SIGNAL = B
   PLOT = ???
   CHART SPEED = 0.20 CM/MIN
   ATTN = 2↑5
   %OFFSET = 10
   ZERO = 19.72

DETECTOR B: FLAME IONIZATION
   CALIBRATION:  H=1477350  L1=1407200  L2=1406990

VALVES:
   VALVE  1 = OFF
   VALVE  2 = OFF
   VALVE  3 = OFF
   VALVE  4 = OFF
```

```
   VALVE  7 = OFF
   VALVE  8 = OFF
   VALVE  9 = OFF
   VALVE 10 = OFF
   VALVE 11 = OFF
   VALVE 12 = OFF

THRESHOLD = 0
PEAK WIDTH = 0.04

AVAILABLE MEMORY (BYTES): 25024

OVEN TEMP INITIAL VALUE 40

OVEN TEMP INITIAL TIME 5

OVEN TEMP LIMIT 250

OVEN TEMP FINAL TIME 35

OVEN TEMP FINAL VALUE 250

INJ 1 TEMP 220

DET 1 TEMP 250

INJ 1 TEMP 220

INJ 1 TEMP 220

DET 1 TEMP 222

DET 1 TEMP 250
```

① 144 min

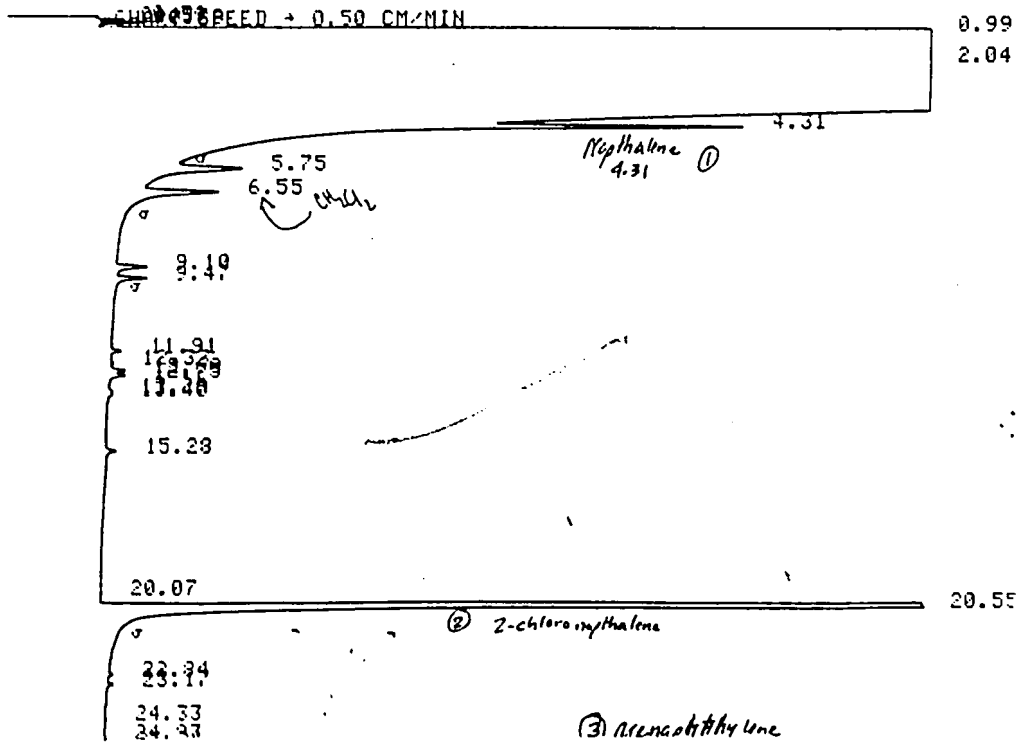

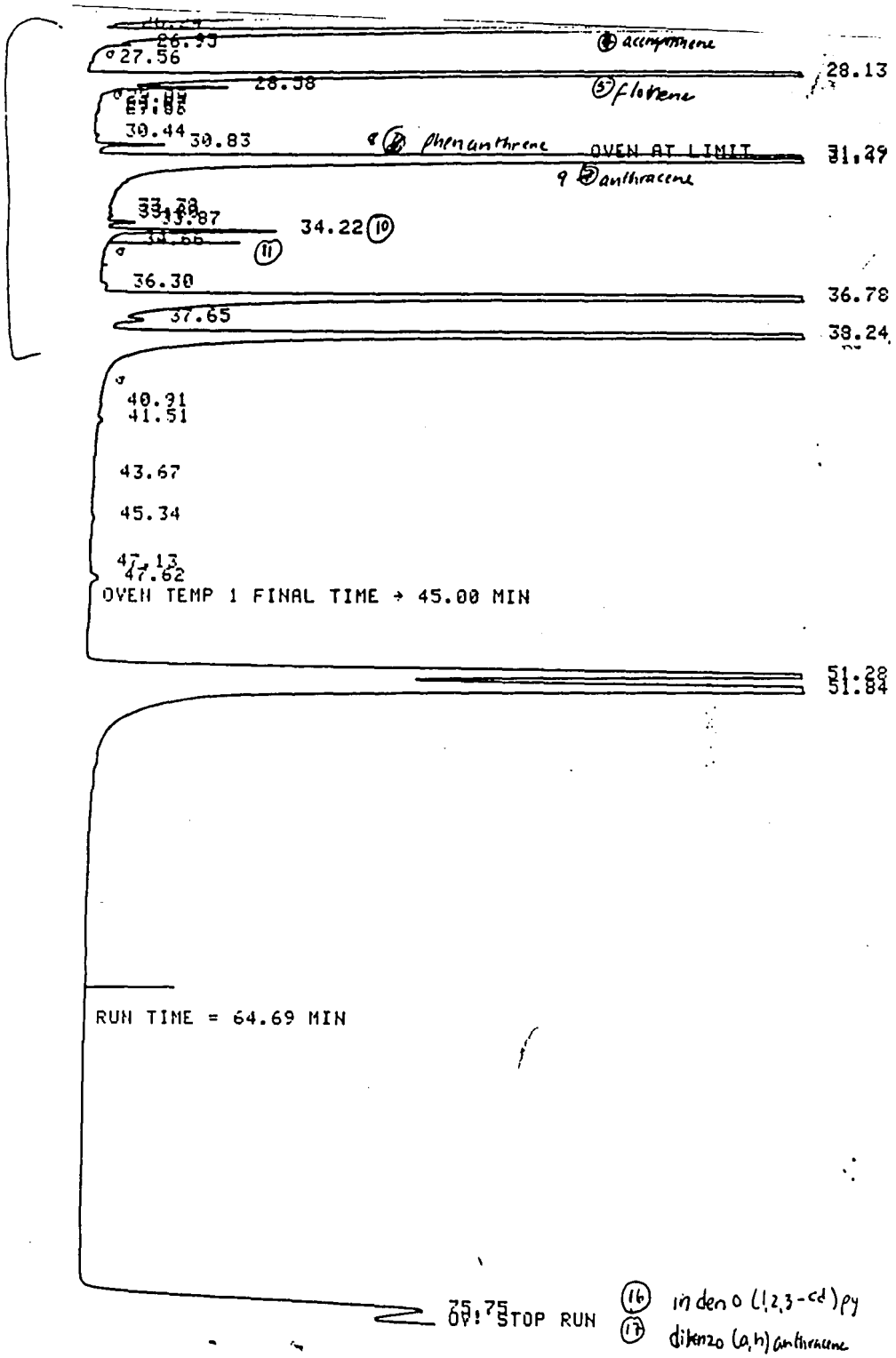

[hp] 5880A MANUAL INJECTION @ 13:36 JAN 4, 1993
AREA %

RT	AREA	TYPE	AREA %

0.36	58.69	BV	0.001
0.49	1.91	BP	0.000
0.57	11.15	PV	0.000
0.68	180.71	VP	0.003
0.99	2524950.00	PV	47.247
2.04	2596680.00	VV	48.590
4.31	6613.41	VV	0.124
5.75	416.45	BB	0.008
6.55	462.69	BP	0.009
9.10	125.02	BB	0.002
9.47	126.01	BP	0.002
11.91	33.15	BB	0.001
12.33	10.89	BV	0.000
12.60	67.07	VV	0.001
12.75	60.96	VB	0.001
13.29	14.00	BV	0.000
13.40	15.73	VB	0.000
15.28	27.81	BB	0.001
20.07	4.63	BB	0.000
20.55	30626.30	BV	0.573
22.84	13.42	BB	0.000
23.17	17.77	BB	0.000
24.33	2.40	BB	0.000
24.97	2.89	BB	0.000
25.24	14.71	BB	0.000
25.80	24617.60	BV	0.461
26.24	49.19	VV	0.001
26.43	24378.40	VV	0.456
27.56	8.92	BB	0.000
28.13	22207.10	BV	0.416
28.58	596.02	VV	0.011
29.09	3.61	BB	0.000
29.37	11.31	BV	0.000
29.53	13.67	VP	0.000
30.44	11.14	BB	0.000
30.83	217.88	BB	0.004
31.29	17836.00	BV	0.334
31.47	19447.60	VB	0.364
33.38	14.96	BP	0.000
33.60	17.64	PB	0.000
33.87	103.46	BB	0.002
34.22	770.47	BV	0.014
34.66	18.21	VP	0.000
36.30	21.14	BB	0.000
36.78	17029.10	BV	0.319
37.65	346.12	VV	0.006
38.24	17817.20	VV	0.333
40.91	14.87	BB	0.000
41.51	35.68	BB	0.001
43.67	10.40	BB	0.000
45.34	31.06	BB	0.001
47.13	16.22	BV	0.000
47.62	91.18	VB	0.002
51.28	11701.20	BV	0.219
51.84	16307.30	VB	0.305
75.75	9807.32	BH	0.184

TOTAL AREA = 5344080.00
MULTIPLIER = 1

OVEN TEMP INITIAL TIME 3

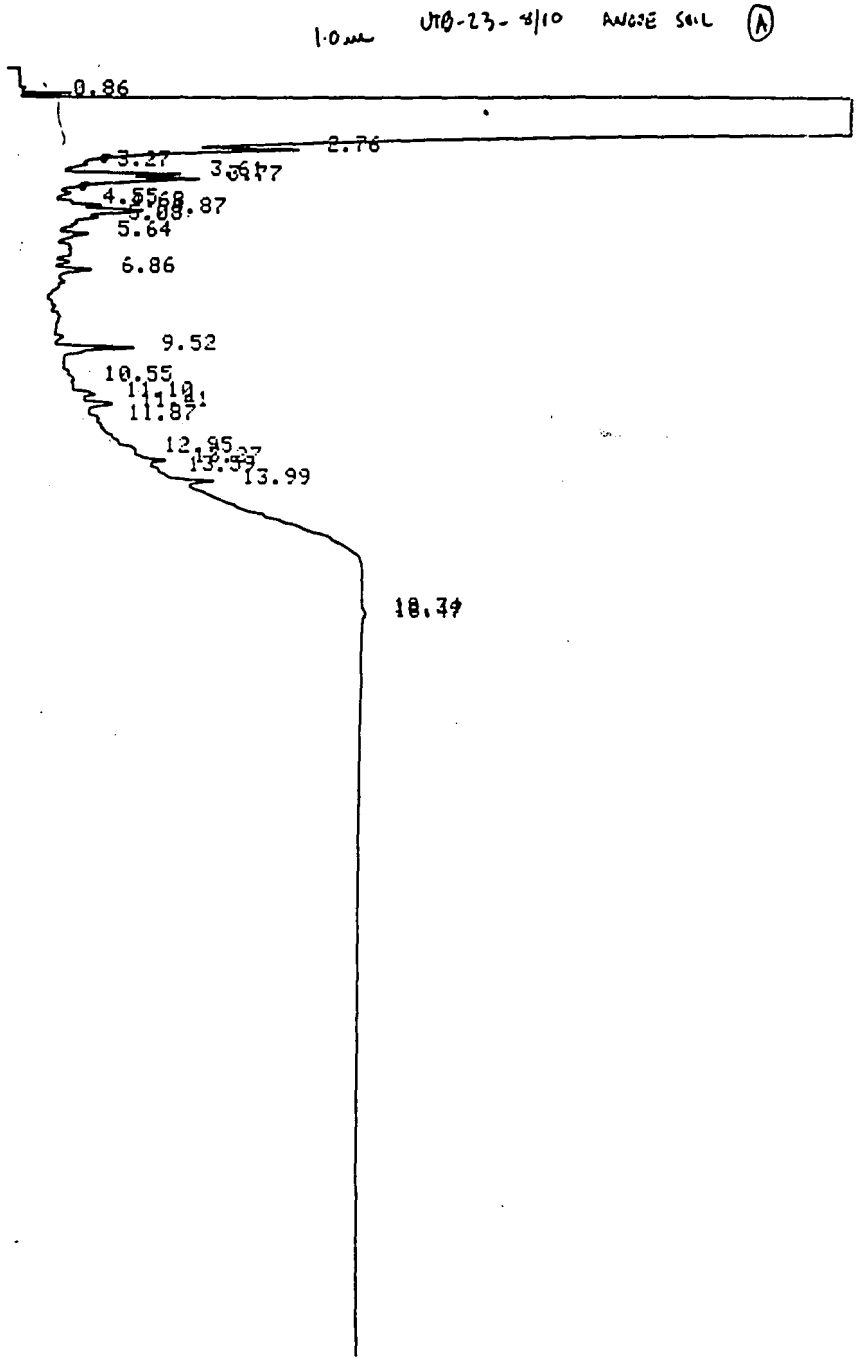
1.0 mm
UTØ-23-4/10 ANDOSE SOIL (A)
0.86
2.76
3.27
3.47
4.55
4.68
5.08
5.87
5.64
6.86
9.52
10.55
11.10
11.87
12.95
13.99
18.74

RUN TIME = 49.50 MIN

[hp]5880A MANUAL INJECTION @ 13:04 FEB 24, 1993
AREA %

RT	AREA	TYPE	AREA %
0.86	6.28	PV	0.000
1.00	2419690.00	BV	99.787
2.76	1528.17	VV	0.063
3.27	13.53	BB	0.001
3.61	448.21	BV	0.018
3.77	890.02	VV	0.037
4.55	48.64	PV	0.002
4.68	173.54	VV	0.007
4.87	535.06	VV	0.022
5.08	201.24	VV	0.008
5.64	185.77	VV	0.008
6.86	175.86	VV	0.007
9.52	384.68	PV	0.016
10.55	29.59	VV	0.001
11.10	98.97	BV	0.004
11.41	138.86	VB	0.006
11.87	17.25	BV	0.001
12.95	41.25	BP	0.002
13.27	79.43	PV	0.003
13.59	3.59	VV	0.000
13.99	142.41	VV	0.006
18.34	8.50	BV	0.000
18.47	14.14	VB	0.001

TOTAL AREA = 2424860.00

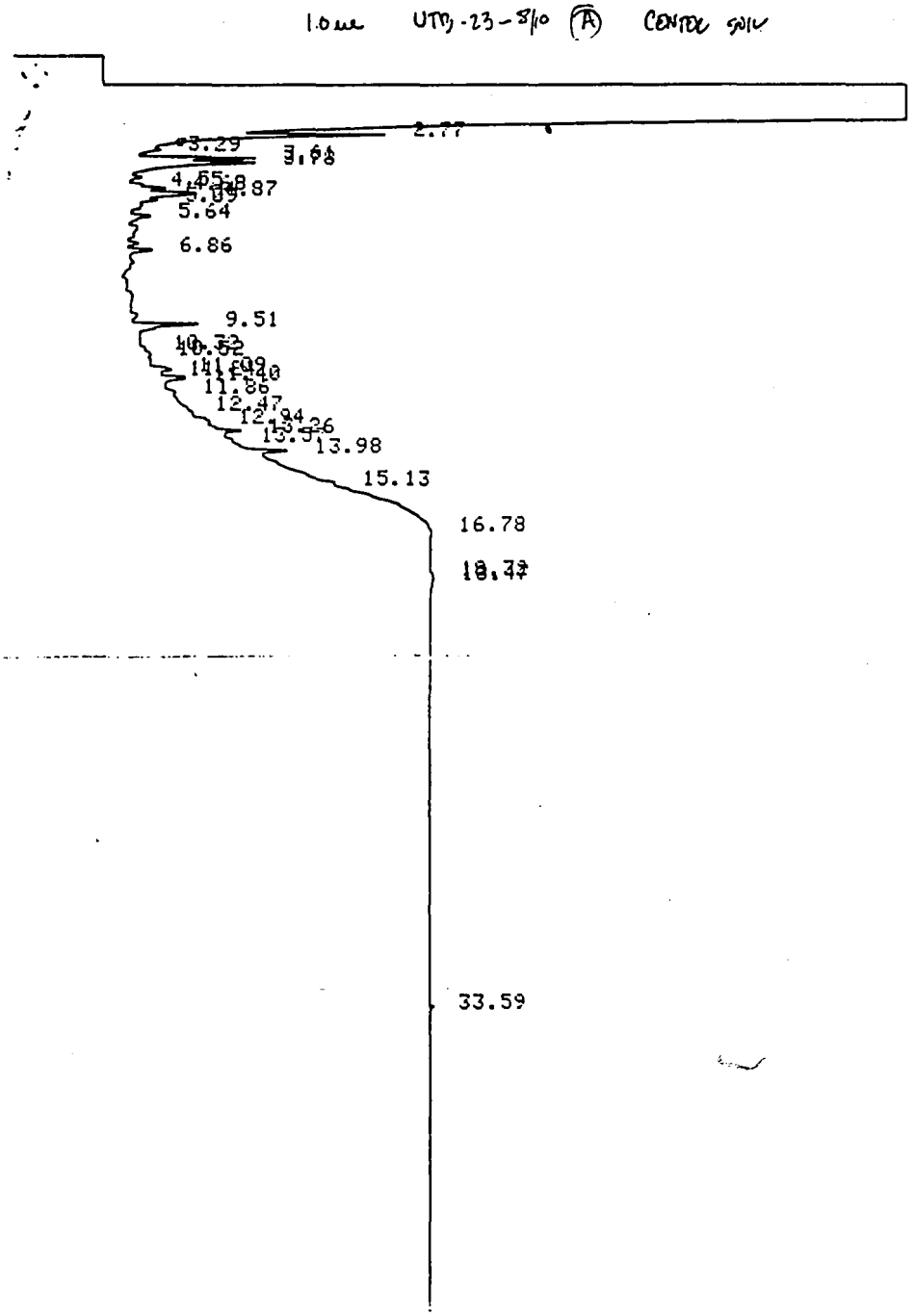
1.0 m UTM-23-8/10 (A) CENTER SOIL
2.77
3.29
3.68
4.87
5.64
6.86
9.51
13.98
15.13
16.78
33.59

RUN STOP RUN 5.48 MIN

[hp] 5880A MANUAL INJECTION @ 13:57 FEB 24, 1993
AREA %

RT	AREA	TYPE	AREA %
1.01	2104930.00	BV	99.794
2.77	1448.96	VV	0.069
3.29	16.30	BB	0.001
3.61	436.55	BV	0.021
3.78	588.29	VB	0.028
4.55	45.64	PV	0.002
4.68	145.87	VV	0.007
4.87	409.37	VV	0.019
5.09	130.04	VV	0.006
5.64	101.61	BP	0.005
6.86	111.31	PB	0.005
9.51	327.07	PV	0.016
10.32	13.22	BV	0.001
10.52	30.31	VV	0.001
11.09	96.01	BV	0.005
11.24	11.49	VV	0.001
11.40	132.24	VB	0.006
11.86	21.35	BV	0.001
12.47	5.86	BV	0.000
12.94	43.31	BP	0.002
13.26	85.21	PV	0.004
13.57	4.16	VP	0.000
13.98	81.50	PP	0.004
15.13	30.95	BV	0.001
16.78	3.04	BB	0.000
18.32	8.31	BV	0.000
18.47	17.70	VB	0.001
33.59	4.04	BH	0.000

TOTAL AREA = 2109280.00
MULTIPLIER = 1

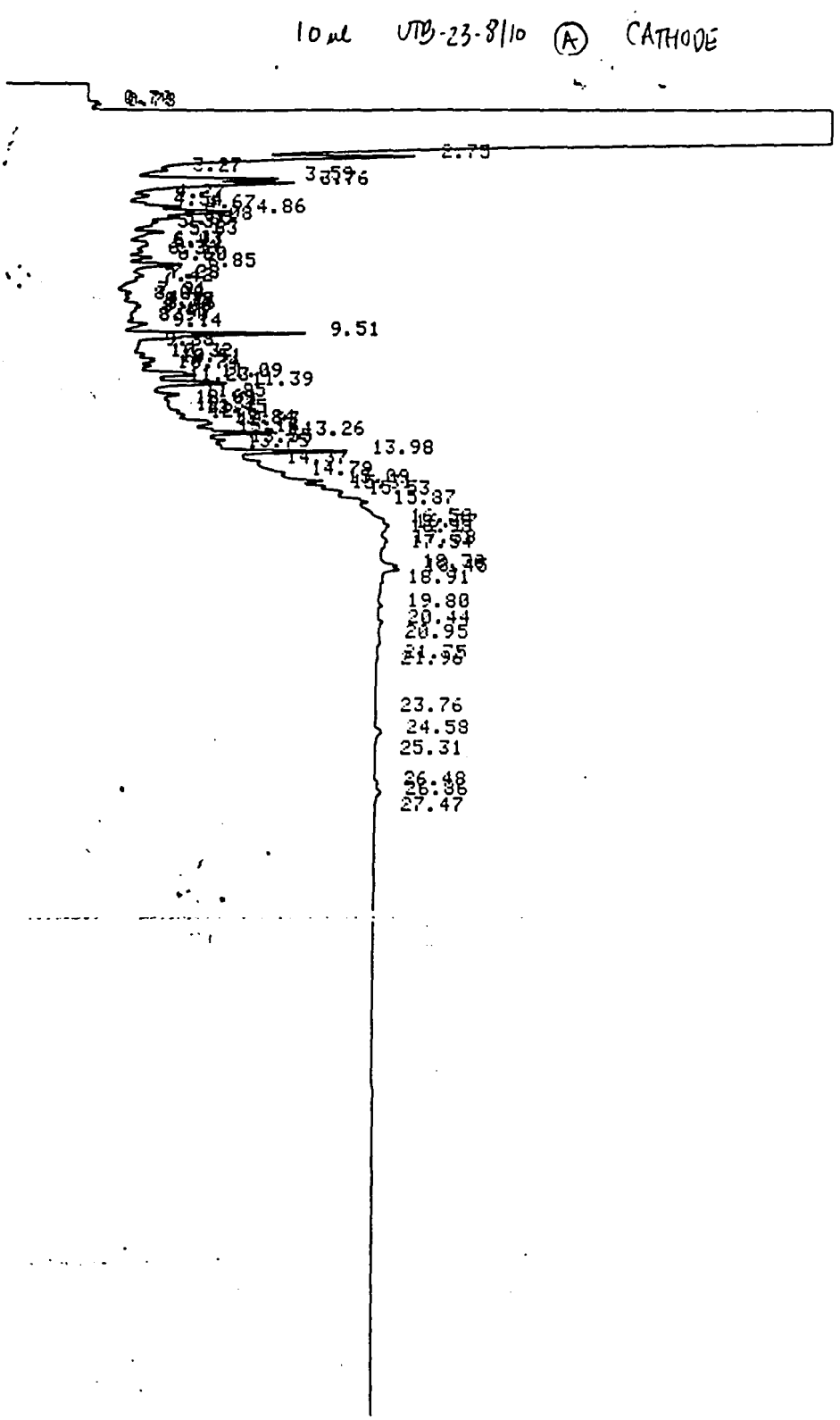
10 µl UTD-23-8/10 (A) CATHODE
2.79
3.27
4.86
9.51
11.39
13.26
13.98
15.87
18.91
19.80
23.76
24.58
25.31
27.47

53.59

OV: STOP RUN

[hp] 5880A MANUAL INJECTION @ 11:00 FEB 25, 1993
AREA %

RT	AREA	TYPE	AREA %
0.70	5.24	BP	0.000
0.78	1.59	BB	0.000
0.99	2773510.00	BV	99.496
2.75	2727.46	VV	0.098
3.27	380.34	VV	0.014
3.59	752.05	VV	0.027
3.76	1304.35	VV	0.047
4.27	110.32	VB	0.004
4.54	60.75	BV	0.002
4.67	229.53	VV	0.008
4.86	697.13	VV	0.025
5.08	269.09	VV	0.010
5.25	144.18	VV	0.005
5.36	129.61	VV	0.005
5.63	269.41	VV	0.010
6.03	90.25	VV	0.003
6.11	140.01	VV	0.005
6.36	131.50	VV	0.005
6.60	168.24	VV	0.006
6.85	404.83	VV	0.015
7.28	195.53	VV	0.007
7.42	147.50	VP	0.005
7.91	44.88	PV	0.002
8.08	37.35	VV	0.001
8.35	43.42	VV	0.002
8.46	64.07	VV	0.002
8.60	32.59	VV	0.001
8.90	10.42	BP	0.000
9.14	114.13	PP	0.004
9.51	916.57	PV	0.033
9.88	14.41	VB	0.001
10.32	39.69	BV	0.001
10.51	99.91	VV	0.004
10.74	43.70	VB	0.002
11.09	305.59	BV	0.011
11.23	44.17	VV	0.002
11.39	438.48	VP	0.016
11.85	85.21	PV	0.003
12.09	29.58	VV	0.001
12.32	6.58	VP	0.000
[illegible]	[illegible]	[illegible]	[illegible]

UTB 23-8/10 (B) Anode. 1.0uL

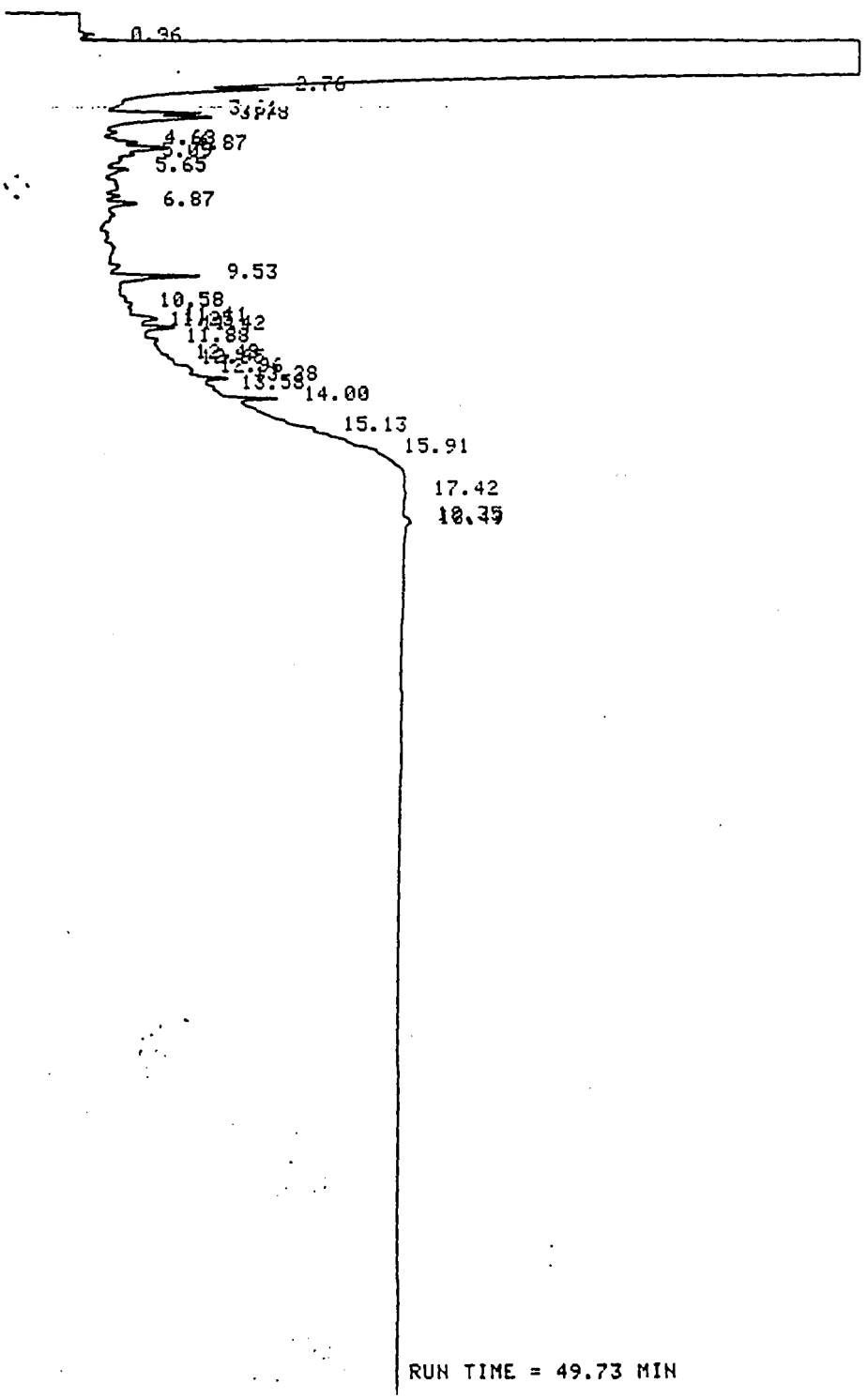

APPENDIX B

MINERALOGY DATA

DETECTED PEAKS FILE 3-AUG-92 18:40

APD1700 Automated Powder Diffractometer System 1

Listed DI file name : SY00:GNH2J03.DI
Original data file name : SY00:GNH2J03.RD
Sample identification : UTB-23-C
Measurement date/time : 3-AUG-92 17:48
Generator settings : 45 kV, 30 mA
Cu alpha1,2 wavelengths : 1.54060, 1.54439 Ang
Step size, sample time : 0.030 deg, 0.90 s, 30.00 s/deg
Monochromator used : Yes
Divergence slit : Automatic (Specimen length: 12.5 mm)

Analysis program number : 35
Peak angle range : 2.000 - 90.020 deg
Range in D spacing : 1.08918 - 44.1372 Ang
Peak position criterion : Top of smoothed data
Cryst peak width range : 0.00 - 2.00 deg
Minim peak significance : 0.75
Number of peaks in file : 43 (Alpha1: 35, Amorphous: 0)
Maximum intensity : 4330. cts, 4810.7 cps

Peak no	Angle (deg)	Tip width (deg)	Peak (cts)	Backg (cts)	D spac (Ang)	I/Imax (%)	Type A1	Type A2	Type Ot	Sign
1	4.0875	0.72	10.	216.	21.5997	0.24	X	X		0.87
2	8.8300	0.09	10.	135.	10.0065	0.24	X	X		0.81
3	12.3725	0.30	32.	85.	7.1482	0.75	X	X		1.10
4	17.6650	0.36	37.	92.	5.0167	0.86	X	X		1.07
5	19.7075	0.15	166.	112.	4.5012	3.84	X	X		0.79
6	20.7850	0.12	773.	123.	4.2702	17.85	X	X		5.13
7	23.5100	0.18	90.	174.	3.7810	2.08	X	X		1.05
8	25.3875	0.60	88.	177.	3.5055	2.04	X	X		1.74
9	26.5725	0.12	4330.	180.	3.3518	100.00	X	X		12.88
10	27.4025	0.09	282.	180.	3.2521	6.52	X	X		1.86
11	27.9900	0.12	441.	182.	3.1852	10.19	X	X		2.88
12	29.6875	0.18	102.	185.	3.0068	2.36	X	X		1.38
13	32.0800	0.36	12.	188.	2.7878	0.27	X	X		0.89
14	34.9650	0.30	156.	156.	2.5641	3.61	X	X		0.79
15	36.4775	0.15	437.	156.	2.4612	10.09	X	X		4.27
16	37.5725	0.36	66.	156.	2.3919	1.52	X	X		0.78
17	39.4050	0.12	353.	159.	2.2848	8.16	X	X		2.40
18	40.2350	0.12	237.	154.	2.2396	5.48	X	X		1.78
19	42.3850	0.21	299.	159.	2.1308	6.91	X	X		7.08
20	45.7175	0.09	216.	149.	1.9830	4.99	X	X		0.78
21	48.0425	0.36	28.	132.	1.8923	0.65	X	X		1.15
22	49.7050	0.09	125.	128.	1.8328	2.90	X	X		1.35
23	50.0650	0.12	778.	128.	1.8205	17.98	X	X		3.98
24	54.7875	0.09	303.	144.	1.6742	6.99	X	X		1.07
25	59.8850	0.09	605.	144.	1.5433	13.98	X			1.62
26	60.0700	0.09	292.	144.	1.5428	6.75		X		0.81
27	61.7325	0.72	100.	149.	1.5015	2.31	X	X		3.39
28	63.9425	0.09	114.	156.	1.4548	2.64	X	X		0.95
29	67.6575	0.09	380.	154.	1.3837	8.78			Ot	1.10
30	68.2525	0.09	497.	154.	1.3730	11.49			Ot	1.15

31	72.0050	0.36	72.	146.	1.3104	1.67	X	X		1.66
32	73.3750	0.12	166.	149.	1.2893	3.84	X	X		1.38
33	75.5775	0.21	193.	154.	1.2571	4.46	X			4.47
34	75.8125	0.09	112.	154.	1.2569	2.60		X		1.51
35	77.5475	0.09	130.	146.	1.2300	3.00	X			1.82
36	77.8025	0.09	76.	144.	1.2296	1.75		X		0.85
37	79.7975	0.09	185.	135.	1.2009	4.27	X			0.83
38	80.0425	0.12	159.	128.	1.2008	3.67		X		0.79
39	81.0825	0.12	149.	128.	1.1851	3.44	X			1.32
40	81.4050	0.15	204.	128.	1.1812	4.72	X	X		1.91
41	81.6825	0.18	86.	125.	1.1808	2.00		X		1.00
42	83.7650	0.12	108.	117.	1.1538	2.50			Ot	0.85
43	87.4725	0.96	16.	119.	1.1142	0.37	X	X		1.10

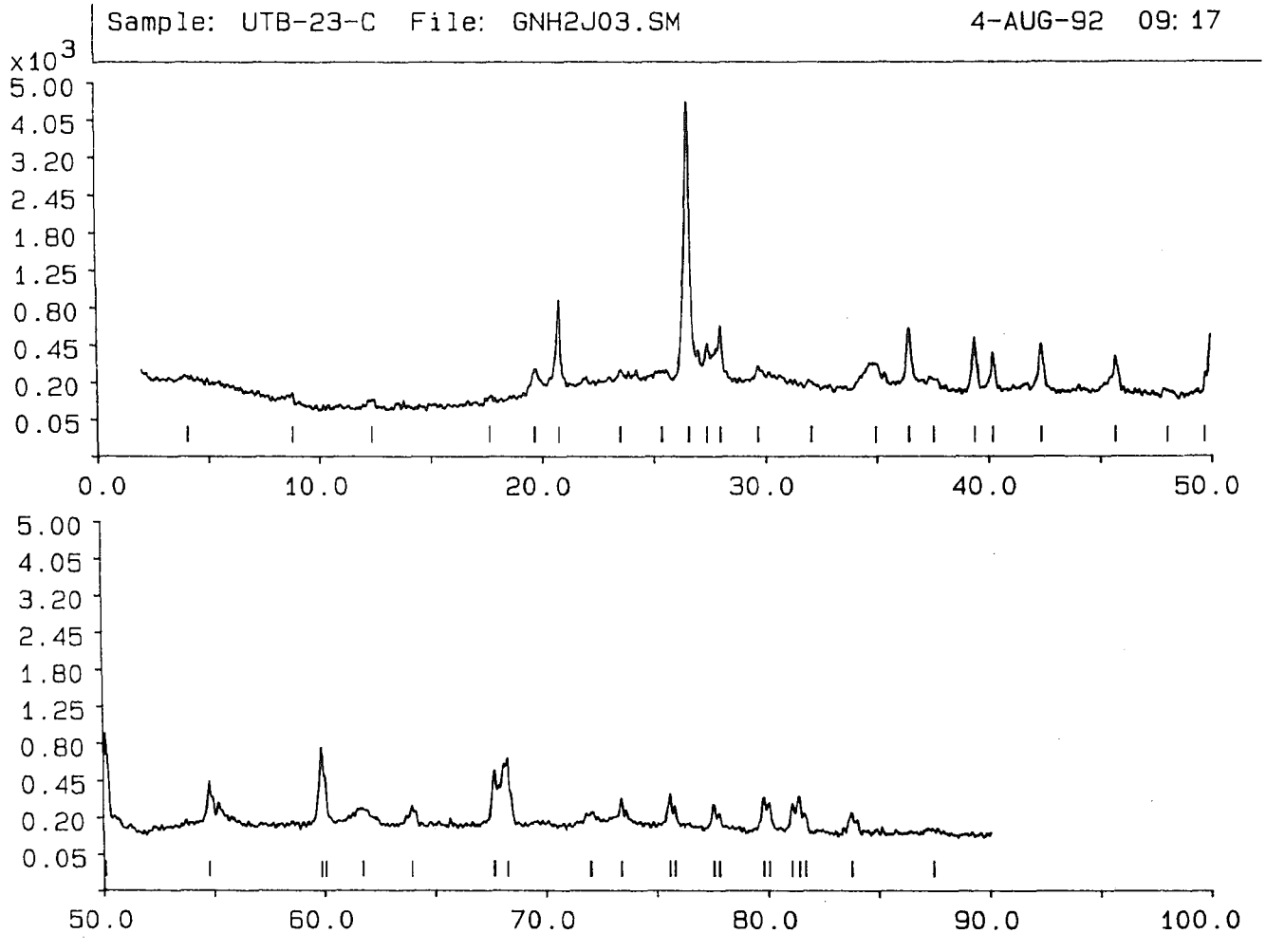
Sample: UTB-23-C File: GNH2J03.SM
4-AUG-92 09:17
x10^3
5.00
4.05
3.20
2.45
1.80
1.25
0.80
0.45
0.20
0.05
0.0
10.0
20.0
30.0
40.0
50.0
5.00
4.05
3.20
2.45
1.80
1.25
0.80
0.45
0.20
0.05
50.0
60.0
70.0
80.0
90.0
100.0

DETECTED PEAKS FILE 3-AUG-92 23:50

APD1700 Automated Powder Diffractometer System 1

Listed DI file name : SY00:GNH3J05.DI
Original data file name : SY00:GNH3J05.RD
Sample identification : UTB-23-Cen
Measurement date/time : 3-AUG-92 22:57
Generator settings : 45 kV, 30 mA
Cu alpha1,2 wavelengths : 1.54060, 1.54439 Ang
Step size, sample time : 0.030 deg, 0.90 s, 30.00 s/deg
Monochromator used : Yes
Divergence slit : Automatic (Specimen length: 12.5 mm)

Analysis program number : 35
Peak angle range : 2.000 - 90.020 deg
Range in D spacing : 1.08918 - 44.1372 Ang
Peak position criterion : Top of smoothed data
Cryst peak width range : 0.00 - 2.00 deg
Minim peak significance : 0.75
Number of peaks in file : 53 (Alpha1: 43, Anomalous: 0)
Maximum intensity : 6084. cts, 6760.0 cps

Peak no	Angle (deg)	Tip width (deg)	Peak (cts)	Backg (cts)	D spac (Ang)	I/Imax (%)	Type A1	Type A2	Type Qt	Sign
1	4.2175	0.36	34.	210.	20.9342	0.55	X	X		0.93
2	12.2800	0.36	18.	85.	7.2019	0.29	X	X		0.87
3	17.5550	0.18	32.	77.	5.0479	0.53	X	X		0.83
4	19.5650	0.15	166.	83.	4.5336	2.74	X	X		0.95
5	20.7375	0.15	756.	83.	4.2799	12.43	X	X		6.76
6	21.8475	0.18	259.	83.	4.0649	4.26	X	X		4.90
7	23.3150	0.09	177.	83.	3.8122	2.91	X	X		1.26
8	24.0700	0.36	94.	83.	3.6943	1.55	X	X		1.05
9	25.3650	0.09	182.	83.	3.5086	3.00	X	X		1.23
10	26.5125	0.18	6084.	83.	3.3593	100.00	X	X		36.31
11	27.3450	0.18	234.	83.	3.2588	3.85	X	X		1.23
12	27.8375	0.12	433.	83.	3.2023	7.11	X	X		3.02
13	29.2350	0.18	207.	83.	3.0523	3.41	X	X		3.16
14	29.7525	0.18	121.	83.	3.0004	1.99	X	X		1.10
15	30.6650	0.18	110.	83.	2.9132	1.81	X	X		1.26
16	32.1850	0.36	27.	83.	2.7790	0.44	X	X		0.89
17	34.8300	0.30	243.	83.	2.5738	4.00	X	X		1.86
18	36.4125	0.18	595.	86.	2.4654	9.79	X	X		7.59
19	37.5275	0.30	112.	88.	2.3947	1.85	X	X		0.91
20	39.3450	0.12	576.	92.	2.2882	9.47	X	X		3.39
21	40.1650	0.21	282.	94.	2.2433	4.64	X	X		6.61
22	41.5925	0.24	64.	98.	2.1696	1.05	X	X		0.89
23	42.3275	0.15	420.	100.	2.1336	6.91	X	X		3.16
24	45.6700	0.09	306.	106.	1.9849	5.03	X	X		1.02
25	47.1200	0.48	38.	100.	1.9272	0.63	X	X		0.95
26	48.1700	0.48	36.	96.	1.8876	0.59	X	X		0.87
27	50.0050	0.15	1116.	90.	1.8225	18.34	X			6.76
28	50.1375	0.09	581.	90.	1.8225	9.55		X		1.48
29	54.7300	0.18	357.	112.	1.6758	5.87	X	X		3.55
30	55.1775	0.09	185.	114.	1.6633	3.04	X	X		0.85

31	59.8025	0.15	829.	102.	1.5452	13.63	X		6.46
32	59.9900	0.06	488.	102.	1.5446	8.03		X	2.24
33	61.6350	0.30	139.	104.	1.5036	2.29	X	X	1.23
34	63.9200	0.12	168.	106.	1.4552	2.74	X	X	0.93
35	67.5925	0.09	676.	100.	1.3848	11.11		Ot	2.00
36	68.1975	0.09	625.	100.	1.3740	10.27		Ot	0.98
37	69.2525	0.30	49.	102.	1.3556	0.81	X	X	0.95
38	73.3075	0.12	216.	110.	1.2903	3.55		Ot	1.70
39	75.5100	0.12	237.	123.	1.2581	3.90	X		1.66
40	75.7375	0.12	149.	123.	1.2579	2.45		X	1.07
41	77.5075	0.18	96.	117.	1.2306	1.58	X		1.95
42	77.8000	0.09	64.	108.	1.2297	1.05		X	1.05
43	79.7325	0.12	246.	102.	1.2017	4.05	X		1.66
44	79.9875	0.09	188.	102.	1.2015	3.08		X	1.48
45	81.0200	0.12	615.	88.	1.1858	10.11	X		4.37
46	81.3125	0.15	484.	88.	1.1823	7.96	X	X	3.31
47	81.5900	0.15	161.	88.	1.1819	2.65		X	1.58
48	83.6875	0.15	151.	88.	1.1547	2.49	X		2.00
49	83.9525	0.12	104.	86.	1.1546	1.71		X	1.20
50	84.8200	0.15	35.	85.	1.1421	0.57	X	X	0.87
51	86.2325	0.72	12.	83.	1.1270	0.19	X	X	0.89
52	87.4025	0.36	24.	79.	1.1149	0.39	X	X	1.12
53	89.6400	0.30	19.	76.	1.0928	0.32	X	X	0.76

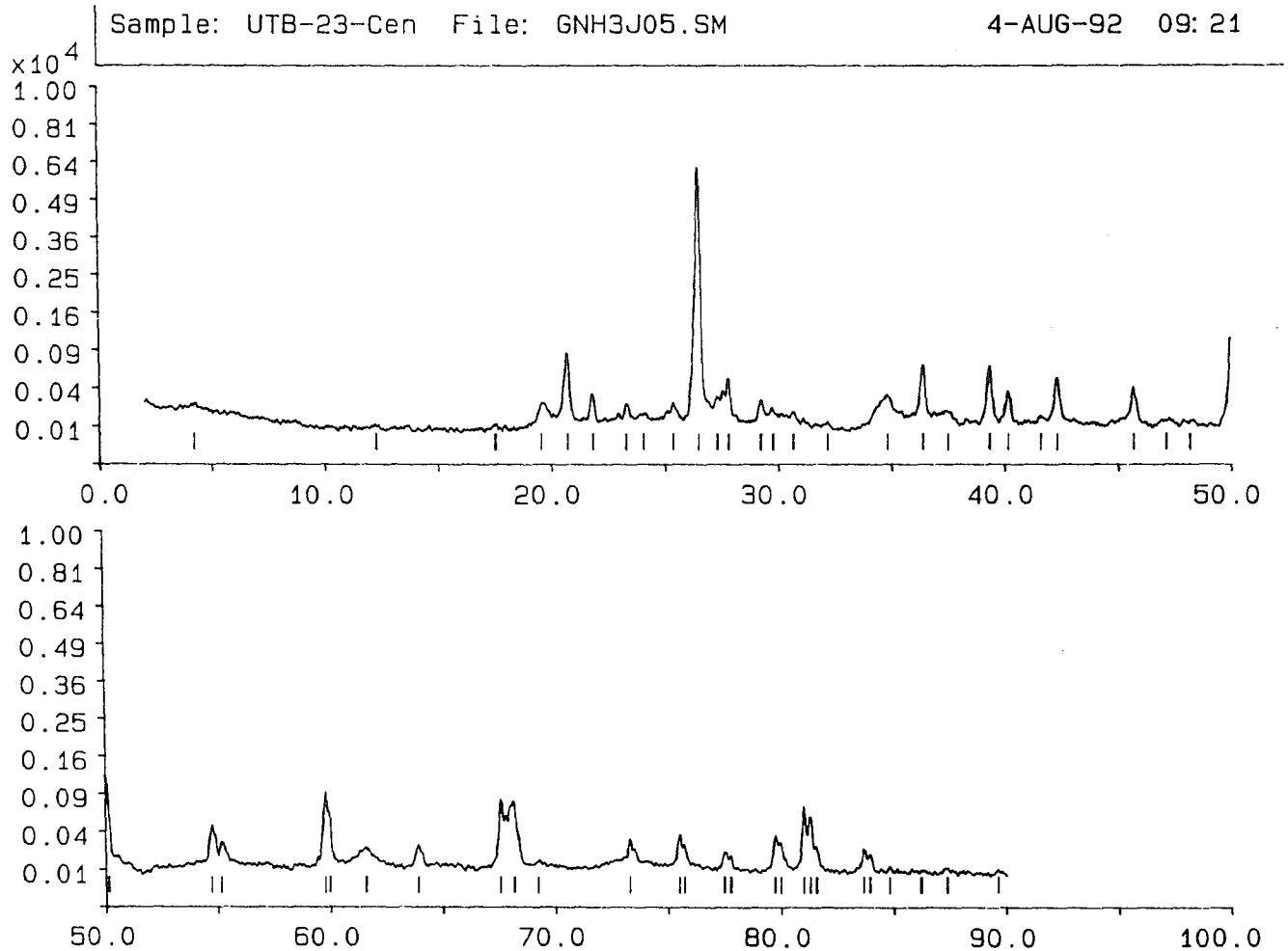
Sample: UTB-23-Cen File: GNH3J05.SM 4-AUG-92 09: 21
x10^4
1.00
0.81
0.64
0.49
0.36
0.25
0.16
0.09
0.04
0.01
0.0
10.0
20.0
30.0
40.0
50.0
1.00
0.81
0.64
0.49
0.36
0.25
0.16
0.09
0.04
0.01
50.0
60.0
70.0
80.0
90.0
100.0

DETECTED PEAKS FILE 3-AUG-92 19:33

APD1700 Automated Powder Diffractometer System 1

Listed DI file name : SY00:GNH1J03.DI
Original data file name : SY00:GNH1J03.RD
Sample identification : UTB-23-D
Measurement date/time : 3-AUG-92 18:40
Generator settings : 45 kV, 30 mA
Cu alpha1,2 wavelengths : 1.54060, 1.54439 Ang
Step size, sample time : 0.030 deg, 0.90 s, 30.00 s/deg
Monochromator used : Yes
Divergence slit : Automatic (Specimen length: 12.5 mm)

Analysis program number : 35
Peak angle range : 2.000 - 90.020 deg
Range in D spacing : 1.08918 - 44.1372 Ang
Peak position criterion : Top of smoothed data
Cryst peak width range : 0.00 - 2.00 deg
Minim peak significance : 0.75
Number of peaks in file : 41 (Alpha1: 35. Amorphous: 0)
Maximum intensity : 3014. cts. 3348.9 cps

Peak no	Angle (deg)	Tip width (deg)	Peak (cts)	Backg (cts)	D spac (Ang)	I/Imax (%)	Type A1	Type A2	Type Dt	Sign
1	4.2950	1.44	17.	185.	20.5566	0.56	X	X		2.75
2	19.4975	0.36	106.	106.	4.5492	3.52	X	X		2.24
3	20.6150	0.15	552.	100.	4.3050	18.32	X	X		5.01
4	21.7700	0.12	119.	100.	4.0791	3.94	X	X		0.87
5	23.2850	0.30	104.	100.	3.8171	3.45	X	X		1.29
6	25.0275	0.48	102.	100.	3.5551	3.38	X	X		0.83
7	26.3875	0.27	3014.	100.	3.3749	100.00	X	X		47.86
8	27.1925	0.09	182.	98.	3.2768	6.05	X	X		0.78
9	27.6025	0.15	196.	98.	3.2290	6.50	X	X		0.83
10	29.1200	0.24	161.	98.	3.0641	5.35	X	X		2.04
11	30.6050	0.15	225.	98.	2.9187	7.47	X	X		3.16
12	34.6075	0.84	128.	98.	2.5898	4.24	X	X		6.17
13	36.2975	0.21	272.	102.	2.4730	9.03	X	X		5.01
14	39.2075	0.21	279.	114.	2.2959	9.25	X	X		6.03
15	40.0325	0.21	123.	114.	2.2505	4.09	X	X		2.34
16	42.2225	0.15	237.	123.	2.1387	7.87	X	X		2.82
17	45.5300	0.12	182.	110.	1.9907	6.05	X	X		1.58
18	47.1825	0.36	46.	104.	1.9247	1.53	X	X		1.66
19	48.0850	0.48	45.	102.	1.8907	1.49	X	X		1.07
20	49.9025	0.18	590.	94.	1.8260	19.59	X	X		6.92
21	52.1550	0.30	28.	86.	1.7523	0.93	X	X		0.78
22	53.0375	0.36	44.	85.	1.7252	1.45	X	X		0.87
23	54.6050	0.09	216.	100.	1.6794	7.17	X	X		2.09
24	57.1250	0.24	26.	114.	1.6111	0.86	X	X		0.78
25	59.6850	0.12	449.	102.	1.5480	14.91	X			2.04
26	59.8975	0.15	269.	102.	1.5468	8.92		X		1.02
27	60.4975	0.18	64.	104.	1.5291	2.12	X	X		0.91
28	61.4200	0.48	94.	106.	1.5083	3.12	X	X		1.82
29	63.7975	0.12	92.	110.	1.4577	3.06	X	X		0.85
30	65.4550	0.60	18.	102.	1.4248	0.61	X	X		0.83

31	67.4725	0.09	433.	92.	1.3870	14.35			Ot	1.58
32	67.9175	0.09	480.	88.	1.3790	15.91	X			1.45
33	68.0950	0.09	488.	88.	1.3792	16.20		X		1.91
34	73.1600	0.06	210.	102.	1.2926	6.98			Ot	3.24
35	75.4200	0.15	142.	114.	1.2593	4.70	X	X		1.58
36	77.4725	0.24	52.	108.	1.2310	1.72	X	X		0.76
37	79.6900	0.12	196.	88.	1.2023	6.50			Ot	1.02
38	80.9325	0.18	130.	86.	1.1869	4.31	X			0.83
39	81.2575	0.15	185.	86.	1.1859	6.14		X		1.32
40	83.6050	0.24	83.	86.	1.1556	2.75	X	X		0.95
41	84.7125	0.36	22.	86.	1.1433	0.73	X	X		0.78

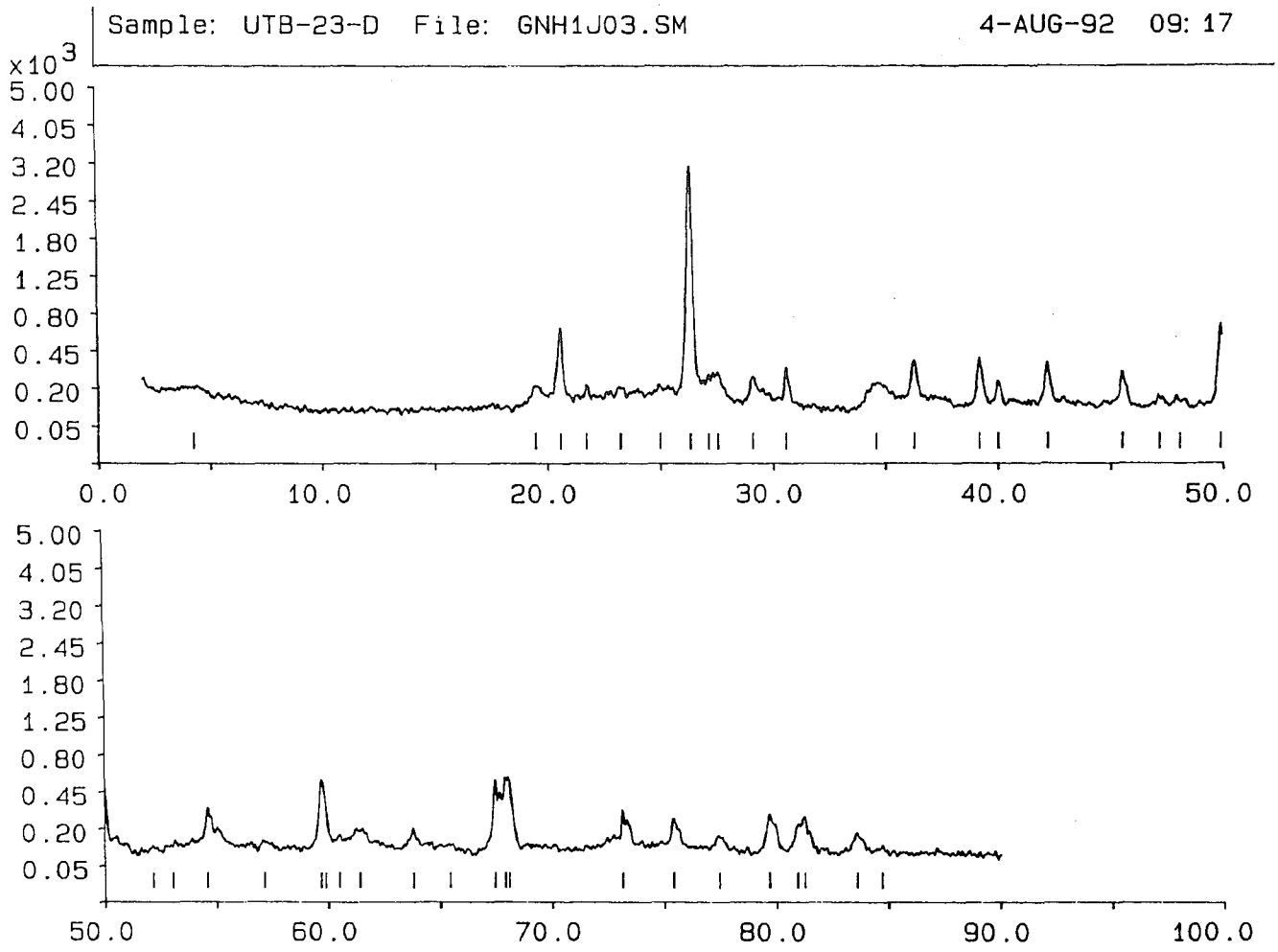
Sample: UTB-23-D File: GNH1J03.SM 4-AUG-92 09: 17
x10^3
5.00
4.05
3.20
2.45
1.80
1.25
0.80
0.45
0.20
0.05
0.0
10.0
20.0
30.0
40.0
50.0
5.00
4.05
3.20
2.45
1.80
1.25
0.80
0.45
0.20
0.05
50.0
60.0
70.0
80.0
90.0
100.0

DETECTED PEAKS FILE 12-AUG-92 17:54

APD1700 Automated Powder Diffractometer System 1

Listed DI file name : SY00:GB1J02.DI
Original data file name : SY00:GB1J02.RD
Sample identification : UTB24T8'-10'
Measurement date/time : 12-AUG-92 16:42
Generator settings : 45 kV, 30 mA
Cu alpha1,2 wavelengths : 1.54060, 1.54439 Ang
Step size, sample time : 0.030 deg, 0.90 s, 30.00 s/deg
Monochromator used : Yes
Divergence slit : Automatic (Specimen length: 12.5 mm)

Analysis program number : 35
Peak angle range : 2.000 - 90.020 deg
Range in D spacing : 1.08918 - 44.1372 Ang
Peak position criterion : Top of smoothed data
Crvst peak width range : 0.00 - 2.00 deg
Minim peak significance : 0.75
Number of peaks in file : 68 (Alpha1: 60, Amorphous: 0)
Maximum intensity : 4100. cts, 4665.6 cps

Peak no	Angle (deg)	Tip width (deg)	Peak (cts)	Backg (cts)	D spac (Ang)	I/Imax (%)	Type A1	Type A2	Type Dt	Sign
1	4.1700	1.20	10.	216.	21.1725	0.24	X	X		1.32
2	5.1100	0.24	14.	177.	14.4536	0.34	X	X		0.85
3	8.6950	0.12	154.	125.	10.1615	3.66	X	X		0.76
4	9.8325	0.15	144.	125.	10.0037	3.43	X	X		1.86
5	12.4425	0.18	154.	83.	7.1082	3.66	X	X		3.09
6	17.6800	0.09	117.	71.	5.0125	2.78	X	X		1.23
7	18.7175	0.18	56.	71.	4.7369	1.34	X	X		1.29
8	19.7100	0.12	151.	71.	4.5006	3.60	X	X		1.05
9	20.7250	0.18	1018.	71.	4.2702	< 24.23	<	X		13.49
10	21.9575	0.18	67.	72.	4.0447	1.60	X	X		1.17
11	22.4525	0.18	94.	72.	3.9567	2.24	X	X		1.05
12	23.3900	0.21	193.	72.	3.8002	4.60	X	X		3.89
13	24.1075	0.18	92.	72.	3.6887	2.19	X	X		0.83
14	25.0625	0.12	262.	72.	3.5502	< 6.25	X	X		1.17
15	26.5500	0.18	4199.	72.	3.3546	< 100.00	X	X		24.55
16	27.4375	0.12	724.	72.	3.2481	< 17.23	X	X		3.39
17	27.8325	0.12	467.	72.	3.2029	< 11.11	<	X		1.29
18	29.6950	0.12	196.	74.	3.0061	4.67	X	X		0.85
19	30.8825	0.21	1840.	74.	2.8931	< 43.83	X	X		23.44
20	32.0050	0.48	76.	74.	2.7942	1.80	X	X		1.07
21	33.4575	0.18	137.	74.	2.6761	3.26	X	X		2.24
22	34.4325	0.36	199.	74.	2.6025	4.73	X	X		1.82
23	34.8900	0.09	317.	74.	2.5695	< 7.55	X	X		1.26
24	36.4650	0.21	538.	74.	2.4620	< 12.82	X	X		9.77
25	37.2525	0.12	190.	76.	2.4119	4.54	X	X		0.89
26	37.6125	0.18	142.	76.	2.3895	3.37	X	X		0.85
27	39.3975	0.18	372.	76.	2.2852	< 8.87	X	X		6.31
28	40.2150	0.12	240.	76.	2.2407	5.72	X	X		1.52
29	41.0425	0.21	296.	76.	2.1974	< 7.05	Y	X		6.31
30	42.3750	0.21	502.	76.	2.1313	< 11.95	X	X		8.91

31	43.6925	0.24	66.	76.	2.0790	1.56	X	X		0.81
32	44.8500	0.12	234.	77.	2.0193	5.57	X	X		1.78
33	45.7500	0.12	335.	77.	1.9816	7.98	X	X		1.15
34	48.0775	0.24	46.	77.	1.8910	1.10	X	X		0.95
35	49.1200	0.30	74.	77.	1.8533	1.76	X	X		2.00
36	50.0600	0.12	870.	81.	1.8206	20.72	X	X		4.27
37	50.4750	0.18	424.	81.	1.8066	10.11	X	X		4.07
38	50.9975	0.12	420.	83.	1.7894	10.01	X	X		2.09
39	54.7875	0.09	286.	104.	1.6742	6.80	X	X		2.75
40	55.3050	0.18	225.	104.	1.6597	5.36	X	X		1.35
41	58.8175	0.36	62.	104.	1.5687	1.49	X	X		1.95
42	59.8525	0.15	718.	98.	1.5440	17.10	X	X		5.13
43	61.6400	0.54	139.	100.	1.5035	3.32	X	X		5.62
44	63.3500	0.24	69.	102.	1.4679	1.64	X	X		1.12
45	63.9025	0.09	166.	102.	1.4556	3.96			Ot	2.00
46	65.0700	0.12	100.	104.	1.4323	2.38	X	X		0.83
47	65.9975	0.60	49.	104.	1.4144	1.17	X	X		2.34
48	67.6125	0.12	488.	106.	1.3845	11.63	X	X		3.16
49	68.2400	0.12	581.	106.	1.3733	13.83	X	X		2.09
50	68.7825	0.09	117.	108.	1.3637	2.78			Ot	0.87
51	69.3725	0.36	53.	108.	1.3536	1.27	X	X		1.02
52	70.4175	0.15	108.	110.	1.3360	2.58	X	X		1.00
53	73.3725	0.12	169.	112.	1.2894	4.02	X			1.26
54	73.6050	0.09	104.	112.	1.2890	2.48		X		0.91
55	74.6850	0.42	83.	108.	1.2699	1.97	X	X		3.69
56	75.5650	0.12	196.	104.	1.2573	4.67	X			2.14
57	75.8225	0.12	104.	102.	1.2567	2.48		X		1.26
58	77.5675	0.12	135.	96.	1.2298	3.20			Ot	1.95
59	79.7975	0.12	237.	86.	1.2009	5.65	X			2.09
60	80.0475	0.09	174.	85.	1.2007	4.15		X		1.66
61	81.0875	0.12	174.	83.	1.1850	4.15	X			2.29
62	81.3800	0.18	259.	83.	1.1815	6.17	X	X		4.47
63	81.6700	0.09	114.	83.	1.1809	2.73		X		1.26
64	82.5800	0.18	45.	81.	1.1674	1.07	X	X		1.35
65	83.7650	0.09	137.	79.	1.1538	3.26	X			1.00
66	84.0025	0.09	88.	77.	1.1540	2.10		X		1.95
67	86.4475	0.15	52.	74.	1.1248	1.23	X	X		0.91
68	87.8325	0.15	94.	77.	1.1106	2.24	X			1.23

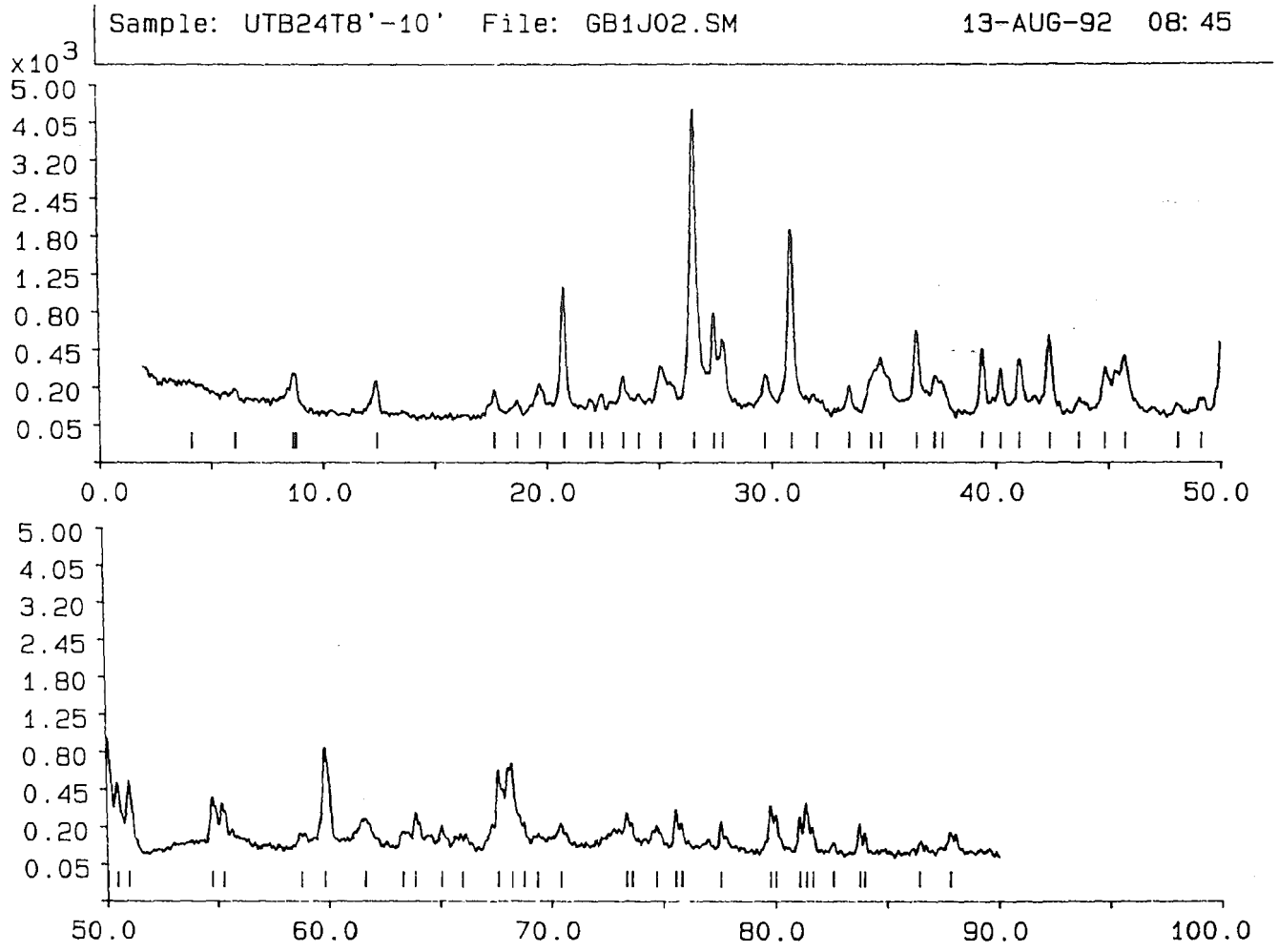
Sample: UTB24T8'-10' File: GB1J02.SM 13-AUG-92 08:45
x10^3
5.00
4.05
3.20
2.45
1.80
1.25
0.80
0.45
0.20
0.05
0.0
10.0
20.0
30.0
40.0
50.0
5.00
4.05
3.20
2.45
1.80
1.25
0.80
0.45
0.20
0.05
50.0
60.0
70.0
80.0
90.0
100.0

DETECTED PEAKS FILE 12-AUG-92 18:27

APD1700 Automated Powder Diffractometer System 1

Listed DI file name : SY00:GB2J02.DI
Original data file name : SY00:GB2J02.RD
Sample identification : UTB24B8'-107'
Measurement date/time : 12-AUG-92 17:34
Generator settings : 45 kV, 30 mA
Cu alpha1,2 wavelengths : 1.54060, 1.54439 Ang
Step size, sample time : 0.030 deg, 0.90 s, 30.00 s/deg
Monochromator used : Yes
Divergence slit : Automatic (Specimen length: 12.5 mm)

Analysis program number : 35
Peak angle range : 2.000 - 90.020 deg
Range in D spacing : 1.08918 - 44.1372 Ang
Peak position criterion : Top of smoothed data
Cryst peak width range : 0.00 - 2.00 deg
Minim peak significance : 0.75
Number of peaks in file : 74 (Alpha1: 70, Amorphous: 0)
Maximum intensity : 4186. cts, 4651.2 cps

Peak no	Angle (deg)	Tip width (deg)	Peak (cts)	Backg (cts)	D spac (Ang)	I/Imax (%)	Type A1	Type A2	Type Bt	Sign
1	4.2550	0.72	14.	153.	20.7497	0.34	X	X		1.55
2	6.1500	0.36	19.	156.	14.3597	0.24	X	X		1.32
3	8.8450	0.18	119.	112.	9.9896	2.84	X	X		5.31
4	12.5450	0.12	94.	74.	7.0503	2.25	X	X		0.85
5	17.7500	0.12	98.	62.	4.9929	2.34	X	X		0.98
6	18.7675	0.18	41.	62.	4.7244	0.98	X	X		1.05
7	19.7450	0.36	117.	64.	4.4927	2.79	X	X		3.02
8	20.6475	0.09	1246.	64.	4.2983	29.77	X	X		3.31
9	20.8475	0.09	876.	64.	4.2575	20.93	X	X		1.48
10	22.0250	0.09	64.	66.	4.0325	1.53	X	X		0.81
11	22.4300	0.18	55.	66.	3.9606	1.31	X	X		0.95
12	23.4850	0.15	130.	66.	3.7850	3.10	X	X		1.26
13	24.0175	0.09	108.	67.	3.7023	2.58	X	X		0.78
14	25.1775	0.21	174.	67.	3.5343	4.16	X	X		1.41
15	26.5675	0.27	4186.	69.	3.3524	100.00	X	X		56.23
16	27.4525	0.15	335.	69.	3.2463	8.00	X	X		2.63
17	28.0075	0.18	164.	69.	3.1832	3.91	X	X		1.45
18	29.4075	0.15	462.	71.	3.0348	11.04	X	X		5.89
19	29.8275	0.18	164.	71.	2.9930	3.91	X	X		1.74
20	30.9225	0.18	1544.	71.	2.8895	36.90	X	X		14.79
21	32.1700	0.36	40.	72.	2.7802	0.95	X	X		0.83
22	33.5225	0.18	106.	74.	2.6711	2.53	X	X		2.69
23	34.4675	0.36	149.	74.	2.6000	3.56	X	X		1.20
24	34.8925	0.30	222.	74.	2.5693	5.30	X	X		1.58
25	36.5250	0.21	437.	76.	2.4584	10.43	X	X		7.94
26	37.3325	0.21	151.	76.	2.4068	3.61	X	X		1.74
27	39.4425	0.21	346.	77.	2.2827	8.26	X	X		9.12
28	40.2975	0.24	259.	77.	2.2368	6.19	X	X		8.32
29	41.1100	0.21	350.	77.	2.1939	8.35	X	X		6.61
30	42.4125	0.21	372.	77.	2.1295	8.90	X	X		7.59

31	43.2000	0.18	45.	77.	2.0925	1.07	X	X	1.07
32	43.7525	0.09	77.	77.	2.0673	1.85	X	X	0.81
33	44.8825	0.09	234.	77.	2.0179	5.59	X	X	2.00
34	45.7150	0.15	286.	76.	1.9831	6.82	X	X	1.62
35	47.0400	0.18	45.	76.	1.9302	1.07	X	X	0.78
36	47.5175	0.18	46.	76.	1.9120	1.10	X	X	1.12
37	48.5425	0.24	61.	76.	1.8739	1.45	X	X	0.91
38	49.2200	0.30	79.	76.	1.8497	1.89	X	X	2.63
39	50.1150	0.12	936.	76.	1.8188	22.37	X	X	3.98
40	50.5400	0.18	412.	76.	1.8045	9.84	X	X	2.82
41	51.0325	0.15	350.	76.	1.7882	8.35	X		2.34
42	51.1575	0.09	266.	76.	1.7841	6.35	X	X	0.89
43	54.8275	0.18	256.	92.	1.6731	6.12	X	X	3.02
44	55.2850	0.09	137.	94.	1.6603	3.27	X	X	0.76
45	57.4875	0.24	30.	102.	1.6018	0.72	X	X	0.83
46	58.9125	0.24	72.	92.	1.5664	1.73	X	X	0.95
47	59.9025	0.18	702.	96.	1.5429	16.78	X	X	7.41
48	61.6850	0.30	121.	102.	1.5025	2.89	X	X	1.12
49	63.3850	0.24	71.	100.	1.4662	1.69	X	X	1.26
50	63.9750	0.12	121.	100.	1.4541	2.89	X	X	1.15
51	65.1575	0.24	79.	100.	1.4306	1.89	X	X	0.89
52	66.0625	0.48	44.	100.	1.4131	1.04	X	X	1.15
53	67.3350	0.15	128.	100.	1.3895	3.05	X		1.07
54	67.6875	0.09	388.	100.	1.3865	9.27		Y	0.85
55	68.1325	0.09	520.	100.	1.3752	12.42	X		0.85
56	68.3175	0.09	471.	100.	1.3753	11.25		X	0.85
57	69.3450	0.18	48.	100.	1.3541	1.14	X	X	0.83
58	70.4750	0.30	71.	98.	1.3351	1.69	X	X	1.23
59	72.9375	0.24	96.	98.	1.2969	2.29	X	X	0.91
60	73.4125	0.12	149.	96.	1.2887	3.56	X	X	1.00
61	74.7825	0.36	46.	92.	1.2685	1.10	X	X	1.26
62	75.6125	0.15	216.	90.	1.2566	5.16	X	X	2.29
63	77.6075	0.12	90.	85.	1.2293	2.16	Y		0.83
64	79.7950	0.12	310.	79.	1.2009	7.40	X		1.70
65	80.0650	0.12	253.	77.	1.2005	6.04		X	1.82
66	81.1325	0.12	144.	77.	1.1845	3.44	Y		1.12
67	81.4125	0.18	225.	77.	1.1811	5.37	X	Y	3.24
68	82.6825	0.36	37.	77.	1.1662	0.89	X	Y	1.55
69	83.7675	0.15	112.	77.	1.1536	2.68	X		1.32
70	84.0775	0.12	76.	77.	1.1502	1.81		Y	0.83
71	84.5700	0.36	22.	77.	1.1446	0.53	X	Y	1.29
72	85.9625	0.15	11.	77.	1.1299	0.26	Y	X	0.81
73	86.5350	0.48	18.	77.	1.1239	0.44	X	X	1.09
74	87.9075	0.60	48.	77.	1.1096	1.14	X	Y	2.09

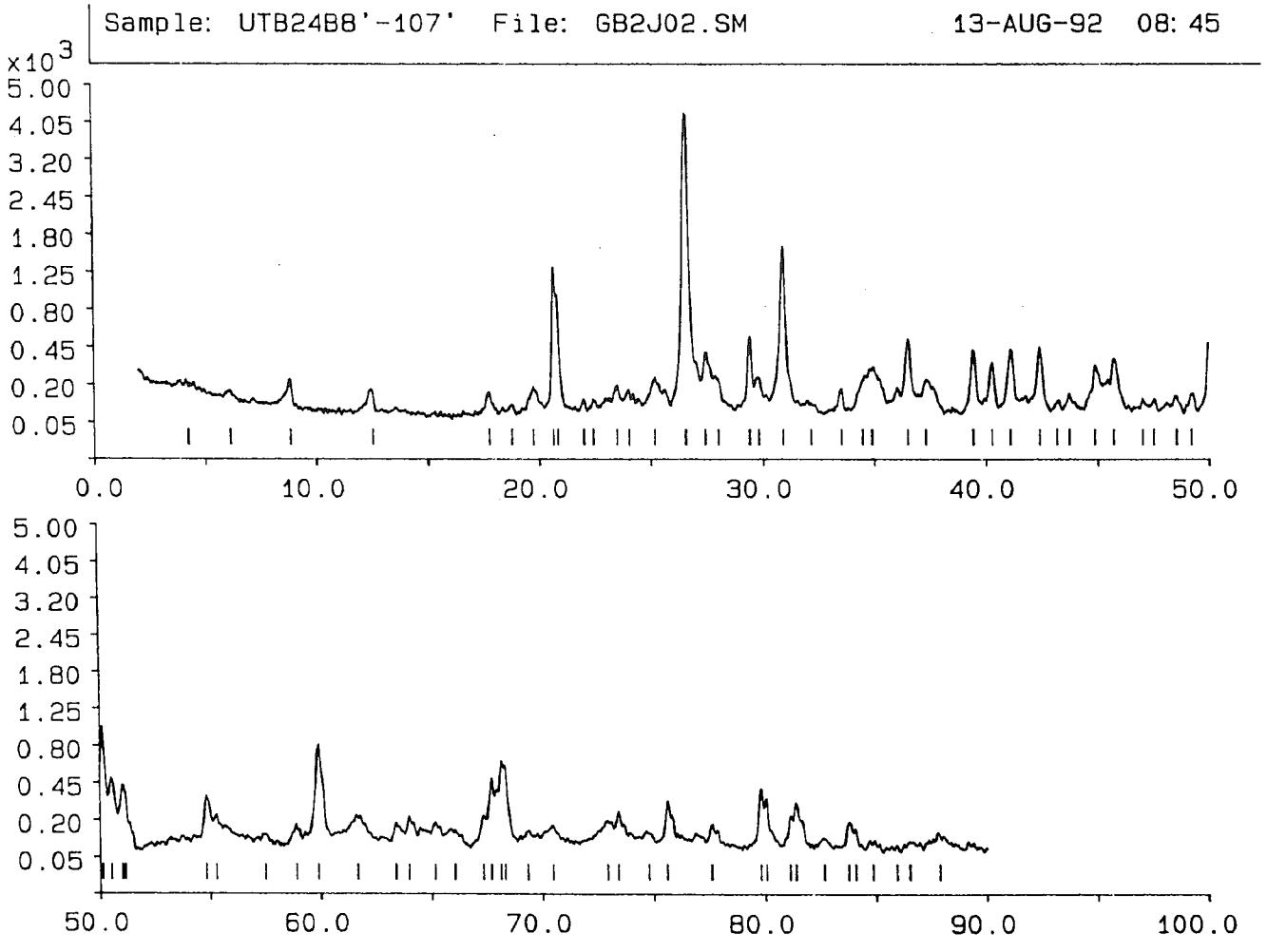
Sample: UTB24B8'-107' File: GB2J02.SM 13-AUG-92 08:45
x10^3
5.00
4.05
3.20
2.45
1.80
1.25
0.80
0.45
0.20
0.05
0.0
10.0
20.0
30.0
40.0
50.0
5.00
4.05
3.20
2.45
1.80
1.25
0.80
0.45
0.20
0.05
50.0
60.0
70.0
80.0
90.0
100.0

DETECTED PEAKS FILE 12-AUG-92 19:20

APD1700 Automated Powder Diffractometer System 1

Listed DI file name : SY00:6B3J02.DI
Original data file name : SY00:6B3J02.RD
Sample identification : UTB24T-10'-12'
Measurement date/time : 12-AUG-92 18:27
Generator settings : 45 kV, 30 mA
Cu alpha1,2 wavelengths : 1.54060, 1.54439 Ang
Step size, sample time : 0.030 deg, 0.90 s, 30.00 s/deg
Monochromator used : Yes
Divergence slit : Automatic (Specimen length: 12.5 mm)

Analysis program number : 35
Peak angle range : 2.000 - 90.020 deg
Range in D spacing : 1.08918 - 44.1372 Ang
Peak position criterion : Top of smoothed data
Cryst peak width range : 0.00 - 2.00 deg
Minim peak significance : 0.75
Number of peaks in file : 77 (Alpha1: 69, Amorphous: 0)
Maximum intensity : 5069. cts, 5632.7 cps

Peak no	Angle (deg)	Tip width (deg)	Peak (cts)	Backg (cts)	D spac (Ang)	I/Imax (%)	Type A1	Type A2	Type Dt	Sign
1	6.2125	0.12	46.	166.	14.2154	0.91	X	X		0.76
2	8.8150	0.12	253.	121.	10.0235	4.99	X	X		2.24
3	12.4725	0.12	199.	83.	7.0912	3.92	X	X		2.40
4	13.7900	0.36	23.	79.	6.4165	0.40	X	X		0.89
5	17.7325	0.12	135.	66.	4.9978	2.65	X	X		1.00
6	18.8250	0.09	61.	67.	4.7101	1.20	X	X		0.76
7	19.7225	0.30	114.	67.	4.4978	2.26	X	X		2.63
8	20.8125	0.12	2218.	69.	4.2646	43.76	X	X		15.14
9	22.4425	0.18	66.	71.	3.9584	1.29	X	X		1.17
10	22.9575	0.24	76.	71.	3.8708	1.49	X	X		1.17
11	23.4475	0.12	166.	71.	3.7910	3.28	X	X		1.17
12	24.0800	0.24	83.	71.	3.6928	1.63	X	X		1.15
13	25.1250	0.18	237.	72.	3.5415	4.68	X	X		2.51
14	25.5475	0.18	161.	72.	3.4839	3.18	X	X		1.29
15	26.5875	0.15	5069.	72.	3.3500	100.00	X	X		23.99
16	27.4100	0.12	428.	74.	3.2513	8.45	X	X		1.78
17	27.8775	0.09	376.	74.	3.1978	7.42	X	X		1.62
18	28.1300	0.12	310.	74.	3.1697	6.11	X	X		1.55
19	29.4175	0.12	538.	76.	3.0338	10.62	X	X		4.17
20	29.7750	0.18	202.	76.	2.9982	3.98	X	X		2.14
21	30.9050	0.15	2601.	77.	2.8911	51.31	X	X		16.22
22	32.1600	0.36	52.	77.	2.7811	1.02	X	X		0.91
23	33.4800	0.18	164.	79.	2.6744	3.23	X	X		3.39
24	34.4675	0.24	156.	79.	2.6000	3.08	X	X		0.79
25	35.0750	0.09	289.	81.	2.5563	5.70	X	X		1.48
26	35.9750	0.12	112.	81.	2.4944	2.22	X	X		0.78
27	36.4950	0.12	488.	81.	2.4601	9.63	X	X		3.09
28	37.3225	0.09	228.	83.	2.4074	4.50	X	X		1.74
29	39.4275	0.21	445.	85.	2.2836	8.78	X	X		10.72
30	40.2425	0.12	250.	85.	2.2392	4.93	X	X		2.19

31	41.1025	0.21	502.	85.	2.1943	> 9.90	X	X		11.22
32	42.3850	0.15	681.	85.	2.1308	>13.44	X	X		6.17
33	43.1575	0.12	66.	85.	2.0945	1.29	X	X		0.76
34	43.7575	0.12	79.	85.	2.0671	1.56	X	X		0.78
35	44.8750	0.21	246.	85.	2.0182	4.86	X	X		4.68
36	45.7750	0.18	310.	83.	1.9806	> 6.11	X	X		2.95
37	46.9725	0.30	46.	83.	1.9329	0.91	X	X		1.12
38	47.5350	0.12	121.	83.	1.9113	2.39	X	X		0.98
39	48.5250	0.18	56.	83.	1.8746	1.11	X	X		1.38
40	49.2075	0.09	77.	83.	1.8502	1.53	X	X		0.91
41	50.0850	0.12	853.	83.	1.8198	>16.82	X	X		4.17
42	50.5175	0.18	543.	83.	1.8052	> 10.71	X	X		4.57
43	51.0125	0.15	529.	83.	1.7889	> 10.44	X	X		3.80
44	54.8025	0.12	331.	102.	1.6738	> 6.53	X	X		2.63
45	55.2350	0.09	149.	104.	1.6617	2.94	X	X		1.20
46	57.4675	0.36	23.	114.	1.6023	0.45	X	X		1.51
47	58.8725	0.30	88.	108.	1.5674	1.74	X	X		2.09
48	59.8925	0.15	807.	108.	1.5431	> 15.91	X			6.17
49	60.0800	0.06	420.	108.	1.5425	> 8.29		X		2.45
50	60.7125	0.18	50.	110.	1.5242	0.99	X	X		0.76
51	61.5750	0.24	130.	110.	1.5049	2.56	X	X		1.17
52	63.4150	0.30	72.	108.	1.4656	1.43	X	X		1.82
53	63.9525	0.12	177.	108.	1.4546	3.49	X	X		1.41
54	65.0950	0.12	98.	106.	1.4318	1.93	X	X		0.83
55	66.0875	0.24	56.	106.	1.4127	1.11	X	X		0.81
56	67.6725	0.15	384.	104.	1.3834	> 7.58	X	X		3.39
57	68.0750	0.09	600.	104.	1.3762	11.84	X			1.95
58	68.2550	0.09	562.	104.	1.3764	11.08		X		1.70
59	69.3400	0.42	62.	102.	1.3541	1.23	X	X		2.04
60	70.4700	0.42	102.	100.	1.3352	2.01	X	X		3.72
61	72.8200	0.30	104.	98.	1.2978	2.05	X	X		1.29
62	73.3825	0.09	166.	96.	1.2892	3.28			Ot	0.95
63	74.6900	0.30	72.	94.	1.2698	1.43	X	X		1.38
64	75.5950	0.12	199.	92.	1.2569	3.92	X			2.19
65	75.8200	0.09	128.	92.	1.2568	2.52		X		1.70
66	76.9475	0.09	64.	90.	1.2381	1.26	X			1.15
67	77.6025	0.12	110.	88.	1.2293	2.17			Ot	1.45
68	79.8350	0.09	266.	85.	1.2004	5.24	X			1.10
69	80.0725	0.09	185.	83.	1.2004	3.65		X		1.00
70	81.1300	0.09	182.	81.	1.1845	2.60	X			1.05
71	81.3975	0.18	279.	81.	1.1813	5.50	X	X		3.63
72	81.6800	0.12	144.	91.	1.1808	2.84		X		0.91
73	82.5575	0.18	53.	79.	1.1676	1.05	X	X		1.07
74	83.7750	0.12	234.	77.	1.1537	4.62	X			2.63
75	84.0700	0.09	121.	76.	1.1532	2.39		X		1.78
76	86.5400	0.48	29.	72.	1.1238	0.55	X	X		0.76
77	87.8475	0.18	81.	76.	1.1104	1.60	X	X		1.29

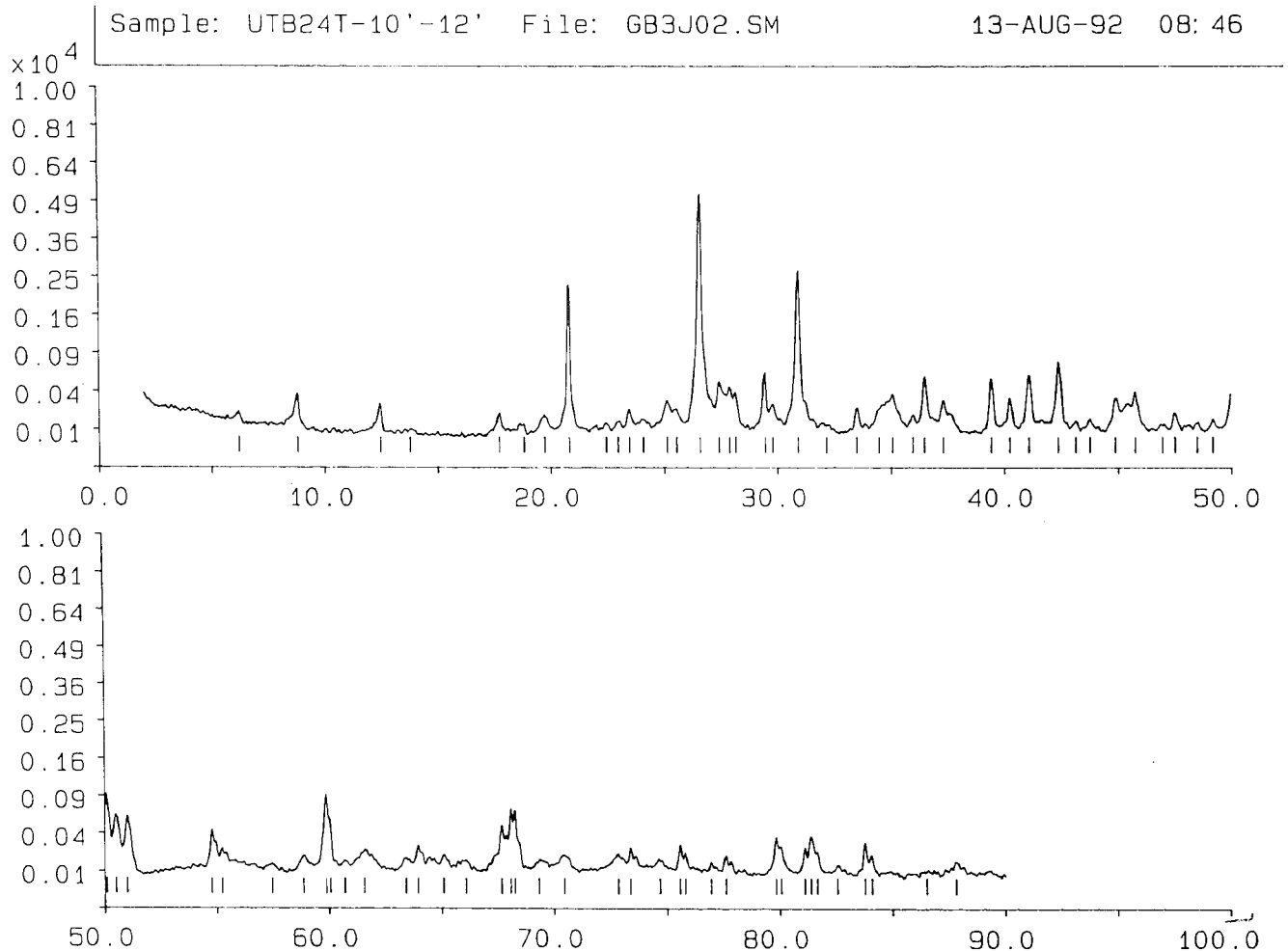
Sample: UTB24T-10'-12' File: GB3J02.SM 13-AUG-92 08: 46
x10^4
1.00
0.81
0.64
0.49
0.36
0.25
0.16
0.09
0.04
0.01
0.0
10.0
20.0
30.0
40.0
50.0
1.00
0.81
0.64
0.49
0.36
0.25
0.16
0.09
0.04
0.01
50.0
60.0
70.0
80.0
90.0
100.0

DETECTED PEAKS FILE 12-AUG-92 20:12

MPD1700 Automated Powder Diffractometer System 1

Listed DI file name : SY00:GB4J02.DI
Original data file name : SY00:GB4J02.RD
Sample identification : UTB24B-10'-12'
Measurement date/time : 12-AUG-92 19:19
Generator settings : 45 kV, 30 mA
Cu alpha1,2 wavelengths : 1.54060, 1.54439 Ang
Step size, sample time : 0.030 deg, 0.90 s, 30.00 s/deg
Monochromator used : Yes
Divergence slit : Automatic (Specimen length: 12.5 mm)

Analysis program number : 35
Peak angle range : 2.000 - 90.020 deg
Range in D spacing : 1.08918 - 44.1372 Ang
Peak position criterion : Top of smoothed data
Cryst peak width range : 0.00 - 2.00 deg
Minim peak significance : 0.75
Number of peaks in file : 80 (Alpha1: 71, Amorphous: 0)
Maximum intensity : 5914. cts, 6570.7 cps

Peak no	Angle (deg)	Tip width (deg)	Peak (cts)	Backg (cts)	D spac (Ang)	I/Imax (%)	Type A1	Type A2	Type Dt	Sign
1	4.0775	1.44	25.	182.	21.6526	0.42	Y	Y		2.34
2	6.1300	0.24	40.	149.	14.4065	0.67	Y	Y		1.05
3	8.7825	0.12	185.	121.	10.0605	3.13	Y	Y		2.04
4	12.4425	0.12	207.	81.	7.1062	3.51	Y	Y		2.88
5	17.6875	0.12	132.	61.	5.0104	2.24	Y	Y		1.23
6	18.7100	0.12	85.	61.	4.7389	1.43	Y	Y		1.07
7	19.6775	0.30	123.	62.	4.5079	2.08	Y	Y		2.57
8	20.7525	0.12	1310.	62.	4.2768	22.16	Y	Y		7.94
9	21.9350	0.09	207.	62.	4.0488	3.51	Y	Y		1.74
10	22.4150	0.18	79.	62.	3.9632	1.34	Y	Y		1.70
11	22.9775	0.12	90.	64.	3.8674	1.53	Y	Y		0.81
12	23.4250	0.24	142.	64.	3.7946	2.39	Y	Y		2.45
13	23.9650	0.12	123.	64.	3.7103	2.08	Y	Y		1.07
14	25.1475	0.12	256.	64.	3.5384	4.33	Y	Y		1.41
15	26.5725	0.12	5914.	66.	3.3518	100.00	Y	Y		16.60
16	27.4000	0.12	467.	66.	3.2524	7.89	Y	Y		2.04
17	27.9425	0.09	424.	66.	3.1905	7.18	Y	Y		1.29
18	29.3400	0.18	441.	66.	3.0416	7.46	Y	Y		5.89
19	29.7750	0.18	240.	66.	2.9982	4.06	Y	Y		3.02
20	30.8725	0.15	2591.	67.	2.8941	43.81	Y	Y		16.22
21	32.1600	0.36	64.	67.	2.7811	1.08	Y	Y		0.79
22	33.4600	0.15	169.	69.	2.6759	2.86	Y	Y		2.24
23	34.4350	0.30	174.	69.	2.6024	2.95	Y	Y		1.02
24	34.8550	0.24	234.	69.	2.5720	3.96	Y	Y		0.93
25	35.2250	0.18	190.	69.	2.5458	3.22	Y	Y		1.86
26	35.9825	0.15	135.	69.	2.4939	2.28	Y	Y		1.45
27	36.4900	0.18	625.	69.	2.4604	10.57	Y	Y		10.00
28	37.2950	0.18	210.	71.	2.4091	3.56	Y	Y		2.51
29	37.7100	0.15	132.	71.	2.3835	2.24	Y	Y		0.87
30	38.4375	0.18	49.	71.	2.3401	0.67	Y	Y		0.91

31	39.3975	0.18	484.	71.	2.2852	8.18	X	X		8.13
32	40.2950	0.18	740.	71.	2.2367	12.51	X	X		9.12
33	41.0675	0.18	420.	72.	2.1961	7.11	X	X		5.37
34	42.3850	0.15	445.	72.	2.1308	7.53	X	X		4.47
35	43.1475	0.09	112.	72.	2.0949	1.90	X	X		1.20
36	43.7350	0.18	74.	72.	2.0681	1.25	X	X		1.15
37	44.8500	0.18	253.	74.	2.0193	4.28	X	X		3.63
38	45.7175	0.15	317.	74.	1.9830	5.36	X	X		2.63
39	47.5075	0.12	92.	74.	1.9123	1.56	X	X		0.89
40	48.5200	0.15	92.	76.	1.8748	1.56	X	X		1.07
41	49.1975	0.12	112.	76.	1.8505	1.90	X	X		0.76
42	50.0475	0.09	955.	76.	1.8211	16.15	X	X		2.69
43	50.5025	0.24	515.	76.	1.8057	8.71	X	X		8.91
44	50.9925	0.12	433.	76.	1.7895	7.32	X	X		2.09
45	54.7850	0.09	324.	98.	1.6743	5.48	X	X		1.48
46	55.3050	0.18	182.	100.	1.6597	3.08	X	X		1.05
47	57.4950	0.30	59.	106.	1.6039	1.00	X	X		1.82
48	58.8500	0.30	77.	108.	1.5679	1.31	X	X		2.14
49	59.8600	0.09	900.	104.	1.5439	15.22	X			2.19
50	60.0500	0.06	506.	104.	1.5432	8.56		X		3.24
51	61.3425	0.30	106.	106.	1.5101	1.79	X			0.98
52	61.6525	0.24	130.	106.	1.5032	2.20	X	X		1.02
53	63.3350	0.09	77.	106.	1.4673	1.31	X	X		1.20
54	63.9650	0.09	142.	106.	1.4543	2.39	X	X		0.98
55	64.6075	0.24	72.	104.	1.4414	1.22	X	X		0.91
56	65.1200	0.30	98.	104.	1.4313	1.66	X	X		1.95
57	65.9525	0.60	45.	104.	1.4152	0.76	X	X		2.09
58	67.3175	0.09	135.	104.	1.3898	2.28			Ot	1.32
59	67.6275	0.09	882.	102.	1.3842	14.92	X			3.31
60	67.8325	0.09	576.	102.	1.3839	9.74		X		1.91
61	68.0600	0.06	493.	102.	1.3765	8.33	X			2.51
62	68.2400	0.06	645.	102.	1.3733	10.91	X	X		5.37
63	68.4325	0.09	259.	102.	1.3732	4.38		X		0.98
64	69.4100	0.36	52.	102.	1.3529	0.88	X	X		1.15
65	70.5150	0.21	104.	102.	1.3344	1.76	X	X		1.17
66	73.3850	0.09	146.	100.	1.3892	2.48			Ot	2.09
67	74.6275	0.24	53.	98.	1.2707	0.90	X	X		0.79
68	75.5650	0.12	310.	96.	1.2573	5.24	X			3.24
69	75.8100	0.09	204.	96.	1.2569	3.46		X		0.91
70	77.6025	0.12	100.	92.	1.2293	1.69	X			1.41
71	79.8000	0.12	207.	88.	1.2009	3.51			Ot	1.66
72	81.1025	0.09	169.	86.	1.1848	2.86	X			0.83
73	81.3975	0.15	361.	88.	1.1813	6.10	X	X		4.47
74	81.6775	0.12	172.	86.	1.1908	2.90		X		1.66
75	82.5675	0.18	40.	86.	1.1675	0.67	X	X		0.95
76	83.7675	0.09	142.	85.	1.1538	2.39	X			0.95
77	84.0375	0.12	76.	85.	1.1536	1.28		X		0.81
78	85.0025	0.36	17.	83.	1.1402	0.28	X	X		0.93
79	86.5325	0.42	31.	83.	1.1239	0.53	X	X		1.02
80	87.8900	0.24	71.	81.	1.1109	1.19	X	X		1.17

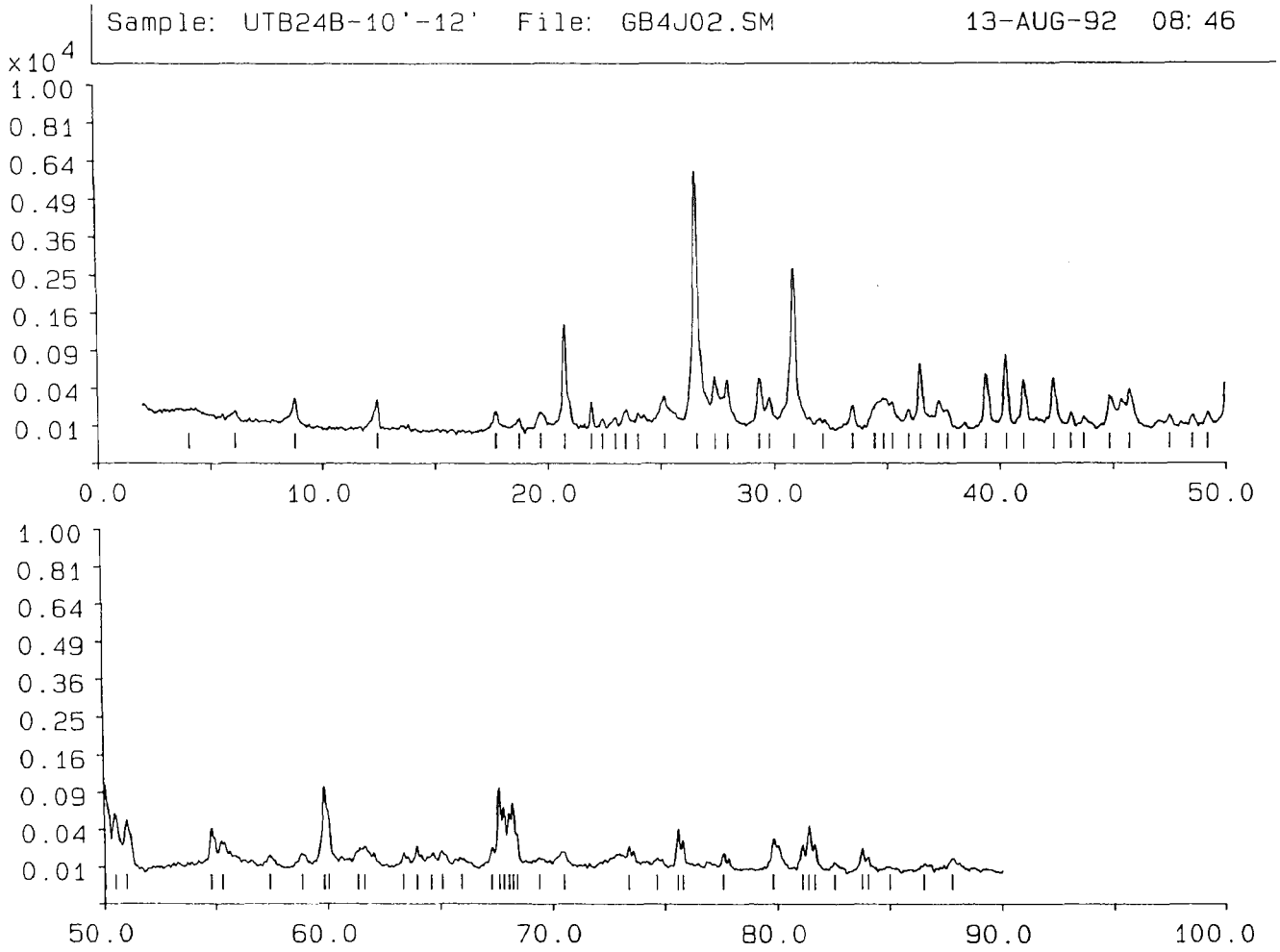
Sample: UTB24B-10'-12' File: GB4J02.SM 13-AUG-92 08: 46
x10^4
1.00
0.81
0.64
0.49
0.36
0.25
0.16
0.09
0.04
0.01
0.0
10.0
20.0
30.0
40.0
50.0
1.00
0.81
0.64
0.49
0.36
0.25
0.16
0.09
0.04
0.01
50.0
60.0
70.0
80.0
90.0
100.0

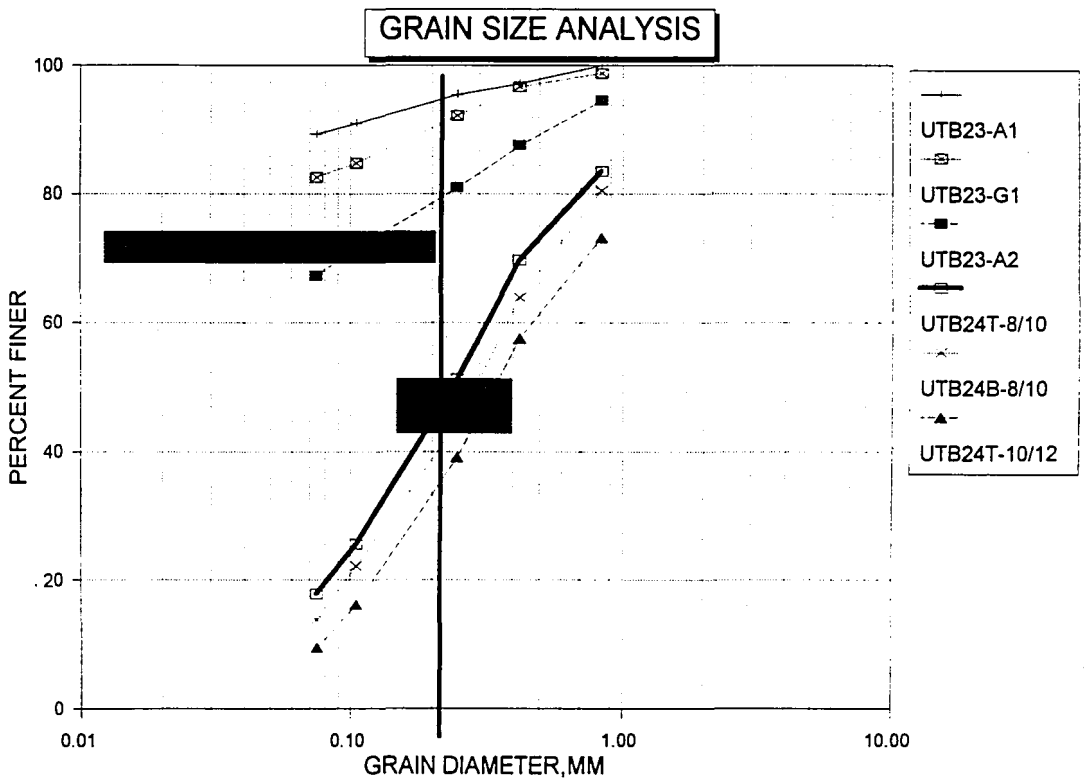
GRAIN SIZE ANALYSIS
100
80
60
40
20
0
PERCENT FINER
0.01
0.10
1.00
10.00
GRAIN DIAMETER,MM
UTB23-A1
UTB23-G1
UTB23-A2
UTB24T-8/10
UTB24B-8/10
UTB24T-10/12

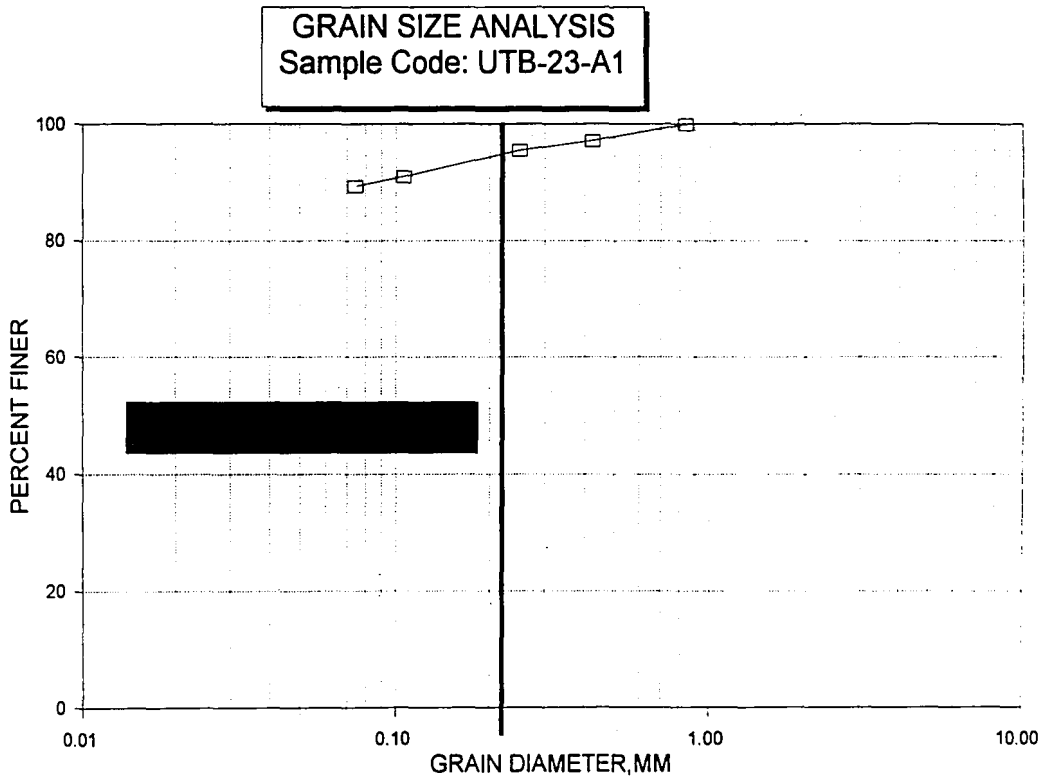
GRAIN SIZE ANALYSIS
Sample Code: UTB-23-A1
PERCENT FINER
100
80
60
40
20
0
0.01
0.10
1.00
10.00
GRAIN DIAMETER,MM

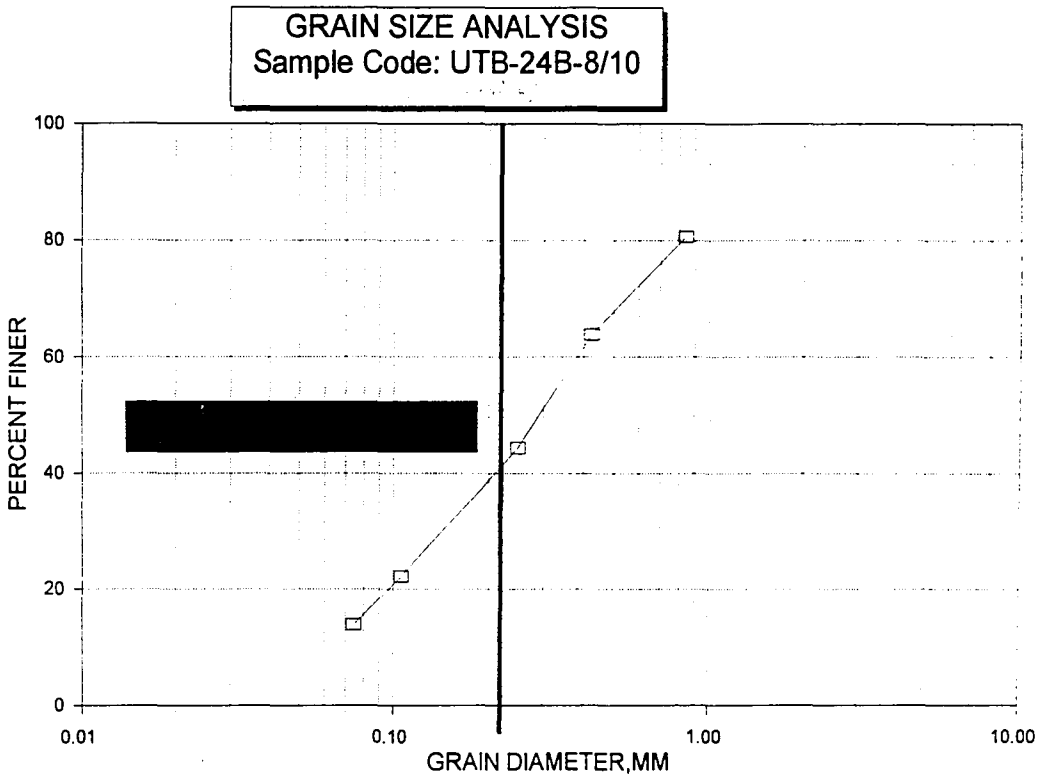
GRAIN SIZE ANALYSIS
Sample Code: UTB-24B-8/10
100
80
60
40
20
0
PERCENT FINER
0.01
0.10
1.00
10.00
GRAIN DIAMETER,MM

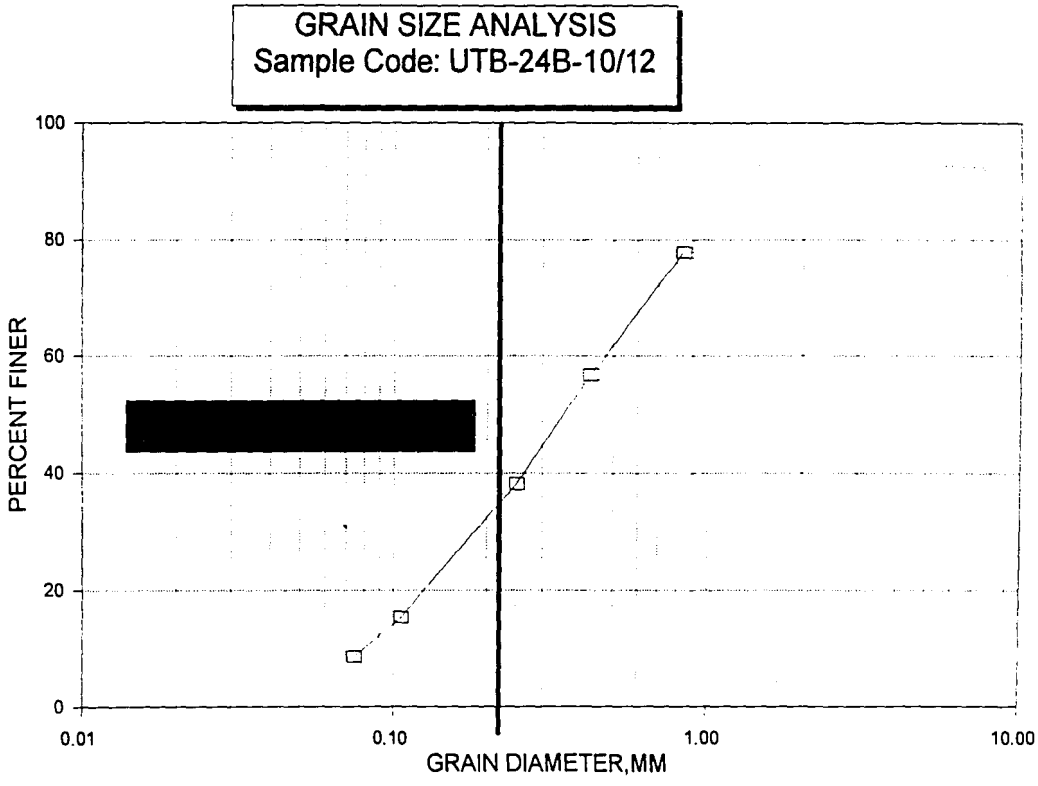
GRAIN SIZE ANALYSIS
Sample Code: UTB-24B-10/12
100
80
60
40
20
0
PERCENT FINER
0.01
0.10
1.00
10.00
GRAIN DIAMETER,MM

APPENDIX C

VOLTAGE GRADIENT PLOTS

and

ELECTROKINETIC FLOW AND CURRENT PLOTS

CURRENT EFFICIENCY
UTB-23-A1 and UTB-23-A2
UTB-23-A1
UTB-23-A2
7
6
5
4
3
2
1
0
0
0.2
W/O SURFACTANT
WITH SURFACTANT

CURRENT EFFICIENCY

UTB-23-A1 and UTB-23-A2

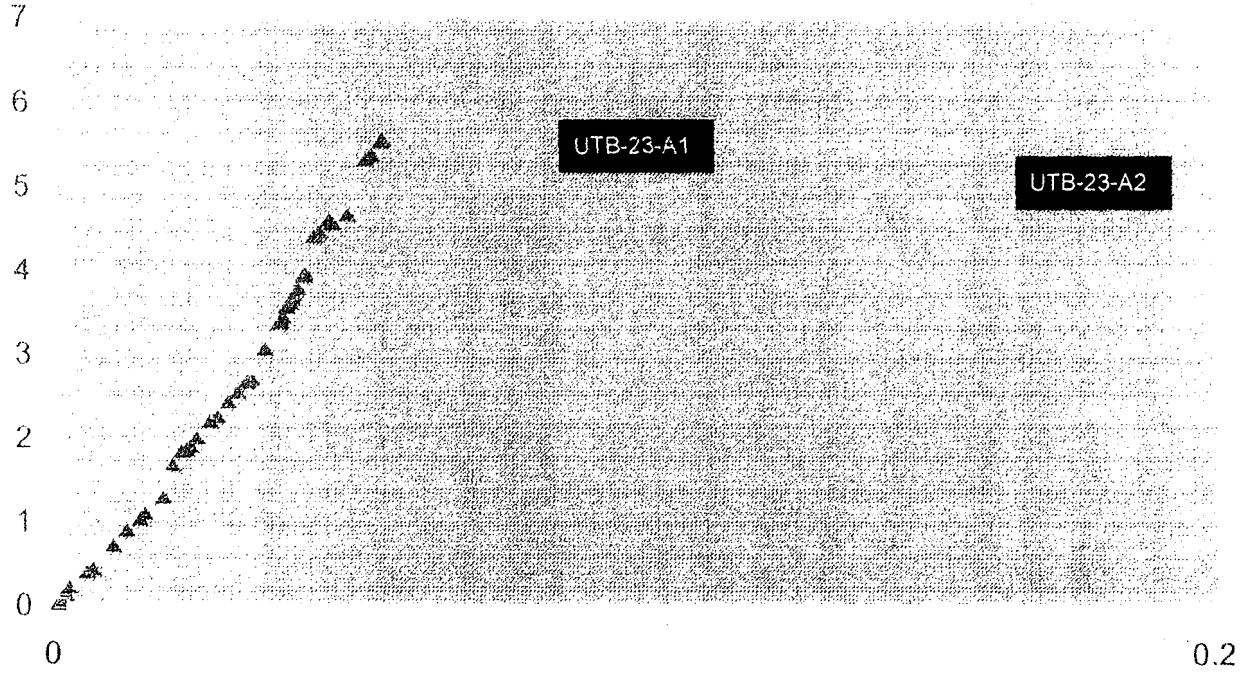

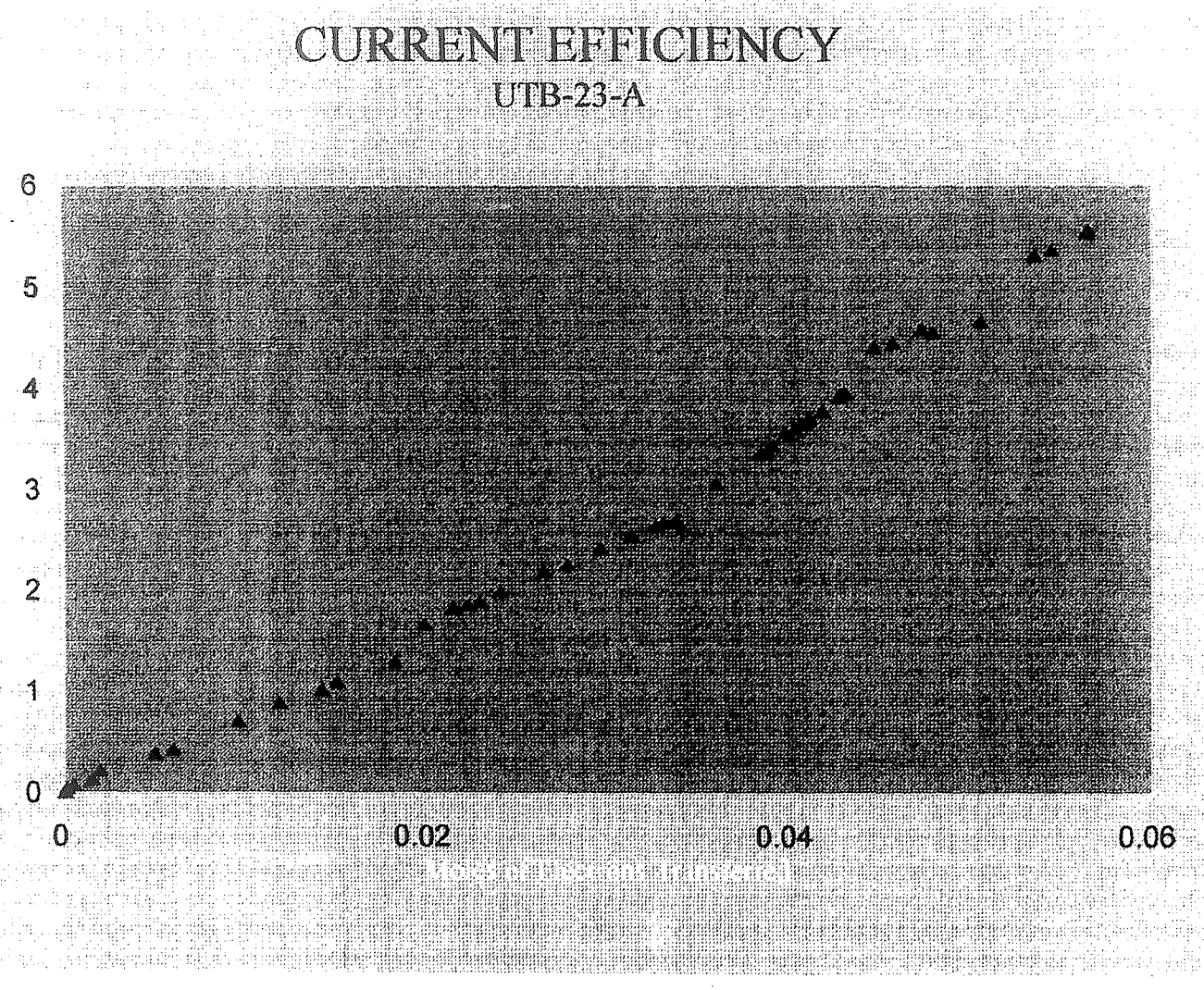
CURRENT EFFICIENCY
UTB-23-A
6
5
4
3
2
1
0
0
0.02
0.04
0.06

CURRENT EFFICIENCY

UTB-23-A

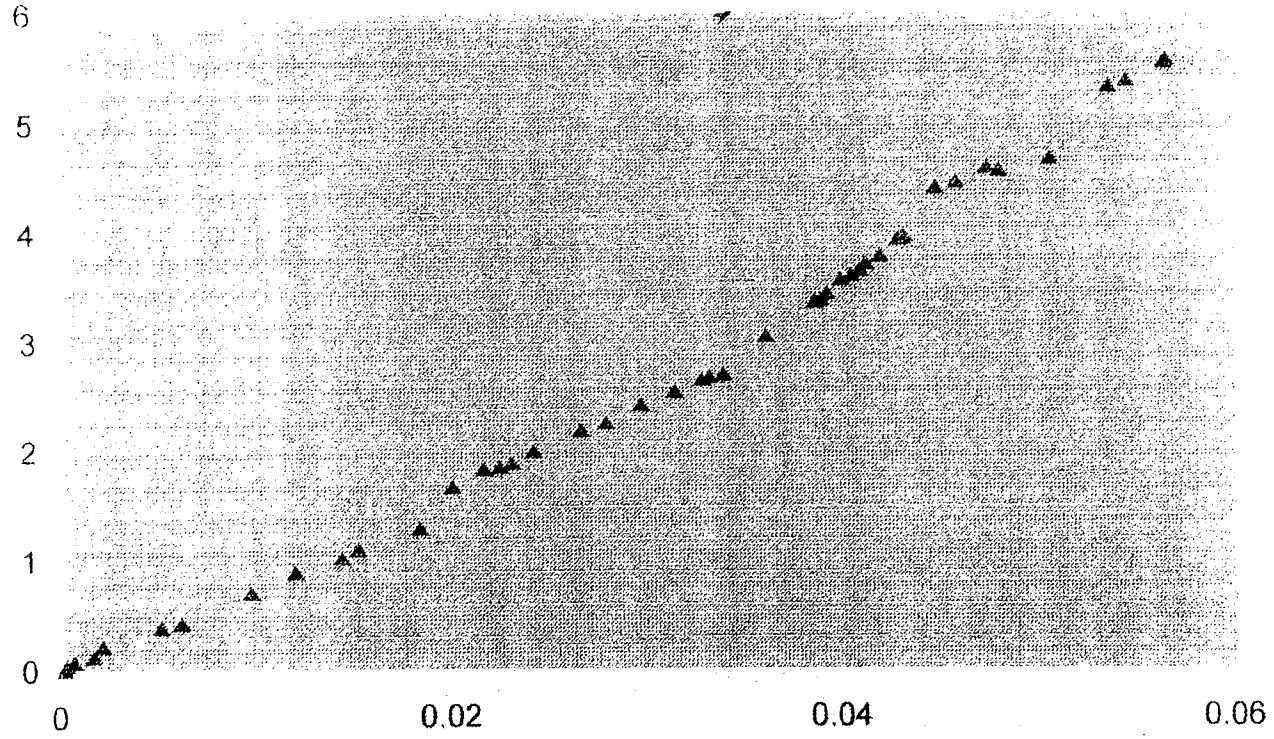

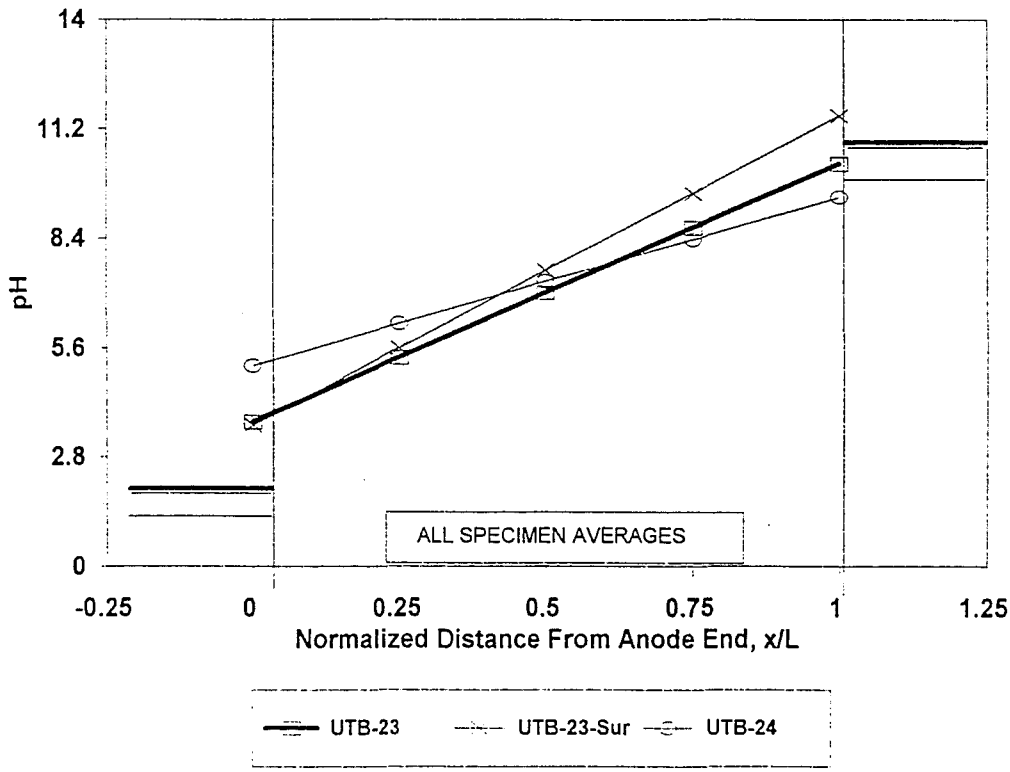
14
11.2
8.4
5.6
2.8
0
pH
-0.25
0
0.25
0.5
0.75
1
1.25
Normalized Distance From Anode End, x/L
ALL SPECIMEN AVERAGES
UTB-23
UTB-23-Sur
UTB-24

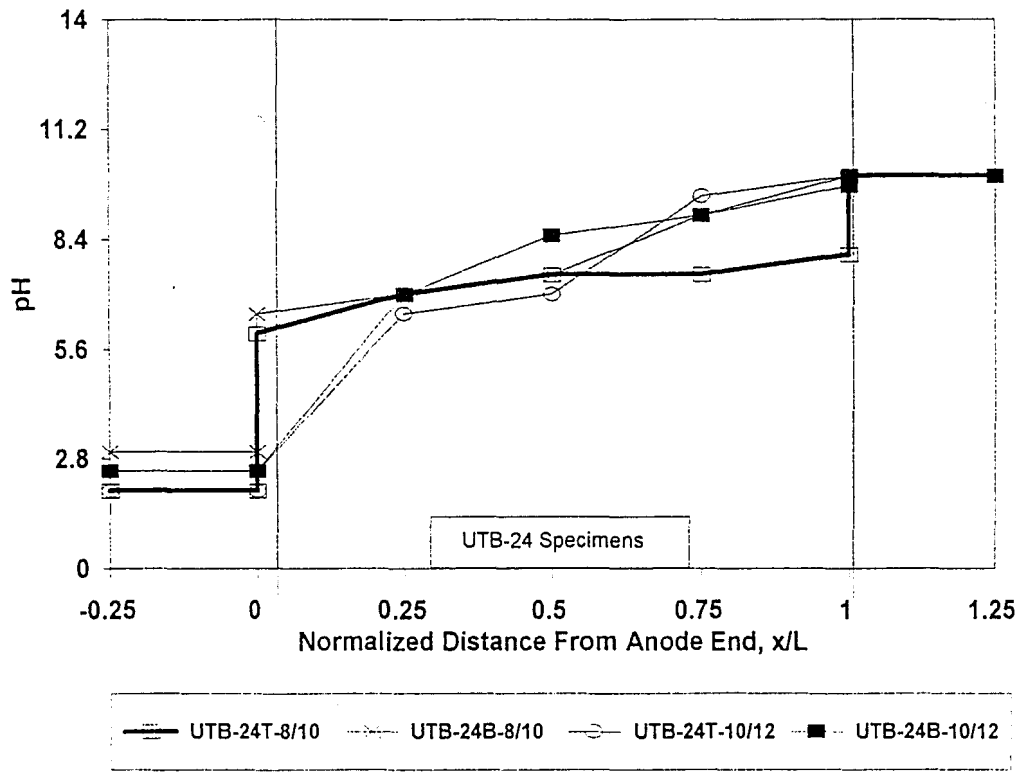
14
11.2
8.4
5.6
2.8
0
pH
-0.25
0
0.25
0.5
0.75
1
1.25
Normalized Distance From Anode End, x/L
UTB-24 Specimens
UTB-24T-8/10
UTB-24B-8/10
UTB-24T-10/12
UTB-24B-10/12

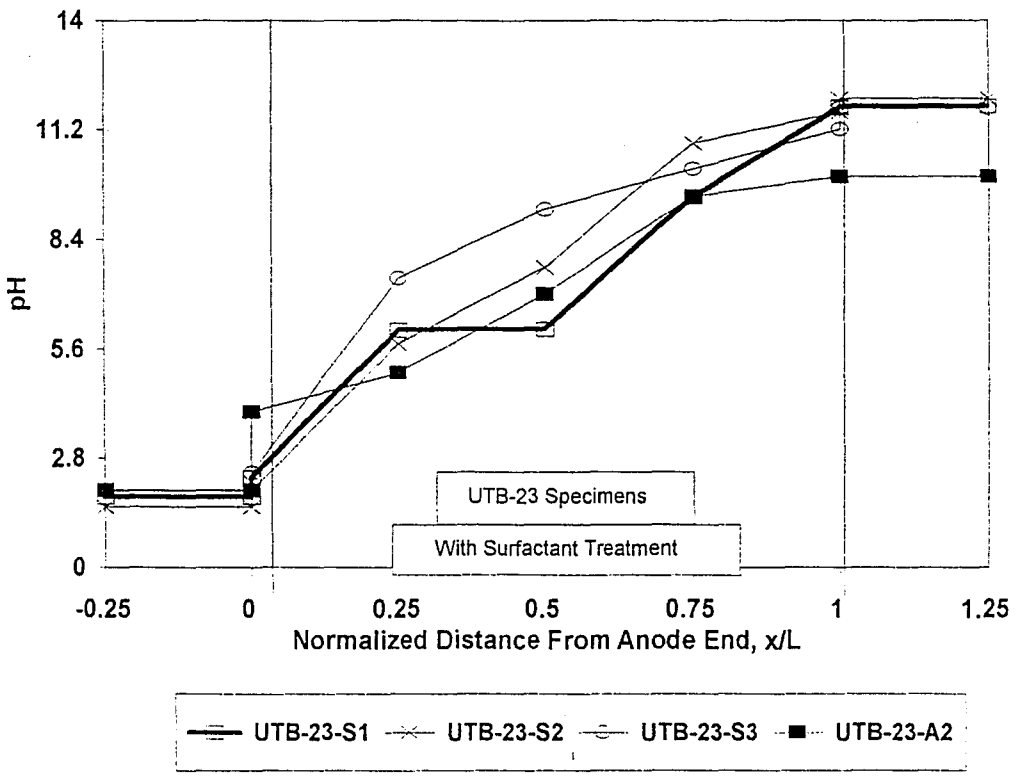
14
11.2
8.4
5.6
2.8
0
pH
-0.25
0
0.25
0.5
0.75
1
1.25
Normalized Distance From Anode End, x/L
UTB-23 Specimens
With Surfactant Treatment
UTB-23-S1
UTB-23-S2
UTB-23-S3
UTB-23-A2

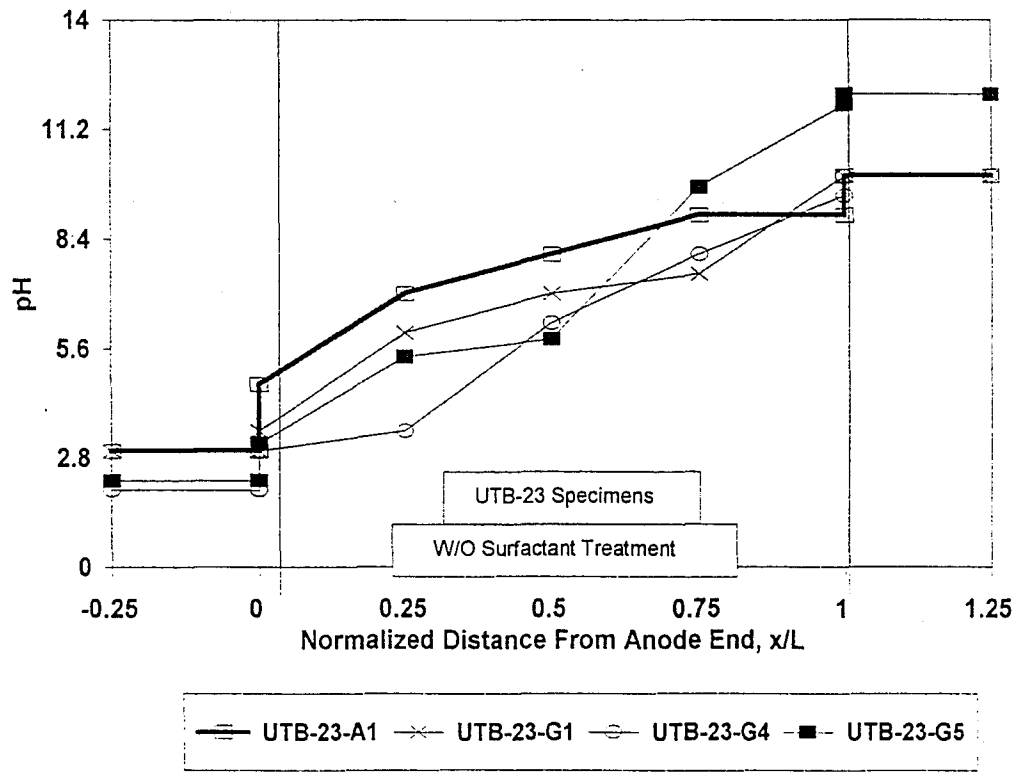
14
11.2
8.4
5.6
2.8
0
pH
-0.25
0
0.25
0.5
0.75
1
1.25
Normalized Distance From Anode End, x/L
UTB-23 Specimens
W/O Surfactant Treatment
UTB-23-A1
UTB-23-G1
UTB-23-G4
UTB-23-G5

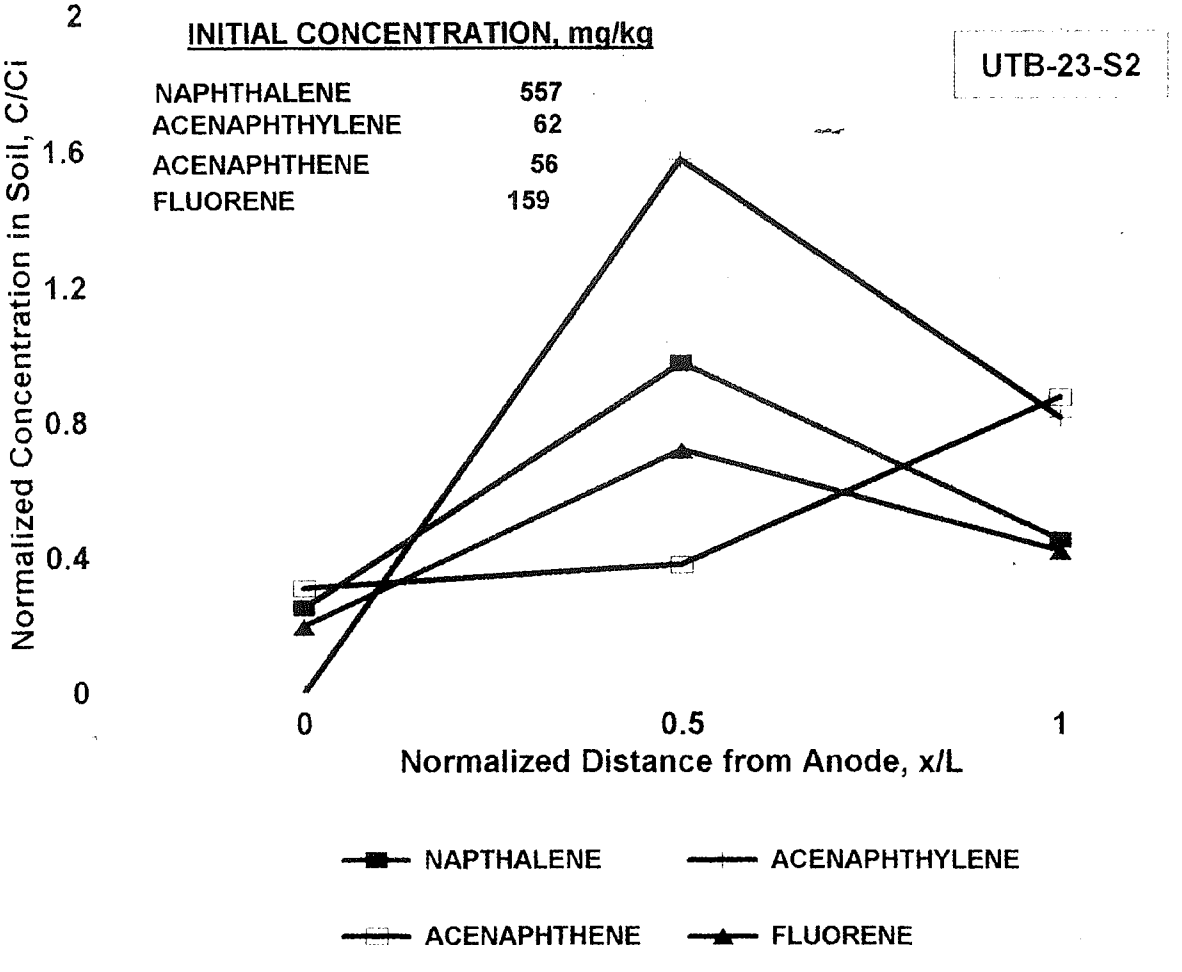
INITIAL CONCENTRATION, mg/kg
NAPHTHALENE 557
ACENAPHTHYLENE 62
ACENAPHTHENE 56
FLUORENE 159
UTB-23-S2
Normalized Concentration in Soil, C/Ci
2
1.6
1.2
0.8
0.4
0
0
0.5
1
Normalized Distance from Anode, x/L
NAPTHALENE
ACENAPHTHYLENE
ACENAPHTHENE
FLUORENE

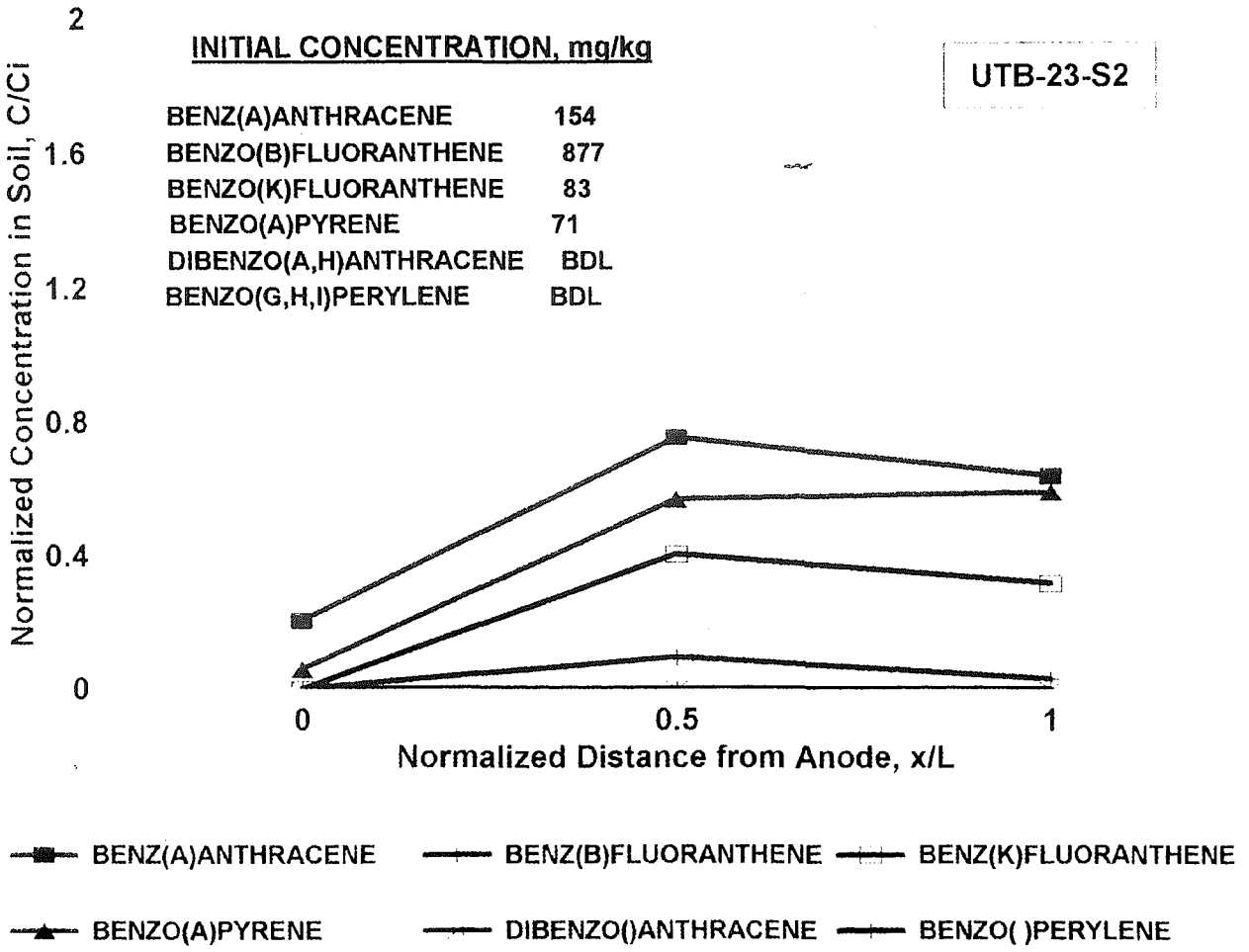
INITIAL CONCENTRATION, mg/kg
BENZ(A)ANTHRACENE 154
BENZO(B)FLUORANTHENE 877
BENZO(K)FLUORANTHENE 83
BENZO(A)PYRENE 71
DIBENZO(A,H)ANTHRACENE BDL
BENZO(G,H,I)PERYLENE BDL
UTB-23-S2
Normalized Concentration in Soil, C/Ci
2
1.6
1.2
0.8
0.4
0
0
0.5
1
Normalized Distance from Anode, x/L
BENZ(A)ANTHRACENE
BENZ(B)FLUORANTHENE
BENZ(K)FLUORANTHENE
BENZO(A)PYRENE
DIBENZO()ANTHRACENE
BENZO( )PERYLENE

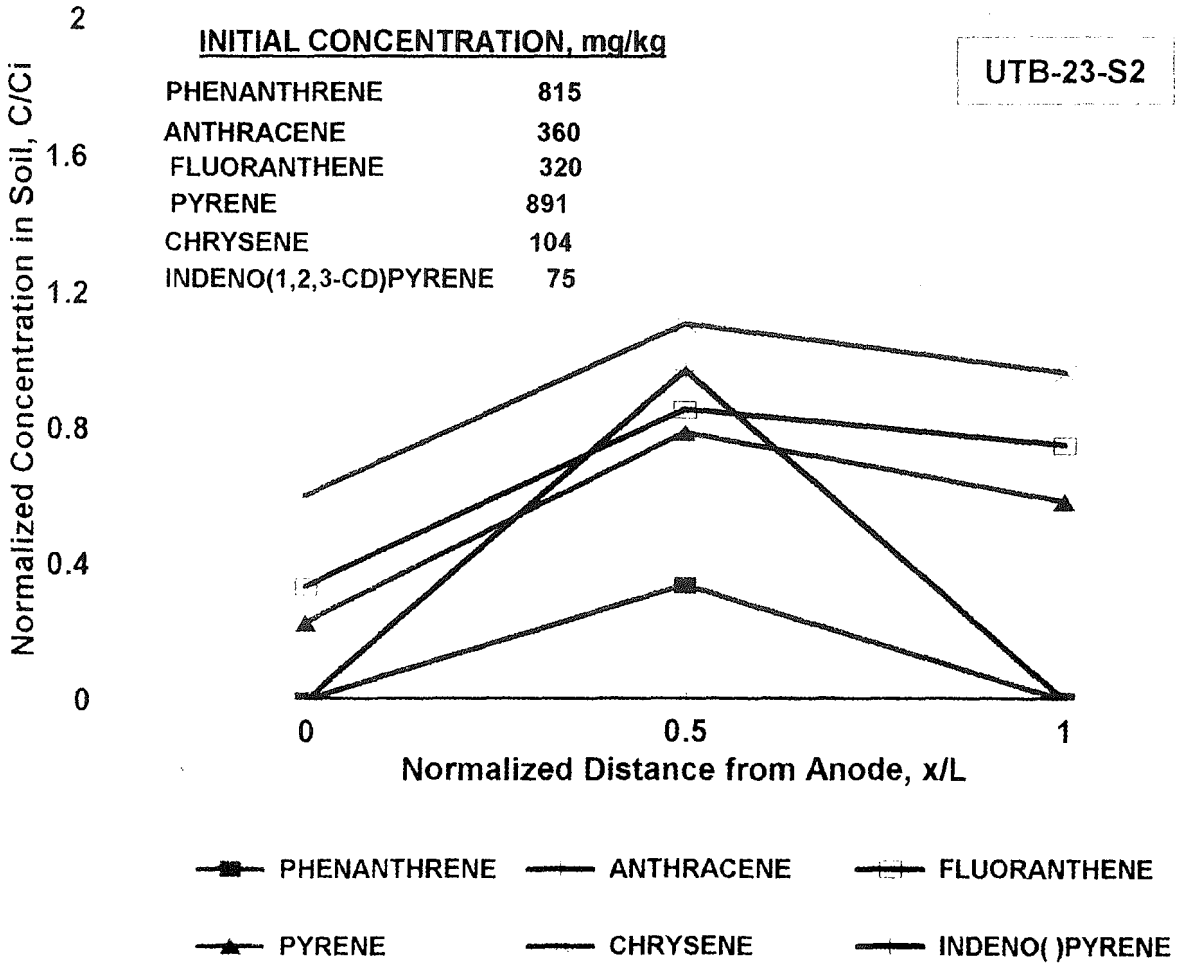
INITIAL CONCENTRATION, mg/kg
PHENANTHRENE 815
ANTHRACENE 360
FLUORANTHENE 320
PYRENE 891
CHRYSENE 104
INDENO(1,2,3-CD)PYRENE 75
UTB-23-S2
Normalized Concentration in Soil, C/Ci
2
1.6
1.2
0.8
0.4
0
0
0.5
1
Normalized Distance from Anode, x/L
PHENANTHRENE
ANTHRACENE
FLUORANTHENE
PYRENE
CHRYSENE
INDENO( )PYRENE

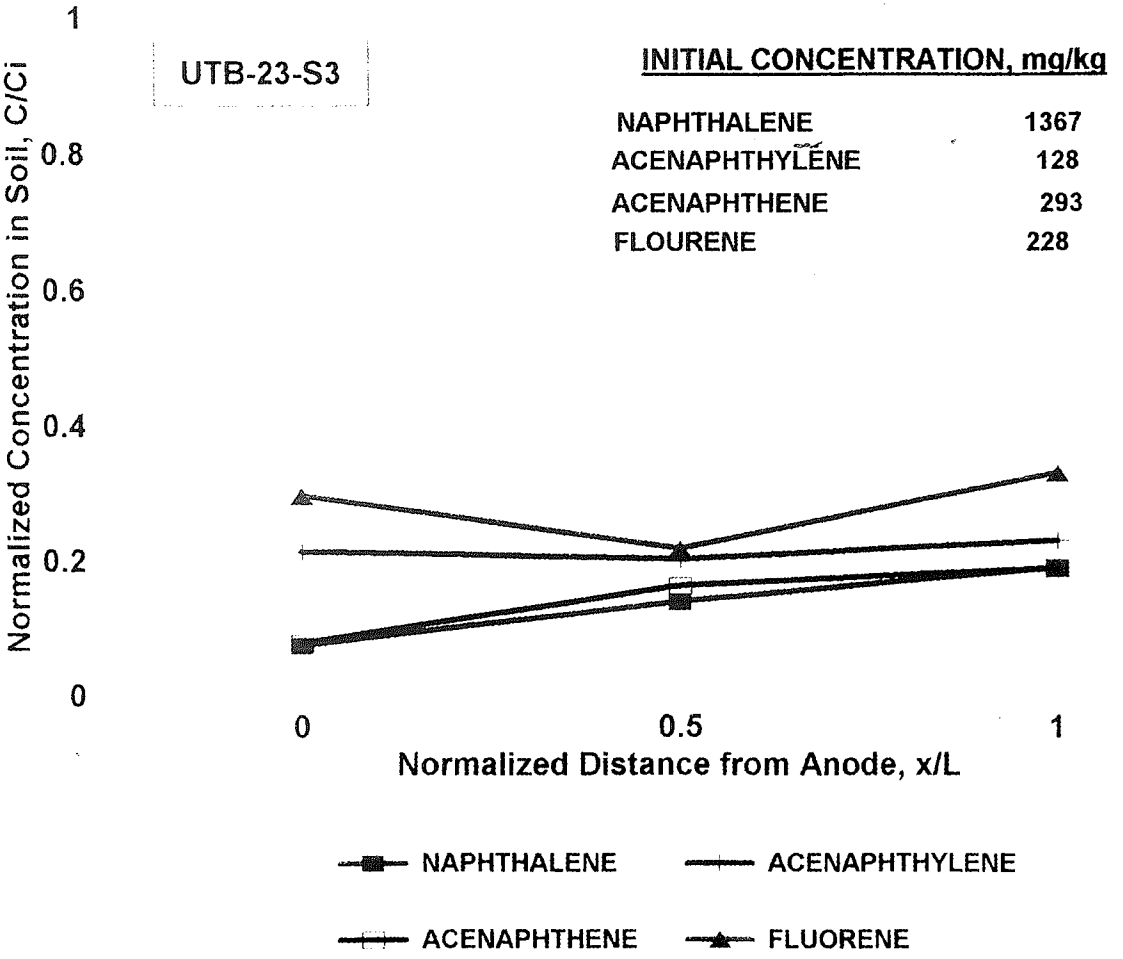
UTB-23-S3
INITIAL CONCENTRATION, mg/kg
NAPHTHALENE 1367
ACENAPHTHYLENE 128
ACENAPHTHENE 293
FLOURENE 228
Normalized Concentration in Soil, C/Ci
1
0.8
0.6
0.4
0.2
0
0
0.5
1
Normalized Distance from Anode, x/L
NAPHTHALENE
ACENAPHTHYLENE
ACENAPHTHENE
FLUORENE

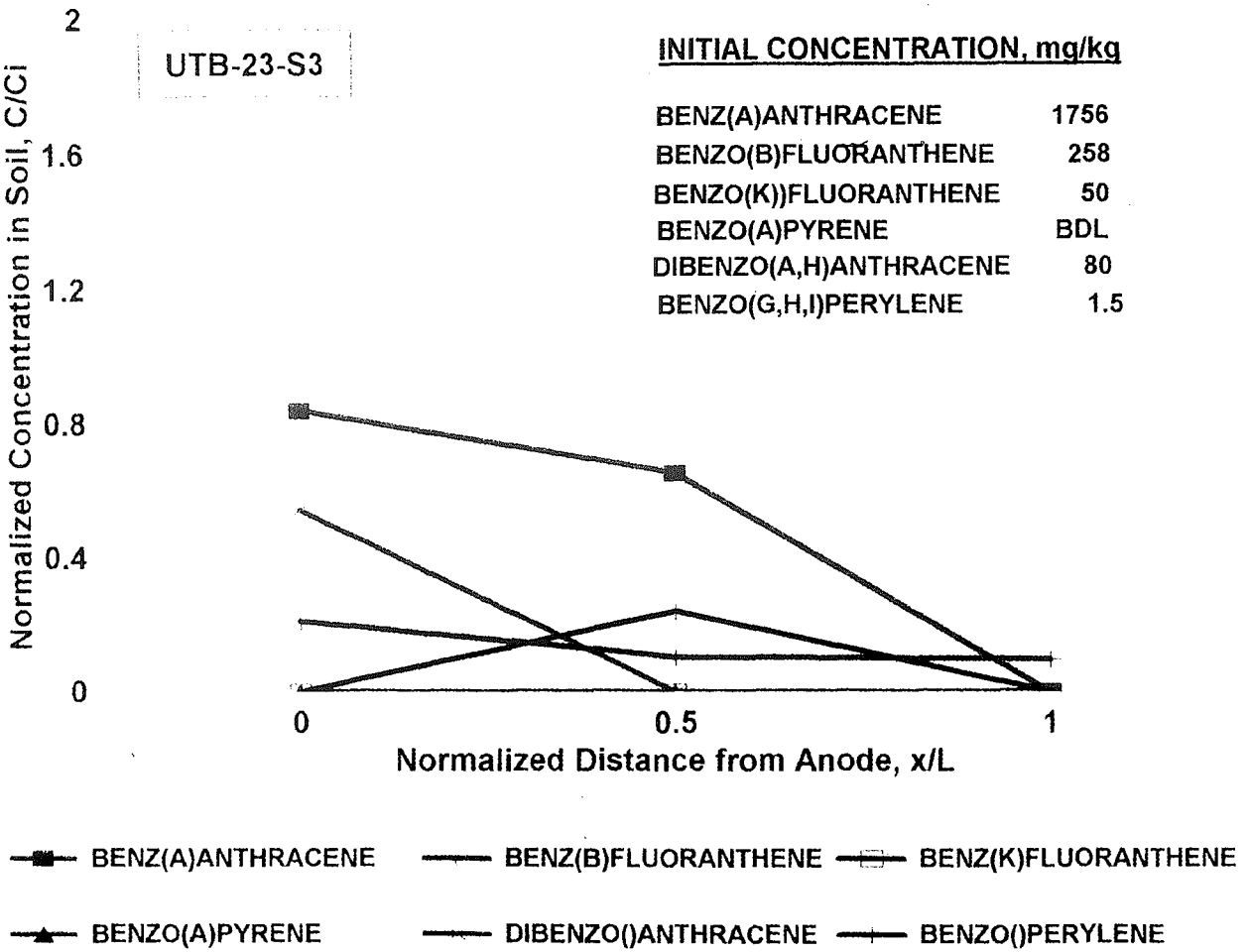
UTB-23-S3
INITIAL CONCENTRATION, mg/kg
BENZ(A)ANTHRACENE 1756
BENZO(B)FLUORANTHENE 258
BENZO(K))FLUORANTHENE 50
BENZO(A)PYRENE BDL
DIBENZO(A,H)ANTHRACENE 80
BENZO(G,H,I)PERYLENE 1.5
Normalized Concentration in Soil, C/Ci
2
1.6
1.2
0.8
0.4
0
0
0.5
1
Normalized Distance from Anode, x/L
BENZ(A)ANTHRACENE
BENZ(B)FLUORANTHENE
BENZ(K)FLUORANTHENE
BENZO(A)PYRENE
DIBENZO()ANTHRACENE
BENZO()PERYLENE

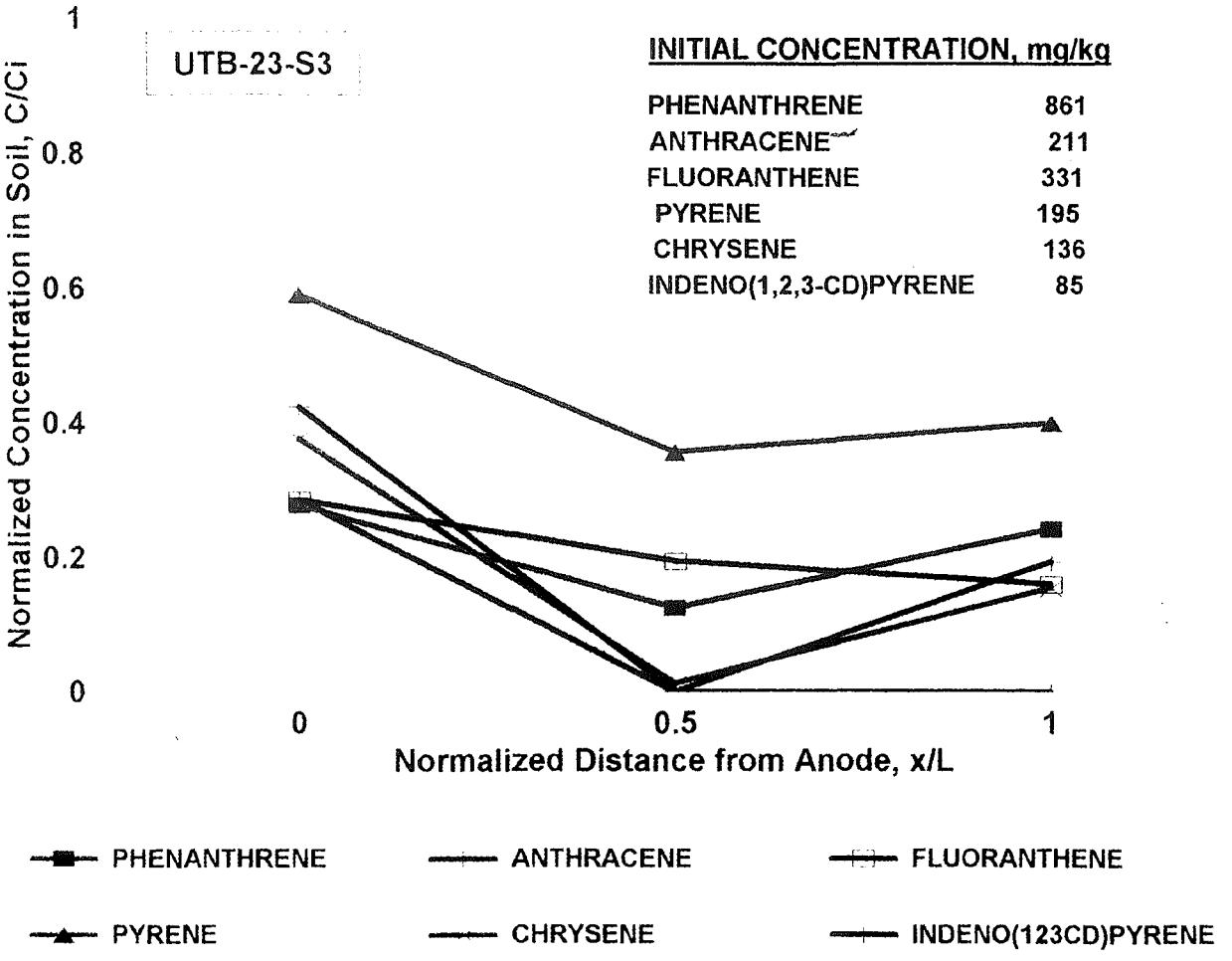
UTB-23-S3
INITIAL CONCENTRATION, mg/kg
PHENANTHRENE 861
ANTHRACENE 211
FLUORANTHENE 331
PYRENE 195
CHRYSENE 136
INDENO(1,2,3-CD)PYRENE 85
Normalized Concentration in Soil, C/Ci
1
0.8
0.6
0.4
0.2
0
0
0.5
1
Normalized Distance from Anode, x/L
PHENANTHRENE
ANTHRACENE
FLUORANTHENE
PYRENE
CHRYSENE
INDENO(123CD)PYRENE

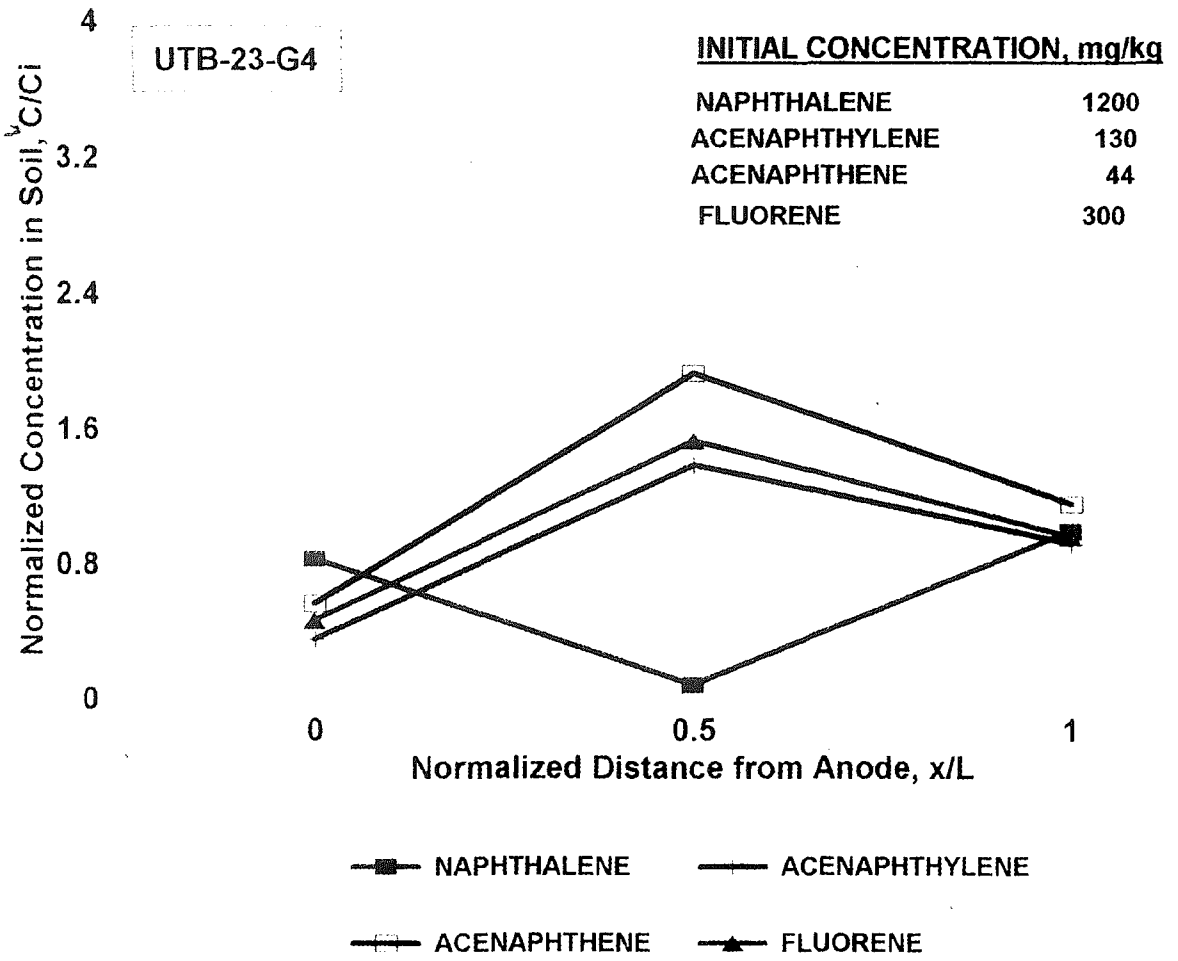
UTB-23-G4
INITIAL CONCENTRATION, mg/kg
NAPHTHALENE 1200
ACENAPHTHYLENE 130
ACENAPHTHENE 44
FLUORENE 300
Normalized Concentration in Soil, C/Ci
4
3.2
2.4
1.6
0.8
0
0
0.5
1
Normalized Distance from Anode, x/L
NAPHTHALENE
ACENAPHTHYLENE
ACENAPHTHENE
FLUORENE

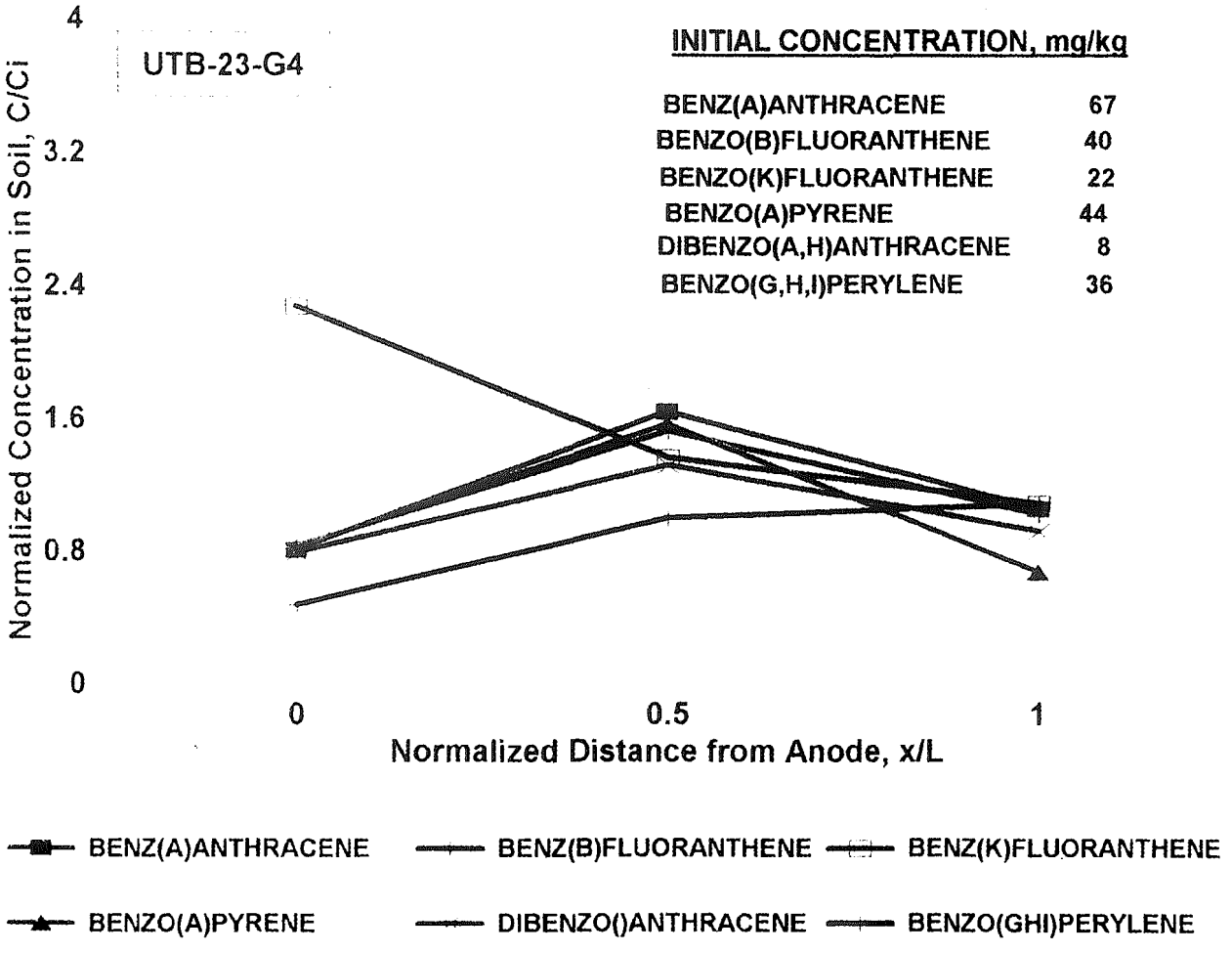
UTB-23-G4
INITIAL CONCENTRATION, mg/kg
BENZ(A)ANTHRACENE 67
BENZO(B)FLUORANTHENE 40
BENZO(K)FLUORANTHENE 22
BENZO(A)PYRENE 44
DIBENZO(A,H)ANTHRACENE 8
BENZO(G,H,I)PERYLENE 36
Normalized Concentration in Soil, C/Ci
4
3.2
2.4
1.6
0.8
0
0
0.5
1
Normalized Distance from Anode, x/L
BENZ(A)ANTHRACENE
BENZ(B)FLUORANTHENE
BENZ(K)FLUORANTHENE
BENZO(A)PYRENE
DIBENZO()ANTHRACENE
BENZO(GHI)PERYLENE

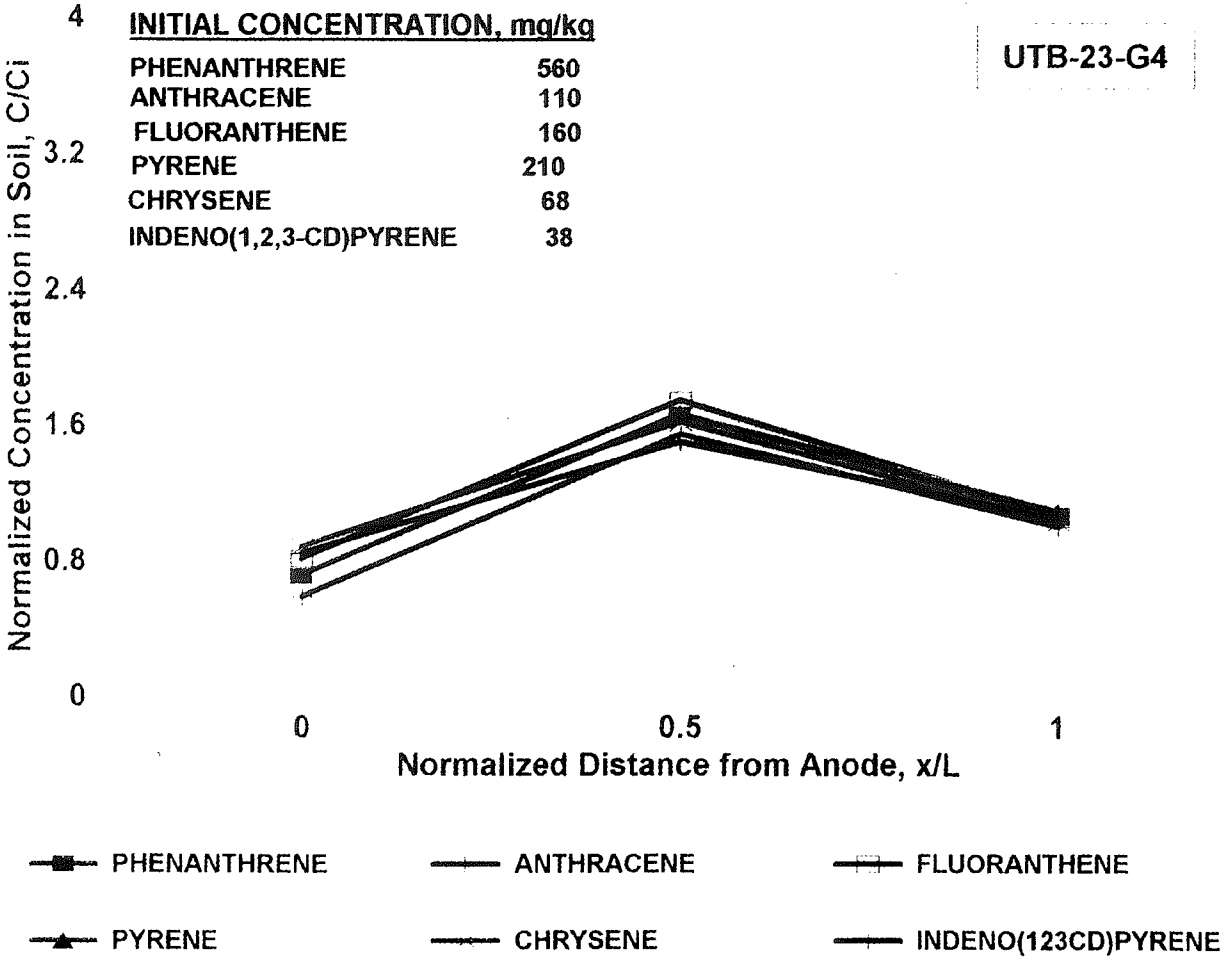
INITIAL CONCENTRATION, mg/kg
PHENANTHRENE 560
ANTHRACENE 110
FLUORANTHENE 160
PYRENE 210
CHRYSENE 68
INDENO(1,2,3-CD)PYRENE 38
UTB-23-G4
Normalized Concentration in Soil, C/Ci
4
3.2
2.4
1.6
0.8
0
0
0.5
1
Normalized Distance from Anode, x/L
PHENANTHRENE
ANTHRACENE
FLUORANTHENE
PYRENE
CHRYSENE
INDENO(123CD)PYRENE

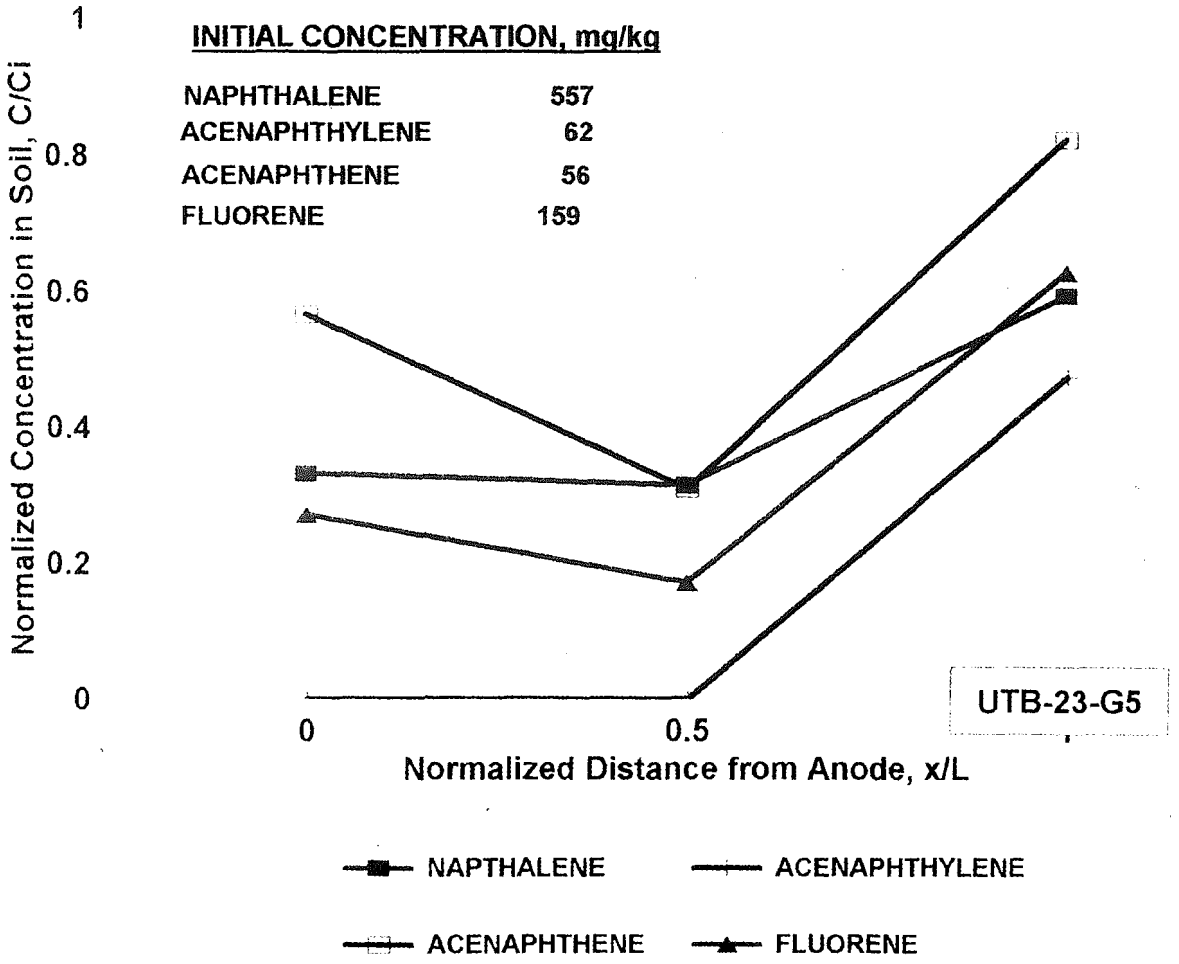
INITIAL CONCENTRATION, mg/kg
NAPHTHALENE 557
ACENAPHTHYLENE 62
ACENAPHTHENE 56
FLUORENE 159
Normalized Concentration in Soil, C/Ci
1
0.8
0.6
0.4
0.2
0
0
0.5
Normalized Distance from Anode, x/L
UTB-23-G5
NAPTHALENE
ACENAPHTHYLENE
ACENAPHTHENE
FLUORENE

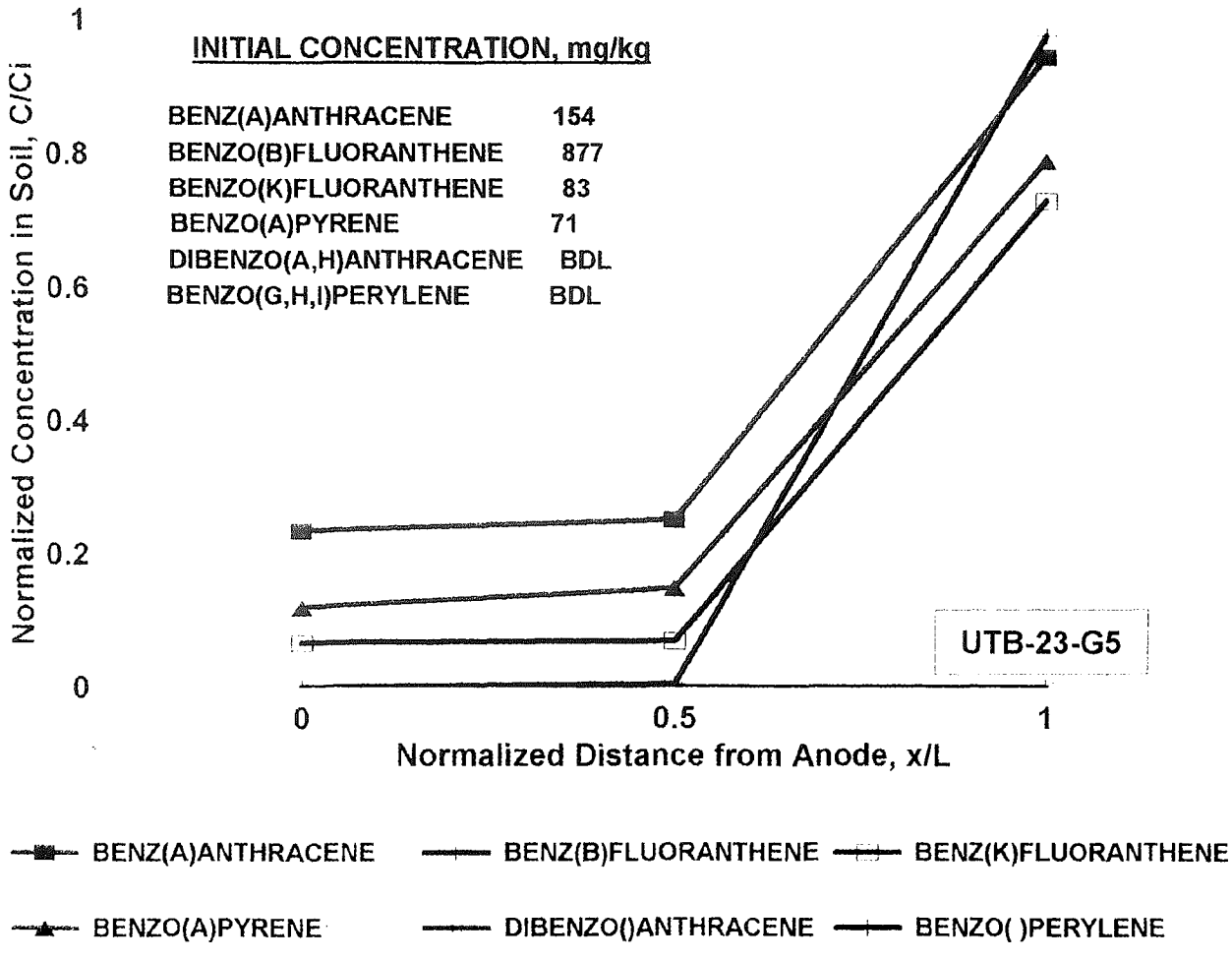
INITIAL CONCENTRATION, mg/kg
BENZ(A)ANTHRACENE 154
BENZO(B)FLUORANTHENE 877
BENZO(K)FLUORANTHENE 83
BENZO(A)PYRENE 71
DIBENZO(A,H)ANTHRACENE BDL
BENZO(G,H,I)PERYLENE BDL
UTB-23-G5
Normalized Concentration in Soil, C/Ci
Normalized Distance from Anode, x/L
0
0.2
0.4
0.6
0.8
1
0.5
BENZ(A)ANTHRACENE
BENZ(B)FLUORANTHENE
BENZ(K)FLUORANTHENE
BENZO(A)PYRENE
DIBENZO()ANTHRACENE
BENZO( )PERYLENE

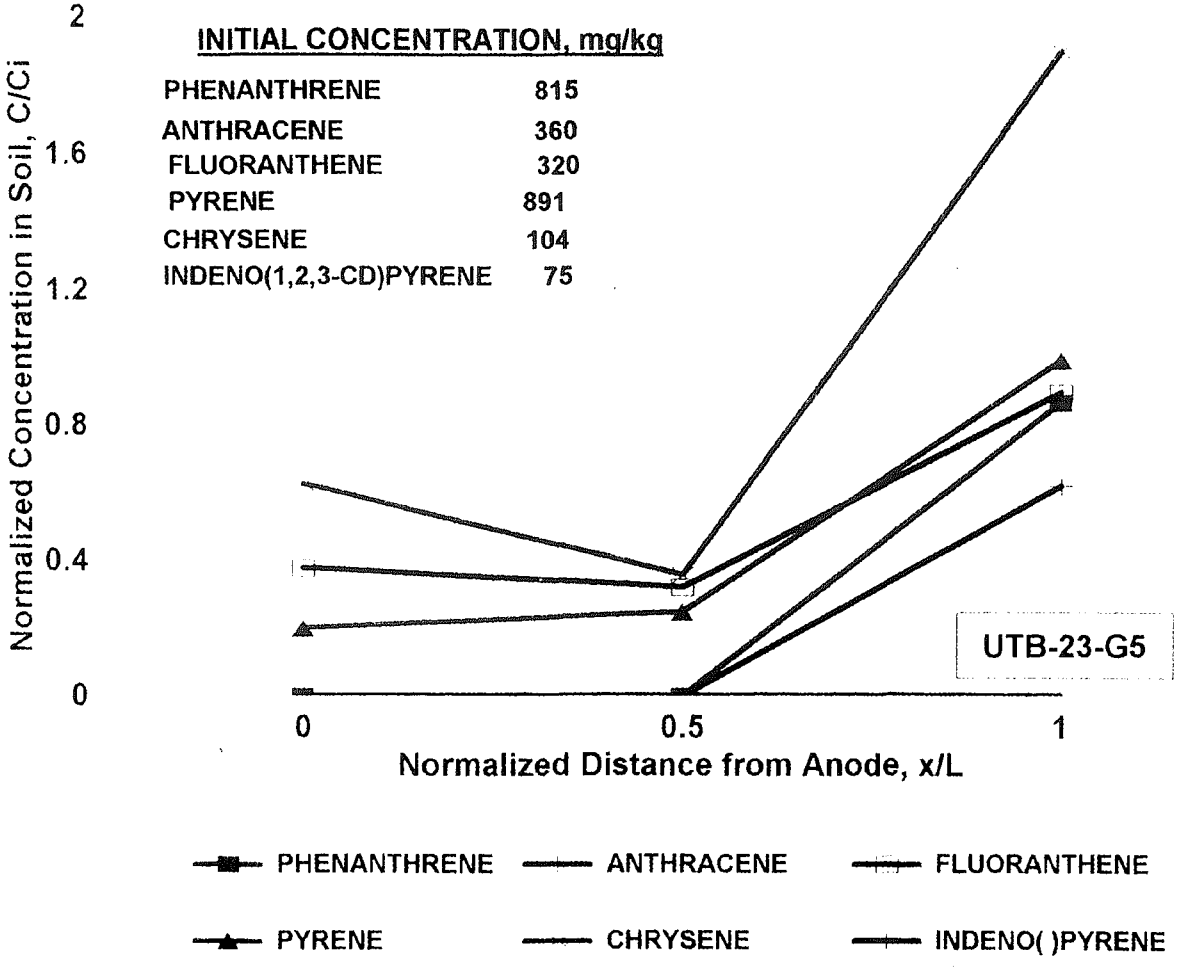
INITIAL CONCENTRATION, mg/kg
PHENANTHRENE 815
ANTHRACENE 360
FLUORANTHENE 320
PYRENE 891
CHRYSENE 104
INDENO(1,2,3-CD)PYRENE 75
Normalized Concentration in Soil, C/Ci
2
1.6
1.2
0.8
0.4
0
0
0.5
1
Normalized Distance from Anode, x/L
UTB-23-G5
PHENANTHRENE
ANTHRACENE
FLUORANTHENE
PYRENE
CHRYSENE
INDENO( )PYRENE

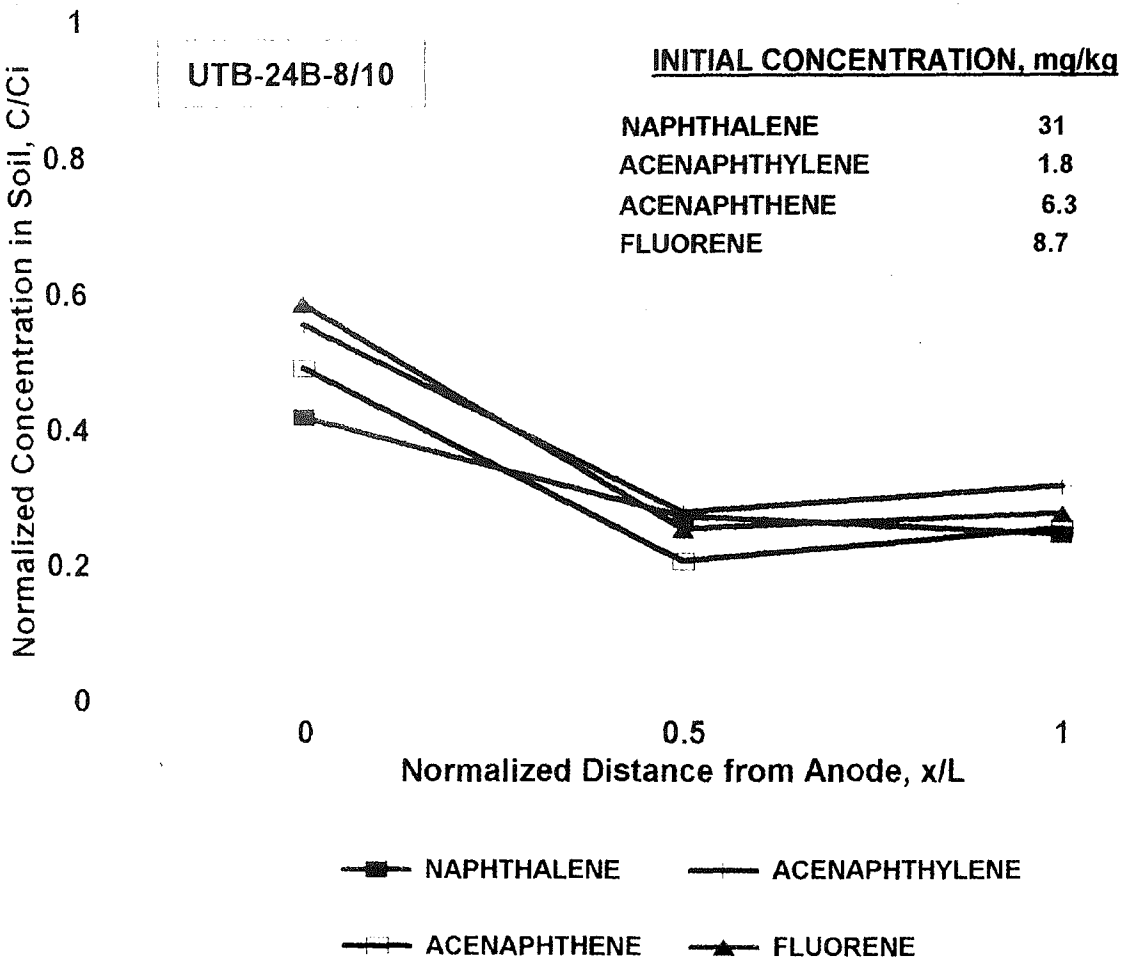
UTB-24B-8/10
INITIAL CONCENTRATION, mg/kg
NAPHTHALENE 31
ACENAPHTHYLENE 1.8
ACENAPHTHENE 6.3
FLUORENE 8.7
Normalized Concentration in Soil, C/Ci
1
0.8
0.6
0.4
0.2
0
0
0.5
1
Normalized Distance from Anode, x/L
NAPHTHALENE
ACENAPHTHYLENE
ACENAPHTHENE
FLUORENE

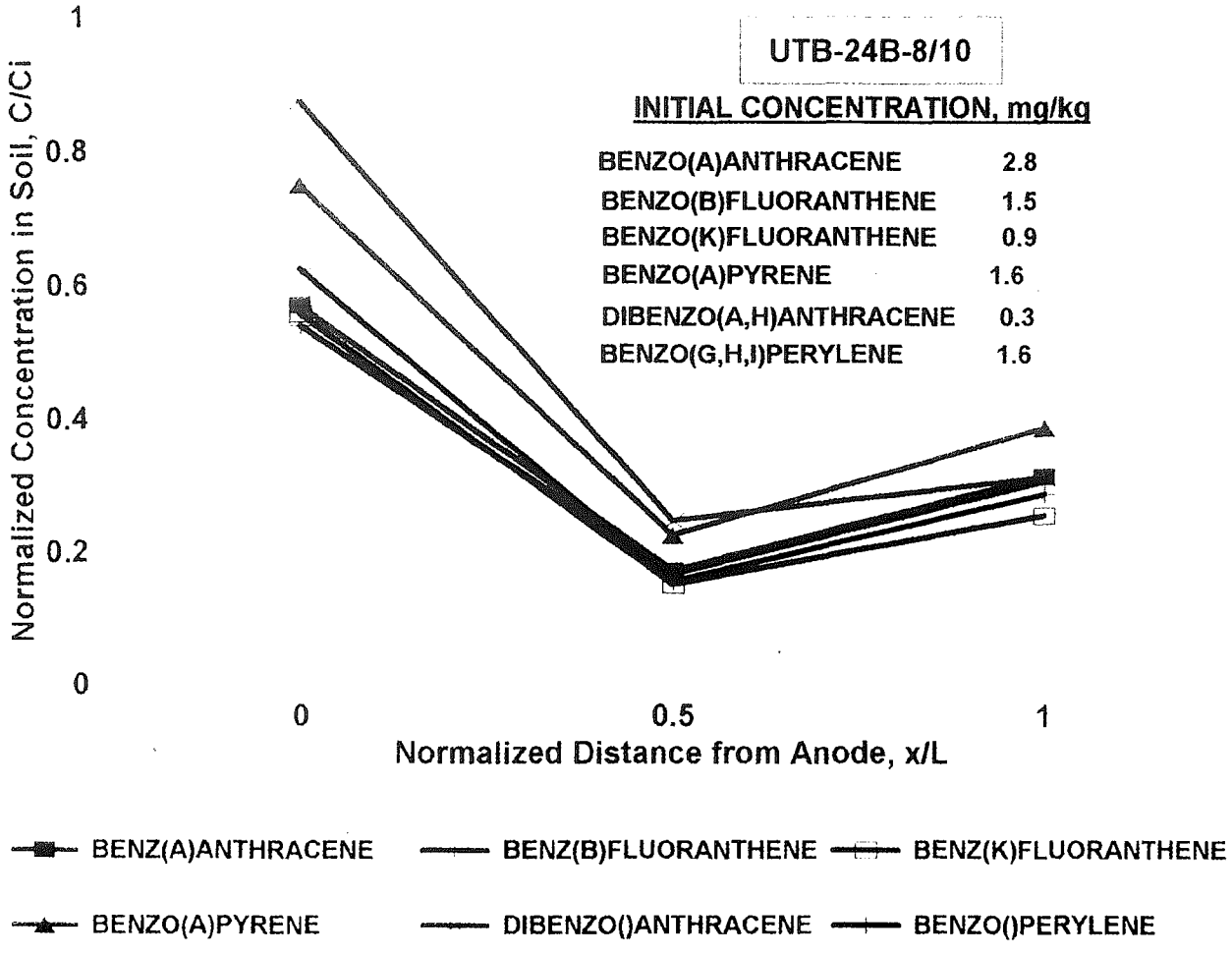
UTB-24B-8/10
INITIAL CONCENTRATION, mg/kg
BENZO(A)ANTHRACENE 2.8
BENZO(B)FLUORANTHENE 1.5
BENZO(K)FLUORANTHENE 0.9
BENZO(A)PYRENE 1.6
DIBENZO(A,H)ANTHRACENE 0.3
BENZO(G,H,I)PERYLENE 1.6
Normalized Concentration in Soil, C/Ci
1
0.8
0.6
0.4
0.2
0
0
0.5
1
Normalized Distance from Anode, x/L
BENZ(A)ANTHRACENE
BENZ(B)FLUORANTHENE
BENZ(K)FLUORANTHENE
BENZO(A)PYRENE
DIBENZO()ANTHRACENE
BENZO()PERYLENE

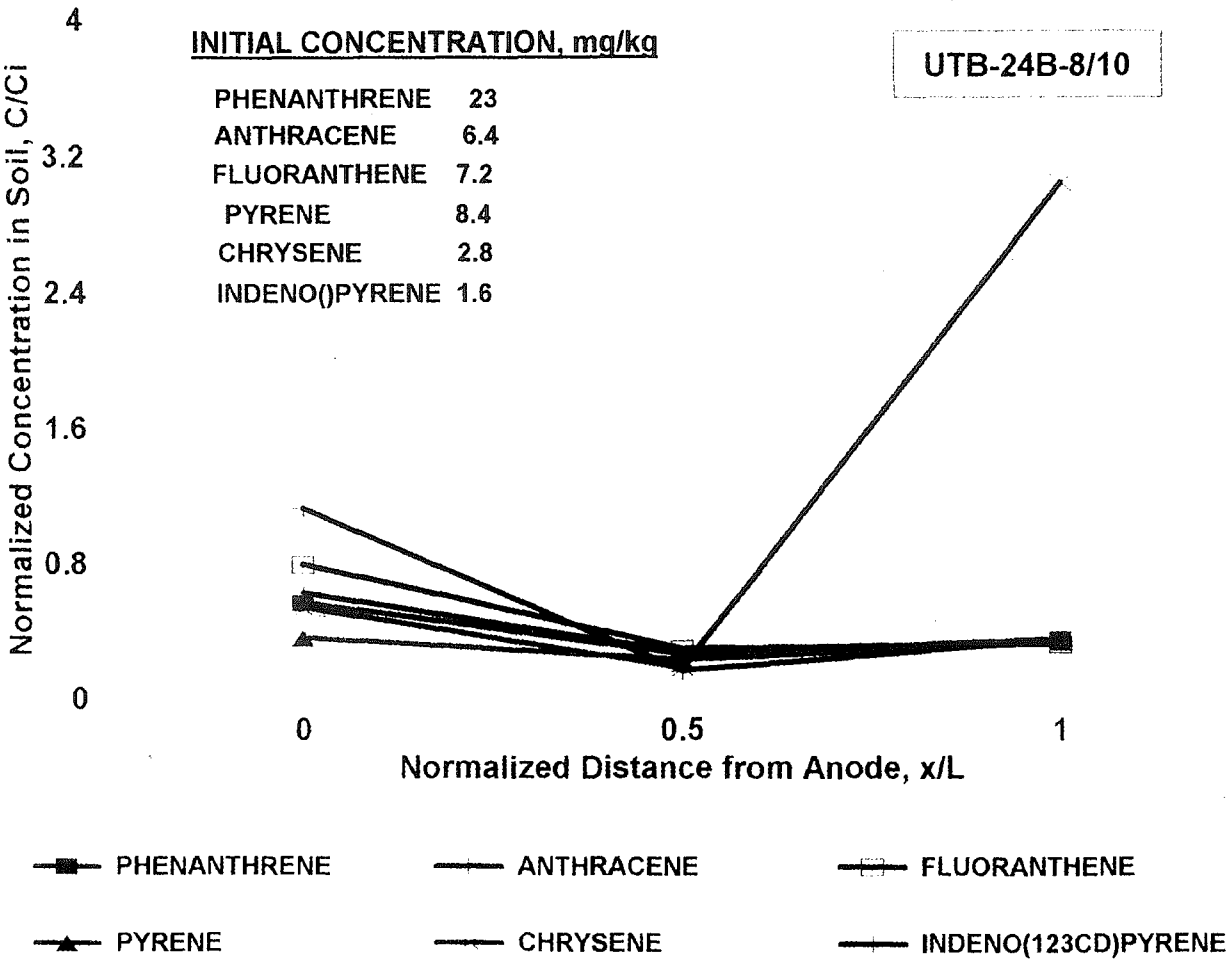
INITIAL CONCENTRATION, mg/kg
PHENANTHRENE 23
ANTHRACENE 6.4
FLUORANTHENE 7.2
PYRENE 8.4
CHRYSENE 2.8
INDENO()PYRENE 1.6
UTB-24B-8/10
Normalized Concentration in Soil, C/Ci
4
3.2
2.4
1.6
0.8
0
0
0.5
1
Normalized Distance from Anode, x/L
PHENANTHRENE
ANTHRACENE
FLUORANTHENE
PYRENE
CHRYSENE
INDENO(123CD)PYRENE

APPENDIX D

CHEMICAL CONCENTRATION DATA

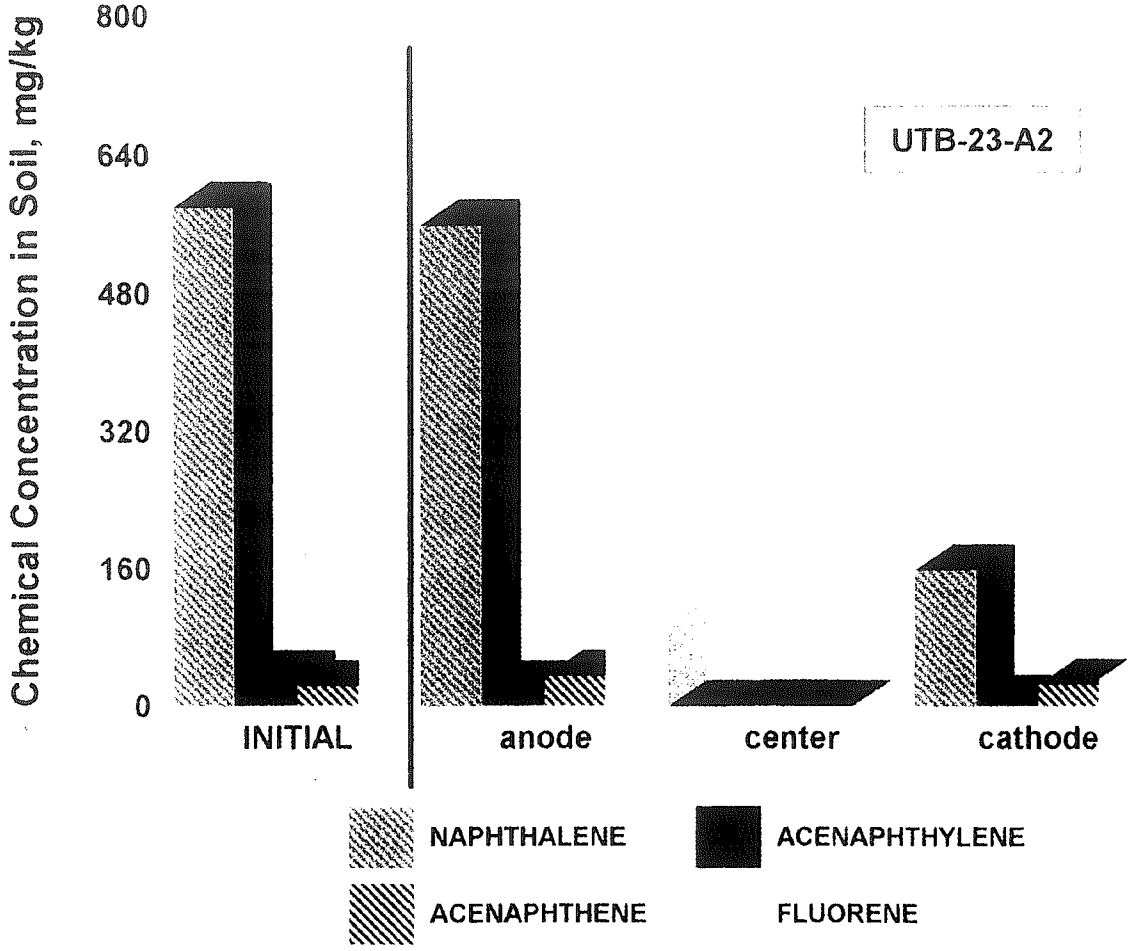
Chemical Concentration in Soil, mg/kg
800
640
480
320
160
0
UTB-23-A2
INITIAL
anode
center
cathode
NAPHTHALENE
ACENAPHTHYLENE
ACENAPHTHENE
FLUORENE

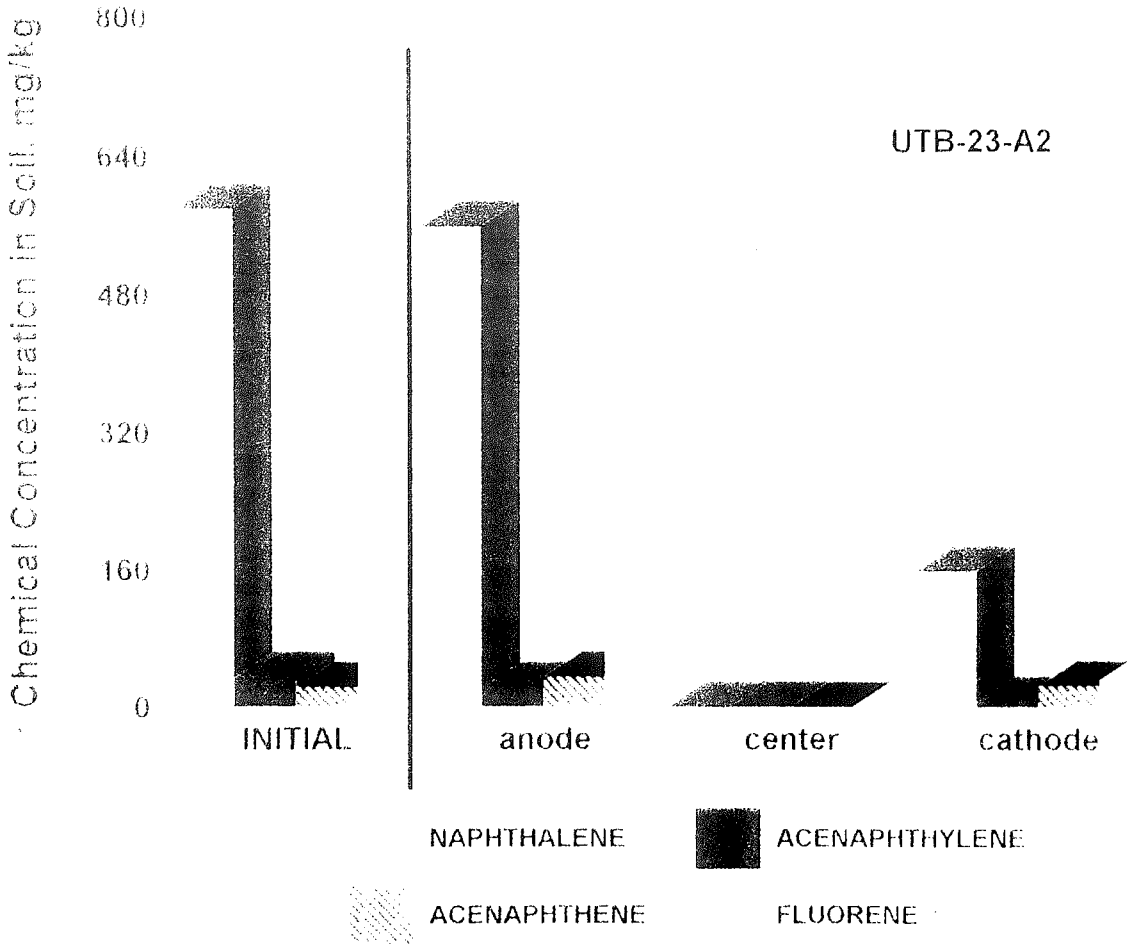
Chemical Concentration in Soil, mg/kg
800
640
480
320
160
0
UTB-23-A2
INITIAL
anode
center
cathode
NAPHTHALENE
ACENAPHTHYLENE
ACENAPHTHENE
FLUORENE

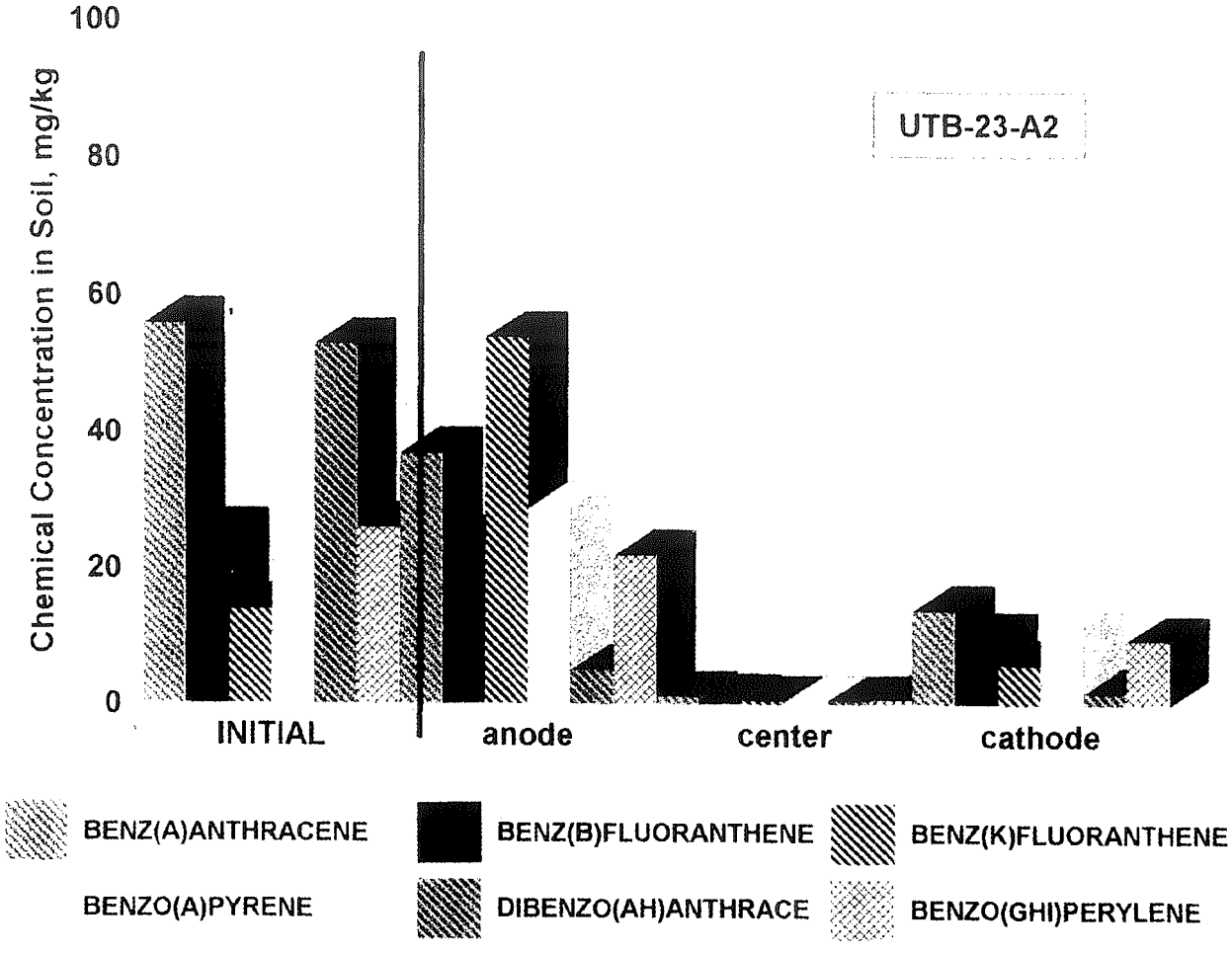
100
80
60
40
20
0
Chemical Concentration in Soil, mg/kg
UTB-23-A2
INITIAL
anode
center
cathode
BENZ(A)ANTHRACENE
BENZ(B)FLUORANTHENE
BENZ(K)FLUORANTHENE
BENZO(A)PYRENE
DIBENZO(AH)ANTHRACE
BENZO(GHI)PERYLENE

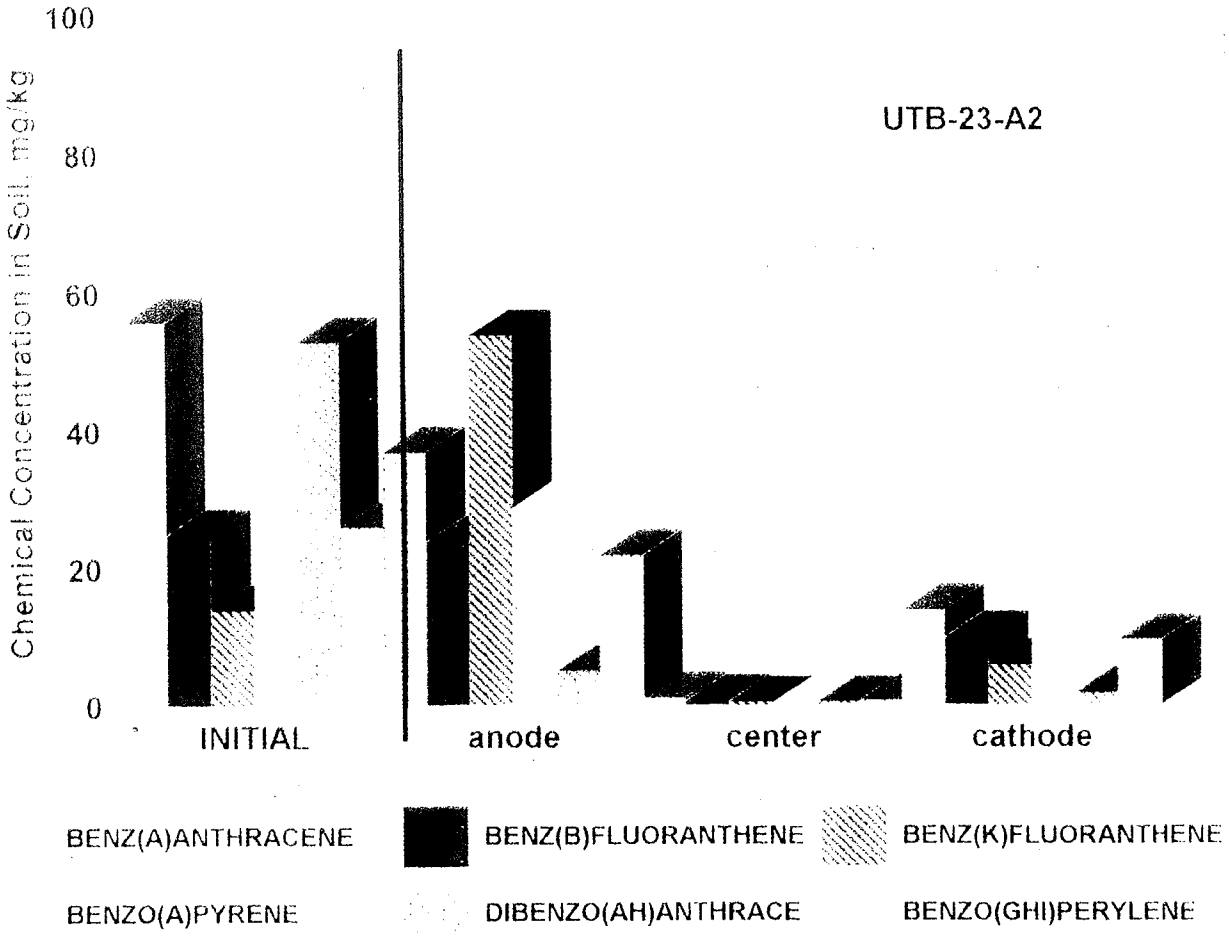
UTB-23-A2
Chemical Concentration in Soil, mg/kg
100
80
60
40
20
0
INITIAL
anode
center
cathode
BENZ(A)ANTHRACENE
BENZ(B)FLUORANTHENE
BENZ(K)FLUORANTHENE
BENZO(A)PYRENE
DIBENZO(AH)ANTHRACE
BENZO(GHI)PERYLENE

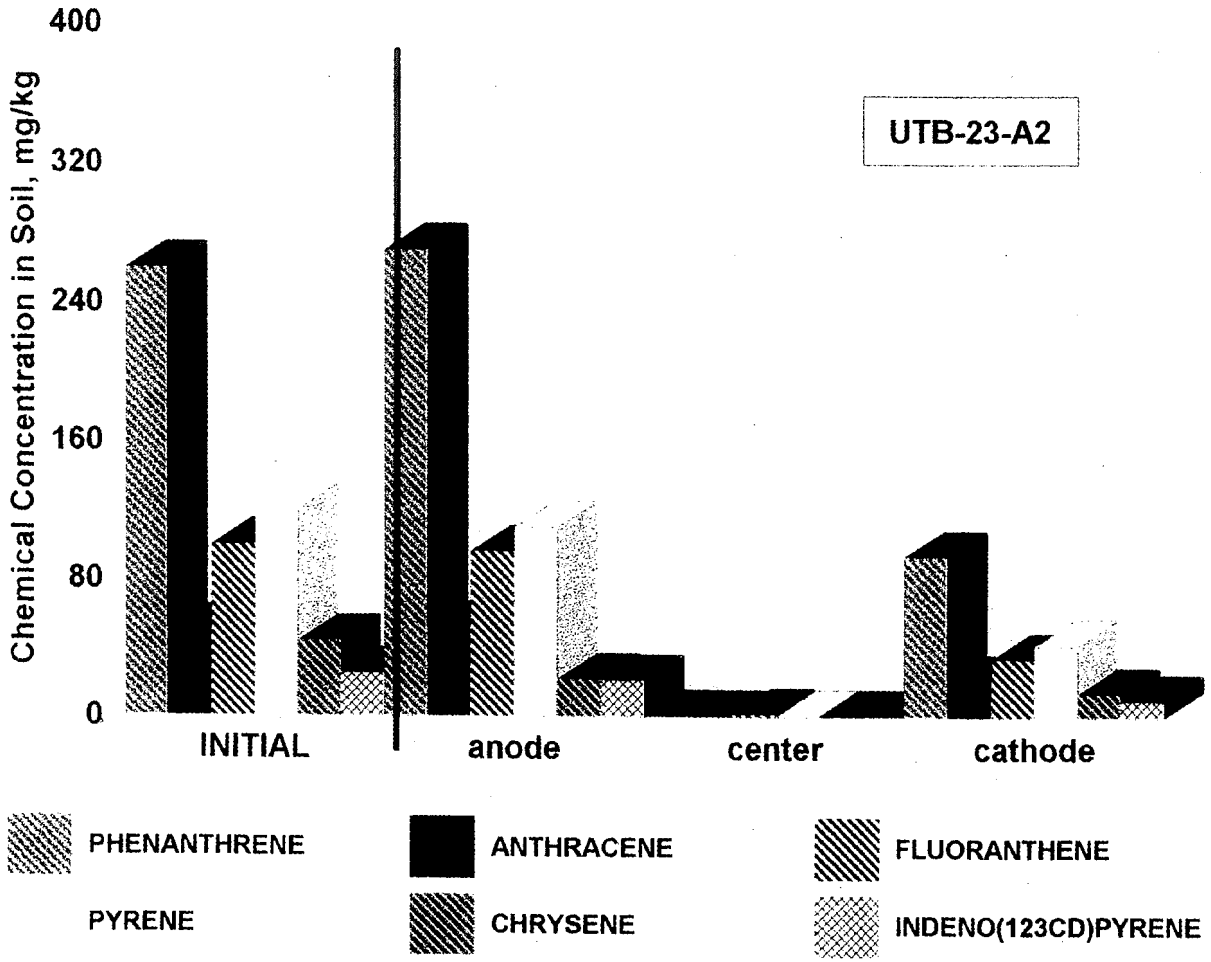
UTB-23-A2
Chemical Concentration in Soil, mg/kg
400
320
240
160
80
0
INITIAL
anode
center
cathode
PHENANTHRENE
ANTHRACENE
FLUORANTHENE
PYRENE
CHRYSENE
INDENO(123CD)PYRENE

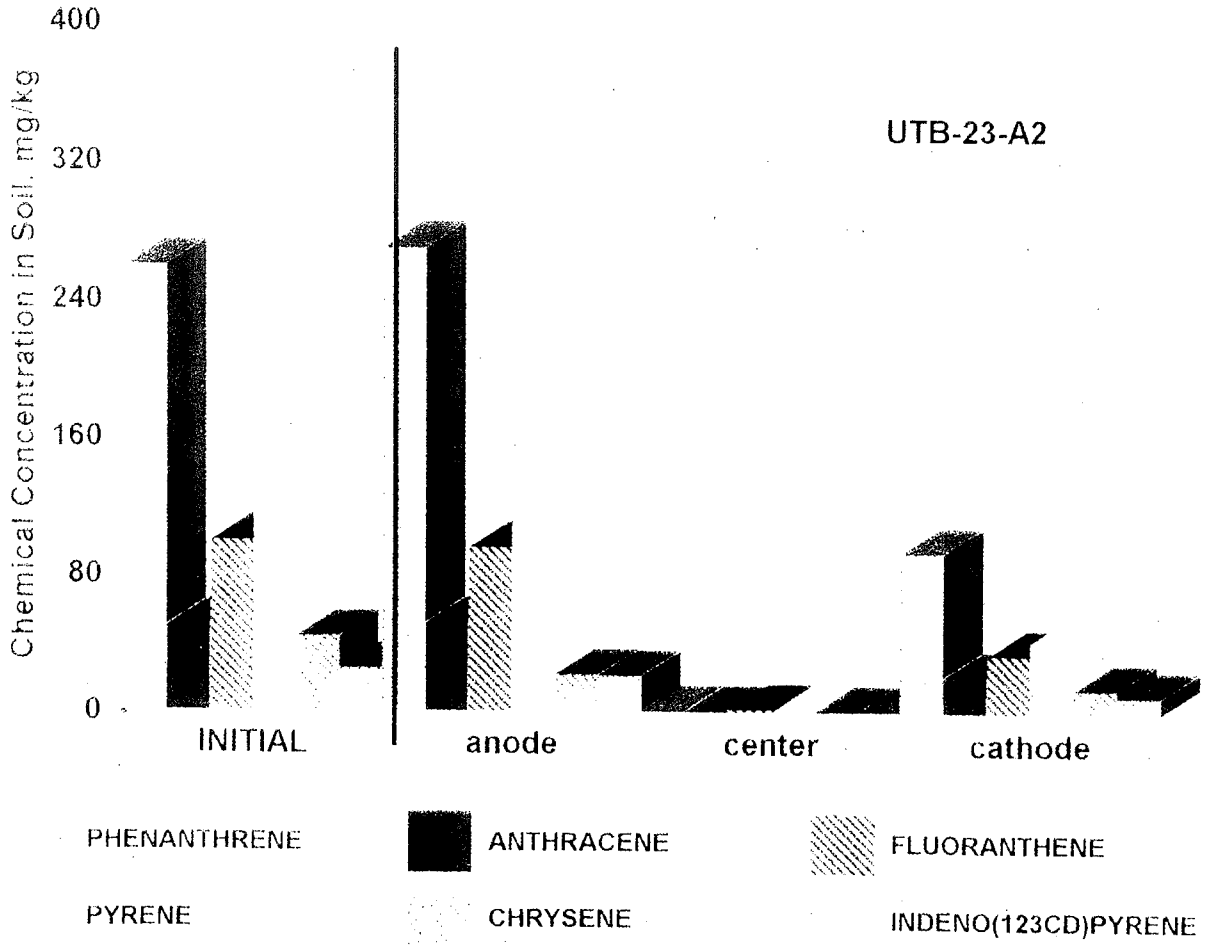
400
320
240
160
80
0
Chemical Concentration in Soil, mg/kg
UTB-23-A2
INITIAL
anode
center
cathode
PHENANTHRENE
ANTHRACENE
FLUORANTHENE
PYRENE
CHRYSENE
INDENO(123CD)PYRENE

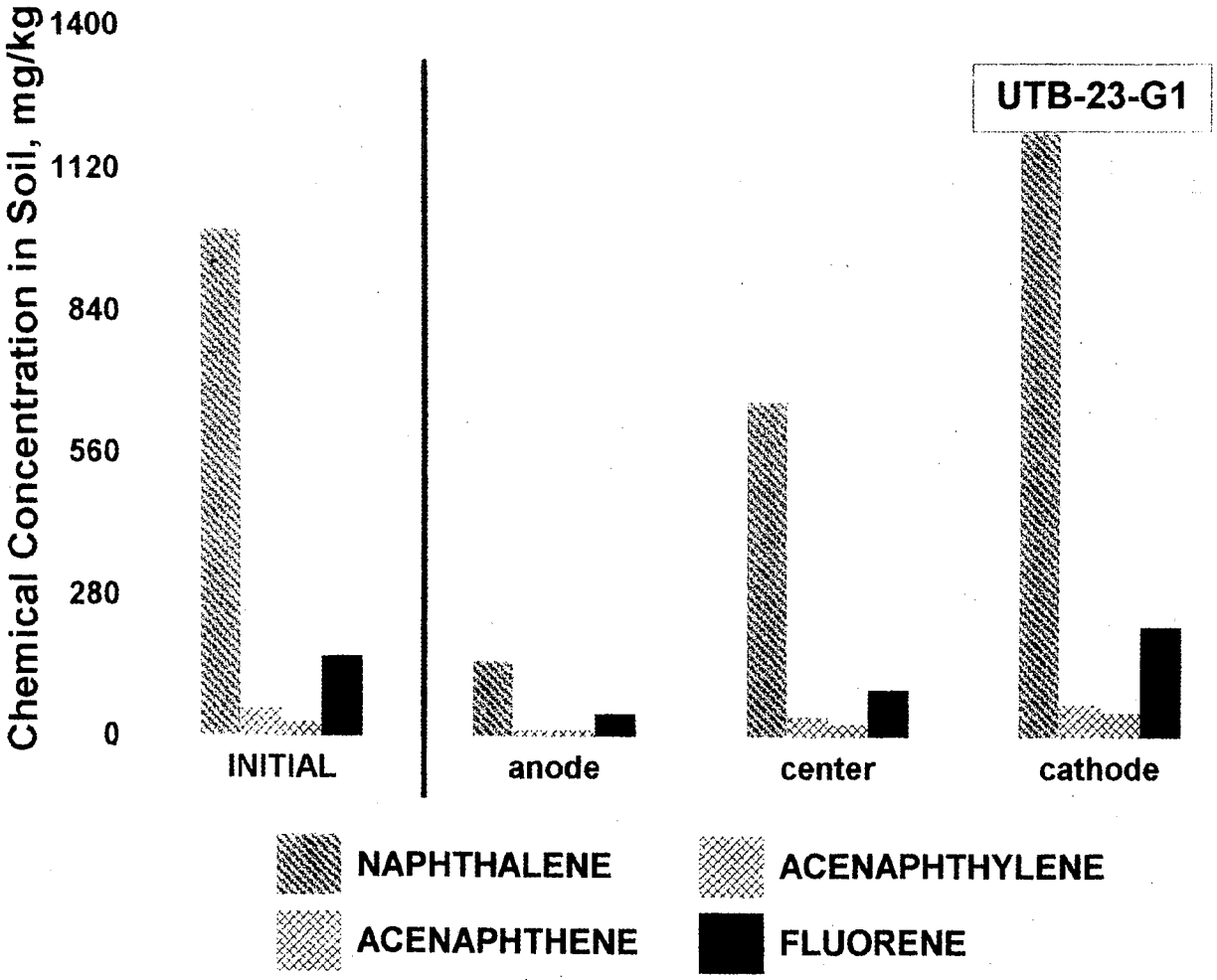
Chemical Concentration in Soil, mg/kg
1400
1120
840
560
280
0
UTB-23-G1
INITIAL
anode
center
cathode
NAPHTHALENE
ACENAPHTHYLENE
ACENAPHTHENE
FLUORENE

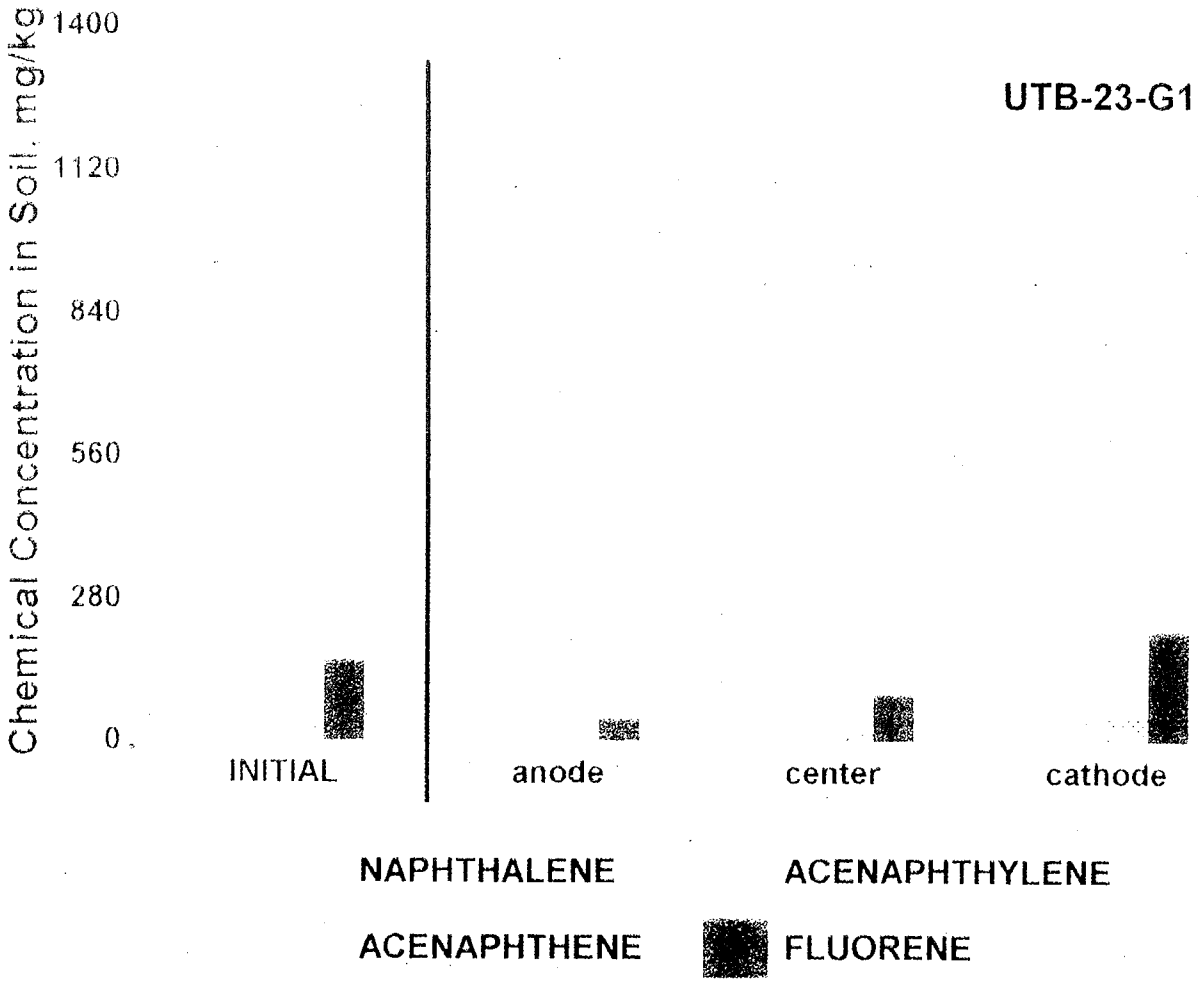
Chemical Concentration in Soil, mg/kg
1400
1120
840
560
280
0
UTB-23-G1
INITIAL
anode
center
cathode
NAPHTHALENE
ACENAPHTHYLENE
ACENAPHTHENE
FLUORENE

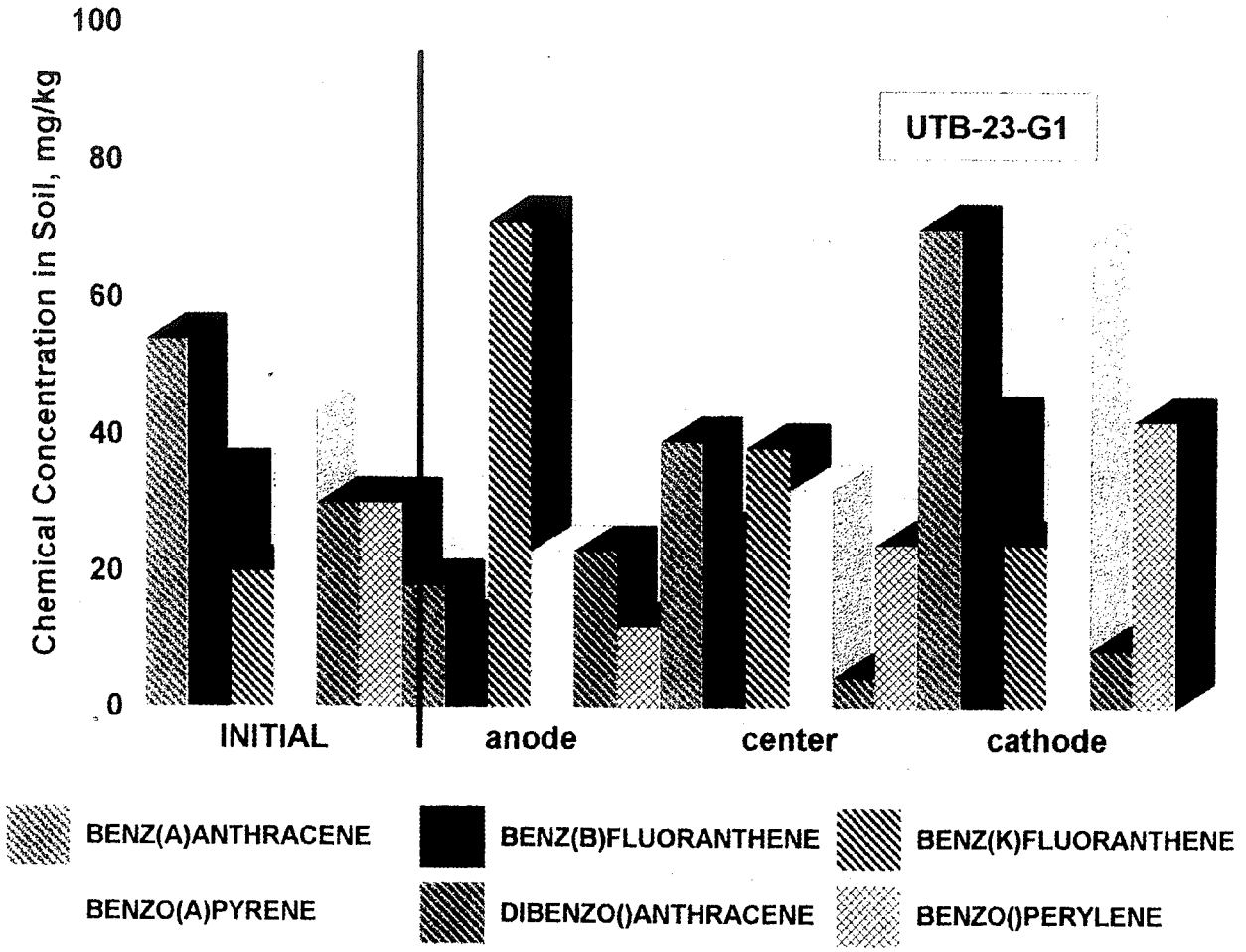
100
80
60
40
20
0
Chemical Concentration in Soil, mg/kg
UTB-23-G1
INITIAL
anode
center
cathode
BENZ(A)ANTHRACENE
BENZ(B)FLUORANTHENE
BENZ(K)FLUORANTHENE
BENZO(A)PYRENE
DIBENZO()ANTHRACENE
BENZO()PERYLENE

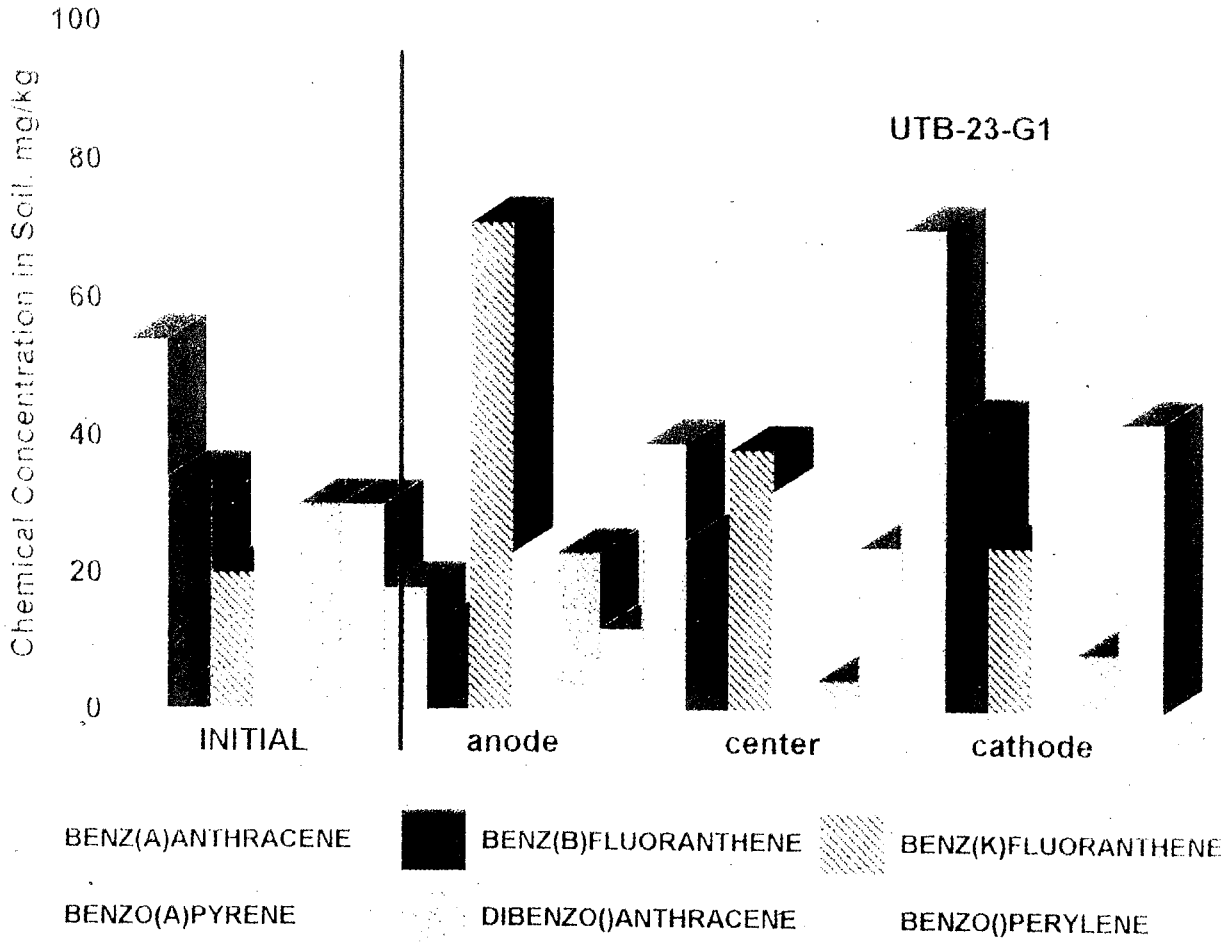
UTB-23-G1
Chemical Concentration in Soil, mg/kg
100
80
60
40
20
0
INITIAL
anode
center
cathode
BENZ(A)ANTHRACENE
BENZ(B)FLUORANTHENE
BENZ(K)FLUORANTHENE
BENZO(A)PYRENE
DIBENZO()ANTHRACENE
BENZO()PERYLENE

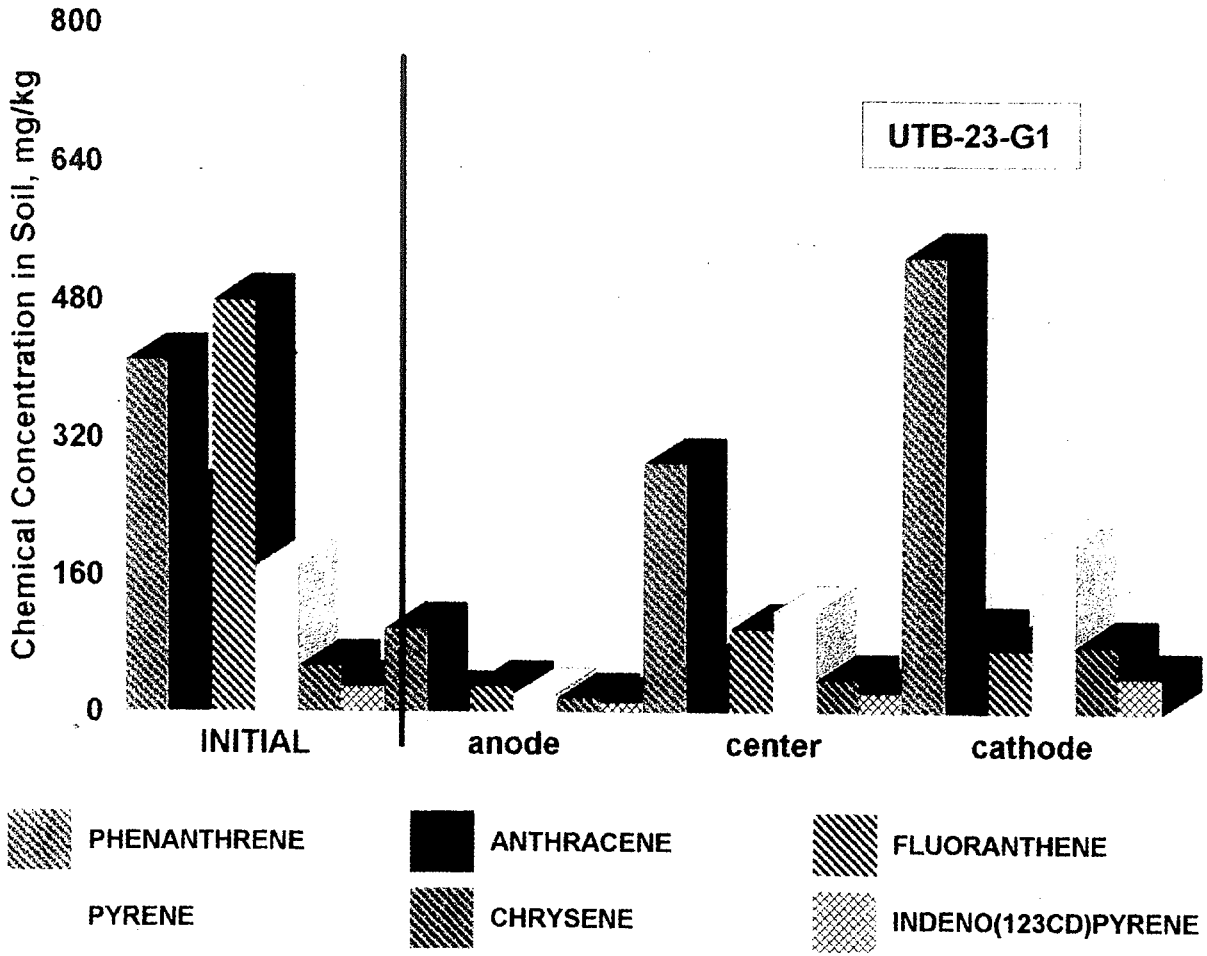
800
640
480
320
160
0
Chemical Concentration in Soil, mg/kg
UTB-23-G1
INITIAL
anode
center
cathode
PHENANTHRENE
ANTHRACENE
FLUORANTHENE
PYRENE
CHRYSENE
INDENO(123CD)PYRENE

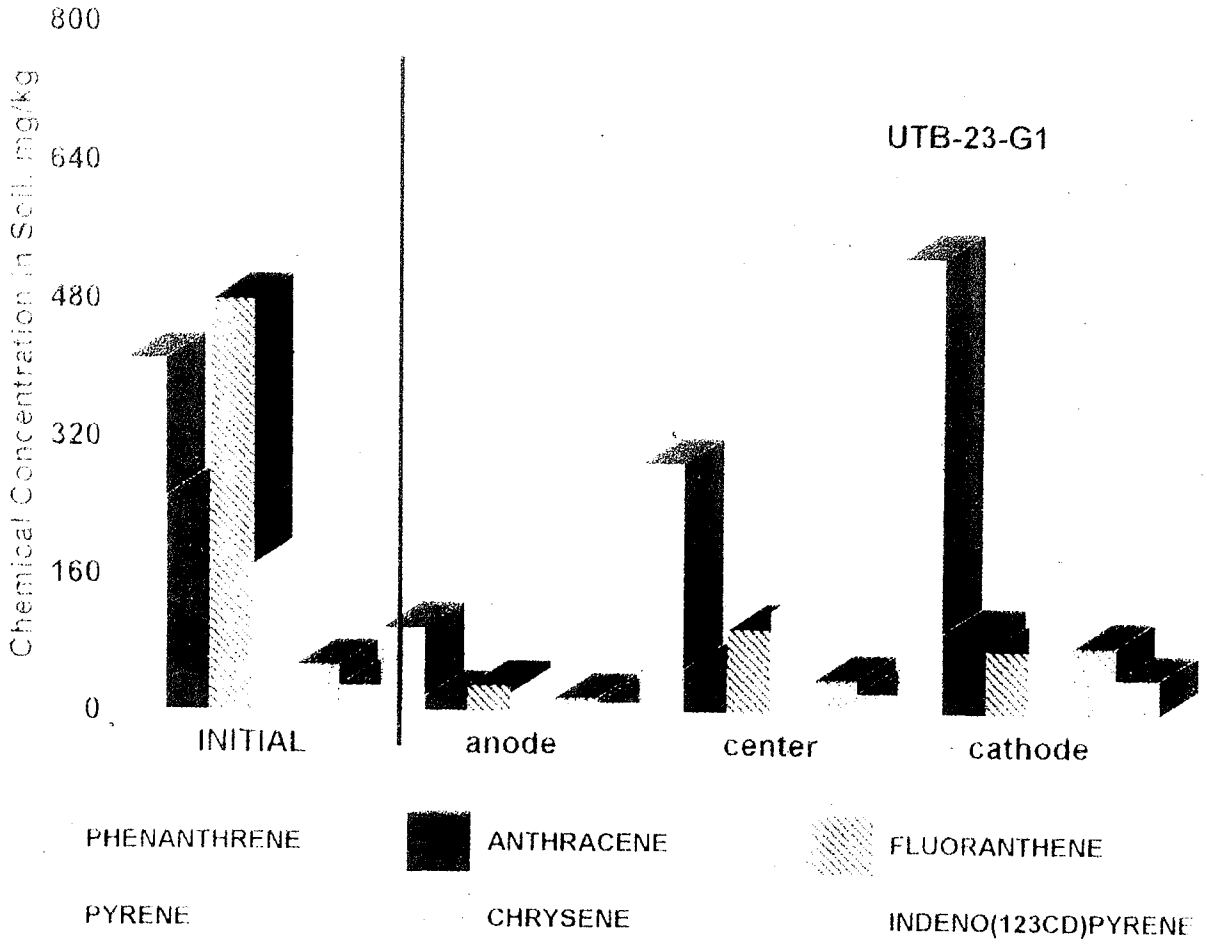
800
640
480
320
160
0
Chemical Concentration in Soil, mg/kg
UTB-23-G1
INITIAL
anode
center
cathode
PHENANTHRENE
ANTHRACENE
FLUORANTHENE
PYRENE
CHRYSENE
INDENO(123CD)PYRENE

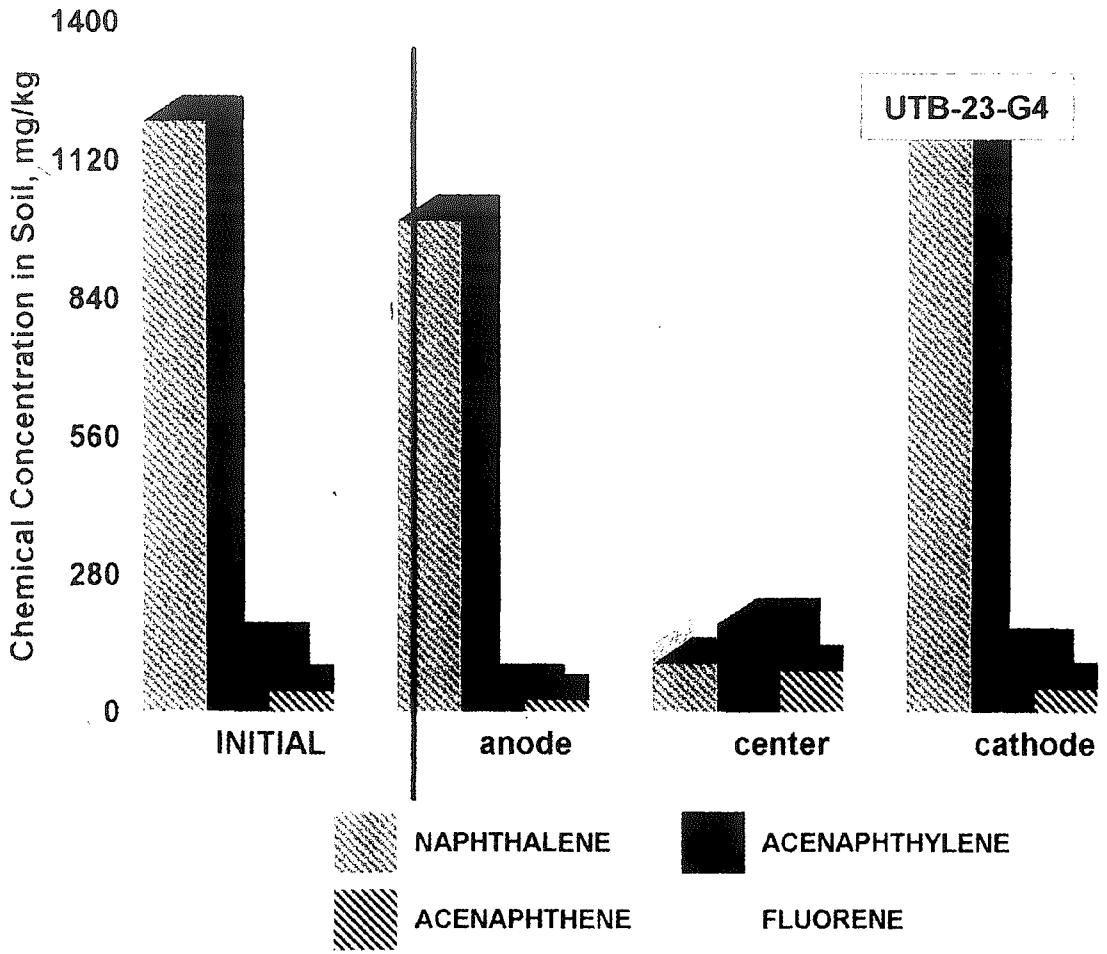
UTB-23-G4
Chemical Concentration in Soil, mg/kg
1400
1120
840
560
280
0
INITIAL
anode
center
cathode
NAPHTHALENE
ACENAPHTHYLENE
ACENAPHTHENE
FLUORENE

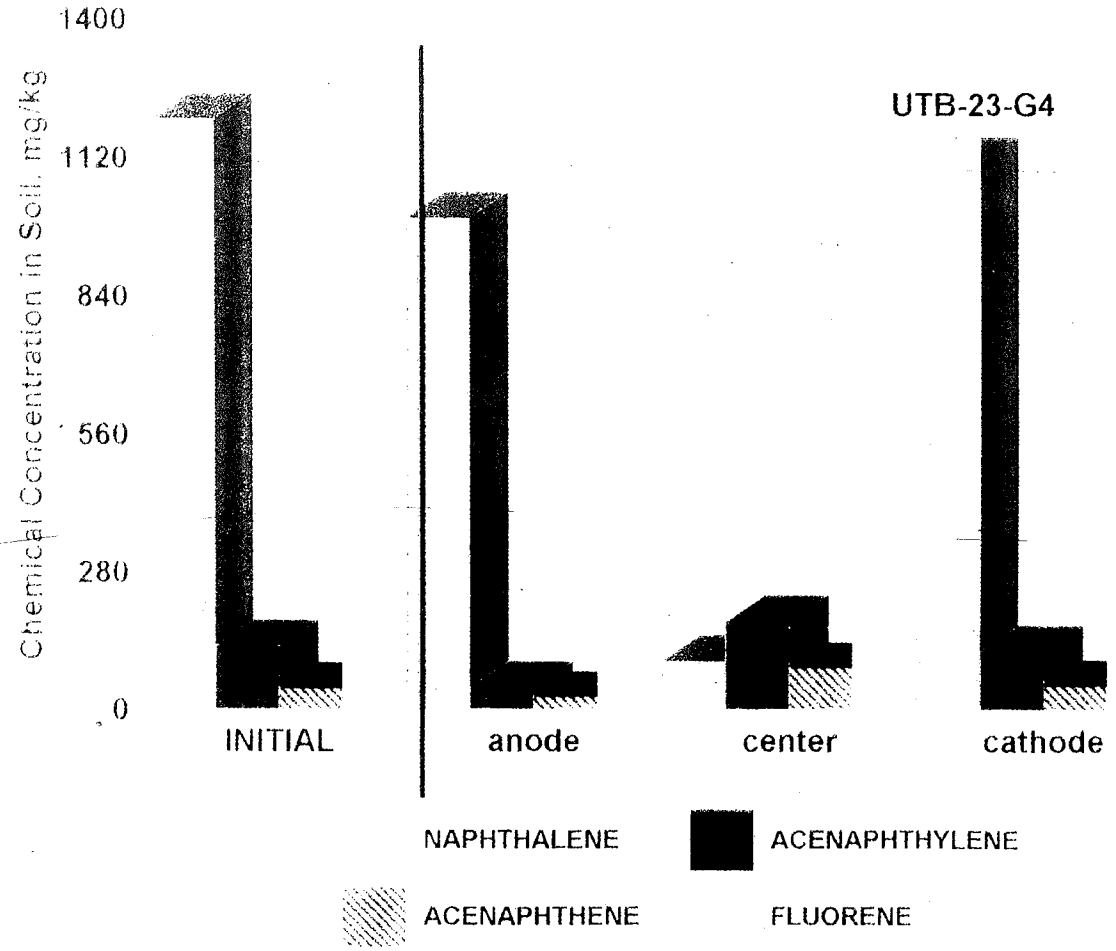
1400
1120
840
560
280
0
Chemical Concentration in Soil, mg/kg
UTB-23-G4
INITIAL
anode
center
cathode
NAPHTHALENE
ACENAPHTHYLENE
ACENAPHTHENE
FLUORENE

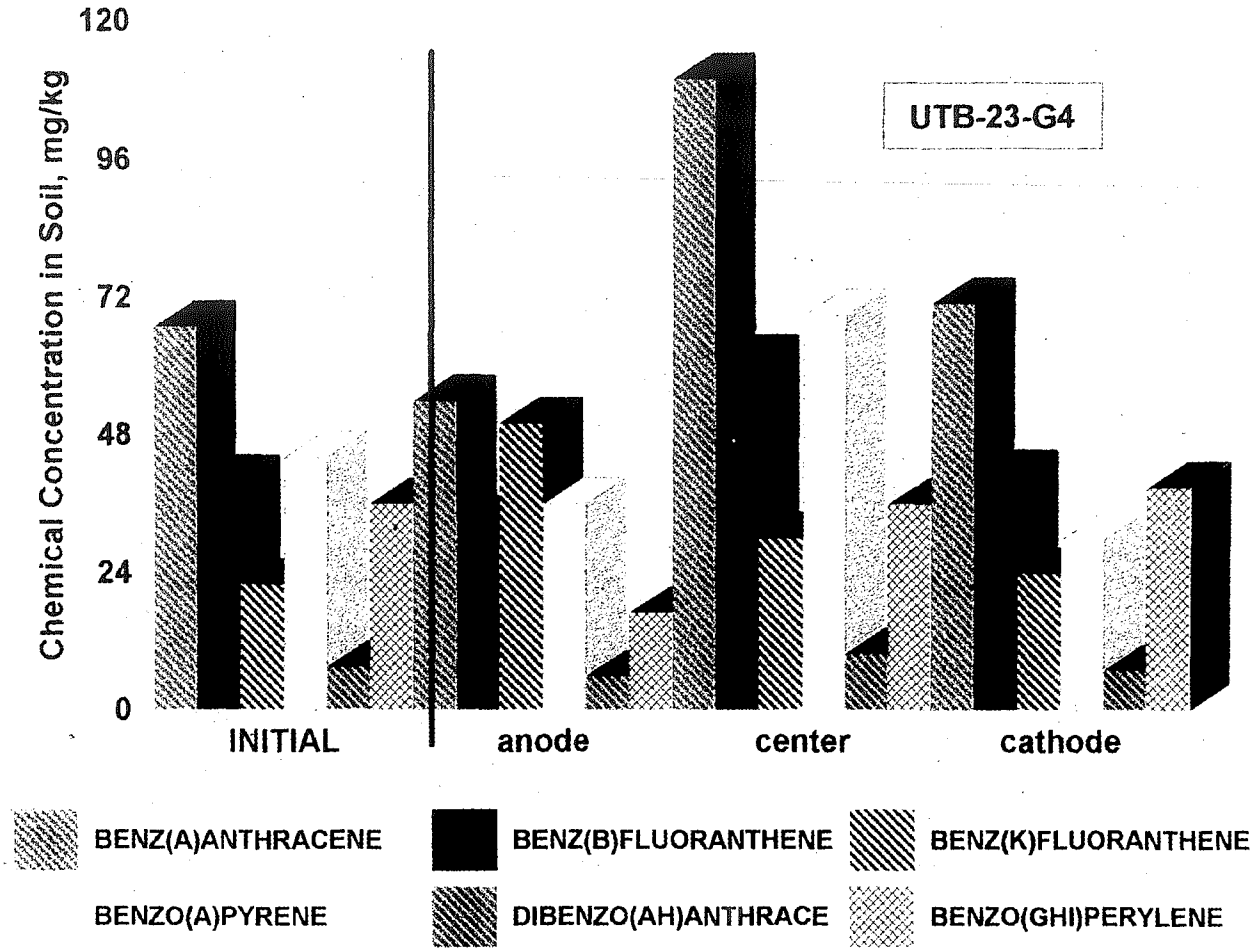
120
96
72
48
24
0
Chemical Concentration in Soil, mg/kg
UTB-23-G4
INITIAL
anode
center
cathode
BENZ(A)ANTHRACENE
BENZ(B)FLUORANTHENE
BENZ(K)FLUORANTHENE
BENZO(A)PYRENE
DIBENZO(AH)ANTHRACE
BENZO(GHI)PERYLENE

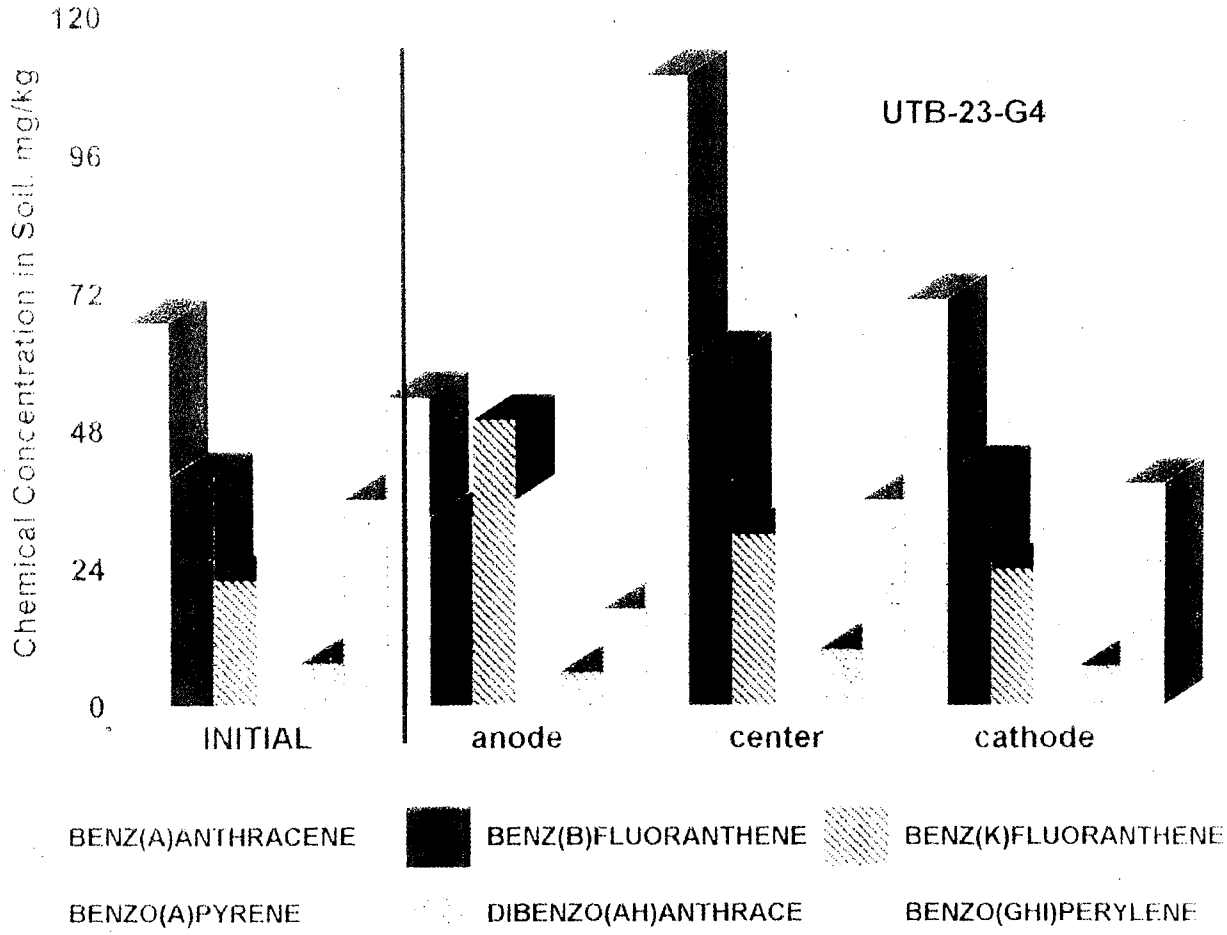
120
96
72
48
24
0
Chemical Concentration in Soil, mg/kg
UTB-23-G4
INITIAL
anode
center
cathode
BENZ(A)ANTHRACENE
BENZ(B)FLUORANTHENE
BENZ(K)FLUORANTHENE
BENZO(A)PYRENE
DIBENZO(AH)ANTHRACE
BENZO(GHI)PERYLENE

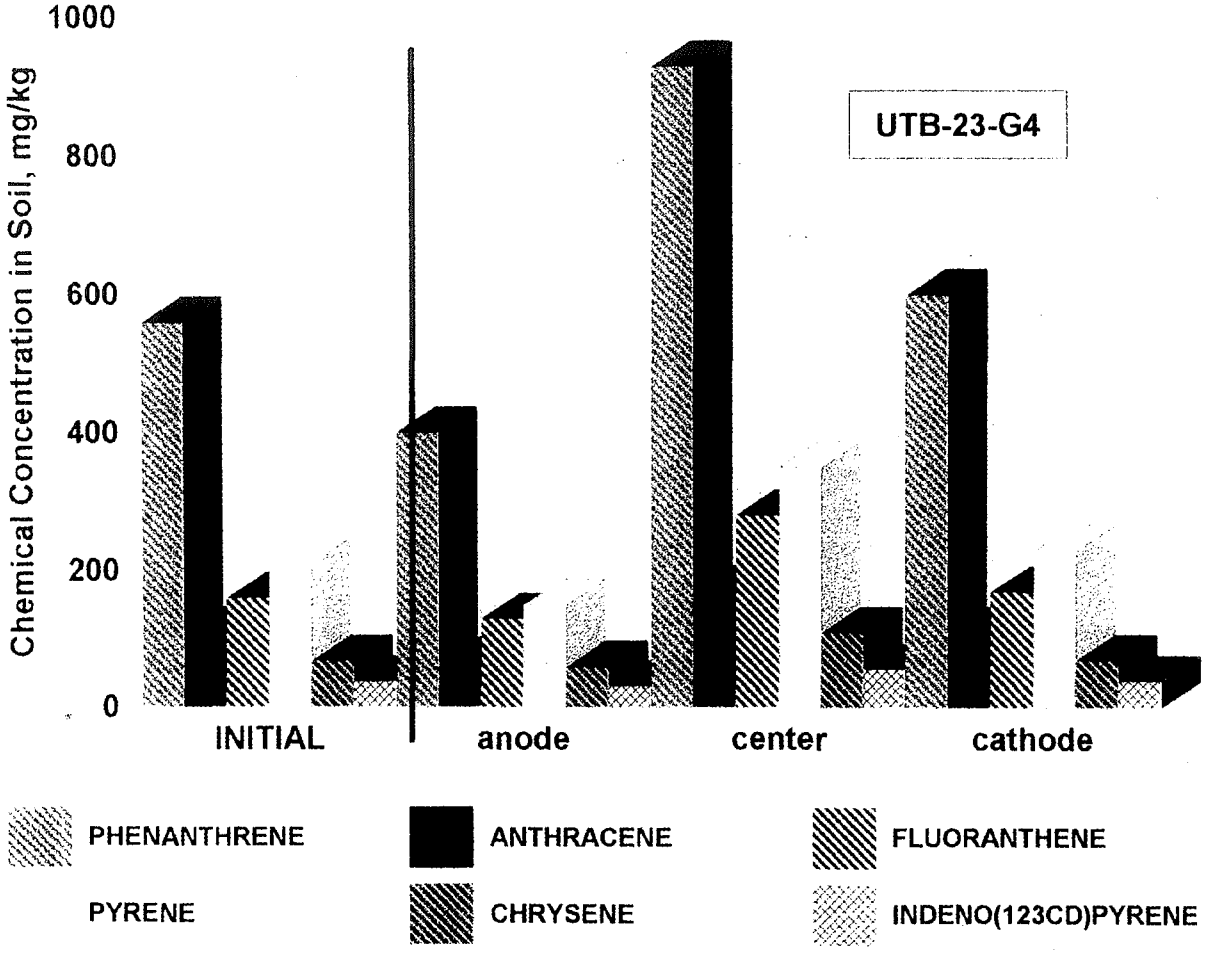
1000
800
600
400
200
0
Chemical Concentration in Soil, mg/kg
UTB-23-G4
INITIAL
anode
center
cathode
PHENANTHRENE
ANTHRACENE
FLUORANTHENE
PYRENE
CHRYSENE
INDENO(123CD)PYRENE

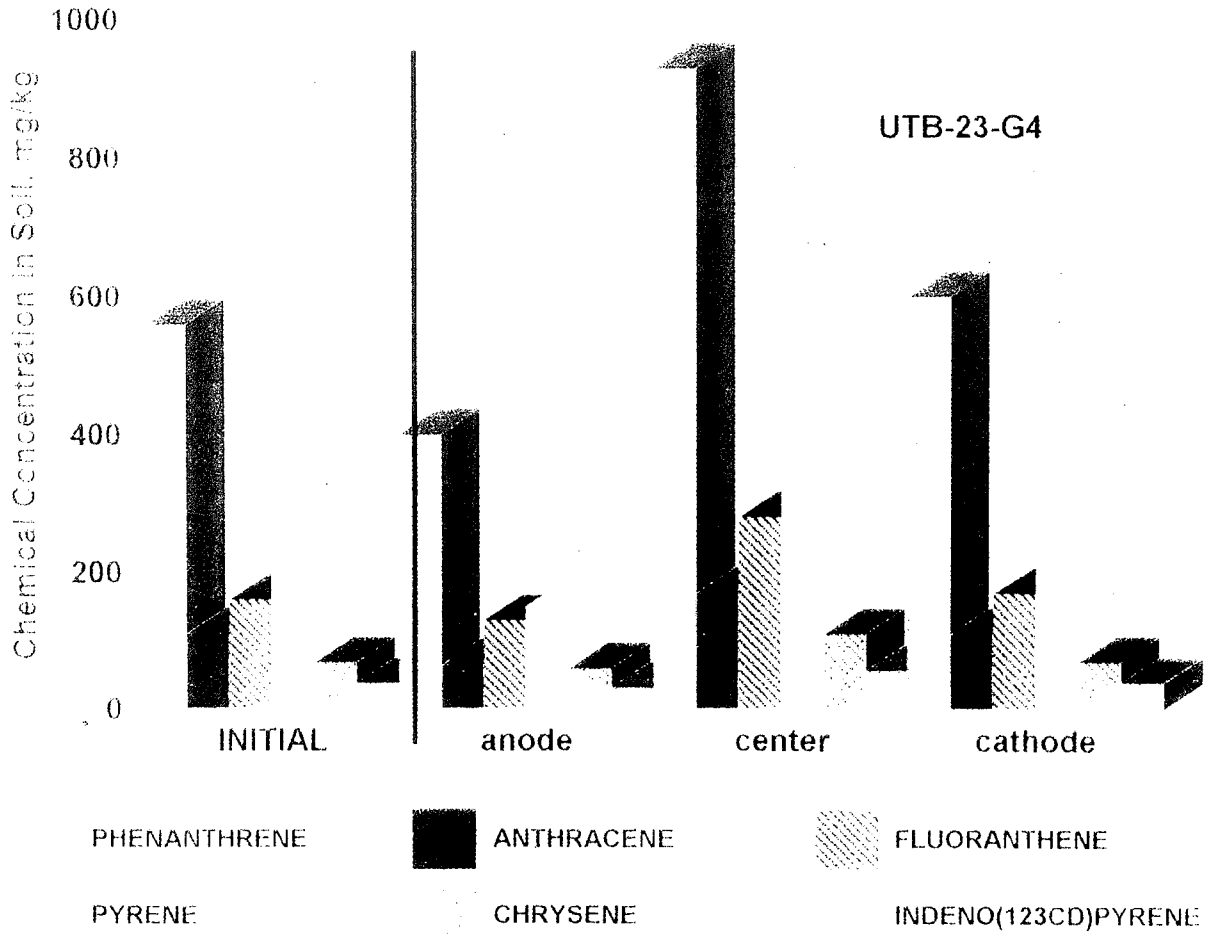
UTB-23-G4
Chemical Concentration in Soil, mg/kg
1000
800
600
400
200
0
INITIAL
anode
center
cathode
PHENANTHRENE
ANTHRACENE
FLUORANTHENE
PYRENE
CHRYSENE
INDENO(123CD)PYRENE

UTB-23-G5
Chemical Concentration in Soil, mg/kg
600
480
360
240
120
0
initial
anode
center
cathode
NAPTHALENE
ACENAPHTHENE
ACENAPHTHYLENE
FLUORENE

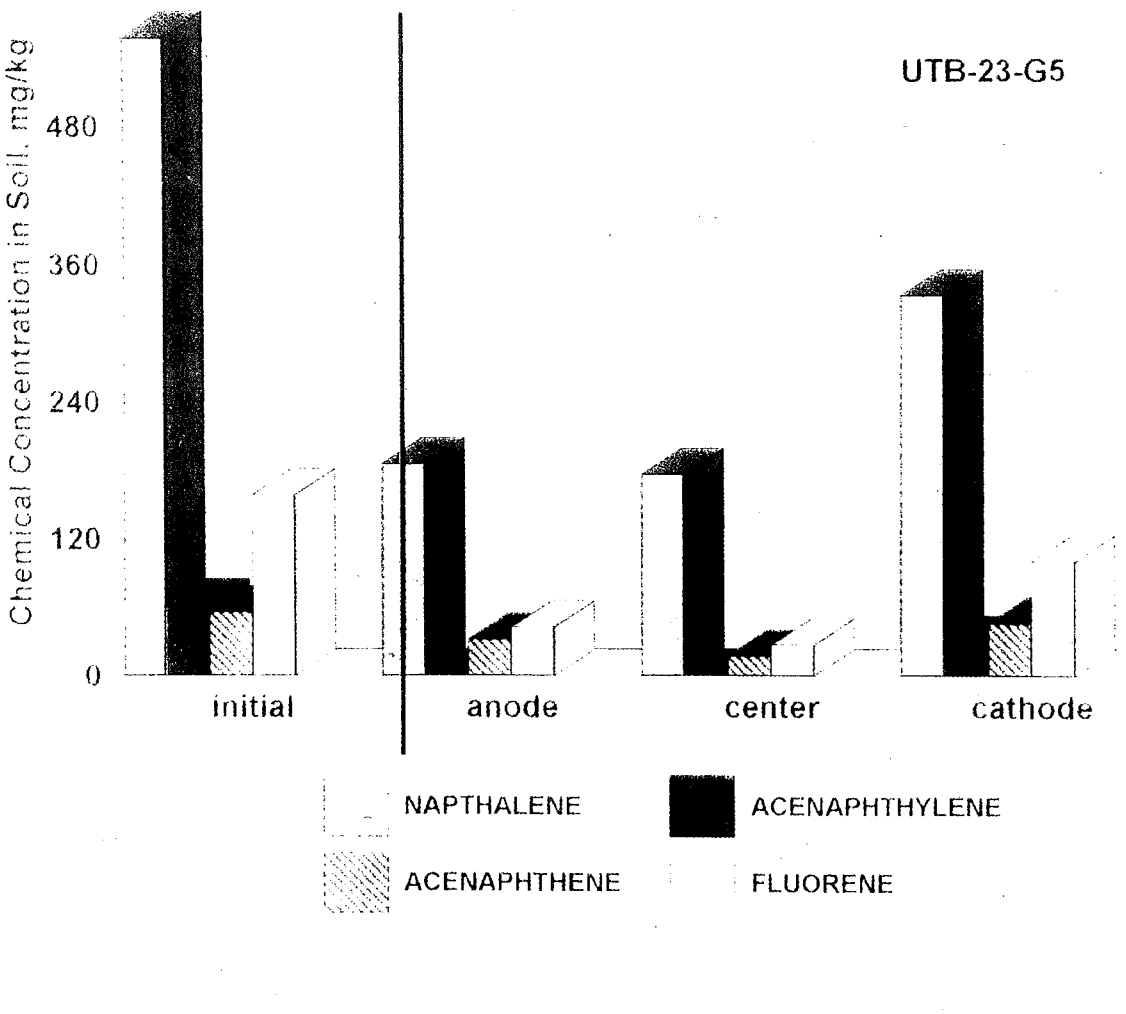
600
480
360
240
120
0
Chemical Concentration in Soil, mg/kg
UTB-23-G5
initial
anode
center
cathode
NAPTHALENE
ACENAPHTHYLENE
ACENAPHTHENE
FLUORENE

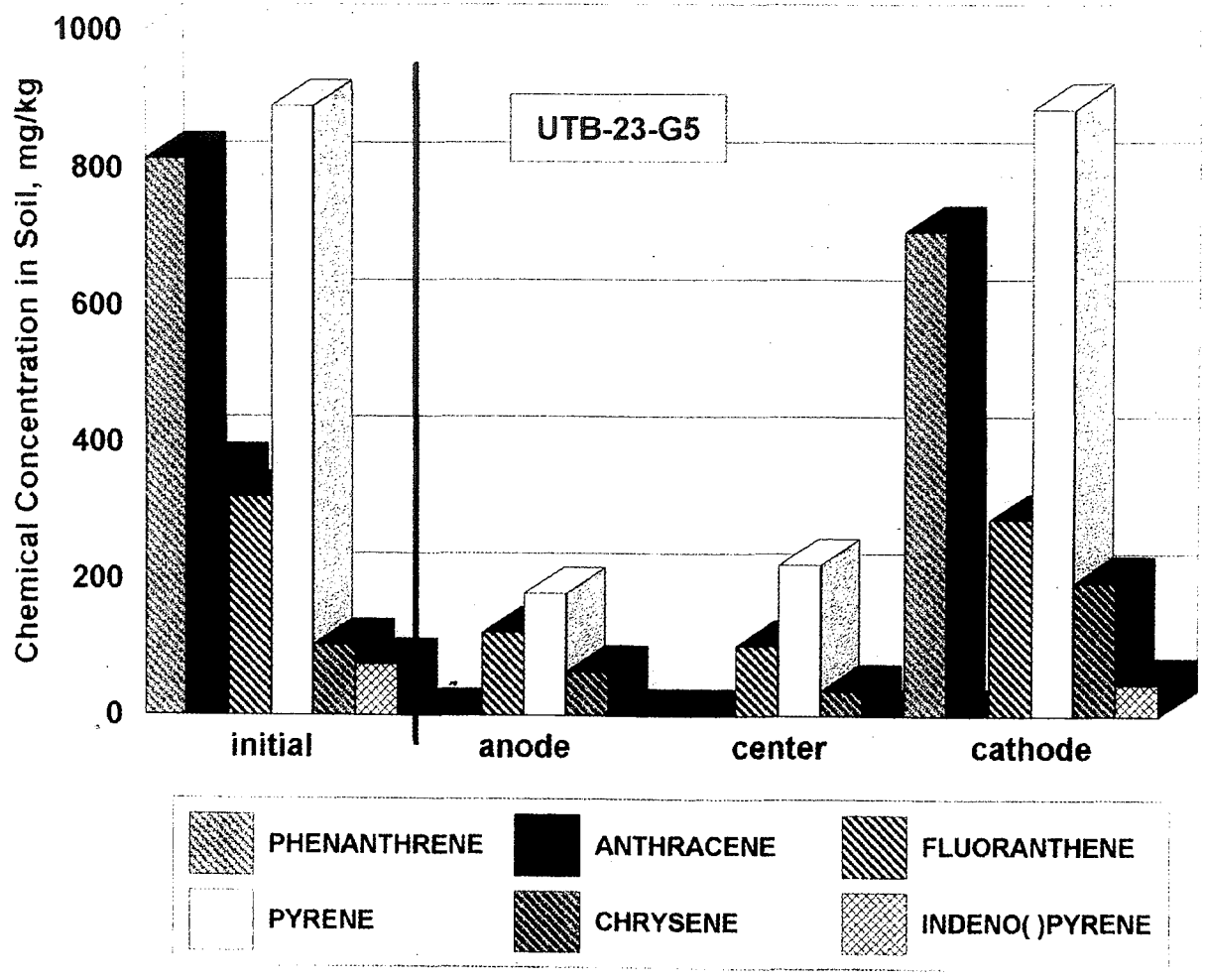
UTB-23-G5
Chemical Concentration in Soil, mg/kg
1000
800
600
400
200
0
initial
anode
center
cathode
PHENANTHRENE
ANTHRACENE
FLUORANTHENE
PYRENE
CHRYSENE
INDENO( )PYRENE

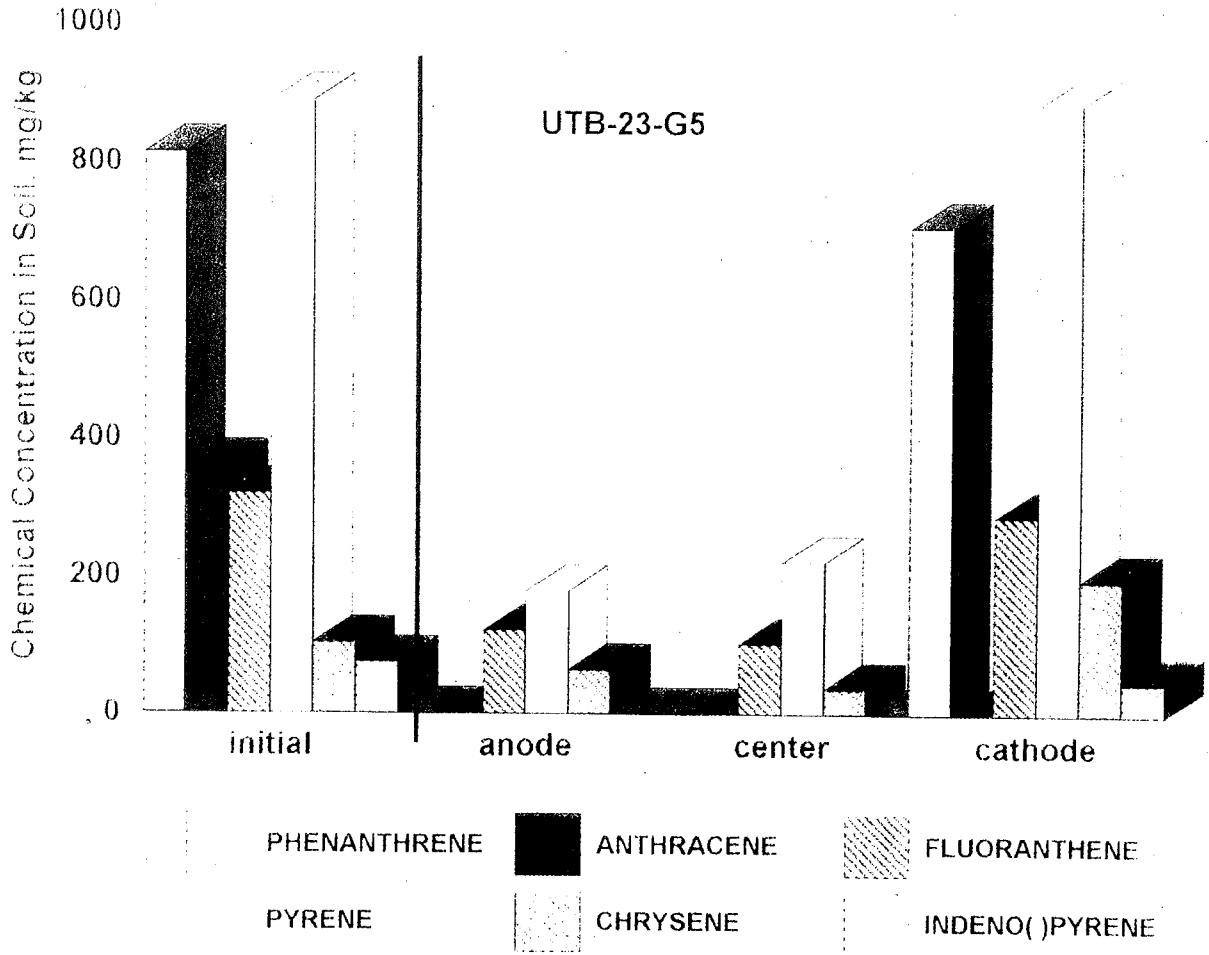
1000
800
600
400
200
0
Chemical Concentration in Soil, mg/kg
UTB-23-G5
initial
anode
center
cathode
PHENANTHRENE
ANTHRACENE
FLUORANTHENE
PYRENE
CHRYSENE
INDENO( )PYRENE

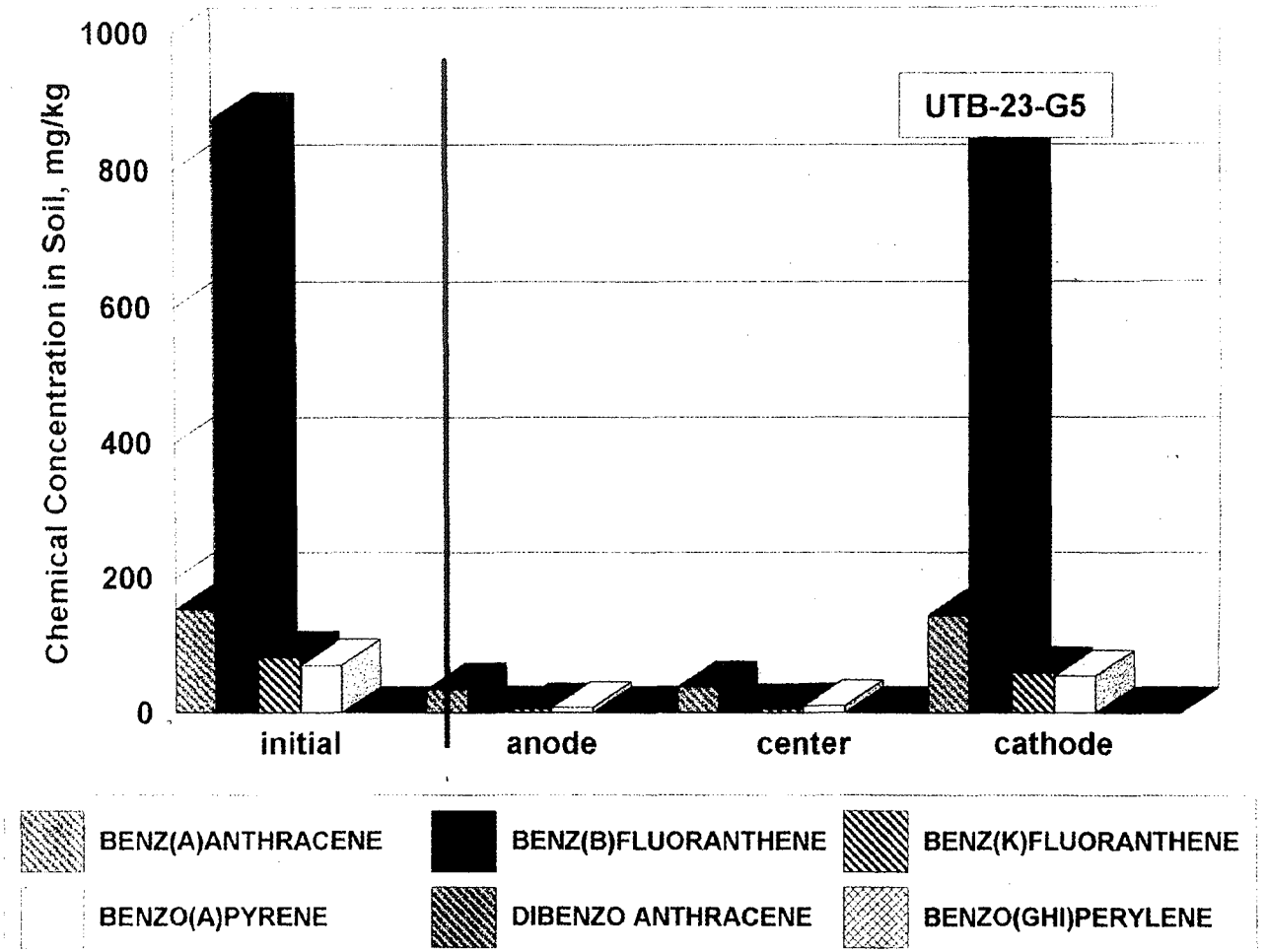
UTB-23-G5
Chemical Concentration in Soil, mg/kg
1000
800
600
400
200
0
initial
anode
center
cathode
BENZ(A)ANTHRACENE
BENZ(B)FLUORANTHENE
BENZ(K)FLUORANTHENE
BENZO(A)PYRENE
DIBENZO ANTHRACENE
BENZO(GHI)PERYLENE

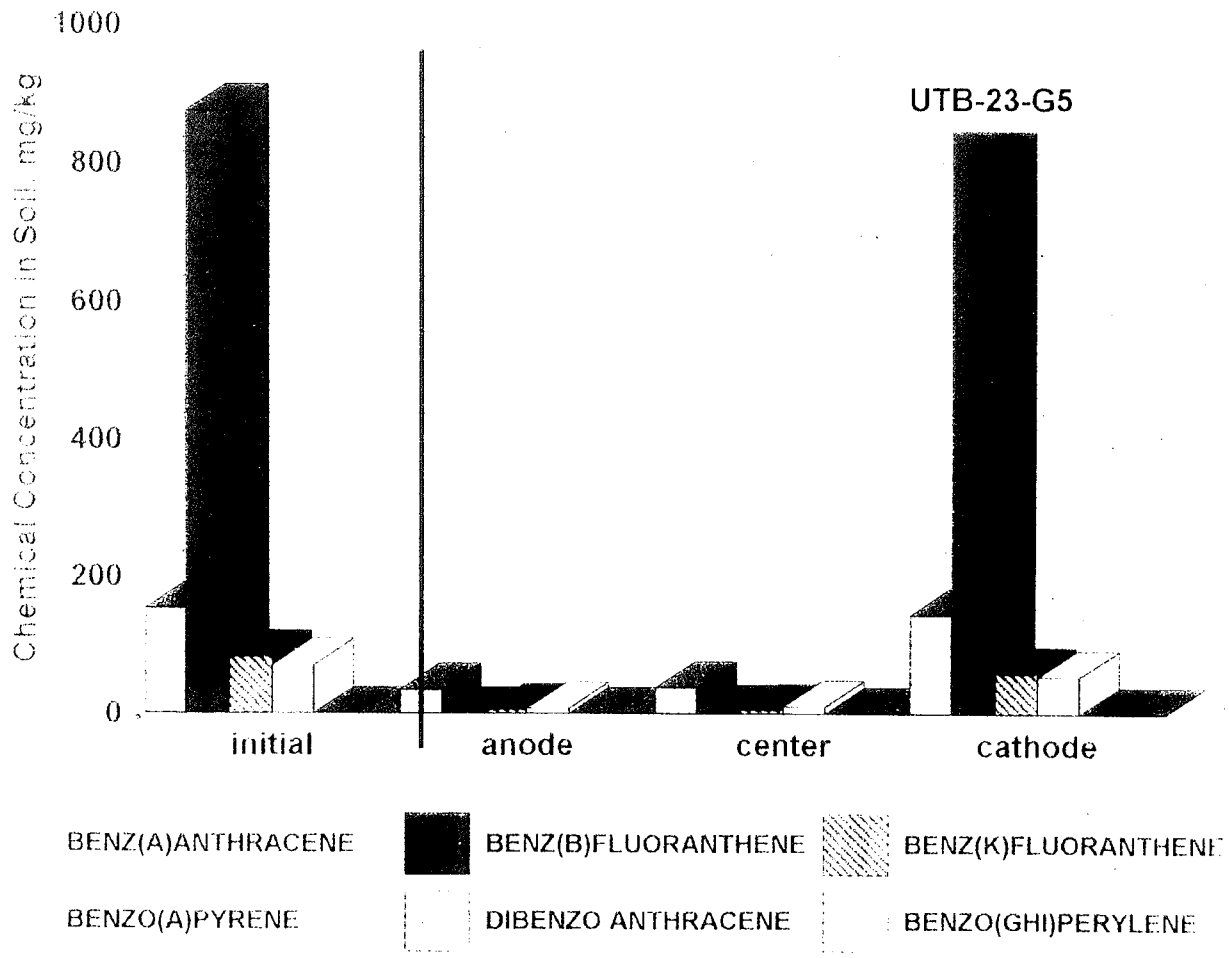
1000
800
600
400
200
0
Chemical Concentration in Soil, mg/kg
UTB-23-G5
initial
anode
center
cathode
BENZ(A)ANTHRACENE
BENZ(B)FLUORANTHENE
BENZ(K)FLUORANTHENE
BENZO(A)PYRENE
DIBENZO ANTHRACENE
BENZO(GHI)PERYLENE

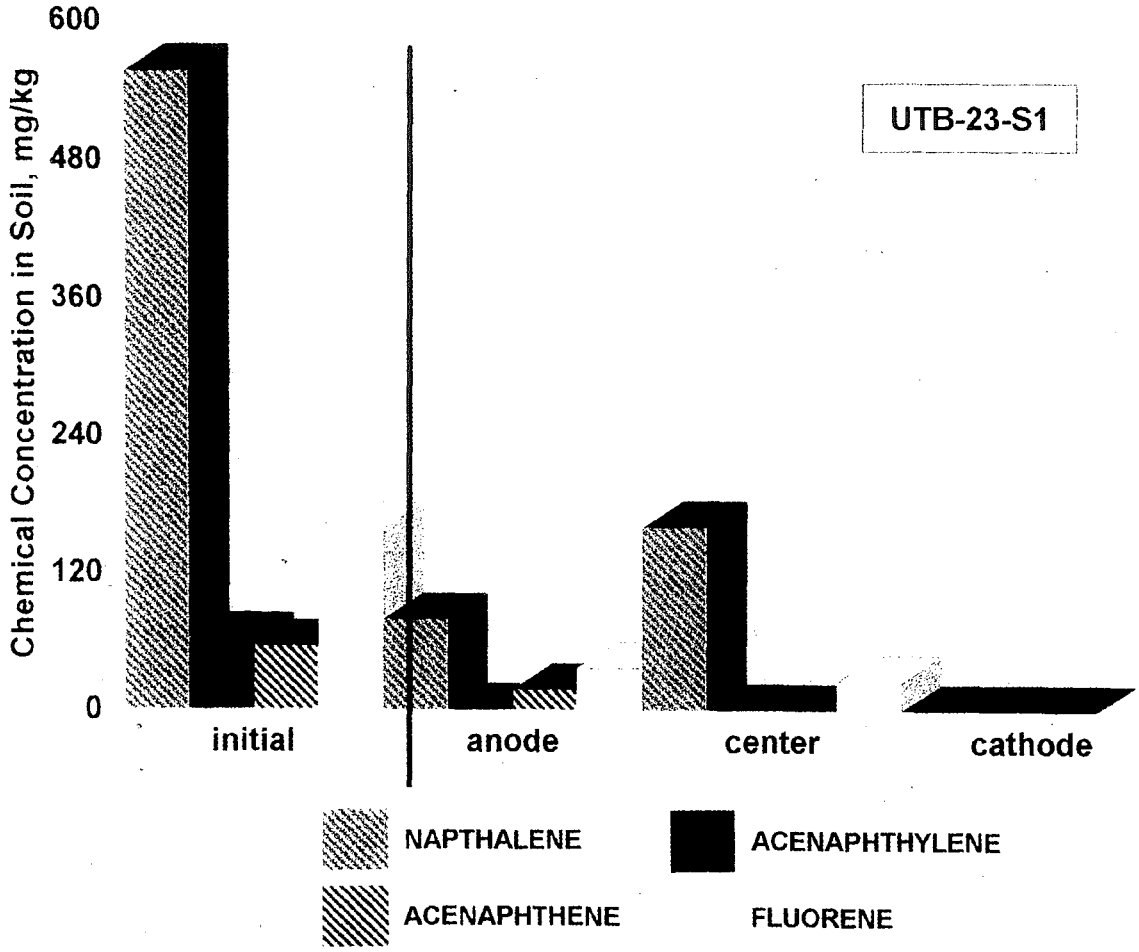
600
480
360
240
120
0
Chemical Concentration in Soil, mg/kg
UTB-23-S1
initial
anode
center
cathode
NAPTHALENE
ACENAPHTHYLENE
ACENAPHTHENE
FLUORENE

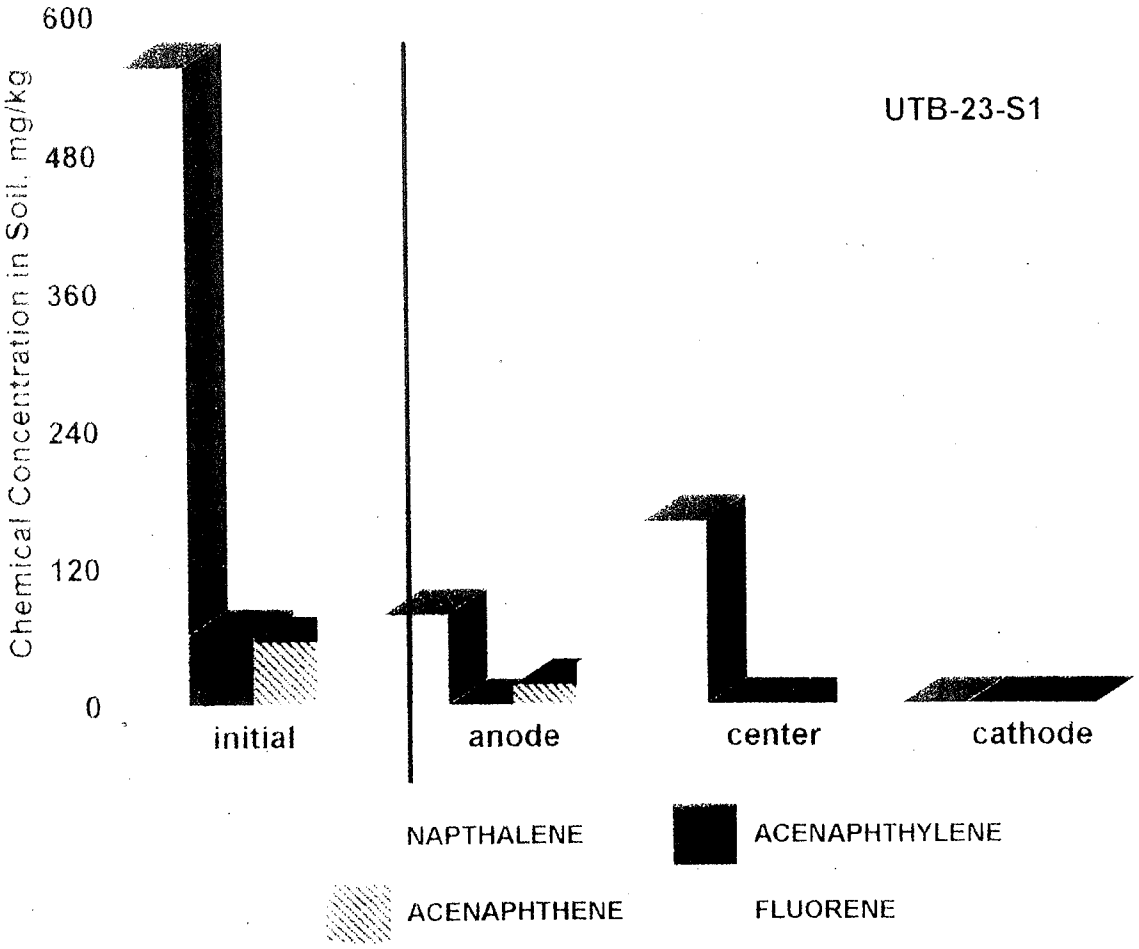
600
480
360
240
120
0
Chemical Concentration in Soil, mg/kg
UTB-23-S1
initial
anode
center
cathode
NAPTHALENE
ACENAPHTHYLENE
ACENAPHTHENE
FLUORENE

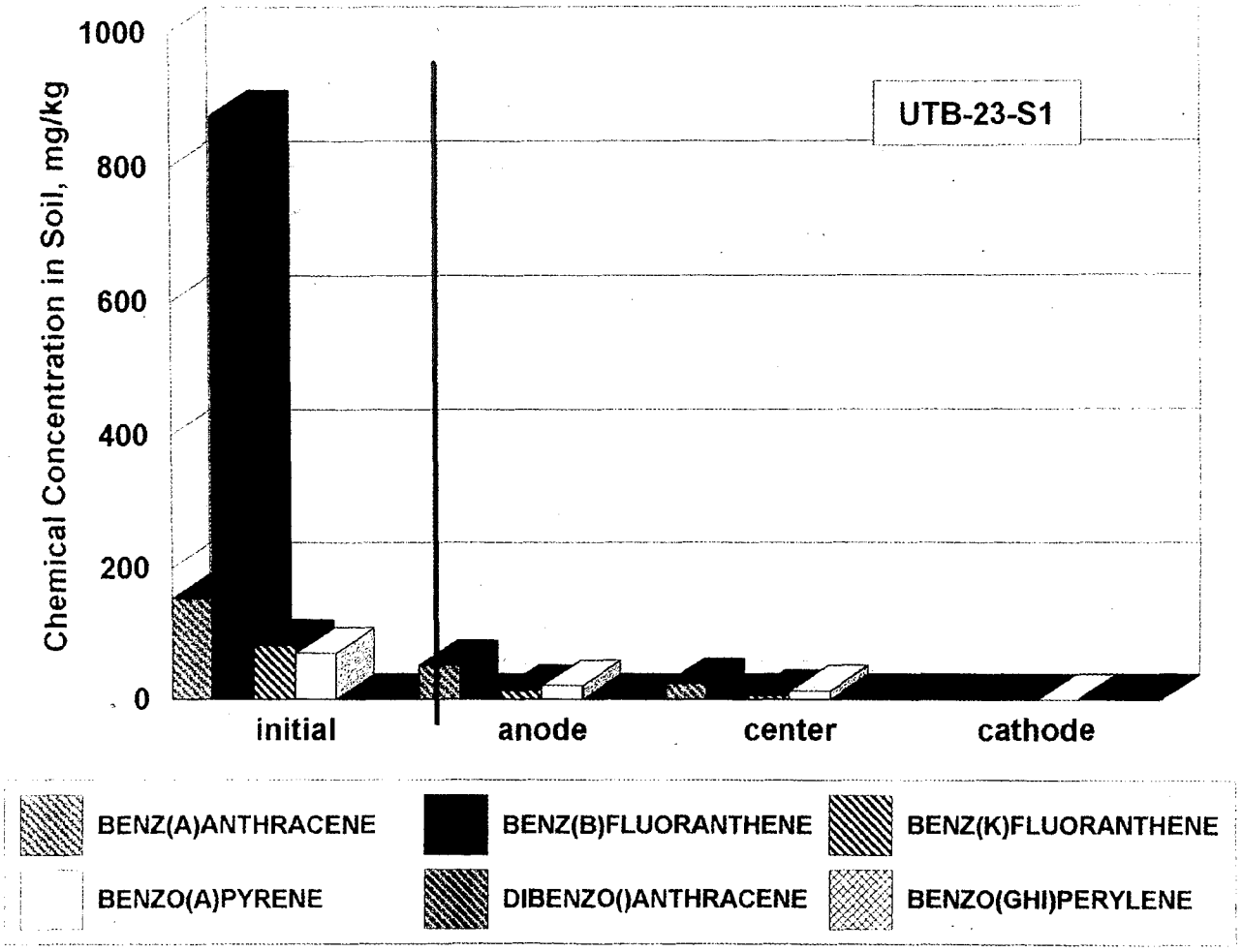
1000
800
600
400
200
0
Chemical Concentration in Soil, mg/kg
UTB-23-S1
initial
anode
center
cathode
BENZ(A)ANTHRACENE
BENZ(B)FLUORANTHENE
BENZ(K)FLUORANTHENE
BENZO(A)PYRENE
DIBENZO()ANTHRACENE
BENZO(GHI)PERYLENE

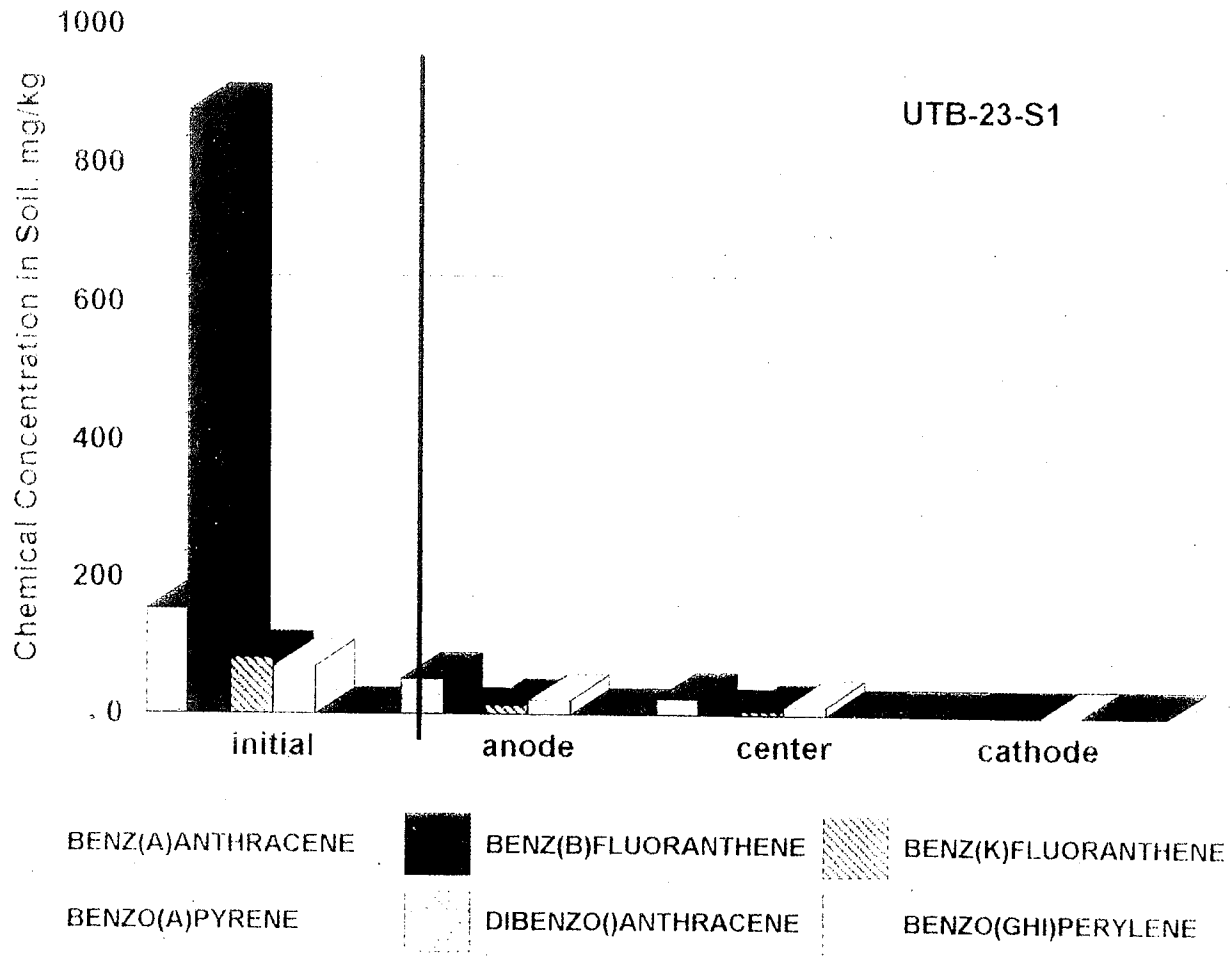
1000
800
600
400
200
0
Chemical Concentration in Soil, mg/kg
UTB-23-S1
initial
anode
center
cathode
BENZ(A)ANTHRACENE
BENZ(B)FLUORANTHENE
BENZ(K)FLUORANTHENE
BENZO(A)PYRENE
DIBENZO()ANTHRACENE
BENZO(GHI)PERYLENE

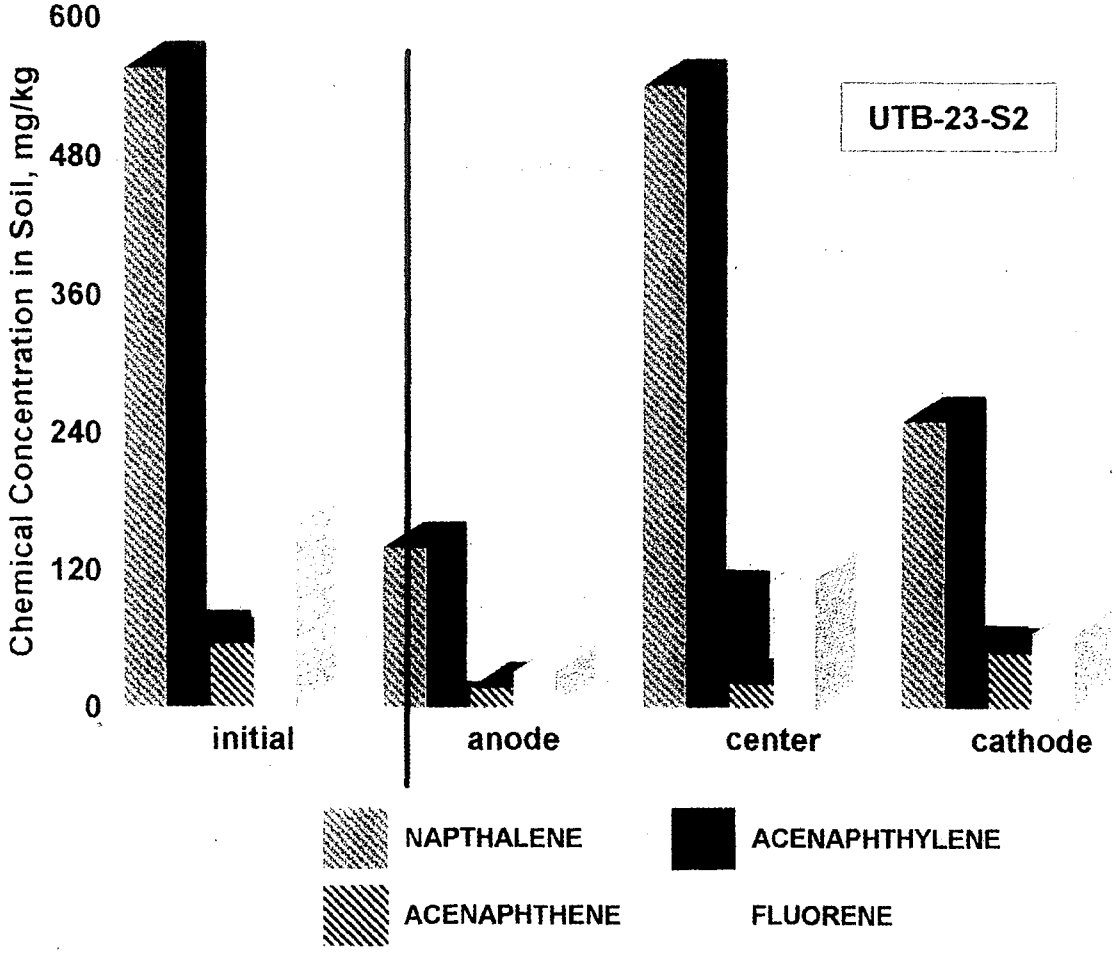
600
480
360
240
120
0
Chemical Concentration in Soil, mg/kg
UTB-23-S2
initial
anode
center
cathode
NAPTHALENE
ACENAPHTHYLENE
ACENAPHTHENE
FLUORENE

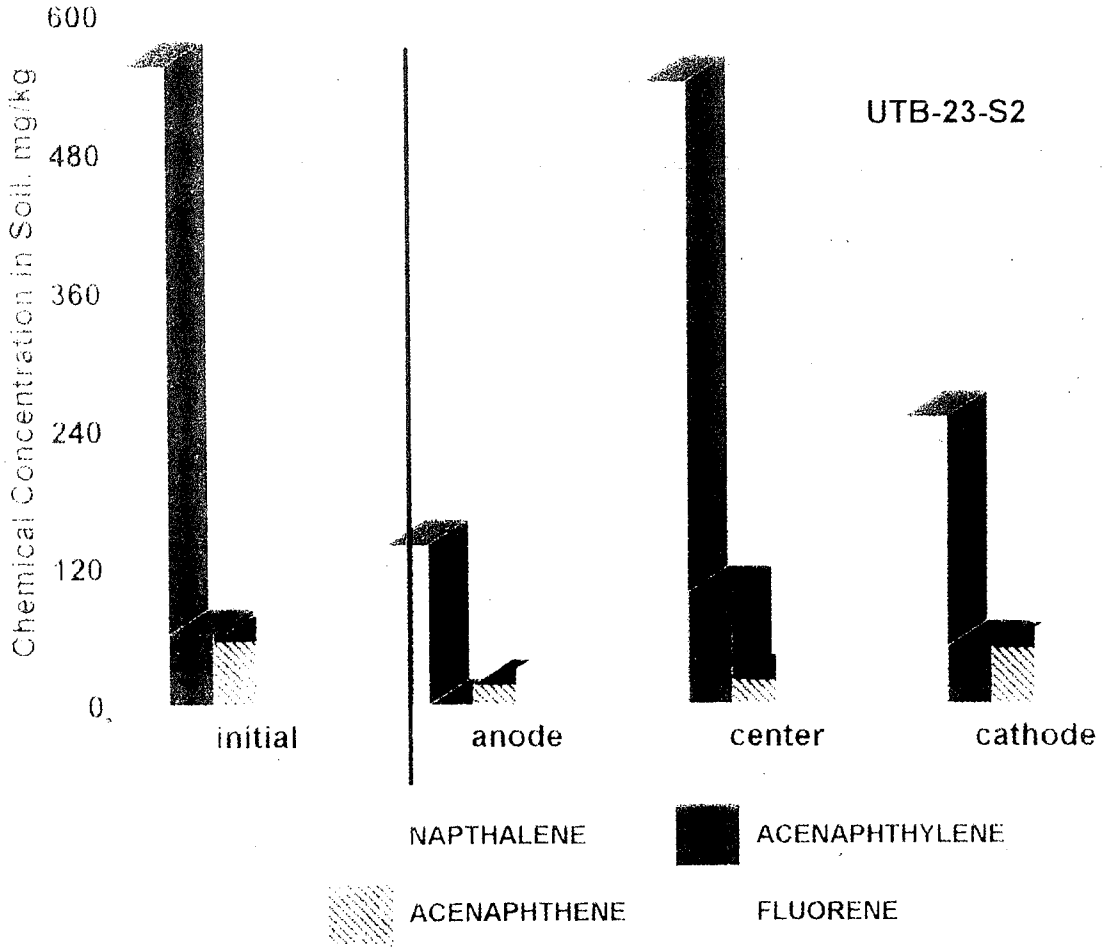
600
480
360
240
120
0
Chemical Concentration in Soil, mg/kg
UTB-23-S2
initial
anode
center
cathode
NAPTHALENE
ACENAPHTHYLENE
ACENAPHTHENE
FLUORENE

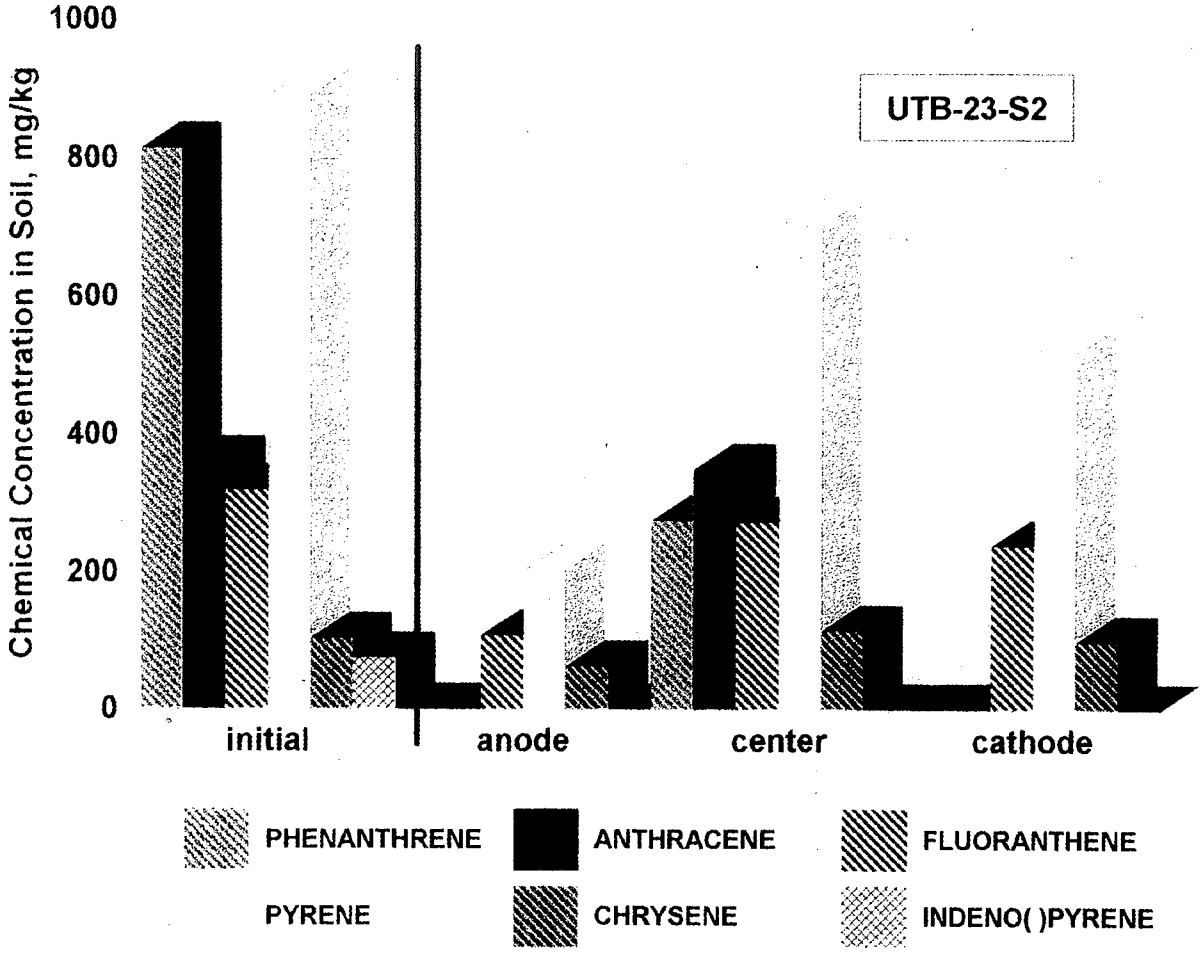
1000
800
600
400
200
0
Chemical Concentration in Soil, mg/kg
UTB-23-S2
initial
anode
center
cathode
PHENANTHRENE
ANTHRACENE
FLUORANTHENE
PYRENE
CHRYSENE
INDENO( )PYRENE

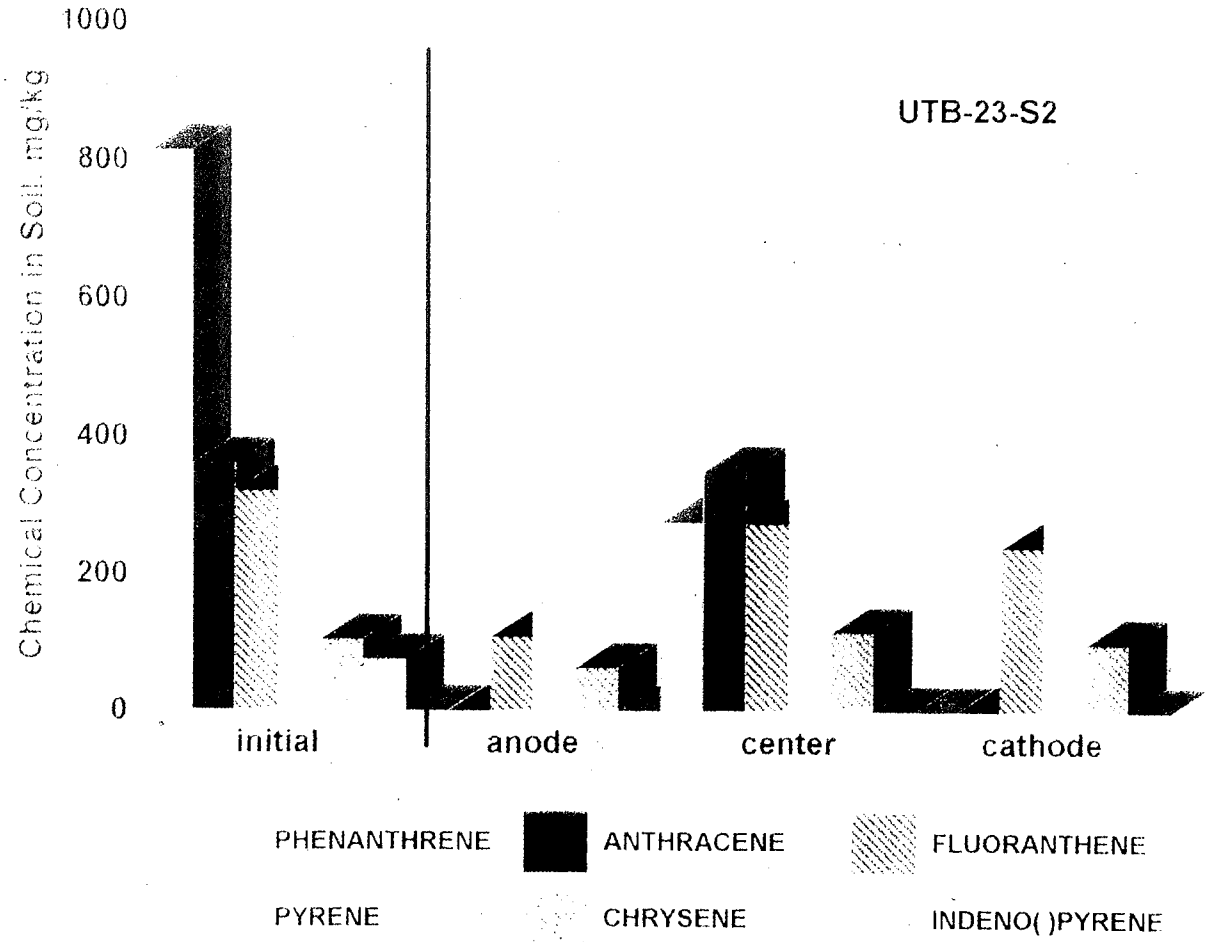
1000
800
600
400
200
0
Chemical Concentration in Soil, mg/kg
UTB-23-S2
initial
anode
center
cathode
PHENANTHRENE
ANTHRACENE
FLUORANTHENE
PYRENE
CHRYSENE
INDENO( )PYRENE

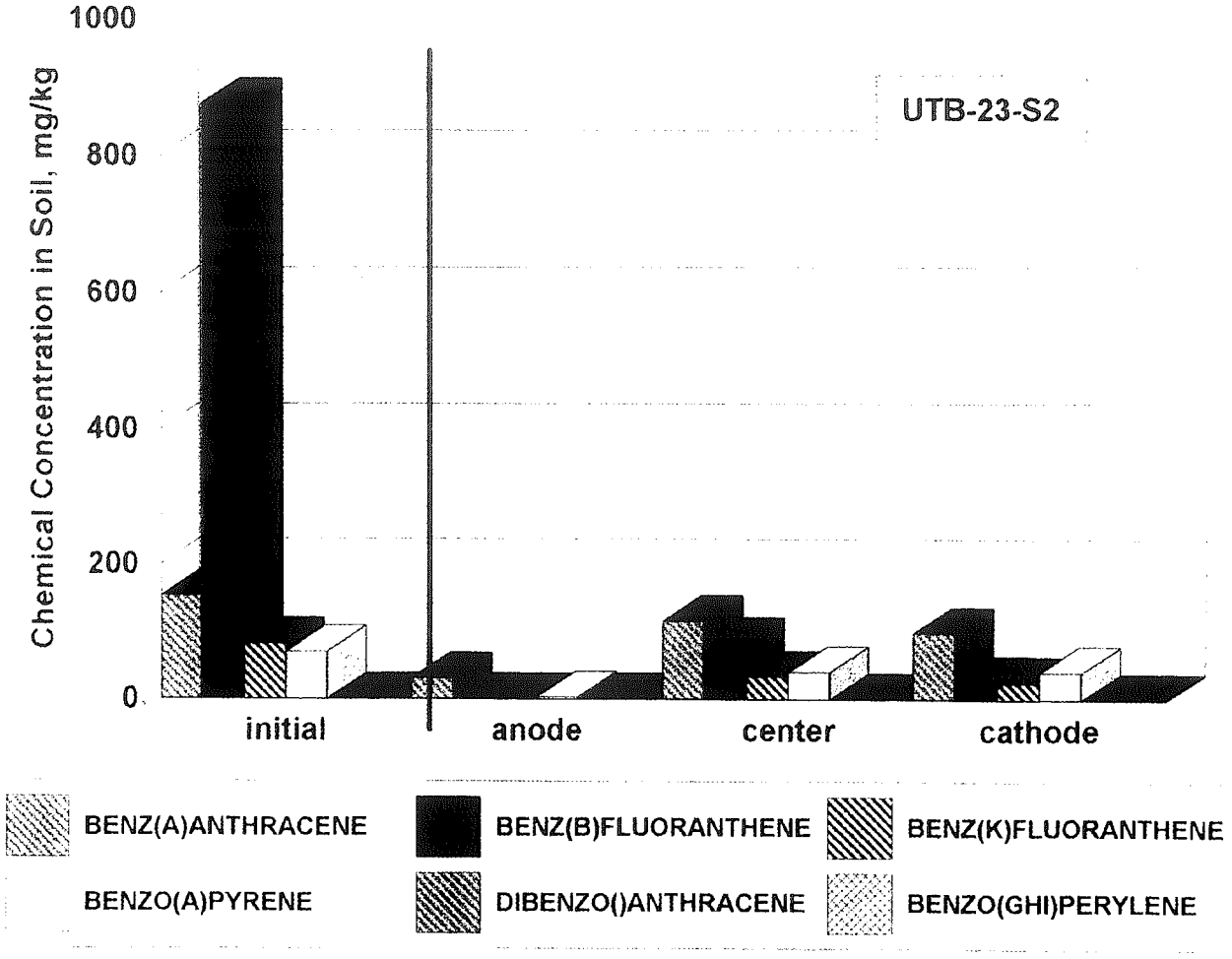
1000
800
600
400
200
0
Chemical Concentration in Soil, mg/kg
UTB-23-S2
initial
anode
center
cathode
BENZ(A)ANTHRACENE
BENZ(B)FLUORANTHENE
BENZ(K)FLUORANTHENE
BENZO(A)PYRENE
DIBENZO()ANTHRACENE
BENZO(GHI)PERYLENE

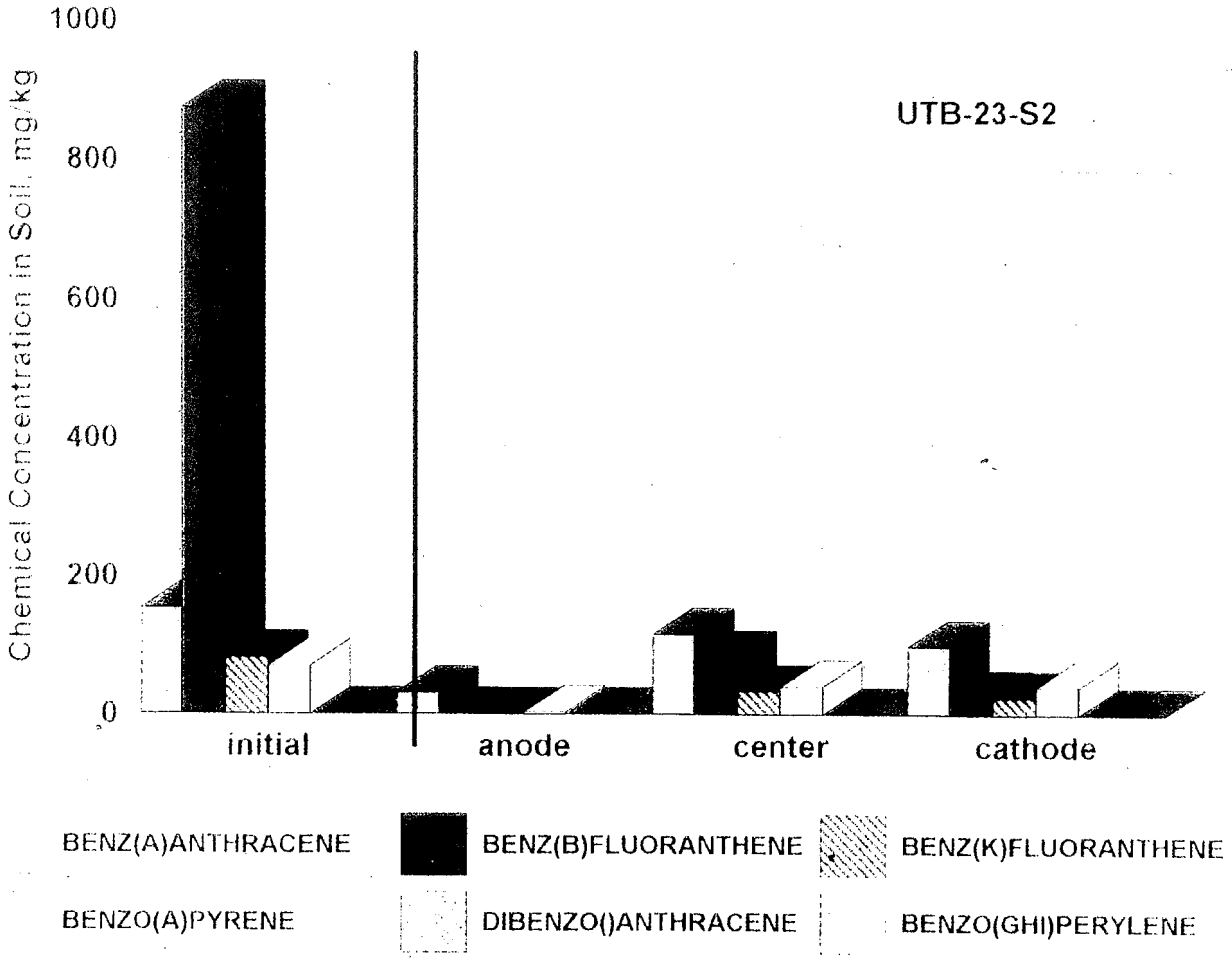
1000
800
600
400
200
0
Chemical Concentration in Soil, mg/kg
UTB-23-S2
initial
anode
center
cathode
BENZ(A)ANTHRACENE
BENZ(B)FLUORANTHENE
BENZ(K)FLUORANTHENE
BENZO(A)PYRENE
DIBENZO()ANTHRACENE
BENZO(GHI)PERYLENE

APPENDIX E

NUCLEAR MAGNETIC RESONANCE SPECTRA PLOTS

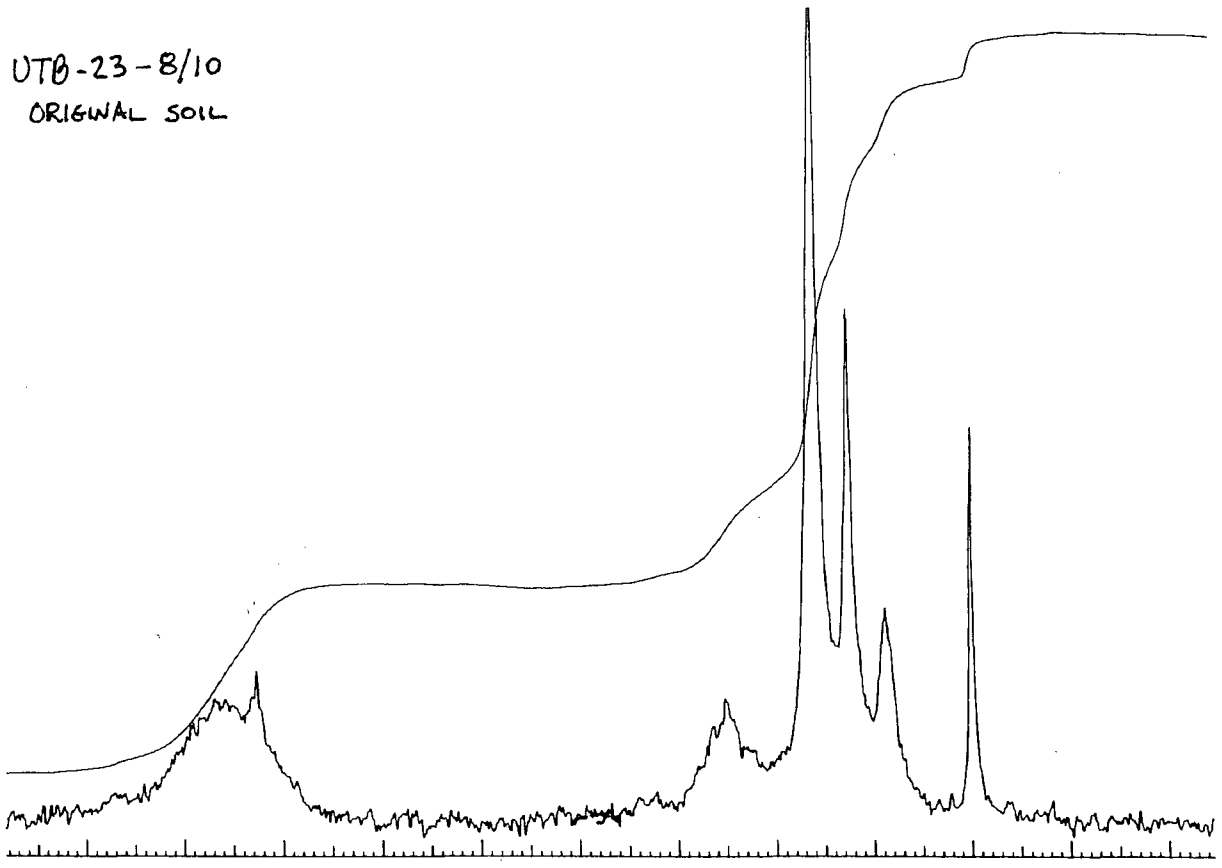
UTB-23-8/10
ORIGWAL SOIL

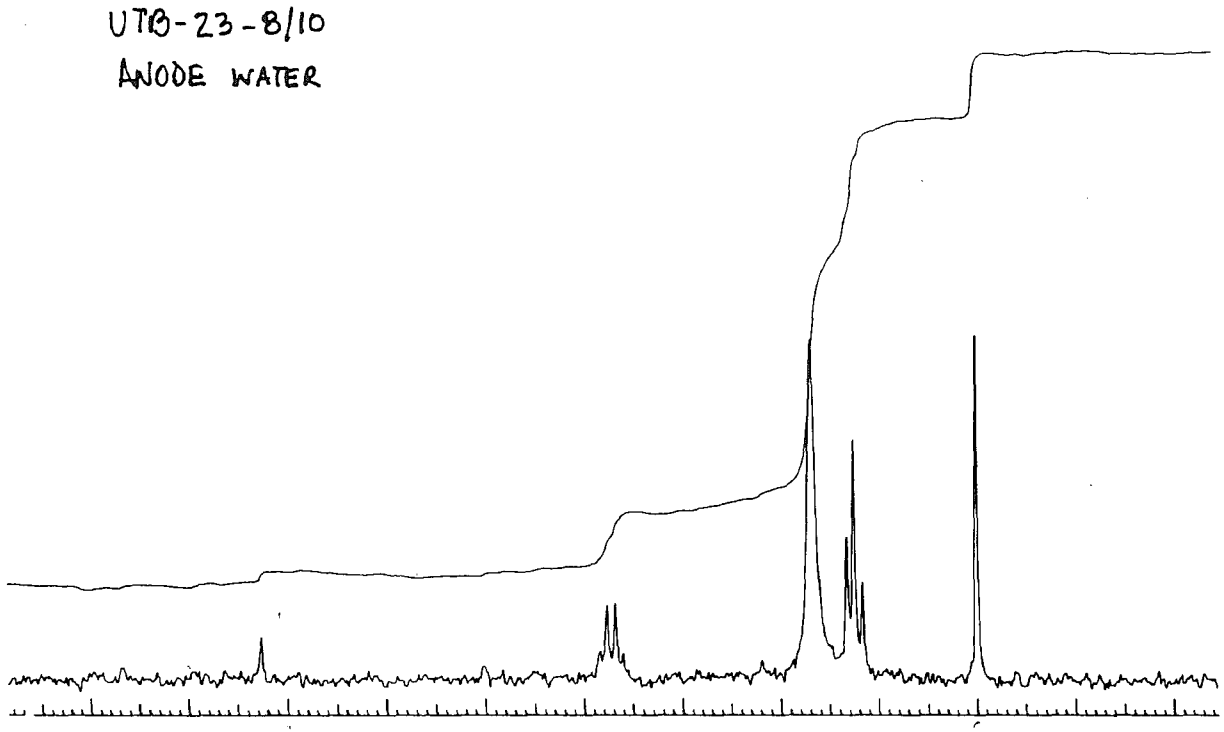
UTB-23-8/10
ANODE WATER

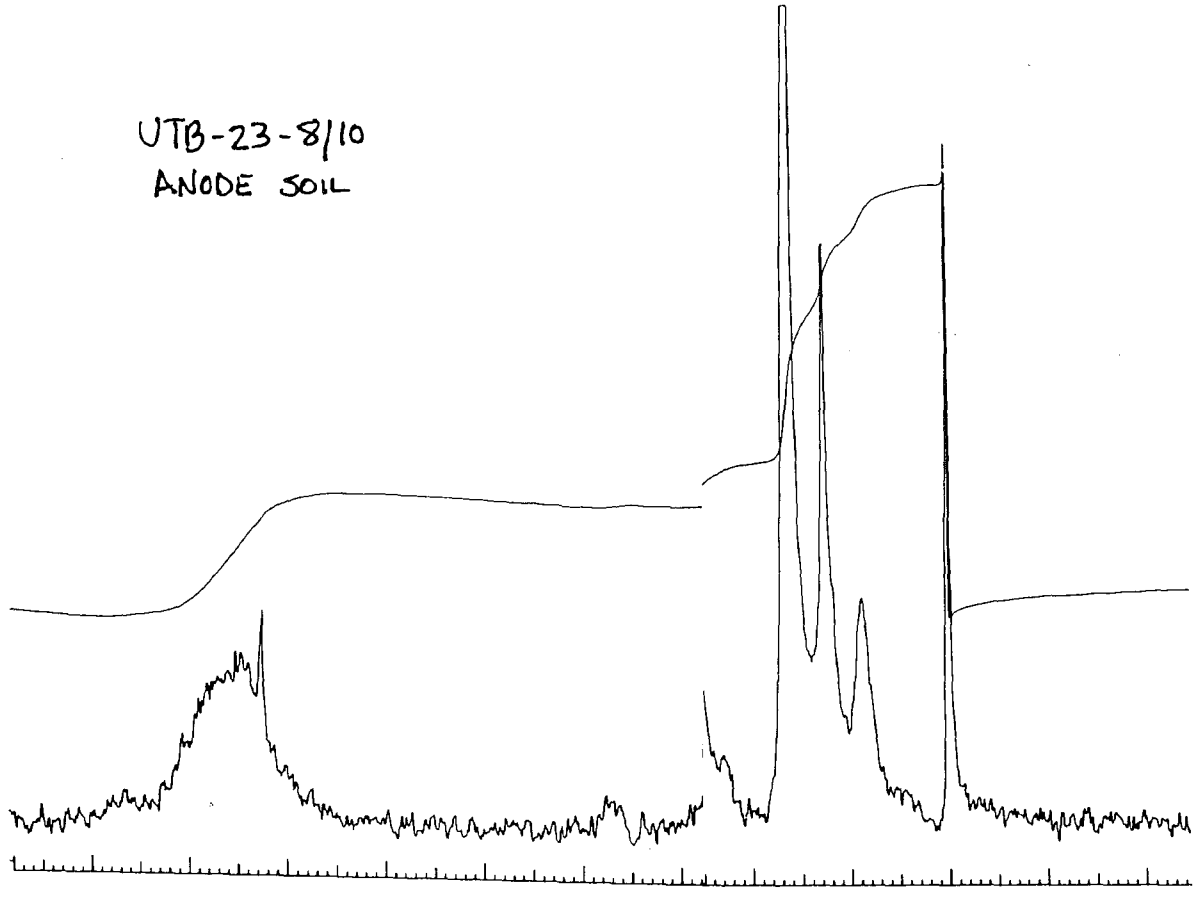
UTB-23-8/10
ANODE SOIL

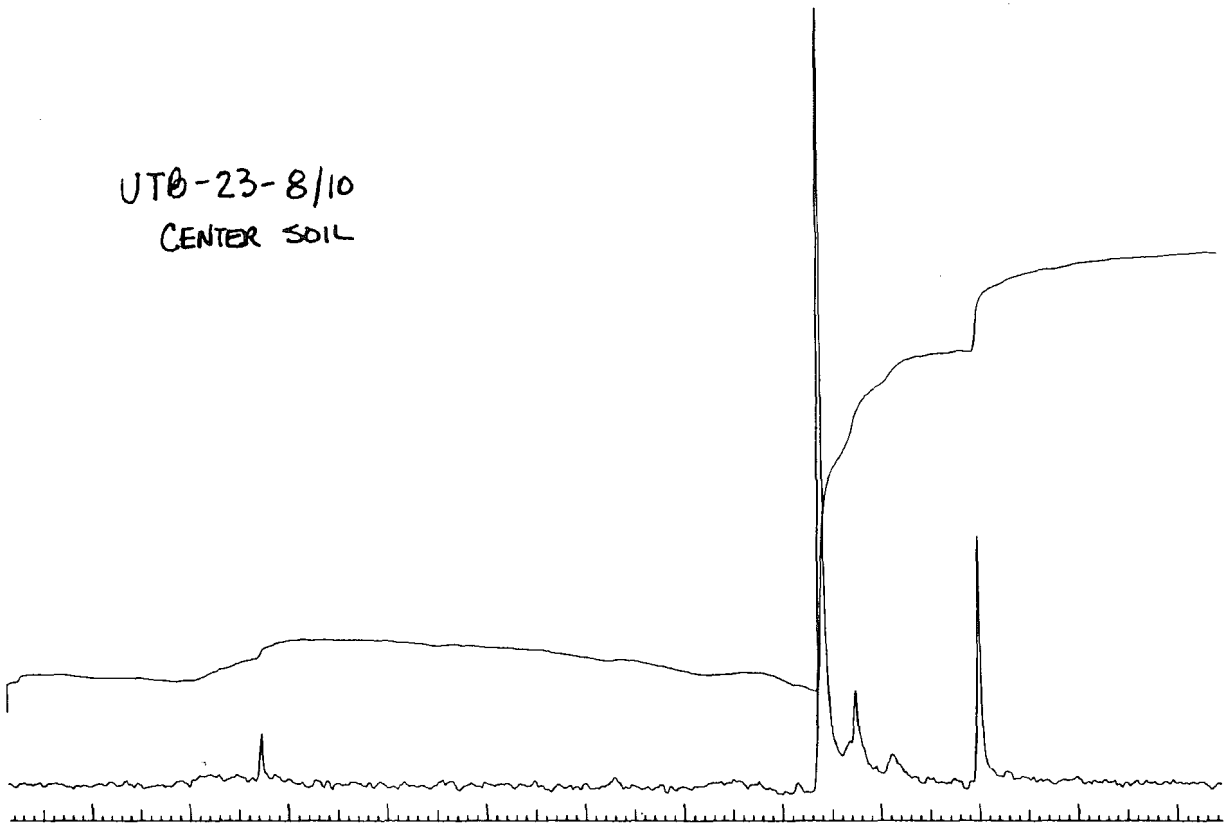
UTB-23-8/10
CENTER SOIL

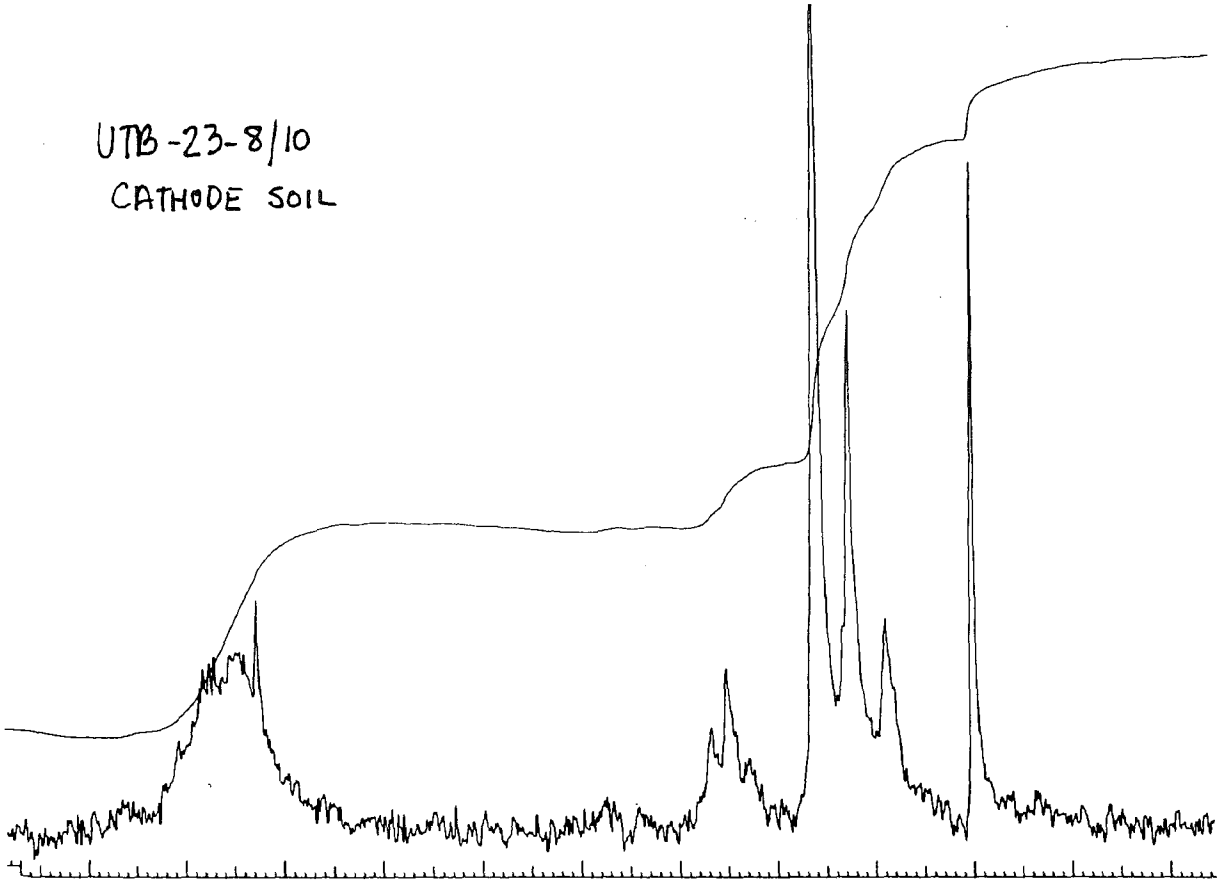
UTB-23-8/10
CATHODE SOIL

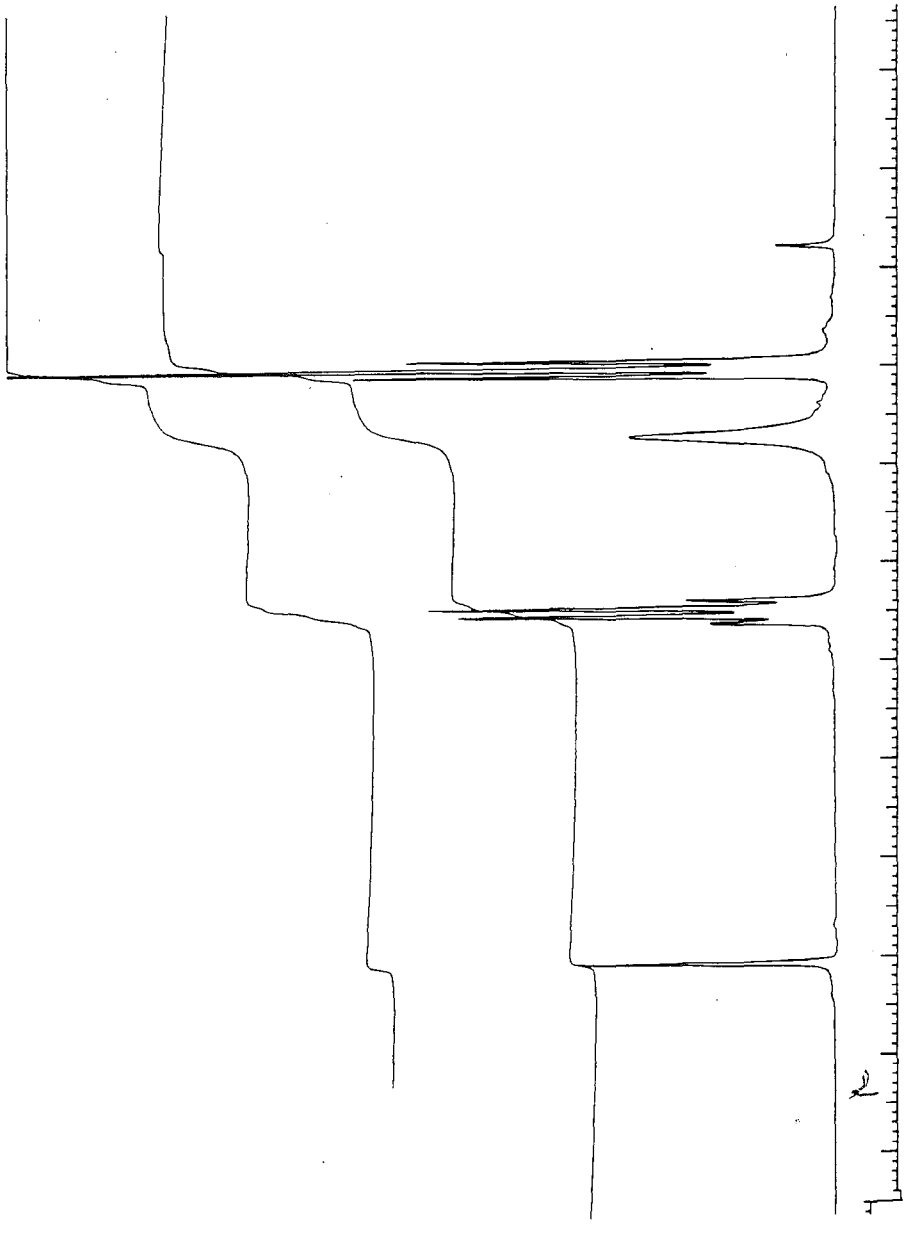

VITA

Gary Newhart was born on November 7, 1957 to Arabella and James Newhart of Springfield, Pennsylvania. He was graduated from Central Bucks High School East in Holicong, Pennsylvania, in May of 1975 and entered the University of Miami, Coral Gables, Florida in August of that year, studying Economics. He transferred to Lehigh University in January of 1978, and began studying Chemistry and Geology. He received a Bachelor of Science degree in Environmental Sciences and Resource Management from Lehigh University in June of 1982.

During the interlude between the Bachelor's degree and the Master's degree, he worked as a research assistant at the Woods Hole Marine Biological Laboratories and the Woods Hole Oceanographic Institute, in Woods Hole Massachusetts, and as a Environmental Engineer at an Engineering firm in Boston, Massachusetts.

In August of 1990, he began graduate school at Lehigh University in pursuit of the Master of Science degree, with special interest in contaminant transport through soil and ground water.

END

OF

TITLE